ROLE OF RHOC IN REGULATION OF STEMNESS IN CERVICAL CARCINOMA

A THESIS TO BE SUBMITTED TO

THE UNIVERSITY OF TRANS-DISCIPLINARY HEALTH SCIENCES AND TECHNOLOGY

FOR THE AWARD OF THE DEGREE OF
DOCTOR OF PHILOSOPHY

BY

PAVANA THOMAS

UNDER THE GUIDANCE OF

DR. SWETA SRIVASTAVA
TRANSLATIONAL AND MOLECULAR BIOLOGY LABORATORY
ST. JOHN'S MEDICAL COLLEGE AND HOSPITAL
BANGALORE-560034

ST. JOHN'S RESEARCH INSTITUTE
DECEMBER 2021

THE UNIVERSITY OF TRANS-DISCIPLINARY HEALTH SCIENCES AND TECHNOLOGY

Private University Established in Karnataka by ACT 35 of 2013

BENGALURU - 560064

CERTIFICATE

This is to certify that the work incorporated in this thesis **"ROLE OF RHOC IN REGULATION OF STEMNESS IN CERVICAL CARCINOMA"** submitted by Ms. Pavana Thomas was carried out under my supervision. No part of this thesis has been submitted for a degree or examination at any university. References, help and material obtained from other sources have been duly acknowledged. I hereby confirm the originality of the work and that there is no plagiarism in any part of the dissertation.

Research Supervisor

Dr. Sweta Srivastava,
Assistant Professor,
Department of Transfusion Medicine and Immunohematology,
Translational and Molecular Biology Laboratory,
St. John's Oncology Centre,
St. John's Medical College Hospital,
Bangalore-560034.

December, 2021

ABSTRACT

Cancer stem cells (CSCs) have been implicated in therapy resistance, and their sensitization is critical to achieve good prognosis. This work provides mechanistic insight into RHOC-mediated regulation of cervical CSCs. Using both cell lines and clinical specimens, it is elucidated that RHOC imparts stem-like ability by up-regulating the expression of stemness genes such as Nanog and CD49f. RHOC was found to activate ERK signalling, resulting in nuclear localization of E2F, leading to increased expression of stemness genes, like CD49f and ALDH. In the nucleus, RHOC was observed to promote DNA hypomethylation by TET2 over-expression. Mechanistically, RHOC interacted with WDR5 and increased H3K4me3 levels, resulting in activation of pluripotency genes, particularly Nanog, eventually yielding an epigenetically altered “hyper-transcriptional” cell. Overall, this work elucidates that RHOC regulates the stemness phenotype by a two-pronged mechanism, comprising of both cytosolic and nuclear means. These data cumulatively highlight the potential use of RHOC as a biomarker to predict CSC load, and positions it, along with TET2 and WDR5, as potential therapeutic targets to improve clinical outcomes.

THE UNIVERSITY OF TRANS-DISCIPLINARY HEALTH SCIENCES AND TECHNOLOGY

Private University Established in Karnataka by ACT 35 of 2013

BENGALURU - 560064

DECLARATION BY THE CANDIDATE

I declare that this thesis entitled "**ROLE OF RHOC IN REGULATION OF STEMNESS IN CERVICAL CARCINOMA**" submitted for the award of Doctor of Philosophy to THE UNIVERSITY OF TRANS-DISCIPLINARY HEALTH SCIENCES AND TECHNOLOGY, Bengaluru, is my original work, conducted under the supervision of my guide Dr. Sweta Srivastava (and co-guide, Dr. Avinash H. Udayashankara). I also wish to inform that no part of the research has been submitted for a degree or examination at any university. References, help and material obtained from other sources have been duly acknowledged.

I hereby confirm the originality of the work and that there is no plagiarism in any part of the dissertation.

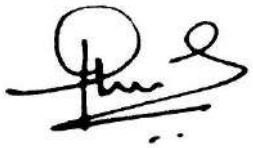

Place: Bengaluru **Signature of the Candidate**

Date: 18th December, 2021

Name of candidate: Pavana Thomas

Reg. No.: 20916020148

December 2021

ACKNOWLEDGEMENTS

Give thanks to the Lord, for He is good; His love endures forever.

-Psalm 118:1

As Ralph Waldo Emerson rightly said- "Life is a journey, not a destination". Multiple individuals have contributed towards my journey so far, and I would like to use this opportunity to express my heartfelt gratitude.

Firstly, my guide, Dr. Sweta Srivastava. Over the years, Dr. Sweta has morphed from someone we used to tip-toe around (and even suppress our sneezes!) to a mentor and even a confidant. Sweta Ma'am has been by my side at every step of the way- teaching, guiding, correcting, tough when necessary, but always understanding. She has been so forthcoming that I would never hesitate to check and recheck the minutest of doubts regarding experiments or anything else. This approachable nature also encouraged me to discuss my results and obtain feedback on a highly regular basis, which helped accelerate my output to an enormous extent. Right from all the "CLOSE THE DOOR!" sessions during which I got an earful for "Not reading enough", to those (extremely) rare occasions where I would get to hear a subtle "Good Pavana" (that was just enough to show that she was pleased with the effort, but also made sure that I did not get complacent), every moment has been etched into memory. Dr. Sweta has shown immense faith in me and my capabilities (often making me wonder why), and has chosen to trust and believe in me even in the most trying situations, when most people would have chosen the convenient way out. Apart from science, interactions with Dr. Sweta over the past few years has made me comprehend the unpleasant side of the world, all the while protecting me from the onslaught of the same until she was certain that I was capable of handling it on my own. Right from understanding scientific concepts, to designing experiments, to managing grants (and even haggling with vendors!), Dr. Sweta has taken the time and effort to train and guide me in every possible sphere. She has always stood by my side and encouraged me to try my hand at every possible scientific technique that could be explored to prove my point. Failure was never a deterrent; instead, it was always considered a stepping stone towards success that was (more often than not) waiting just around the corner. As they say, the darkest hour of the day is just before dawn, Dr. Sweta has inculcated in me the will to try umpteen routes and never ever give up until I see light at the end of the tunnel. I am indebted to Dr. Sweta for the knowledge and experiences she has imparted (scientific and otherwise) and I now realize that my mother was

right- I should be thanking the Almighty every single day for blessing me with a guide like Dr. Sweta. I could not have been luckier...!

I am grateful to my Doctoral Advisory Committee (DAC) comprising of Prof. Hosahalli Subramanya (Director, Institute of Bioinformatics and Applied Biotechnology, Bangalore), Dr. Avinash H Udayashankara (Assistant Professor, Department of Radiation Oncology, St. John's Medical College Hospital, Bangalore) and Prof. Amit Kumar Mandal (Clinical Proteomics Unit, SJRI). Prof. Subramanya has been encouraging, kind, insightful, and his scientific comments have contributed immensely towards building my project. He has always taken time out of his extremely busy schedule to discuss my work, and has put me in touch with multiple scientists on his team in order to help me achieve the objectives outlined in my thesis. Dr. Avinash has been keen and highly inquisitive of my work and his clinical insights have helped me understand the disease and patient requirements better. He has greatly helped in clinical sample accruement which has helped me validate my findings with patient specimens. The proteomics lab headed by Dr. Mandal has been of tremendous help in training me with the 2D electrophoresis. Dr. Mandal has always made sure that the equipment in his lab was made available to me for the numerous standardizations and the final gel runs. Sir has also willingly and patiently listened to my work presentations and given me valuable inputs that have helped me approach my research question better. My DAC members have been a constant source of support and encouragement over the past few years and I am immensely thankful to them for that.

I would not be who I am today if not for my parents. I have been fortunate to have Mrs. Annie Thomas and Major V Thomas Xavier as my Ma and Pa. From the moment I was born, my mother resolved to ensure that I would never be left wanting for love and attention. That I be financially independent when I became an adult was of utmost importance to her. Towards this end, Ma has read my text books, underlined the portions she felt were important, prepared question papers, revised and re-revised with me (to a point where she knew the subject better than I did!), all the while enduring the horrible tantrums I used to throw when forced to read the topics that I found boring. Every subject has a specific way that it should be approached- and Ma was brilliant at making sure that I learnt it exactly in the way it should be. Every concept was drilled into me with utmost clarity. Accolades and recognition in the academic's arena followed, but pride was close on its heels. All this while, Ma was in the background, constantly toiling and braving the odds. I now realize that with training like that, ANYONE would have

succeeded academically. I was only fortunate enough to be the recipient of the same. In fact, looking back, it was Ma who was more deserving of all the attention that was directed towards me. I was too naïve to realize it back then, I realize it now. I will forever be indebted to her. My father, a retired army officer, has also been instrumental in my up-bringing. I was never made aware of the difficulties we faced financially. If I ever asked for a book, an original, unblemished version of the book in mint condition would be on my table the very next day, no questions asked. I was never made aware of the burden of responsibilities that he perpetually carried on his shoulders. Instead, Pa would often try to lighten the mood with his humour (often misguided and amusing to him alone!). In a world where it is becoming increasingly difficult to survive under the weight of societal expectations, my parents have allowed me to carve my own path and build a career of my choosing. While some individuals of my generation (surprisingly, mostly male!), seem to be extremely worried about my impending nuptials, my parents have been a constant source of support, and have always maintained that my happiness is of utmost importance. They are in every sense the "coolest" parents ever, and I hope to inherit at least a tiny fraction of this "coolness" when I am their age! Thank you, Ma and Pa, for everything!

My fellow labmates have contributed in many ways to my growth. Mr. Shankar Rao Patil has been instrumental in training me with basic techniques in Molecular Biology and Cell Culture. Right from lessons on how to hold a pipette, he has been extremely patient with me and I owe my bench skills to him. Ashwini, Liz, Dhanya, Deepak, Katte, Lynn, Srinag, Lokendra, Yashaswini, Mugdha, Shikha, Annapurna, Pratyusha, Simanti, Harini, Ayesha, Chirag, Suraj, Ashwin, Sarah, Bisma, Krishnapriya, Ranjana, Roopy, Savitha, Amul, Jane, Binta, Vishal, Haritha, Swagatika, Sohan, Deepika, Bhavani, Shristi, Swati, Sawani and Samyuktha- I have learnt a lot from all of you and I cherish the wonderful times that we spent together. Though the trajectories of life may have taken us in different directions, I am extremely glad that our paths crossed at some point and that I got to know each of you personally. The laughter and the tears shed (mostly from laughing!) will be remembered fondly.

Apart from my labmates, I have been blessed with friends who have encouraged me every step of the way. A special mention to Ashwini, Babitha, Kavya and Yashaswini. Thank you for the innumerable bouts of laughter, which would more often than not leave people around us wondering if we were okay. But most of all, thank you for refraining from asking the most dreaded question- When are you finishing your PhD??

This work would not have been possible if not for the support from various departments across the campus. I would like to thank Dr. Nirmala Srikantia, Head, Department of Radiation Oncology for allowing us to use the linear accelerator for the radiation experiments. I am also extremely grateful to her entire team- Ms. Shibina N, Mr. K Ravindra Babu, Mr. Niranjan Immanuel and Mr. R.P Kathiressan, for help with the radiation experiments. They have carved out time to schedule my experimental work along with the patient appointments that continue incessantly throughout the day. I would specifically like to mention Mr. Ravindra, who has generously volunteered on multiple occasions to stay beyond working hours so that my radiation experiments could be completed. Thank you!

I would like to extend my gratitude to Dr. Tony Raj (Dean, SJRI) and Dr. George D'souza (Dean, SJMC) for their support. I would also like to thank Ms. Geetha K.P and Ms. Riya Francis from the Accounts Department, Ms. Ramya Mohan from the Grants Office, Ms. Lincy Thomas and Mr. Alen Babu from HR, Secretaries- Ms. Vanaja and Ms. Cynthia, Mr. Venu and Mr. Prakash for help with the documentation work, raising of purchase orders and clearing of bills. Smooth functioning of labs would not be possible without your help. I would also like to thank Mr. Ravi Kumar, Assistant Registrar (Academics), The University of Trans-Disciplinary Health Sciences and Technology, for his easy accessibility, prompt responses, patience and immense help with the paperwork.

I would like to thank all the patients who have volunteered to give a portion of their biopsies towards this work. Your contribution today will hopefully help in understanding the workings of this dreadful disease tomorrow.

I would like to thank the Council for Scientific and Industrial Research (CSIR), which has provided me with a fellowship during the course of my Ph.D. I would also like to thank the Department of Science and Technology (DST), Department of Biotechnology (DBT) and Rajiv Gandhi University of Health Sciences (RGUHS) for funding this work.

It would be apt to say that numerous people have had a role to play in the work that has been presented in this thesis. It is possible that I may have missed mentioning a few names, but this omission is purely due to oversight alone. The contribution of every individual is highly appreciated and will be warmly remembered.

Acharya Chanakya, one of the great scholars of ancient India, famously said- “Learn from the mistakes of others, you can’t live long enough to make them all yourselves!”. Going by the success rate of my experiments, I seem to have made mistakes that could last not one, but two lifetimes! However, the process of falling, getting up and moving forward has been highly rewarding and fruitful and I hope to put these experiences to good use in the future.

“For I know the plans I have for you, declares the Lord, plans for welfare and not for evil, to give you a future and a hope.”

-Jeremiah

CONTENTS

List of Tables

List of Figures

List of Acronyms

Acronym	Expansion
5mC	5-methyl cytosine
ABCG	ATP-binding cassette super-family G
AICDA	Activation-induced cytidine deaminase
Akt	Ak strain transforming
ALDH	Aldehyde dehydrogenase
AML	Acute Myeloid Leukaemia
ASH2L	Absent, small, homeotic disks-2-like
ASIR	Age-standardized incidence rate
ASMR	Age-standardized mortality rate
ATF2	Activating Transcription Factor 2
Atorva	Atorvastatin
AV	Aloe vera
BCA	Bicinchoninic acid
BCSC	Breast cancer stem cell
BER	Break-excision repair
bFGF	Basic fibroblast growth factor
BLAST	Basic Local Alignment Search Tool
BP	Biological processes
BSA	Bovine serum albumin

CAD	Caspase activated DNase
CC	Cytoplasmic component
CDK2	Cyclin-dependent kinase 2
c-EBPα	CCAAT enhancer-binding protein alpha
CENP-A	Centromere protein A
CF	Cytosolic fraction
CF	Cytosolic fraction
CHAPS	3-[(3-cholamidopropyl)dimethylammonio]-1-propanesulfonate
ChIP	Chromatin immunoprecipitation
ChIP-qPCR	Chromatin immunoprecipitation quantitative PCR
CML	Chronic Myelogenous Leukaemia
CML	Chronic Myelogenous Leukemia
CREB	cAMP response element-binding protein
CSCs	Cancer Stem Cells
CTCs	Circulating Tumour Cells
DAPI	4′,6-diamidino-2-phenylindole
DFF	DNA Fragmentation Factor
DMEM	Dulbecco's Modified Eagle Medium
DMSO	Dimethylsulfoxide

DNA	Deoxyribonucleic Acid
DNMT	DNA methyltransferase
dNTPs	Deoxynucleoside triphosphates
DSB	Double-strand break
DSP	Dithiobis Succinimidyl Propionate
DTT	Dithiothreitol
Dvl2	Disheveled2
ECM	Extracellular Matrix
EDTA	Ethylenediamine tetraacetic acid
EMT	Epithelial to Mesenchymal Transition
ERK	Extracellular-signal-regulated kinase
ESI Q-TOF	Electrospray ionization Quadrupole-Time-of-Flight
EtOH	Ethanol
FACS	Fluorescence-activated Cell Sorting
FAK	Focal adhesion kinase
FBS	Foetal Bovine Serum
FPKM	Fragments Per Kilobase Million
FPP	Farnesylpyrophosphate
FSG	Fish Skin Gelatin
GAPDH	Glyceraldehyde 3-phosphate dehydrogenase

GDP	Guanosine Diphosphate
Gli1/2	Glioma-associated oncogene
GO	Gene Ontology
GPP	Geranylgeranylpyrophosphate
GTP	Guanosine Triphosphate
H3	Histone3
H3K4me3	Trimethylation of lysine 4 on histone 3
HBSS	Hank’s Balanced Salt Solution
HDAC	Histone Deacetylase
HDAC	Histone deacetylase
HDI	Human Development Index
HDM	Histone Demethylase
Hes1	Hairy and enhancer of split-1
HIV	Human Immunodeficiency Virus
HMG-CoA	β-Hydroxy β-methylglutaryl-CoA
HMT	Histone Methyltransferase
HNSCC	Head and neck squamous cell carcinoma
HPLC	High performance liquid chromatography
HPV	Human Papilloma Virus
HR	Homologous recombination
IBC	Inflammatory breast cancer

IFNK	Interferon Kappa
IHC	Immunohistochemical
IKKβ	Inhibitor of nuclear factor kappa-B kinase subunit beta
IL	Interleukin
IP	Immunoprecipitation
iPSC	Induced pluripotent stem cell
IQGAP-1	IQ-domain GTPase activating protein 1
JAK/STAT	Janus Kinase/Signal Transducer and Activator of Transcription
KMT	Lysine methyltransferases
LD	Lethal dose
LEF1	Lymphoid Enhancer Binding Factor 1
LIF	Leukemia Inhibitory Factor
MAPK	Mitogen-activated protein kinases
miRNA	Micro Ribonucleic Acid
MLC	Myosin Light Chain
MLL	Mixed lineage leukemia
MMLV-RT	Moloney Murine Leukemia Virus-Reverse Transcriptase
MMPs	Matrix Metalloproteases
MPI	Multi-protease inhibitor

mRNA	Messenger Ribonucleic Acid
MS	Mass spectrometry
MS/MS	Tandem Mass Spectrometry
MTT	3-(4,5-dimethylthiazol-2-yl)-2,5-diphenyltetrazolium bromide
Na_3VO_4	Sodium orthovanadate
NaCl	Sodium chloride
NaF	Sodium fluoride
NF	Nuclear fraction
NF-κβ	Nuclear Factor kappa-light-chain-enhancer of activated B cells
NHEJ	Non-homologous end joining
NOD/SCID	Nonobese diabetic/severe combined immunodeficiency
OCSC	Ovarian cancer stem cells
OCT4	Octamer-binding transcription factor 4
PBS	Phosphate buffered saline
PCR	Polymerase chain reaction
PFA	Paraformaldehyde
PI3K	Phosphoinositide 3-kinase
PMN	Pre-Metastatic Niche
PMSF	Phenylmethylsulfonyl fluoride

POLA2	DNA Polymerase Alpha 2, Accessory Subunit
POSTN	Periostin
PTCH1	Patched 1
PTEN	Phosphatase and tensin homolog
qPCR	Quantitative real time polymerase chain reaction
RANK	Receptor Activator of NF-κβ signalling
RbBP5	Retinoblastoma-binding protein-5
Rho	Ras homologous
RhoGAPs	Rho GTPase Activating Proteins
RhoGDIs	Rho Guanine Dissociation Inhibitors
RhoGEFs	Rho Guanine Exchange Factors
RNA	Ribonucleic Acid
ROCK	Rho-associated protein kinase
SAM	S-adenosyl-L-methionine
SCC	Squamous Cell Carcinoma
SCJ	Squamous Columnar Junction
SCR	Scrambled siRNA
SDS	Sodium dodecyl sulfate
SET	Su(var)3-9, Enhancer-of-zeste and Trithorax
SHH	Sonic hedgehog
siRNA	Small interfering RNA

SOX2	SRY (sex determining region Y)-box 2
SP	Side-population
Ta	Annealing Temperature
TAE	Tris-acetate-EDTA
TBE	Tris-borate-EDTA
TBS	Tris buffered saline
TCF-4	Transcription Factor 4
TET	Ten Eleven Translocation
TET	Ten eleven translocation dioxygenases
TGF-β	Transforming growth factor beta
Tm	Melting Temperature
VEGF	Vascular endothelial growth factor
WDR	WD repeat-containing protein
Wnt	Wingless-related integration site
WST	Water Soluble Tetrazolium Salt (4-[3-(4-Iodophenyl)-2-(4-nitro-phenyl)-2H-5-tetrazolio]-1,3-benzene sulfonate)
wtR	Wild-type RhoC

CHAPTER-I

Introduction

1.1 Cervical Cancer

According to the Global Cancer Observatory Database, cervical cancer is the 4th most common cause of cancer affecting women in the world today after breast, lung and colorectal cancers (Globocan 2020). There have been approximately 570,000 fresh cases and 311,000 deaths due to cervical cancer in 2018 alone. The global age-standardized incidence rate (ASIR) for cervical cancer is 13.1 per 100,000 whereas the age-standardized mortality rate (ASMR) stands at 6.9 per 100,000 (Arbyn et al., 2020). Developing countries have been observed to bear the maximum burden of the disease, contributing to more than 85% of cervical cancer incidences. China and India alone account for a third of the global incidences of the disease, and 35% of global deaths due to cancer of the cervix (Arbyn et al., 2020). **Figure 1.1** is a representation of the global incidence and mortality due to cancer of the cervix, with regions in Africa, Asia and certain parts of South America observed to be among the most affected.

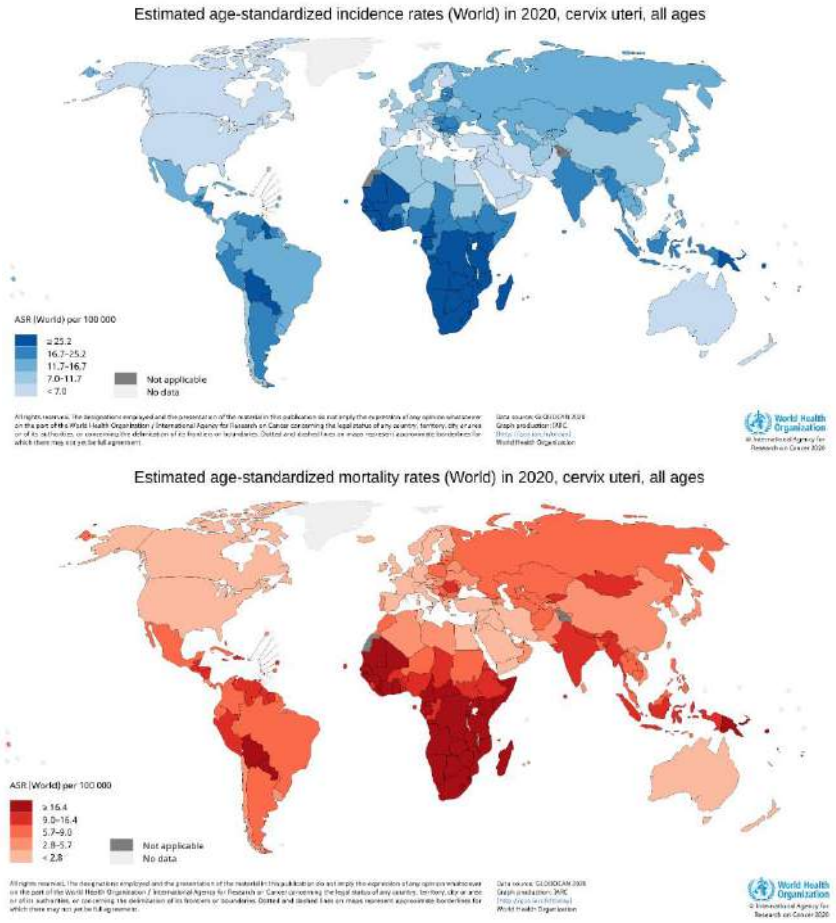

Figure 1.1: Distribution of ASIR (in blue) and ASMR (in red) of cervical cancer in 2020 as per WHO.

The Human Development Index (HDI), is a numerical value assigned to countries for overall progress in key aspects of human life by accounting for numerous factors that affect health, education and standard of living. Analysis of cervical cancer incidence and mortality rates on the basis of HDI, revealed a stark contrast between countries classified under the high HDI category and those in the lower rungs. The ASIR and ASMR for cervical cancer among the low HDI countries was found to be 26.7 per 100,000 and 20 per 100,000 whereas the very-high HDI group of countries exhibited an ASIR and ASMR of 9.6 per 100,000 and a meagre 3 per 100,000 respectively (Globocan 2020). Further, cervical cancer was found to be the primary cause of death due to cancer in 42 countries that comprise the low-HDI group, whereas it was only the 19th cause of cancer mortality in Finland, a country belonging to the high HDI tier (Arbyn et al., 2020). As per 2020 data, India's HDI stands at 0.645, ranking our country at a dismal 131 amongst 189 countries globally. **Figure 1.2** depicts the stark difference in cervical cancer incidences in low HDI and high HDI countries. Cervical cancer is the second most common cancer occurring in women in low and medium HDI countries (the most common being cancer of the breast). It drops significantly in high HDI countries occupying the 5th position among the most common malignancies, while not even appearing in the top 7 cancers affecting individuals in countries with very high HDI.

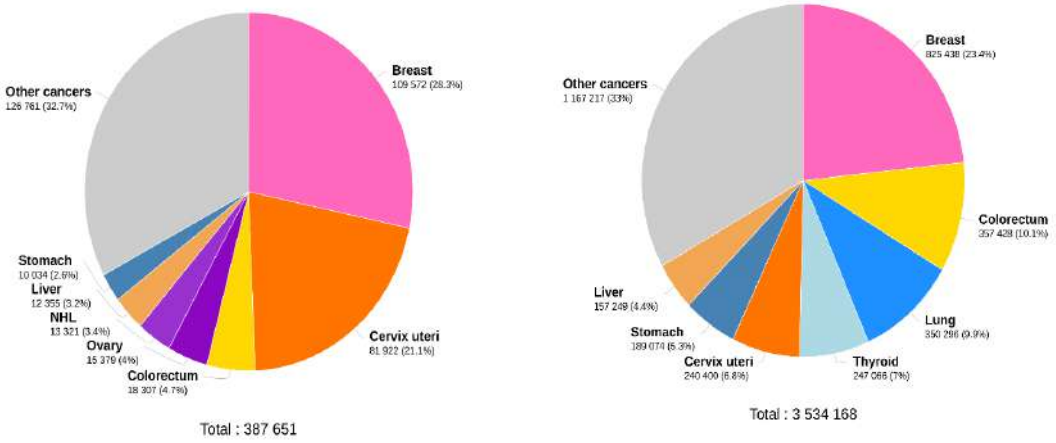

Figure 1.2: Pie chart representation of the percentage of cancer incidence in low (left) and high HDI countries (WHO, 2020).

Infection by the Human Papilloma Virus (HPV) has been identified as the main etiological factor contributing to cervical cancer incidences, with nearly 99% of cervical cancer patients found to have detectable levels of HPV DNA. Other factors include sexually-transmitted

infections like HIV (Human Immunodeficiency Virus), *Chlamydia trachomatis*, smoking and regular use of oral contraceptives. Papillomaviruses are ubiquitously present and have been known to be responsible for the development of epithelial lesions in rabbits and cows, apart from humans. The role of papillomaviruses as oncogenic agents was first reported in rabbits in the year 1933 (Shope and Hurst, 1933). HPV comprises of the following components:

a) dsDNA (nearly 8000 bp in length)

b) Viral proteins (classified into early and late proteins)

Based on the gene products, the HPV genome is organized into the following segments-a) E- Early genes b) L- Late genes c) LCR- Long control region/NCCR- Non-coding region/URR- Upstream regulatory region.

The Early genes are responsible for viral replication and cancer-initiation in the host, whereas the Late genes encode for the structural viral capsid proteins. **Figure 1.3** is a diagrammatic representation of the organization of the HPV genome.

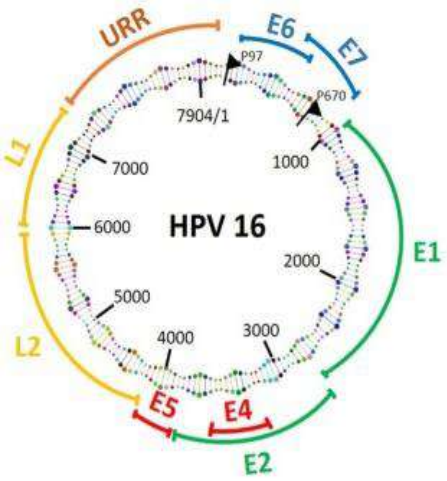

GENES	ACTIVITY
L1	Major Capsid protein
L2	Minor Capsid protein
E1	Replication of Viral genome and its maintenance
E2	Initiation of viral DNA replication; regulates transcription of E6 and E7
E4	Release of viral particles
E5	Enhances growth factor signaling pathways
E6	Inhibits p53 and causes loss in cell cycle regulation
E7	pRb mediated deregulation of cell cycle

Figure 1.3: Organization of the HPV 16 genome (Pal and Kundu, 2020).

The 5’ end of the genome begins with the early coding region comprising of 6 genes- E1, E2, E4, E5, E6 and E7. While E1 and E2 regulate replication and transcription of viral DNA, E5-E7 are responsible for the deregulation of various signalling pathways and checkpoints in the host that eventually lead to oncogenesis. E4 is deemed to be involved in viral release and transmission (Doorbar, 2013). E2 is a transcriptional regulator that modulates the expression of E6 and E7 genes. Integration into the host DNA disrupts E2, thereby leading to uncontrolled

increase in transcription of E6 and E7 proteins. The E6 and E7 proteins bind to and lead to consequent degradation of the tumour suppressors p53 and Rb. E6 and E7 therefore play vital roles in alteration of host gene expression and release of cells from cell-cycle checkpoints resulting in carcinogenesis. **Figure 1.4** represents the mechanism of oncogenesis post HPV infection.

Figure 1.4: Mechanism of oncogenic transformation by HPV (Pal and Kundu, 2020).

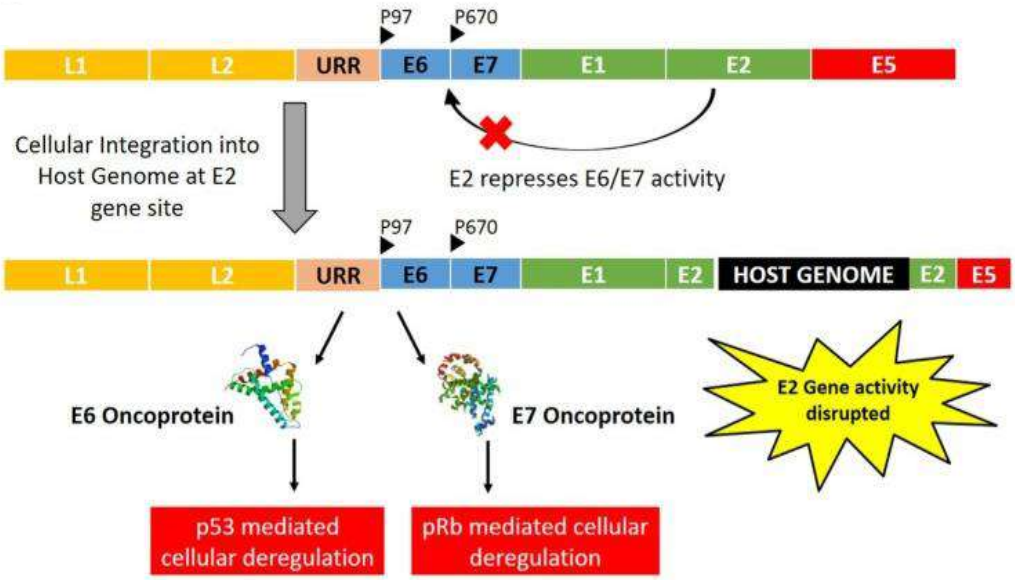

Currently more than 100 types of HPV have been identified. Of these, 35 have been found to be associated with cancers of the anogenital epithelium including that of the cervix, vulva, vagina, rectum and penis. The others have been known to cause benign (warts) as well as malignant skin lesions. Based on the propensity of these HPV types to cause invasive cancer, they have been divided into high-risk and low-risk categories. The high-risk types include 16, 18, 31, 33, 35, 39, 45, 51, 52, 56, 58, 59, 68 and 70. The low-risk HPVs are 6, 11, 42, 43 and 44. Most HPV infections are cleared by the immune system. However, based on the HPV genotypes and intrinsic host factors, some infections may lead to the development of invasive

cancers over the course of a few decades. **Figure 1.5** depicts the several stages of HPV infection and parallel progression of the disease.

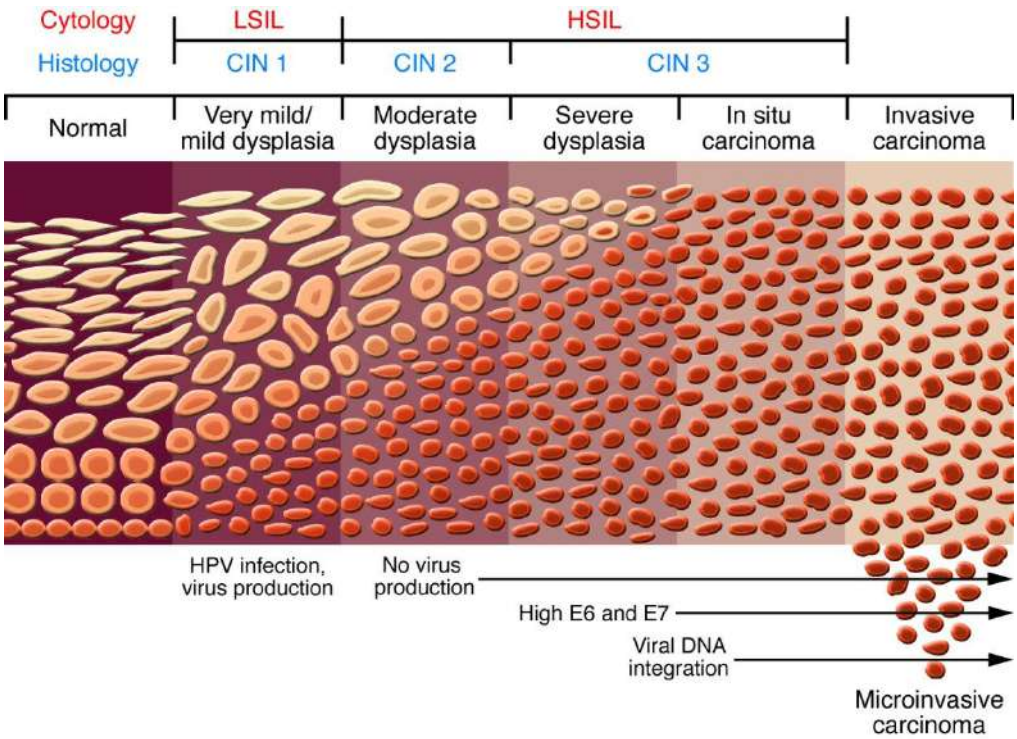

Figure 1.5: HPV infection and cervical cancer progression (Lowy and Schiller, 2006).

HPV infection occurs mainly at the Squamous Columnar Junction (SCJ), the region between the ectocervix and endocervix. These cells are most susceptible to HPV infection, thereby making cancer of the cervix more common than vaginal cancers despite the presence of HPV in the vagina. Post infection in the cellular transformation zone or SCJ, pre-cancerous lesions are formed, which later transforms to cancer of the invasive type. A minimum latency period of at least 7 years has been observed between infection and cancer diagnosis. **Figure 1.6** diagrammatically represents the female anatomy and the location of the transformation zone.

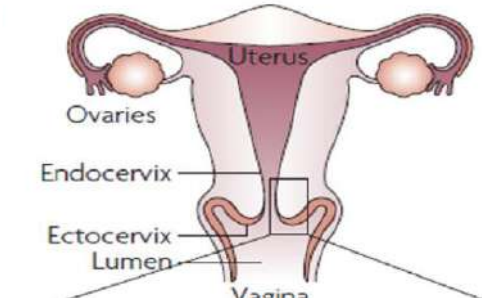

Figure 1.6: A diagram of the female reproductive system indicating the transformation zone (Suzuki et al., 2010).

Based on histology, cervical cancer can be classified into 3 broad types-

a) Squamous cell carcinoma- These develop in the epithelial cells and constitute around 90% of cervical cancer cases. They may be further classified into-

- Keratinizing
- Non-keratinizing
- Basaloid
- Verrucous
- Papillary

b) Adenocarcinoma- This cancer type develops in the glandular cells of the endocervix and constitute about 10% of identified cases. Adenocarcinomas may be categorized into-

- Mucinous
- Villoglandular
- Endometroid

- Clear cell

c) Mixed type- These are the rarest type of cervical cancer and have features of both the squamous and adeno types.

Depending on the extent of spread of the malignancy, cancer of the cervix may be divided into various stages-

Stage of the Disease		**Extent of spread**
I		Restricted to the cervix alone.
II	A	Upper two-thirds of the vagina. No spread to the parametrium.
	B	Involvement of parametrium.
III	A	Lower third of vagina. No spread to pelvic wall.
	B	Spread to pelvic wall.
	C	Involvement of pelvic and/or para-aortic lymph nodes, but no spread to distant sites.
IV	A	Spread to adjacent organs.
	B	Spread to distant organs.

Table 1.1: Stages of cervical cancer and the extent of spread (FIGO 2020).

The mode of treatment is dependent on the stage at which the disease is diagnosed. If the disease is diagnosed in Stage 1, the treatment is primarily hysterectomy, which may be followed by chemoradiation therapy. Stage 2 diagnosis is generally followed by chemoradiation therapy. This may be sometimes preceded by surgery if diagnosed in Stage 2A1. Stages 3 and 4 are treated with chemoradiation therapy, with treatment of Stage 4 disease being largely palliative.

Since the identification of HPV as the single largest cause for cancer of the cervix, multiple primary and secondary prevention strategies have been formulated. Prophylactic HPV vaccines constitute the primary prevention approach, with early evidence suggesting high efficacy of

protection against both infection and formation of pre-cancerous lesions in vaccinated individuals naïve to the infection. Currently, there are three HPV vaccines available in the global market-

- Cervarix (a bivalent vaccine against HPV strains 16 and 18).
- Gardasil (a quadrivalent vaccine against HPV types 16, 18, 6 and 11).
- Gardasil 9 (a nonavalent vaccine against HPVs 16, 18, 6, 11, 31, 33, 45, 52 and 58).

Secondary preventive methods include-

- Screening patients utilizing HPV assays.
- Treatment of pre-cancerous lesions.

Incorporation of the above into the healthcare framework of a country can result in significant improvement in cervical cancer incidences. The WHO has currently set a goal of achieving an ASIR of 4 per 100,000 by stringent adherence to primary and secondary preventive measures. However, as per 2018 data, only a fourth of girls aged below 10 years reside in the 85 countries that have made HPV vaccines available commercially. Of these, only 13% are citizens of low-HDI countries, whereas the rest constitute the high-HDI group. Further, mathematical modelling predicts that achieving the ambitious goal of an ASIR of 4 per 100,000 may be possible in a few decades in countries with ample resources at their disposal, while the less fortunate regions of the world may take up to the end of the 21st century to achieve a similar result.

Survival and disease-free recovery are heavily dependent on the stage of diagnosis. The 5-year survival rate of women diagnosed in Stage 1A1 was found to be 95.1%, whereas survival in women presenting with late-stage disease (Stage 4) was a meagre 5.3% (Jayant et al., 2016). Unfortunately, women in developing countries present with late-stage tumours, often post metastasis, eventually resulting in decreased overall survival. It must be noted that metastatic disease is widely considered incurable. It is therefore imperative to understand the molecular mechanisms at play behind spread of the disease, which could enable devising effective treatment strategies to avoid resistance and recurrence.

1.2 Cancer Progression and Theories

Cancer initiation and progression has been attempted to be explained using 3 theories -

a) Clonal Evolution Theory

This model, first proposed by Peter C Nowell in the year 1976, postulates that all cancers arise from one single aberrant cell (Nowell, 1976). The basis of the clonal evolution theory was decades of research by various groups which pointed towards a possible unicellular origin of cancer. Cells constituting the primary tumour were found to have similar genetic aberrations, indicative of the cancer originating from a single cell (Sandberg and Hossfeld, 1970). Further, homogeneous production of immunoglobulins in plasma cell tumours and activation of the same X chromosome member in all cells of a given tumour in women suggested that cancers could arise from a single clone (Linder and Gartler, 1965). According to this model, neoplastic growth is initiated by a single alteration in a cell which was previously normal, thereby providing it with certain proliferative advantages over its non-malignant precursor. This altered cell then undergoes further genetic changes on account of genomic instability, leading to "mutant clones". Most of these clones are eliminated due to unfavourable characteristics or immune surveillance. However, some clones with marked privileges serve as precursors to malignant growth. These clones are then sequentially chosen by a process of natural selection and evolution to yield cellular pools that are increasingly abnormal by virtue of both phenotypic and genetic features.

The model states that such clones may be actively proliferating or undergo a period of latency before unleashing its uncontrolled proliferative abilities. The first event that initiates the cascade has been defined as being "unrestrained" and a possible consequence of a combination of extrinsic and intrinsic factors that could remain undetectable cytogenetically. However, in certain instances they may be easily detectable as in the case of the Philadelphia chromosome in Chronic Myelogenous Leukaemia (CML). The clonal evolution model also takes into cognizance the role of the tumour microenvironment in cancer progression. It states that the rate at which the cancer develops could be attributed either to the extent of accumulation of genetic abnormalities in tumour cells or due to the "selective pressures" imposed by the tumour environment. **Figure 1.7** is a diagrammatic representation of the principle of the clonal evolution theory.

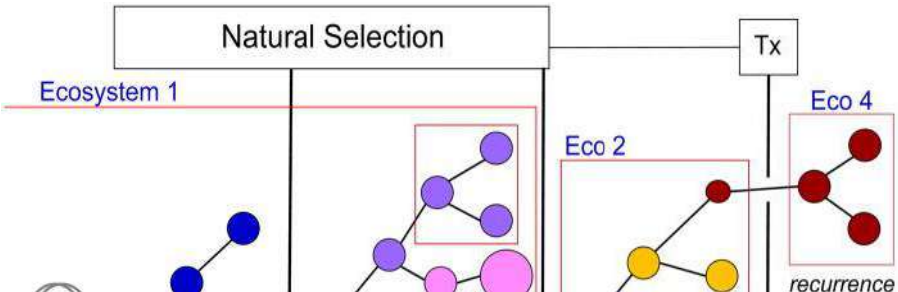

Figure 1.7: A schematic representation of the clonal evolution theory (Greaves and Maley, 2012).

b) Hierarchical/CSC model

This model emphasizes that tumour initiation and progression is solely due to the CSC population, a pool of cells that are highly potent, but miniscule in number. The model states that a hierarchical organization of tumour cells is possible based on their potential to develop tumours. Therefore, according to the CSC model, elimination of every tumour cell is not necessary to tackle the disease. Further, the model emphasizes that determination of the "fate" of a cell only (whether it can form tumours or not) is not the ideal therapeutic route since cells with tumorigenic potential may not always result in tumours owing to unfavourable microenvironments and immunogenic response (Shackleton et al., 2009). Instead, approaches that would specifically target the CSC pool could be more efficient at preventing therapy resistance and relapse.

The prediction of the "stemness status" of a cell can be made via the presence/absence of markers for stemness on tumour cells. However, the mere presence of markers on a cell is not adequate to confirm tumorigenic ability. It is highly essential for this observation to be followed with functional assays that demonstrate the ability of cells to recapitulate tumour growth (Shackleton et al., 2009). The transplantation assay of stem-like cells in NOD/SCID mice and observing for growth of tumours is the widely used approach to determine stemness capability **(Figure 1.8)**.

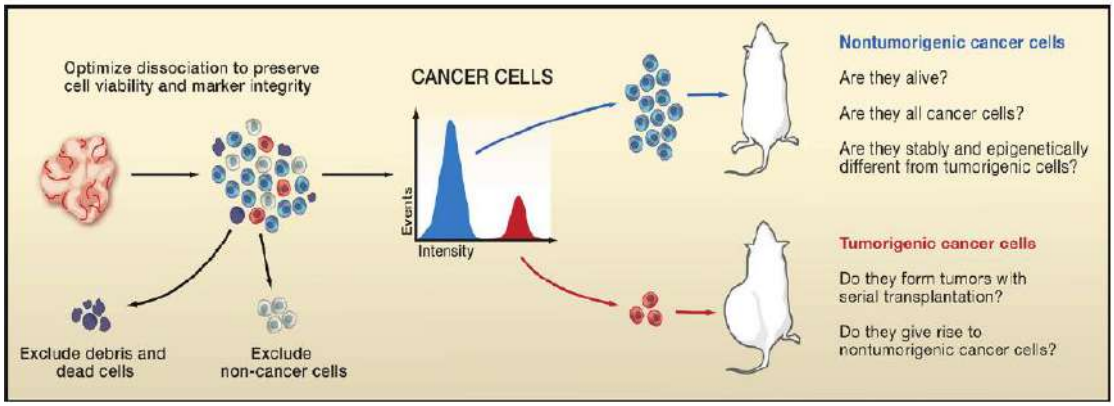

Figure 1.8: The transplantation assay for "stem-like" ability (Shackleton et al., 2009).

However, this method has been found to grossly under-estimate tumorigenic capability of cells (Quintana et al., 2008). This has been attributed to discordancy between mouse ligands and receptors on human cells. Further, most tumorigenic models involve heterotypic transplantation (at sites other than the organ of origin), which has been found to drastically decrease rates of successful engraftment. There is therefore a dire need for an ideal model that could help gain better insight and understand the mechanistic of CSC-driven tumour induction.

Cancers of the breast, brain, colon and leukaemia have been found to follow this model, while there are certain others that do not (Al-Hajj et al., 2003; Dalerba et al., 2007; Dick et al., 1997; Kelly et al., 2007; Singh et al., 2004). Currently, the widely accepted consensus is that one model of tumour formation alone cannot be completely relied on. Cancer initiation, relapse and therapy response is a highly complex, convoluted phenomenon that could be best explained by accounting for the ability of tumour cells to differentiate and dedifferentiate at will, best explained by the more recent CSC plasticity model.

c) Plasticity model

Tumours have been identified as heterogenous masses comprising of both the rapidly proliferating tumour bulk (non-CSCs) and the quiescent CSC pool. However, recent evidence has demonstrated that these two states are not mutually exclusive of each other and are in fact, dynamic cellular populations capable of inter-conversion (Chaffer et al., 2011; Chaffer et al., 2013; Quintana et al., 2010). For example, it was found that $CD133^-$ cells were capable of forming tumours in nude rats and that the resulting tumours contained $CD133^+$ cells, thereby belying the CSC model concept (Wang et al., 2008a). This plasticity has been observed to be governed by core transcriptional networks. Numerous studies have proven the integral role of transcription factors like OCT 3/4, SOX, NANOG and KLF4, and epigenetic modifications in modulation of cellular plasticity (Ben-Porath et al., 2008; Eun et al., 2017; Gu et al., 2007; Poli et al., 2018). The impact of extrinsic factors like the microenvironment on tumour cell plasticity have also been elucidated in numerous studies (Hjelmeland and Rich, 2011; Lequeux et al., 2019; Pattabiraman and Weinberg, 2014). Further, cellular plasticity has also been linked to the processes of EMT and MET, essential for metastasis. While cells undergoing EMT have previously been associated with increased stemness potential (Mani et al., 2008; Shibue and Weinberg, 2017), recent evidence has unearthed that cells that have initiated the EMT process are more "stem-like" than cells that have fully gained mesenchymal properties. Therefore, cells that represent characteristics of both the epithelial and mesenchymal type display enhanced stemness characteristics as compared to those that are closer to either the epithelial or mesenchymal states (Jolly et al., 2018). **Figure 1.9** is an overview of the plasticity model.

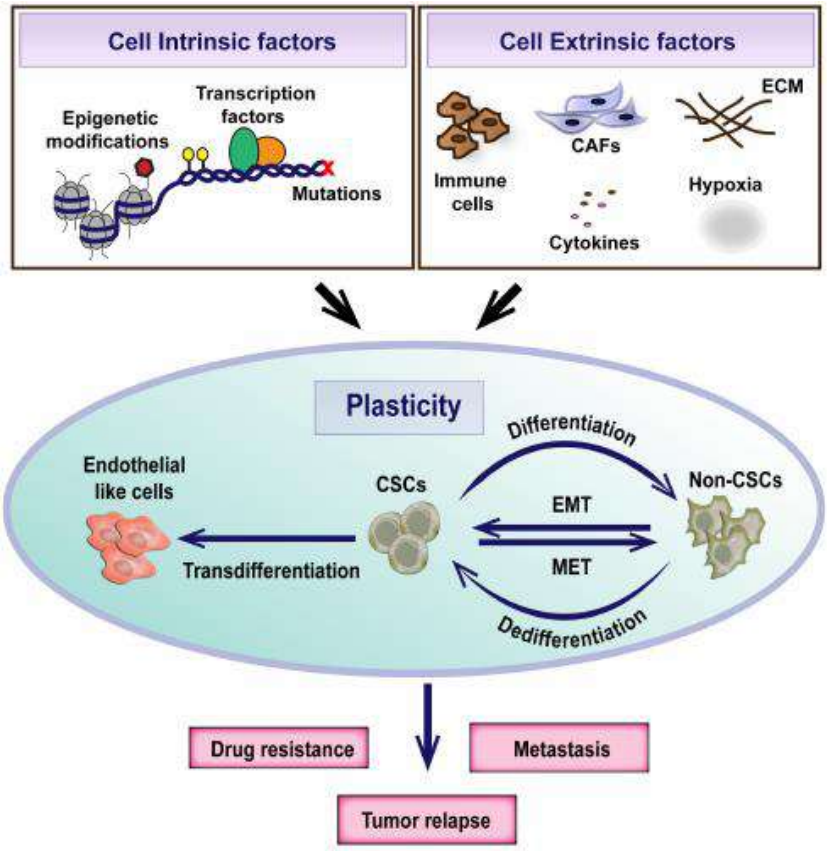

Figure 1.9: The plasticity model of tumour initiation and progression (Thankamony et al., 2020).

This model therefore reiterates that CSC and non-CSC states are fluid, with cells capable of transitioning between these two states, governed by intricate transcriptional networks and microenvironmental factors. This poses enormous challenges to the scientific community, making the study of CSCs and the identification of mechanisms of CSC maintenance, the key to effective therapy.

1.3 Metastasis

Metastasis may be defined as the spread of cancerous cells from the primary site to neighbouring or distant organs (Seyfried and Huysentruyt, 2013). Till date, metastatic disease is the principal cause for cancer mortality, accounting for nearly 90% of cancer-related deaths worldwide (Chaffer and Weinberg, 2011). Around 4 million cells are believed to be shed per gram of tumour on a daily basis, of which only 0.01% form metastases (Fidler, 1970). This

can be attributed to the highly demanding and dynamically changing environments that tumour cells must endure to detach from the primary organ and colonize at a secondary, distant site. The metastatic cascade can be sequentially categorised into 5 steps- invasion, intravasation, circulation, extravasation and colonization. Each of these processes is governed by tightly regulated molecular mechanisms and signalling pathways. A schematic representation of the overall metastatic cascade has been outlined in **Figure 1.10**.

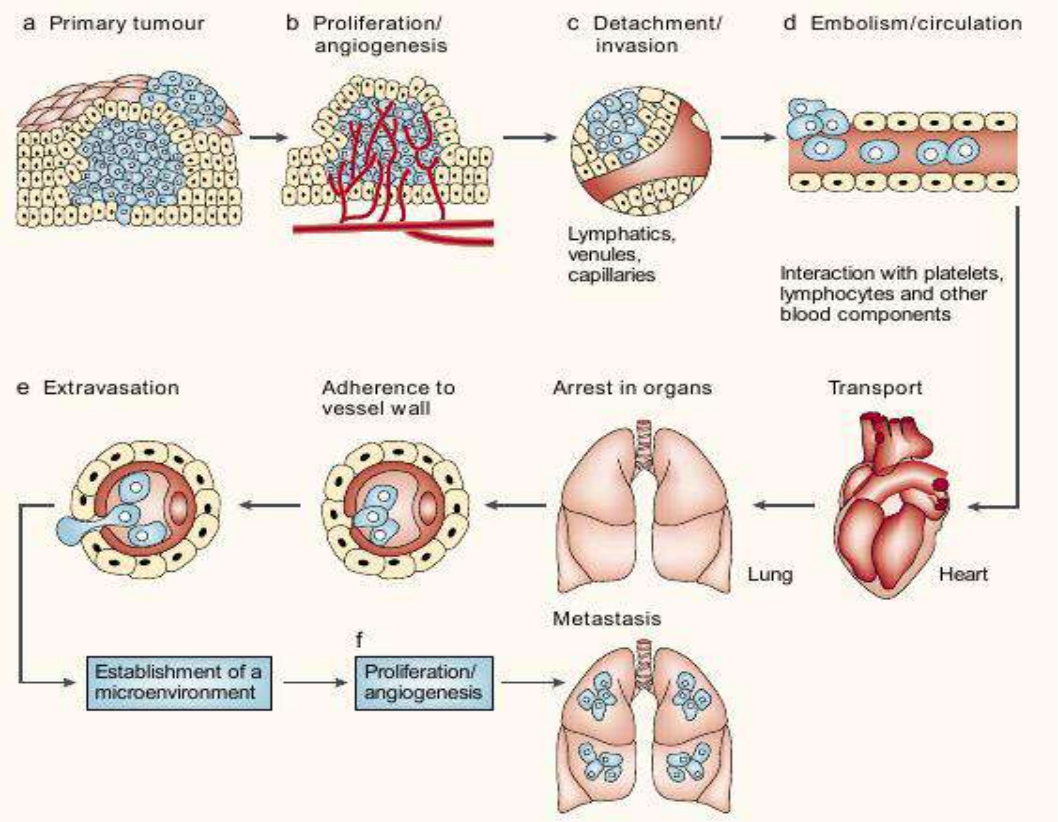

Figure 1.10: The metastatic cascade (Fares et al., 2020).

a) Invasion-

The first step towards establishment of a distant tumour outgrowth is detachment from the primary tumour and invasion through the basement membrane. Epithelial cells are characterised by rigidity and high affinity to the surrounding extracellular matrix (ECM) components. An epithelial cell must therefore undergo epithelial to mesenchymal transition (EMT) and imbibe mesenchymal properties of motility and invasion in order to disseminate from the primary organ. Emerging evidence now suggests that epithelial and mesenchymal

states are not binary choices (Nieto et al., 2016). They are in fact, stages that a cell transitions through, with cells marked by a combination of both epithelial and mesenchymal characteristics being found to be the most effective at forming distant metastases (Pastushenko et al., 2018). The EMT process involves progressive loss of epithelial markers like EpCAM and E-cadherin and gain of mesenchymal markers like vimentin (Pastushenko and Blanpain, 2019).

Additionally, remodelling of ECM components like proteoglycan, collagen, laminin and fibronectin via matrix metalloproteases (MMPs) constitutes a major step of tumour invasion and dissemination. MMPs are zinc-dependent endopeptidases that utilize specific ECM proteins as substrates, allowing invading cells to tunnel through the matrix and finally breach the basement membrane (Gialeli et al., 2010). This breach of the basement membrane heralds the transition from a benign *in-situ* growth to an invasive carcinoma.

b) Intravasation-

Intravasation involves movement of tumour cells into the bloodstream by breaching the endothelial lining. This may occur actively or passively (Bockhorn et al., 2007). Active intravasation constitutes directed movement of tumour cells following a gradient of chemokines and aided by pro-inflammatory factors. In this scenario, tumour cells follow a similar method of invading the bloodstream as immune cells, i.e by diapedesis.

Passive intravasation occurs as tumour cells shed into blood vessels that support the tumour. These vessels are leaky and allow for easy movement of cells across them. The process may also be mitosis-driven, with dividing cells along the periphery of the endothelium leading to disruption of the endothelial membrane and consequent systemic circulation (Wong and Searson, 2017).

c) Circulation

Cells that have intravasated into blood vessels are termed as circulating tumour cells (CTCs). CTCs travel either via the bloodstream or the lymphatic system. They may move as single cells or as clusters in association with other CTCs, stromal cells, immune components and platelets. Platelets serve as a shield around the CTC cluster and protect them from being recognized by immune cells. They also double up as a mechanical structure, protecting the clusters from the

shear stress encountered during circulation (Gay and Felding-Habermann, 2011). As a consequence, CTC clusters have been found to be more efficient at forming metastases in comparison with single-cell CTCs (Aceto et al., 2014).

Importantly, CTCs must be capable of enduring detachment, anoikis and other harsh conditions prevalent in circulation. The survival and ability to extravasate at secondary sites rely heavily on the interactions between the CTCs and the immediate circulatory components. CTCs are known to be influenced by chemokine and cytokine gradients, which continuously direct their movement through the vasculature towards a favourable metastatic niche (Bonecchi et al., 2009). In addition to this, shear forces exerted by blood flow also dictate sites at which CTCs would eventually home into. Regions of the endothelium where shear force exceeds the adhesive capacity of CTCs have been observed to have greater incidences of extravasation (Follain et al., 2018). Therefore, homing is influenced by both microenvironmental and mechanical factors.

d) Extravasation

As CTCs travel through minute capillaries, they become entrapped. Once stagnant, CTCs would either divide and move into tissue via microvascular rupture or be forced to undergo transendothelial migration (van Zijl et al., 2011). This process is controlled by ligand-receptor interactions, chemokine gradients and other circulating non-tumour cells (Reymond et al., 2013). Integrins on the CTC surface determine the specific site of extravasation. The liver and bone, which consist of highly permeable sinusoidal vessels, have been observed to have higher rates of metastasis than other organs which are protected by tight basement membranes (Fouad and Aanei, 2017). Extravasation into these organs would require mediation of genetic and molecular mechanisms. It has been observed that CTCs from certain primary tumours have a propensity to extravasate into specific organs in the body. This phenomenon came to be known as metastatic organotropism (Langley and Fidler, 2011). For example, breast and lung cancers preferentially home into bones, whereas cancers of the pancreas and colon metastasize majorly into liver tissues.

e) Colonization

Secondary sites of metastasis are not a passive choice. In fact, scientific evidence proves that the primary tumour primes probable secondary sites even prior to the initiation of the metastatic process (Peinado et al., 2017). The process involves extracellular vesicles, secretory factors, immune-suppression and ECM remodelling, together forming a suitable microenvironment for the homing of CTCs. This tailored microenvironment is known as the pre-metastatic niche (PMN). Cancer cell-host interactions and exosomes carrying mRNA or miRNA are therefore instrumental in "educating" the PMN to favourably receive CTCs (Peinado et al., 2011).

Once CTCs home into distant favourable niches, they may proliferate or remain dormant for years on end. This observed dormancy after invasion into secondary sites may be attributed to delayed acclimatization to the microenvironment or an inherent dormancy signature ascribed onto these cells prior to dissemination from the primary tumour. Such cells are characterized by decreased WNT signalling, increased stemness signatures and weak expression of extracellular antigens to enable evasion of immune response. This is maintained by an intricate balance between ERK and p38 signalling pathways **(Figure 1.11)**. While dormancy is marked by up-regulation of the p38 pathway and suppression of ERK signalling, tumour cells are "woken up" or reactivated by enhanced ERK signalling and reduced p38 mediated molecular pathways.

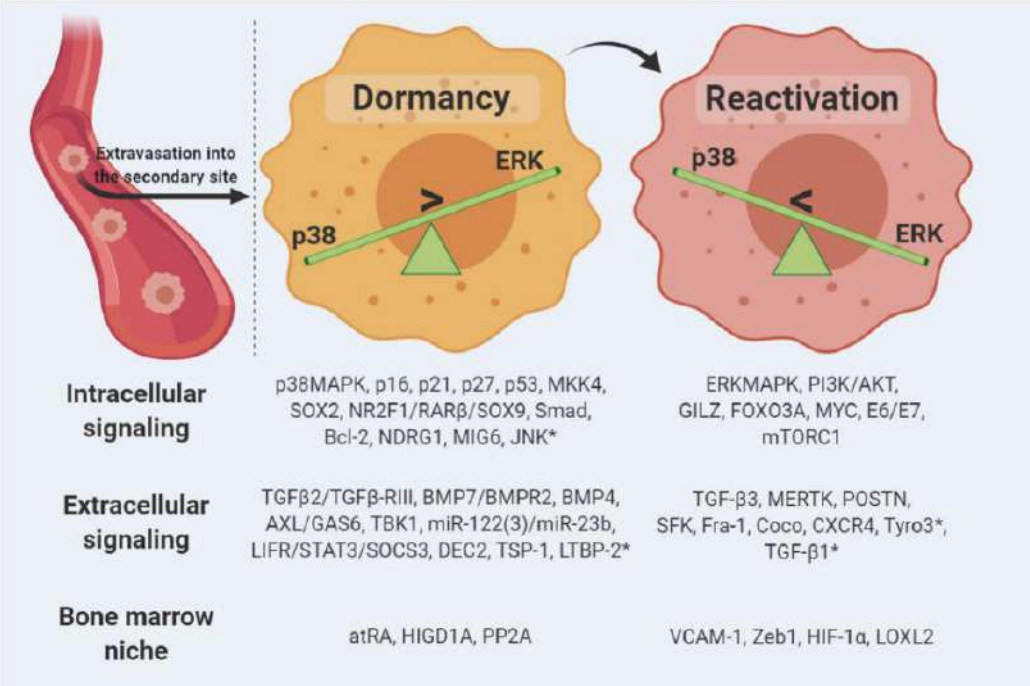

Figure 1.11: The fine balance between dormancy and proliferation (Fares et al., 2020).

Over the centuries, two basic models of metastasis have come to the fore-

a) Seed and Soil Model

Proposed first by Stephen Paget in 1889, after examining 735 post mortem data of women with breast cancer, the theory suggests that distribution of metastases is not a random process. Akin to budding of plants, Paget hypothesised that successful metastasis requires favourable interactions between CTCs (the "seed") and their microenvironment (the "soil") (Paget, 1889). This theory was later proved by multiple scientists. A report by Kinsey in 1960 described how metastatic melanoma cells specifically metastasized into normal lung and ectopically placed lung tissue only (Kinsey, 1960). Our understanding of metastatic disease today reiterates the concepts proposed by Paget's work, with growth, survival, angiogenesis and colonization known to be influenced by both CTCs and the metastatic niche. However, this work was met with criticism in the immediate decades following this hypothesis.

b) Anatomical/Mechanical Model

James Ewing strongly contested Paget's theory. In the year 1928, Ewing suggested that tumour dissemination and colonization is dictated purely by circulation. He postulated that metastasis was a random process governed by direction of blood flow. According to Ewing's theory, tumour cells would follow the circulatory route and non-specifically colonize in the first organ encountered. For example, gastrointestinal tumours colonize mainly in the liver since the hepatic portal venous system is the first complex vascular network that these CTCs encounter after dislodging from the primary tumour. This theory was widely accepted by the scientific community for the better part of the 20th century. However, evidence by Schackert and Fidler in 1988, upheld Paget's work which had been largely disregarded until then. They observed that murine melanoma cell lines and a fibrosarcoma cell line despite being injected through a common route (carotid artery), formed metastases at different sites in the brain (Schackert and Fidler, 1988). It was further proven that the observed homing was not random and was not determined by vasculature only. This paper suggested that complex interactions between tumour cells and the microenvironment would determine the point of culmination of the metastatic cascade. Further studies over the past few decades have unravelled that the extent to

which either the "seed and soil" or the "anatomical-mechanical" hypotheses are operational is highly dependent on the tumour. The discovery of a sub-population of tumour cells called cancer stem cells (CSCs) has provided deeper insight into the intricate metastatic process. The plasticity exhibited by these CSCs, which may be defined as the ability to dynamically alternate between differentiated and undifferentiated states, has been credited with both metastatic spread and non-response to therapy, making CSC research an exciting field of study.

1.4 Cancer Stem Cells (CSCs)

The first mention of a possible association between stem-like cells and cancer can be traced back to Johannes Muller. Muller, in the year 1838, called for a possible association between embryonic cells and cancer outgrowths due to morphological similarities. Following this, Cohnheim in 1877 attributed cancer to embryonic cells that have remained undifferentiated or "unused" during the process of development (Grundmann, 1985). He called such cells "embryonic rests" and hypothesised that upon receipt of appropriate blood supply, such pockets have the ability to proliferate uncontrollably leading to cancer. However, these claims could not be verified experimentally. In 1907, Max Askanazy first used the term "stem cells" or "stamzellen" to describe these embryonic remnants (Maehle, 2011).

The idea that cancer was a result of embryonic cells that were left undifferentiated during the course of development was largely believed to be true, with differentiation patterns in cancer remaining a neglected field of study, until John E Dick's work on Acute Myelogenous Leukaemia (AML) in the 1990's. John Dick convincingly showed that $CD34^{+}/CD38^{-}$ AML cells when injected into mice in highly limiting numbers were capable of initiating cancer (Lapidot et al., 1994). These cells were characterized by exceptionally high self-renewal, with tumorigenic potential progressively decreasing with an increase in differentiation. Further, they were found to successfully form tumours upon serial transplantation into mice, with tumours thus formed having a combination of self-renewal and differentiation signatures (Bonnet and Dick, 1997). This was a classical trait of stem cells, which are known to generate both self (stem-like) and differentiated cells.

Post this ground-breaking finding, numerous groups have since uncovered CSCs as the primary reason for cancer initiation in multiple models. Further, ample proof has been generated to imply that dedifferentiation of cells results in cancer incidence as opposed to the "embryonic remnant" theory put forward by Cohnheim in the 19^{th} century. The plasticity of CSCs has been

observed to give them an edge over the bulk tumour, allowing them to adapt and survive at different stages of tumour progression, in a dynamically changing microenvironment, beginning from the site of tumour initiation and ending at a distant metastatic site. Apart from self-renewal, these cells have also been credited with high drug efflux capacity and better DNA repair, consequently leading to therapy resistance, metastasis and relapse (Hirschmann-Jax et al., 2004; Srivastava and Krishna, 2009). CSC development has been attributed to deregulation of signalling pathways and epigenetic modifications leading to increased stem-like characteristics.

a) Signalling Pathways Involved in CSC Generation and Maintenance

Numerous signalling networks have been implicated in the self-renewal and survival of CSCs. These include the Wnt, Notch, Hedgehog, NF-κβ, PI3K and JAK/STAT pathways amongst several others.

The Wnt pathway is essential for embryogenesis and plays an important role in proliferation, survival, migration and determination of cell polarity in normal tissues (Kahn, 2014). Mutations and deregulation of this pathway has been perceived to be important in CSCs of breast, colon, lung, skin, urinary tract and blood cancers (Holland et al., 2013). WNT1 when constitutively over-expressed in mice models, was found to result in 6 times greater the number of CSCs than control mammary glands (Shackleton et al., 2006). Downstream effectors of the Wnt pathway like β-catenin, TCF-4 and LEF1 were observed to be up-regulated in breast CSCs, while inhibition of WNT1 resulted in decreased expression of stemness markers and reduced tumoursphere formation capability (Jang et al., 2015). Deletion of β-catenin resulted in loss of tumorigenicity, with $CD34^{+}$ skin-derived CSCs failing to form tumours upon secondary transplantation, whereas over-expression of non-degradable β-catenin resulted in an increase in the stem cell population (Malanchi et al., 2008). Further, knockdown of Disheveled2 (Dvl2) was found to result in decreased tumorigenicity in gliomas (Pulvirenti et al., 2011). These and other studies underline the importance of Wnt signalling in CSC expansion.

Binding of DLL and JAG proteins of one cell to Notch receptors on another cell activates the Notch signalling pathway (Karamboulas and Ailles, 2013). Notch signalling plays a crucial role in normal human physiology, influencing differentiation patterns in organs that require constant regeneration like the skin, intestine and the haematopoietic system (Chiba, 2006). Recent evidence is suggestive of a definitive role for Notch signalling in CSC maintenance in pancreatic and oesophageal cancer. CSCs derived from clinical samples revealed up-regulation of the Notch pathway as evidenced by increased expression of NOTCH 1/3, JAG 1/2 and HES1, a downstream effector of Notch signalling, in pancreatic cancer (Abel et al., 2014). As expected, inhibition of this pathway was found to result in decreased tumoursphere formation, increased cell death and compromised cell cycle progression (Abel et al., 2014). Similar knockdown of the Notch pathway in oesophageal adenocarcinoma cells led to decreased stemness gene expression, decreased CSC survival and loss of secondary transplantation ability in mice, further ascertaining that the Notch signalling axis controls CSC population survival (Wang et al., 2014).

The Hedgehog pathway is known to control patterning of various organs by regulating proliferation, migration and differentiation during embryogenesis (Petrova and Joyner, 2014). Though inactive in most adult tissues, aberrant activation of Hedgehog signalling has been implicated in CSC regulation in various cancers. Mutations in the Patched 1 gene (*PTCH1*), a suppressor of the Hedgehog signalling pathway, has been observed in patients presenting with basal cell carcinoma and medulloblastoma (Kim et al., 2003; Peterson et al., 2015). Molecular profiling of glioma-derived CSCs revealed over-expression of key mediators of the Hedgehog pathway- *GLI1*, *SHH* and *PTCH1* (Clement et al., 2007). In colon cancer, patient-derived CSCs were found to exhibit up-regulation of *GLI1* and *GLI2* with respect to non-metastatic controls (Varnat et al., 2009). Significantly, inhibition of Hedgehog signalling led to decreased self-renewal and survival ability in multiple myeloma and glioma models, suggestive of a crucial role for Hedgehog signalling in CSC development and maintenance (Clement et al., 2007; Peacock et al., 2007).

The NF-κβ pathway is a core signalling mechanism that regulates proliferation, cell cycle, differentiation and inflammatory responses (Hayden and Ghosh, 2008). Mutations causing hyperactivation of this pathway have been implicated in numerous haematological malignancies and gastrointestinal, gynaecological, head and neck and breast tumours (Karin, 2009; Prasad et al., 2010). Constitutive expression of the RANK (Receptor Activator of NF-κβ signalling) ligand has been implicated in expansion of breast CSCs, whereas inhibition of

this pathway led to decreased self-renewal ability as observed by a decrease in secondary transplantation capability, accompanied with diminished *NANOG* and *SOX2* promoter activity (Liu et al., 2010; Pellegrini et al., 2013). Finally, inhibition of IKKβ led to reduced metastases in the lung and decreased frequency of CSCs in the few metastatic foci thus formed (Chen et al., 2015a).

PI3K/PTEN signalling is central to normal cellular physiology, regulating survival, proliferation and cell cycle progression. The pathway is governed by numerous upstream regulators including cytokines, integrins and various growth factors (Hemmings and Restuccia, 2012). Emerging evidence implies a possible involvement of this pathway in CSC regulation. Inactivation of PTEN (an antagonist of PI3K signalling), was observed to lead to enhanced survival, invasion, migration and increased expression of core stemness markers NANOG, SOX2 and OCT4 in the glioblastoma model (Duan et al., 2015). In AML, increased miR-126 resulted in maintenance of the "stem-like" phenotype via PI3K signalling (Lechman et al., 2016). Similarly, experimental evidence suggested that miR-10b, a silencer of PTEN, led to enhanced self-renewal of CSCs in the breast cancer model, thereby indicating that CSCs could be governed by this signalling axis (Bahena-Ocampo et al., 2016).

The JAK/STAT pathway is a highly conserved signalling mechanism that is involved in normal functioning of various systems in the body, particularly immunogenic response. Significantly, this pathway has been shown to play a major role in maintenance of self-renewal properties of embryonic stem cells (Stine and Matunis, 2013). Deregulation of this signalling cascade has been seen to aid CSC maintenance in various tumour models. STAT1, IFNK, IL-6 and other key signalling molecules involved in JAK/STAT signalling were found to be over-expressed in prostate cancer CSCs (Birnie et al., 2008), whereas activated STAT3 was found to be significantly enriched in CSCs derived from breast cancer (Zhou et al., 2007). Glioma-derived CSCs were found to be regulated via LIF (Leukemia Inhibitory Factor) mediated JAK/STAT signalling (Penuelas et al., 2009). Further, inhibition of this pathway was observed to lead to decreased stem-like ability *in-vitro* in glioma and breast cancer, and decreased serial transplantation efficiency in mice in the AML model (Cook et al., 2014; Sherry et al., 2009; Zhou et al., 2007).

Multiple signalling pathways have been demonstrated to contribute towards CSC maintenance and repopulation. It must also be noted that these pathways do not always follow a linear path. Instead, they form an intricate network, with convergence and cross-talk between signalling

mechanisms being highly prevalent (Matsui, 2016). Therefore, blocking one arm of this complex may not yield the desired therapeutic outcome, as other signalling axes may be activated in response, thereby continuing to support the elusive CSC pool. Therefore, a multi-pronged approach of targeting an array of diverse signalling pathways might be the key to effective cancer therapy.

b) Epigenetics in CSC maintenance

Epigenetics, which may be defined as heritable modifications to the DNA that affect transcription, without any change to the DNA sequence (Waddington, 2012), is emerging as an interesting field of study in relation to cancer initiation and progression. Very often, signalling pathways in collusion with changes to the epigenomic landscape are deemed to be responsible for non-response to therapy and relapse (Cheng et al., 2019). Epigenetic alterations can be broadly classified into DNA methylation and histone modifications.

DNA methylation involves the covalent transfer of a methyl group onto the 5^{th} carbon atom of the cytosine ring. In mammalian DNA, this modification is mostly limited to CpG dinucleotides and is associated with gene silencing (Ramsahoye et al., 2000). DNA methylation is brought about by DNA methyltransferases (DNMTs), which catalyse the transfer of a methyl group from S-adenosyl-L-methionine (SAM) to cytosine (Schubeler, 2015). DNMTs are of 5 types- DNMT1, DNMT2, DNMT3a, DNMT3b and DNMT3L, with DNMT1, DNMT3a and DNMT3b being the most widely studied. While the activity of DNMT1 is restricted to helping maintain original methylation signatures by allowing methylation of hemimethylated DNA strands produced during replication, DNMTs3a and 3b are de-novo methyltransferases capable of establishing new methylation patterns (Goyal et al., 2006; Okano et al., 1999). Though DNA methylation signatures are largely stable and subjected to minimal alterations, DNA demethylation has been observed in certain situations that demand gain of pluripotency. This process is actively controlled by the TET (ten eleven translocation) group of enzymes, which through oxidation and glycosylation result in removal of the methyl group from the cytosine moiety (Tahiliani et al., 2009). Global DNA hypomethylation has previously been associated

with CSC maintenance in various tumour models (El Helou et al., 2014; Ferrer et al., 2020; Liu et al., 2020).

Apart from direct modifications to the DNA, epigenetic changes also encompass alterations to histones- proteins that help package DNA. These modifications have been observed both at the tail regions and in core histone proteins. The modifications include methylation and acetylation (at lysine and arginine residues), phosphorylation (at serine and threonine residues), sumoylation and ubiquitylation, with acetylation and methylation being the most prevalent (Audia and Campbell, 2016). Histone acetyltransferases (HATs) and histone deacetylases (HDACs) control acetylation at various sites on histones. Similarly, histone methyltransferases (HMTs) and histone demethylases (HDMs) regulate the methylation modifications. Depending on the type of modification and the site at which the modification takes place, transcription may be activated or repressed. For instance, while H3K4, H3K79 and H3K36 methylations are associated with gene activation, addition of methyl groups to H3K9, H4K20 and H3K27 lead to suppression of gene expression (Volkel and Angrand, 2007). Covalent histone modifications leading to repression of tumour suppressor genes and activation of genes responsible for metastatic spread have been implicated in myriads of tumour models. Mutations or perturbation in levels of p300 (a histone acetyltransferase), has been linked to progression of AML and gastric adenocarcinoma (Chaffanet et al., 2000; Muraoka et al., 1996). SUV39H1 (a lysine methyltransferase which results in trimethylation of H3K9), has been associated with repression of genes involved in iPSC reprogramming (Becker et al., 2016). Consequently, SUV39H1-low cells have been observed to have increased migratory abilities in the cervical cancer model (Rodrigues et al., 2019).

As evident from the data above, CSCs are supported by a combination of both extracellular signalling mechanisms and epigenetic modifications to the DNA that allow them to evade chemotherapy and radiation treatment (Toh et al., 2017). Since conventional forms of cancer therapy are designed to target the rapidly proliferating cellular pool, quiescent CSCs remain largely unaffected. Further, owing to the toxicity and long-term side effects of these modes of treatment, there is an urgent requirement for natural compounds that could sensitize CSCs to conventional therapy, with minimal damage to non-cancerous tissue. Additionally, it has become crucial to identify, if possible, a molecule that acts as a common trigger, setting the activation of these pathways into motion, leading to cancer progression, and many times, relapse.

1.5 RHOC and Its Role in Tumour Progression

RHOC is a protein that belongs to the Rho family of small Guanosine Triphosphatases (GTPases) (Ridley, 2006), which are small signalling G-proteins that regulate cytoskeletal organization and thus affect numerous cellular functions, like cell division, motility, and polarity. Rho GTPases carry out their functions by switching between the active Guanosine Triphosphate (GTP)-bound and inactive Guanosine Diphosphate (GDP)-bound states **(Figure 1.12)** (Hall, 1992; Hall, 1998; Hall, 2005; Ridley, 1997). This switch in states is tightly regulated by RhoGAPs (Rho GTPase Activating Proteins), RhoGEFs (Rho Guanine Exchange Factors) and RhoGDIs (Rho Guanine Dissociation Inhibitors) (Moon and Zheng, 2003). RhoGAPs support the intrinsic GTPase activity of RhoGTPases, converting them from the GTP-bound state to GDP-bound, thereby leading to their deactivation (Lamarche and Hall, 1994). RhoGEFs on the other hand help maintaining RhoGTPases in the active state by facilitating their switch from the GDP-bound form to the GTP-bound form (Zheng, 2001). The third regulator protein, the RhoGDIs, stabilize RhoGTPases in the GDP form, consequently playing an important role in determining localization of the protein (Olofsson, 1999). **Figure 1.12** is a schematic representation of the molecules involved in activation of RHOC.

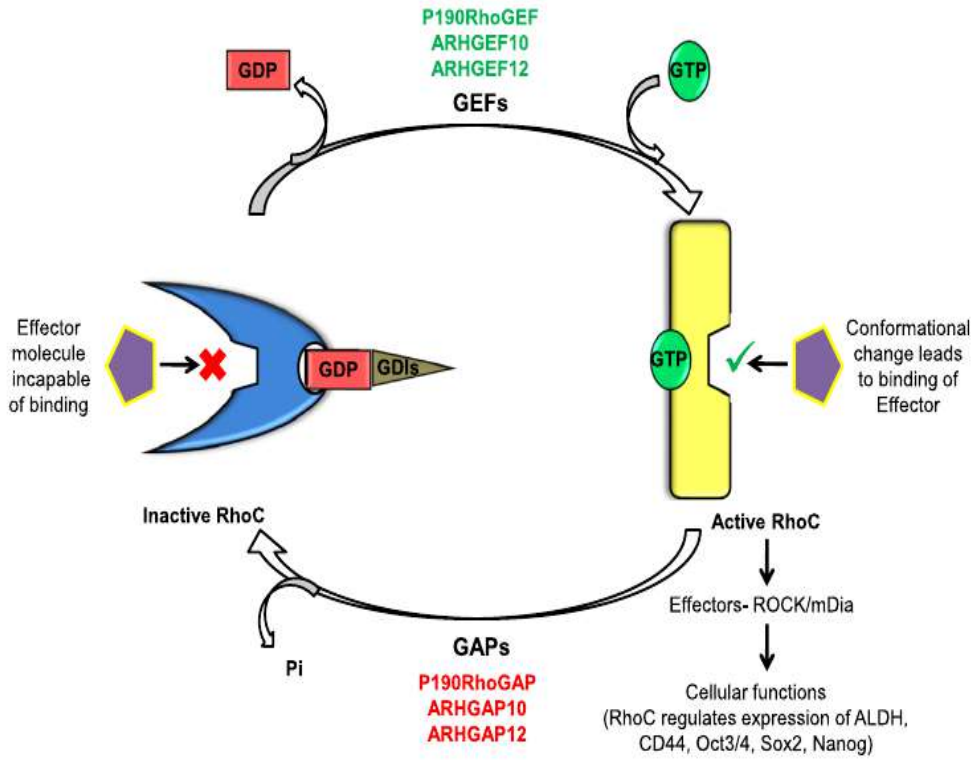

Figure 1.12: Mechanism of activation of RHOC (Thomas et al., 2019).

Rho GTPases control organization of the actin cytoskeleton via formation of stress fibres and focal adhesion complexes (Hall, 1998). Rho proteins, via the Rho associated kinases (ROCK) regulate myosin light chain (MLC) phosphorylation resulting in smooth muscle contraction (Kimura et al., 1996). Therefore, via regulation of the actin cytoskeleton, Rho proteins play an important role in cell migration, polarity, cell division, membrane trafficking and transcription (Hall et al., 1993). Multiple reports have also confirmed that RHOC plays an important part in cancer progression.

The role of RHOC in carcinoma progression has been extensively clarified by several research groups over the years. The first report, which suggested that RHOC contributed to progression of cancer, was by Suwa et al. in the year 1998. This group investigated changes in the expression levels of the Rho family of genes—RHOA, B and C in pancreatic ductal carcinoma. It was discovered that the expression of the RHOC gene was significantly higher in metastatic tumours than in primary tumours, whereas RHOA and RHOB did not show significant changes in expression under these conditions. Also, increased RHOC expression significantly correlated with poor prognosis of patients, unlike RHOA and RHOB, which showed no such correlation (Suwa et al., 1998). Following this study, several other groups reported the role of RHOC in numerous cancers, including those of the breast, skin, ovaries, liver and head and neck, among several others (Carr et al., 2003; Kamai et al., 2003; Shikada et al., 2003; Shinto et al., 2003; van Golen et al., 2000b; Wang et al., 2003). Increased expression of RHOC is therefore positively correlated to poor prognosis.

RHOC has been implicated in multiple tumour phenotypes in various tumour models. RHOC was found to be up-regulated in 90% of inflammatory breast cancer (IBC) specimens in comparison with stage-matched non-IBC controls. Further, over-expression of RHOC in non-malignant human mammary epithelial cells, led to these cells expressing oncogenic characteristics like anoikis resistance, increased migratory and invasive properties. Finally, injection of these cells into mice was observed to result in successful tumour formation (van Golen et al., 2000b). A similar observation of increased RHOC expression in hepatocellular carcinomas led to the conduction of experiments to investigate the oncogenic potential of RHOC (Xie et al., 2013). Over-expression of RHOC in normal hepatocytes was observed to result in increased proliferation, clonogenic ability, migratory and invasive properties.

Significantly, these cells successfully formed tumours when transplanted into mice in comparison with cells containing the empty vector alone. These studies pointed towards a possible role for RHOC in tumour initiation.

In another study, hepatocellular carcinoma cells stably over-expressing the RHOC protein were observed to display increased proliferative capacity, whereas siRNA mediated knockdown of RHOC led to decreased proliferation, accompanied by a reduction in percentage of cells in the divisive phases of the cells cycle (S and G2/M), reduced expression of markers regulating cell cycle progression and increased apoptosis, establishing that RHOC plays a definitive role in controlling proliferative ability of hepatocellular carcinoma (Wang et al., 2003). A study on gastric cancer cells revealed that RHOC via its downstream effector IQ-domain GTPase activating protein 1 (IQGAP-1) augments proliferative ability by increasing the levels of cell cycle proteins cyclin D and cyclin E1, with depletion of RHOC resulting in the opposite effect (Wu et al., 2012). Various other studies have indicated that RHOC promotes proliferative potential of tumours along with enhancement of invasive and migratory abilities (Faried et al., 2006; Srivastava et al., 2009; Xu et al., 2017).

The switch from a locally confined tumour to an invasive metastatic form is the most damaging alteration, allowing the tumour to disseminate, eventually leading to poor prognosis. As described previously, metastasis is a complex process that involves numerous steps including invasion, intravasation, circulation, extravasation and homing. Therefore, successful formation of metastases is preceded by an elaborate change in gene expression, leading to gain of cellular phenotypes that aid metastatic spread. Identification of the internal switch that leads to the aforesaid events is crucial to designing effective therapeutic measures. Interestingly, DNA array analysis of metastatic melanoma cells by Clark et al. revealed that RHOC was highly essential for metastasis (Clark et al., 2000). Experimental evidence on the lung adenocarcinoma cell line, A549, suggested that cytoskeletal regulation by RHOC resulted in increased invasive ability, by mediating the EMT process initiated by TGF-β signalling (Lu et al., 2016). Over-expression of RHOC was observed to result in gain of mesenchymal markers in ovarian cancer cell lines, accompanied by enhanced proliferation, migration and invasion abilities (Gou et al., 2014). In breast cancer, it was observed that while both RHOC and RHOA equally contributed to cell proliferation, RHOC was indispensable for invasion (Lang et al., 2017). Apart from migration and invasive abilities, metastatic spread requires cells to possess the ability to intravasate and survive in the bloodstream under non-adherent conditions. RHOC via its downstream effectors, ROCK1 and ROCK2 was seen to regulate adhesion and trans-

endothelial migration of prostate cancer cells (Reymond et al., 2015). Subsequently, depletion of RHOC was found to lead to reduction in the formation of metastatic outgrowths in lungs (Ikoma et al., 2004). RHOC over-expression in human mammary epithelial cell lines resulted in increased production of angiogenic factors like VEGF, bFGF, IL-6 and IL-8 in the conditioned media as compared to cells containing the vector alone. Further, inhibition of RHOC resulted in consequent reduction of these factors, proving RHOC's role in regulation of angiogenesis in breast cancers (van Golen et al., 2000a). Finally, a study by Srivastava et al. proved that NOTCH1 via RHOC controlled proliferation, EMT, anoikis resistance and angiogenesis in the cervical cancer model (Srivastava et al., 2009). Further, since HPV infection is known to cause significant changes to the gene expression landscape, RHOC expression could be modulated by HPV in cervical cancer cells, hence driving their progression. **Figure 1.13** gives an overview of the contributory role of RHOC in various aspects of tumour progression.

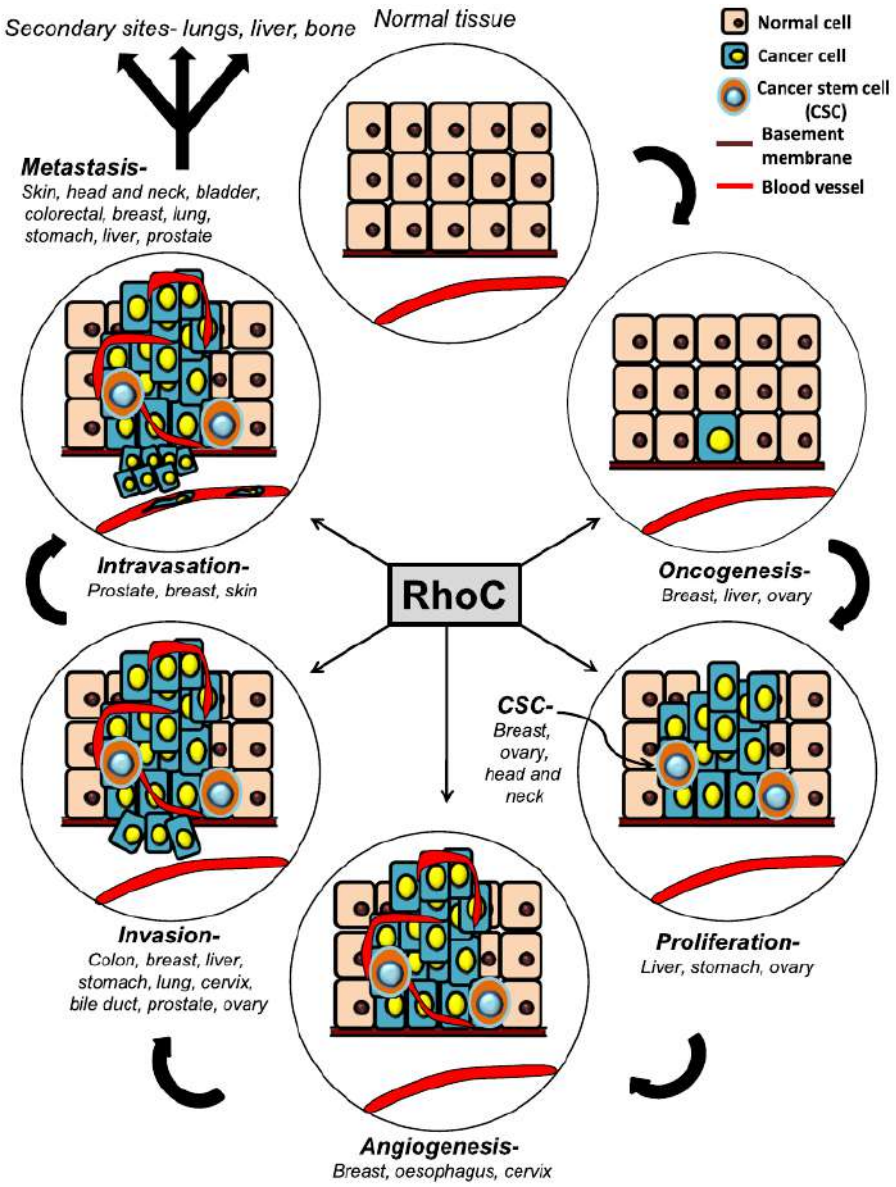

Figure 1.13: RHOC and its involvement in tumour progression (Thomas et al., 2019).

Since the observed phenotypic alterations brought about by RHOC require cells to undergo large-scale molecular expression changes and gain a "plastic" nature that would enable them to dynamically switch between various states, the involvement of RHOC in maintaining stemness ability was inevitable. An important finding by Rosenthal et al. indicates a strong correlation between RHOC and ALDH, a breast cancer stem cell (BCSC) marker (Rosenthal et al., 2012). Using the aggressive BCSC cell line SUM149, Rosenthal et al. show that cells with active ALDH (ALDH+) have higher levels of RHOC than those with inactive ALDH (ALDH−). Tumorigenicity studies utilizing a limiting number of 50 cells in mice resulted in

no induction of tumours in mice injected with ALDH+/shRHOC cells, whereas 5 out of 9 mice with ALDH+/scrambled cells formed tumours. Moreover, incidences of lung metastases were found to be around five times higher in mice injected with ALDH+/scrambled cells compared to those injected with ALDH+/shRHOC cells, indicating the stem-like property of cells containing RHOC. Finally, a tissue microarray of breast cancer samples from 136 patients indicated a high correlation between RHOC and ALDH1, further supporting RHOC's association with ALDH.

The role of RHOC in CSC maintenance has also been illustrated in head and neck squamous cell carcinoma (HNSCC) by Islam et al. (Islam et al., 2014). Using UM-SCC-1 and UM- SCC-47 cell lines, they show that the siRNA mediated inhibition of RHOC led to decreased expression of ALDH, CD44, OCT3/4, SOX2 and NANOG, in addition to a diminished formation of tumourspheres. Further, Islam et al. determine that tumourspheres have increased levels of RHOC and genes associated with stemness compared to cells grown as monolayers, whereas the inhibition of RHOC leads to a reduction in the expression of stemness genes, which points towards RHOC's possible role in CSC induction. Islam et al. then demonstrate that RHOC leads to stemness induction in head and neck cancer by activation of STAT3 via IL-6.

In a study by Sang et al., ovarian cancer stem cells (OCSCs) were sorted using the CD117 marker from A2780-PM and A2780-PTX-PM- two drug-resistant and invasive ovarian cancer cell lines (Sang et al., 2016). These OCSCs were found to have elevated expressions of RHOC. The MTT (3-(4,5-dimethylthiazol-2-yl)-2,5-diphenyltetrazolium bromide) assay revealed that cells inhibited for RHOC had decreased cell proliferation and drug resistance. Further, inhibition of RHOC by RHOC-specific siRNA led to decreased expression of stemness markers like CD133 and CD117, as observed by real-time quantitative PCR, suggesting a possible role of RHOC in the formation of OCSCs. It may be thus appropriate to deduce that overexpression of RHOC results in enhanced plasticity/stemness of cancer cells. **Figure 1.14** reveals the probable contribution of RHOC to stemness maintenance by allowing dynamic dedifferentiation of bulk tumour cells and transit amplifying cells to CSCs.

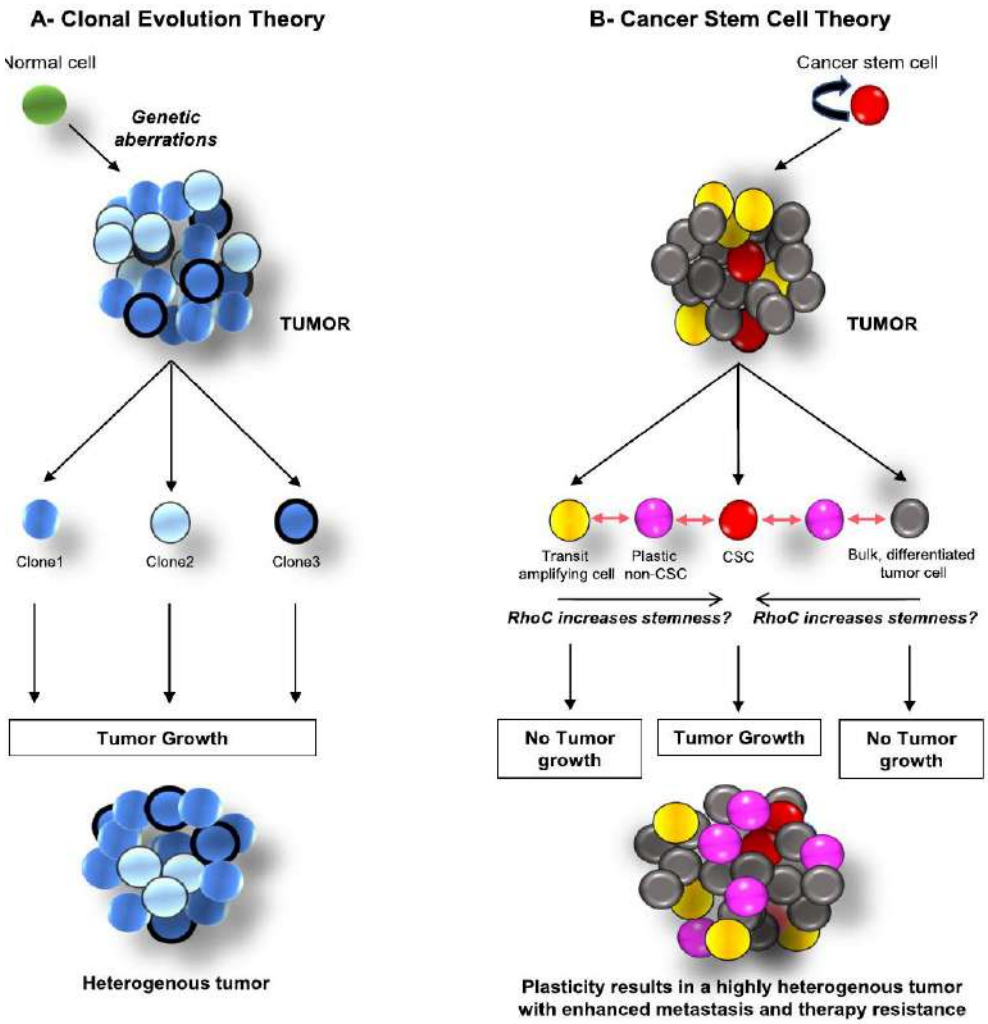

Figure 1.14: Possible contribution of RHOC in imparting plasticity to tumour cells (Thomas et al., 2019).

Though studies have indicated that RHOC could result in increased stemness ability of cells, details regarding the mechanism governing this finding remain sketchy. Further, no study thus far has described RHOC's contribution to CSC maintenance in cervical cancer. Considering that women in developing countries are diagnosed at late stages of the disease, making effective therapeutic intervention a challenge, identification of the molecular switch governing metastatic spread and stem-like ability gains paramount importance.

This work establishes that RHOC plays a definitive role in stem cell maintenance in cervical cancer. The work goes on to describe how RHOC via the ERK pathway leads to enhanced expression of cytosolic stemness markers like CD49F and ALDH. Importantly, the study attaches a novel role for RHOC in epigenetic regulation. Through active DNA hypomethylation and interaction with WDR5, (a histone modifier that results in the active transcriptional mark,

H3K4me3), RHOC over-expressing cells were found to enhance expression of core transcriptional factors that regulate pluripotency like NANOG and SOX2. Subsequently, RHOC over-expressing cells displayed resistance to radiation owing to robust DNA repair machinery, with depletion of RHOC successfully sensitizing these cells to radiation treatment. Finally, ethanolic extracts of Aloe vera were found to decrease the stem-like ability and EMT phenotype in SiHa cells, thus unveiling a natural compound that could potentially function as a sensitizer of CSCs to conventional forms of therapy.

Hypothesis

and

Objectives

2.0 HYPOTHESIS

The contribution of RHOC to cancer progression is well-established (Thomas et al., 2019). Studies have shown that RHOC regulates proliferation (Wu et al., 2012), EMT (Lu et al., 2016), metastasis (Lang et al., 2017), angiogenesis (Wang et al., 2008b), resistance to anoikis (Srivastava et al., 2009) and resistance to radiation (Pranatharthi et al., 2019) across various tumour models. For a cell to metastasize, it must be capable of detaching from the primary tumour, wading through the blood stream, identifying a suitable distant site for colonization and finally homing into and proliferating at the secondary site, eventually forming metastases (Valastyan and Weinberg, 2011). This indicates that metastatic cells must be able to dynamically switch between various phenotypes to enable metastatic spread.

Stem cells are known for their "plastic" nature and their inherent ability to toggle between various phenotypes depending on external microenvironmental cues, thus equipping them with the machinery to survive and thrive under trying conditions (Das et al., 2020). This implies that the cells that eventually break away from the tumour to successfully form metastases must be "stem-like". Sure enough, CSCs have been associated with EMT (Tanabe et al., 2020), metastatic spread (Shiozawa et al., 2013) and poor response to therapy (Zhou et al., 2021). With RHOC known to be linked to most of the phenotypes that are signs of poor prognosis in cervical cancer (Srivastava et al., 2009), it was envisaged that RHOC could play a key role in maintenance of stem-like properties in cancer of the cervix.

Therefore, the hypothesis of this study was-

RHOC modulates stemness in cervical cancer.

3.0 OBJECTIVES

Since the hypothesis of the study was that RHOC helps in the maintenance of stemness in cervical cancer, experiments were designed that could help understand the molecular mechanisms behind this theory. Initial studies were aimed at determining whether RHOC regulated stem-like ability in cervical cancers. Next, the specific mechanisms by which RHOC imparts stemness advantage to cervical cancer cells was explored. Finally, the effect of natural extracts (Aloe vera) in abrogating stemness was investigated.

Overall, the objectives of the study may be outlined as follows-

1) To test the role of RHOC in maintenance of CSCs in cervical cancer.
2) To understand the mechanism of action of RHOC in CSC maintenance.
3) To correlate the expression of RHOC and stemness genes in cervical carcinoma using human patient samples.
4) To evaluate the effect of Aloe vera on stemness in cervical cancer.

CHAPTER -II

Materials and Methods

4.1 Cells Lines Used and Culturing Conditions

Squamous cervical carcinoma derived SiHa and CaSki cell lines were used in this study. The SiHa cell line originates from a Grade II Squamous cell Carcinoma, whereas CaSki cells are isolates from metastatic outgrowths of cervical cancer in the small intestine. The cell lines were cultured using Dulbecco's Modified Eagle Medium (DMEM) (Invitrogen Catalogue number: 12100046), supplemented with 10% FBS (Foetal Bovine Serum) (HiMedia Catalogue number: RM10409) and penicillin-streptomycin (Invitrogen Catalogue number:15140148) at 37°C and 5% CO_2. The cultures were tested for mycoplasma contamination on a regular basis.

Plasmids that were used for creation of stable cell lines were as follows- pcDNA3 (Invitrogen, Carlsbad, USA), RHOC over-expressing plasmid with the wild-type RHOC gene used as insert and a plasmid containing the dominant-negative form of RHOC as the insert (UMR cDNA Resource Center). Cells that were successfully transfected were selected by treating with the antibiotic G418 (Invitrogen Catalogue number: 11811023). A concentration of 1mg/ml was used for selecting SiHa cells, and 300µg/ml was used for selection of CaSki cells harbouring the plasmid. SiHa cells were transfected with pcDNA3 to obtain the stable cell line SiHa-N, that had only the pcDNA3 vector. SiHa-R cells stably over-expressed the wild-type RHOC protein. Similarly, CaSki-N cells were transfected with pcDNA3 and CaSki-dnR over-expressed the dominant negative form of RHOC.

4.2 Transfection

Lipofectamine 2000 (Invitrogen Catalogue Number: 11668019) and Hiperfect (Qiagen Catalogue Number: 301705) reagents were utilized for transfection experiments. All siRNAs were procured from Ambion, Invitrogen. Cells were seeded in DMEM supplemented with 10% FBS at 70% confluency on the day prior to commencement of transfection experiments.

4.2.1 Lipofectamine-based transfections-

Cells were incubated with opti-MEM media (Invitrogen Catalogue Number: 11058021) devoid of growth factors for 1h at 37°C and 5% CO_2. The target siRNA (at the desired

concentration) and Lipofectamine 2000 reagent (3µl for a 35mm dish) was mixed in two separate tubes containing 50µl of opti-MEM each, and allowed to stand at room temperature for 5mins. They were then combined, mixed and incubated at room temperature for 15mins. After 15mins, fresh media was added and the volume was made up to 1ml. The media in the culture dishes was discarded, replaced with fresh media containing the transfection complexes and incubated for 5h at 37°C and 5% CO_2. After 5h, the media containing transfection complexes was removed and replaced with fresh opti-MEM. Post incubation for 1h, media was replaced with fresh DMEM containing 10% FBS. The cells were retrieved 48-72h post transfection and subjected to the desired assays. Scrambled siRNA was utilized as the negative control.

4.2.2 Hiperfect-based transfections-

Transfection complexes comprising of siRNA and Hiperfect transfection reagent (3µl for a 35mm dish) were made in an eppendorf tube in 100µl DMEM (devoid of FBS). The complexes were allowed to stand at room temperature for 10mins. Media was replaced with 900µl of fresh DMEM supplemented with 10% FBS and the complexes were added onto the cells. The dishes were swirled to allow homogenous distribution of the reagents and incubated at 37°C and 5% CO_2. Cells were retrieved 48-72h post transfection.

The siRNAs and the quantities used per ml of the media are indicated in **Table 4.1**.

Target gene	**Quantity (in pico moles)**	**Catalogue Number**
RHOC	30	120759, 120897
E2F1	50	107658
TET2	50	126964
WDR5	50	136959
Scrambled (negative control)	At the same concentration as the target siRNA	AM4611

Table 4.1: Quantities of siRNAs used and their manufacturing details.

4.3 Clonogenic Assay

The clonogenic assay scores for self-renewal ability (Puck and Marcus, 1956; Rafehi et al., 2011). Cells were seeded in limiting numbers that would not allow interaction with neighbouring cells. Eventually, only cells that are capable of surviving independent of other cells will grow and form clones. A clone is defined as a group of cells more than 50 in number that arise from a single cell. The number clones formed is proportional to the self-renewal ability.

1000 cells were seeded in 100mm dishes in DMEM supplemented with FBS. The colonies formed were allowed to grow over a period of 14 days. They were then stained with 0.05% crystal violet, imaged and counted.

4.4 Soft Agar Assay

The soft agar assay helps identify cells that have self-renewal capability in conjunction with anoikis resistance abilities (Borowicz et al., 2014). Cells are seeded in a semi-solid agar medium, suspended over a layer of agar of higher percentage, that prevents attachment to the culture dish. Only cells capable of surviving under these conditions would form colonies, which are scored based on the size. The size and number of colonies is a direct read-out of stem-like ability. Small colonies were identified as those that measured 20-30µm in diameter, medium colonies were 40-50µm and the large colonies were graded as those in the range of 60-100µm.

5000 cells were seeded in 0.33% agar containing DMEM over a layer of 0.5% agar with DMEM and fetal calf serum in a 35mm dish (Srivastava et al., 2009). The dishes were topped up with 200µl media every 3 days. At the end of 21 days, colonies from 10 random fields were imaged and counted using a Leica DM IL LED Fluorescence microscope.

4.5 Anoikis Assay

This assay also measures self-renewal and anoikis resistance abilities (Folkman and Moscona, 1978). Here, dishes are coated with a polymer that prevents attachment of

cells to the dish. The number of colonies formed under such conditions are determined, and is considered to be a measure of self-renewal and resistance to anoikis.

Cells were seeded in dishes coated with poly-hydroxyethylmethacrylate (Sigma Catalogue Number: P3932-25G) and allowed to grow over a period of 7 days. The spheroidal colonies thus formed were measured, imaged and counted from 10 random fields using a Leica DM IL LED Fluorescence microscope.

4.6 RNA Isolation

The media was removed and cells were washed thoroughly with PBS. The PBS was removed completely and 1ml of TRIzol (Invitrogen Catalogue Number: 15596026) was added per 10^7 cells. Cells in TRIzol can be stored at -30°C for upto 6 months. RNA was then isolated as per the procedure detailed below.

The sample in TRIzol was thawed completely and 200µl of chloroform (Fisher Scientific Catalogue Number: 22465) was added. The sample was vortexed well for 20-30s and centrifuged at 12,500rpm for 15mins at 4°C. After centrifugation, the formation of three distinct layers was observed. The upper transparent aqueous phase contains the RNA, the pink organic phase contains the proteins and the opaque interphase consists of the DNA. The clear aqueous phase was carefully removed into another tube, without disturbing the other layers. 500µl of chilled isopropanol (Merck Catalogue Number IG0I600404) was added into the collected aqueous phase. The tube was mixed by inversion and incubated on ice for 10mins to allow precipitation of RNA. The tube was then spun at 12,500rpm for 10mins at 4°C. The supernatant was discarded carefully and the pellet was washed first with 75% ethanol (Merck, Catalogue Number: 100983) followed by a 100% ethanol wash. The RNA pellet was dried to ensure that no traces of ethanol remain. The dried pellet was dissolved in nuclease-free water (Invitrogen Catalogue Number: AM9916) and incubated for 5mins at 55°C to enhance solubility.

The RNA was quantified using the Qubit RNA Broad Range Assay kit (Invitrogen Catalogue Number: Q10210) on the Qubit fluorimeter. 500ng of RNA was also run on a 1% TBE gel to check the quality of RNA. Non-degraded RNA appears as three distinct, intact bands when subjected to gel electrophoresis. This corresponds to the each of the ribosomal RNAs-28s, 18s, 5.8s and 5s RNAs. The 5.8s and 5 s RNA appear

as a single band. If the RNA was found to be non-degraded and of sufficient quantity, it was converted to cDNA on the same day. The remaining RNA was stored at -80°C.

4.7 cDNA Preparation

The RNA isolated was converted to cDNA for further analysis by PCR. The MMLV-Reverse transcriptase kit (Catalogue Number: 28025013) from Invitrogen was utilized for this purpose. 1µg of RNA was converted to cDNA. 0.8µl of random hexamers (Invitrogen Catalogue Number: 48190011) at a working concentration of 300ng/µl was added to 1µg RNA in a 0.2ml PCR vial. The volume was made up to 12.5µl with nuclease-free water. The mixture was incubated at 70°C for 10mins. 7µl of a master mix containing the components listed in **Table 4.2** was added-

Component	Volume (in µl)
5X First Strand Buffer	4
0.1M Dithiothreitol	2
10mM dNTPs (Invitrogen Catalogue Number: R0181)	1

Table 4.2: Components of the master mix used in cDNA preparation.

The tube was then incubated at 37°C for 2mins. 0.5µl of the MMLV-RT enzyme was added into the tubes and incubated under the conditions detailed in **Table 4.3**. The prepared cDNA was stored at -30°C.

Temperature	Time
25°C	10mins
37°C	60 mins
70°C	15mins

Table 4.3: Incubation conditions for cDNA preparation.

4.8 Primer Designing and Standardization

Customized oligos were designed for each gene. The gene sequences were accessed from NCBI (https://www.ncbi.nlm.nih.gov/) and primers were manually designed. For analysis of mRNA transcripts, the primers were designed to ensure that either the forward or the reverse primer spanned an exon-exon junction. This was done to prevent amplification of possible DNA that could have cross-contaminated the RNA samples during the isolation process. The Tm of the primers were between 64-66°C and the GC content ranged from 40-60%. The 3' end of the primer culminated with G/C, T/A, G/C to ensure non-sticky, specific binding. The specificity of the primer was checked using Nucleotide BLAST (https://blast.ncbi.nlm.nih.gov/Blast.cgi). For qPCR, the product sizes were limited to 150-200bp.

The annealing temperature (Ta) of the primers was ascertained by running a gradient PCR (Details regarding PCR are given in Section 4.9). The Ta is mostly found to be around 5°C lesser than the Tm of the primer. The gradient was set up in such a way that the possible Ta served as the mid-point of the gradient. The PCR products were subjected to gel electrophoresis in TAE buffer. The optimum Ta was decided based on the intensity of the bands thus obtained. The sequences of the primers used in this study is given in **Table 4.4**.

Gene		**Primer sequence (5'→3')**
GAPDH	Forward	GAAGGTGAAGGTCGGAGTC
	Reverse	GAAGATGGTGATGGGATTTC
Notch3	Forward	CACGAGGATGCTATCTGTGACAC
	Reverse	CTCGTCCACATCCTGGTCACATG
POSTN	Forward	CATCACATCGGACATATTGGAG
	Reverse	AGCTTCGGAAGCCACTTTGTC
ALDH1	Forward	CATGAAGATCATGGAGATGTCAG
	Reverse	TGTGAGGAAGTTGGCCATCAG

ABCG2	Forward	GATCCAAGTGGATTATCTGGAG
	Reverse	CCGTCAGAGTGCCCATCACA
CD49F	Forward	ACTGGAAAGGGATTGTTCGTGT
	Reverse	GCTCCACTGTGATTGGCTCT
Oct4	Forward	GTACTCCTCGGGTCCCTTTCC
	Reverse	CAAAAACCCTGGCACAAACT
SOX2	Forward	ACACCAATCCCATCCACACT
	Reverse	GCAAACTTCCTGCAAAGCTC
NANOG	Forward	TTCCTTCCTCCATGGATCTG
	Reverse	TCTGCTGGAGGCTGAGGTAT
TET2	Forward	CATTCAGCAGCACACCCTCTC
	Reverse	TAGTTGAATTCAGCAGCTCAGTC
WDR5	Forward	CTCAGAGCAAGCCTACACCTG
	Reverse	ATGAACTTGCCAGCCACTCTC
AICDA	Forward	GACACCACTATGGACAGCCTC
	Reverse	AGCACTGTCACGCCTCTTCAC
NANOG promoter (1)	Forward	CTCAAATCAAGAAATCACCCTAATG
	Reverse	CAGGAATATGGTTCAACAGGAAT
NANOG promoter (2)	Forward	ATTCCTGTTGAACCATATTCCTG
	Reverse	TGTTAGAGAAATAGGACCTCCAG

Table 4.4: Sequences of primers used.

4.9 Polymerase Chain Reaction (PCR)

The PCR has emerged as an important tool for the study of DNA and RNA since its inception by Kary Mullis in 1985 (Mullis et al., 1986). PCR works by using DNA polymerase sourced from the bacterium *Thermus aquaticus*, a species of bacterium capable of tolerating extremely high temperatures. The DNA polymerase from these bacteria have an optimum temperature of 72°C and is extremely stable at temperatures upto 95°C. This property makes it ideal for use in PCR, which utilizes repeated cycles of high temperatures for denaturing the double-stranded DNA template. The components and the volumes used in PCR are listed in **Table 4.5**. The Taq Polymerase kit from Invitrogen (Catalogue Number: EP0405) was utilized.

Component	**Volume**
Nuclease-Free water	5.8µl
10X Taq Buffer	1µl
25mM $MgCl_2$	0.6µl
10mM dNTP	0.5µl
10µM Forward Primer	0.5µl
10µM Reverse Primer	0.5µl
Template DNA	1µl
Taq Polymerase	0.1µl
Total	10µl

Table 4.5: Components of the Polymerase Chain Reaction (PCR).

Once the components were carefully pipetted out into a 0.2ml tube, the tubes were placed in an Eppendorf thermal cycler with the following cycling conditions-

Process	Temperature	Time	
Initial Denaturation	95°C	10mins	
Denaturation	95°C	10s	Cycling Stage
Annealing	Primer dependent	30s	Number of cycles=35
Extension	72°C	30s	
Final Extension	72°C	1min	

Table 4.6: Cycling conditions for PCR.

The PCR products thus obtained were loaded on an agarose gel made of 1X TAE buffer. The percentage of the gel used was dependent on the size of the PCR product. Larger molecules require larger pore sizes to pass through, which is provided by gels with decreased agarose percentages. Therefore, the percentage of the gel used was inversely proportional to the size of the PCR product. SYBR safe (Invitrogen Catalogue Number: S33102), a fluorescent DNA binding dye was used to stain the DNA. Gels were run in TAE buffer and visualized under the BIO-RAD ChemiDoc XRS+.

4.10 Real-time Quantitative PCR (qPCR)

Gene expression was studied by qPCR. Real time qPCR has been used extensively for the past few decades to study gene expression and alterations to the DNA including duplications, deletions, point mutations and many others (Aldea et al., 2002). The technique utilizes SYBR green, a fluorescent, DNA intercalating dye that binds to double-stranded DNA. As the PCR progresses, the number of double-stranded PCR products increase exponentially. SYBR green binds to these double-stranded DNA molecules and emits a fluorescent signal, the intensity of which proportionally increases with PCR amplification and is recorded in real-time. However, since this assay uses the property of SYBR green to bind to any double-stranded DNA in the mix, with no specificity to the desired PCR product, non-specific signals from possible primer-dimer

pairs could interfere with the final results. This was overcome by taking extra precaution while designing primers to ensure minimal complementarity between primers to avoid self-dimerization or formation of dimers between the forward and reverse primers. The melt curves generated during the dissociation stage of the qPCR run were also checked to verify the presence of a single peak, indicative of amplification of a single PCR product.

The cycle number at which the fluorescent signal crosses the threshold intensity is defined as the Cycle threshold number (Ct value). If the number of copies of the gene of interest was large to begin with, this threshold intensity is attained during the initial cycles, because of which such samples will have a low Ct value. On the other hand, samples with very low copies of the gene under consideration will take a larger number of cycles to reach the same threshold intensity. Therefore, the Ct value associated with these samples will be larger. The Ct values obtained after the run were normalized against a housekeeping gene whose expression does not change across the analysed samples. The difference in Ct values thus obtained between control and test samples post normalization, is raised to the power of 2 to arrive at the final change in gene expression between samples, expressed in folds over the control sample.

Here, the TB GreenTM Premix Ex TaqTM II mix (Catalogue Number: RR820A) from TAKARA was used to analyse changes in gene expression. The components and the volumes of reagents added are given in **Table 4.7**.

Components	**Volumes**
Nuclease-free water	3µl
Forward primer (10µM)	0.5µl
Reverse primer (10µM)	0.5µl
Template cDNA	1µl
SYBR Green master mix	5µl
Total	10µl

Table 4.7: Reaction components for qPCR.

Table 4.8 gives details regarding the cycling conditions used for qPCR.

Temperature	Time	
50°C	20s	
95°C	10mins	
95°C	15s	Cycling stage
60°C	30s	Number of cycles=40
72°C	30s	
95°C	15s	
60°C	1min	Dissociation stage
95°C	15s	
60°C	15s	

Table 4.8: Cycling conditions for qPCR.

The samples were run on a 7500 Fast Real Time PCR machine from Applied Biosystems using the ΔΔCt method. Fold changes in gene expression were computed using the Ct values thus obtained.

4.11 Genomic DNA isolation

Genomic DNA was isolated using the salting out method (Miller et al., 1988). Cells were re-suspended in 600µl of cell lysis buffer and 3µl proteinase K (10mg/ml) (Sigma Catalogue Number: P2308) was added and incubated at 55°C for 3h. Post the incubation, 200µl of 5M potassium acetate was added, vortexed and centrifuged at 14,000rpm for 3mins. The proteins were precipitated out and the supernatant was collected in another tube. 600µl of chilled isopropanol was added to precipitate the

DNA. The tubes were mixed by inversion and incubated on ice for 10mins. The tubes were spun at 14,000rpm for 1min. 1ml of chilled absolute ethanol was added and the tubes were spun at 14,000rpm for 1min. The pellet was air dried and nuclease-free water was added to dissolve the DNA. The tubes were incubated at 55°C for 5mins to facilitate complete dissolving of the pellet. Quantification of the DNA isolated was done using the DNA High Sensitivity kit (Invitrogen Catalogue Number: Q33230) on the Qubit fluorimeter. 500ng of DNA was also run on a 1% TAE gel in order to check the quality of DNA isolated. The composition of the buffers used are mentioned in the Appendix A1 section.

4.12 Methylation-Sensitive Restriction Digestion of DNA

Restriction enzymes identify and cleave at specific sites in the DNA termed as recognition sequences. Some enzymes are unable to cleave at regions where the cytosines have a methyl group added onto them. These are called methylation-sensitive restriction enzymes (Nelson et al., 1993). Restriction digestion by these enzymes is therefore used to study changes in DNA methylation patterns (Hashimoto et al., 2007).

*Hpa*II (NEB Catalogue Number: R0171S) was used to study changes in DNA methylation. 1µg genomic DNA was taken in a tube and 5units of *Hpa*II was added in 1X cut-smart NEB buffer. The tubes were incubated at 37°C for 1h followed by incubation at 80°C for 20mins to deactivate the enzyme. The digested products were run on a 1.2% TAE gel alongside undigested DNA. Changes in the extent of digestion were determined by analysing the intensity of the bands obtained after gel electrophoresis. Densitometry analysis using the ImageJ software was performed to quantify the digestion.

4.13 WST-1 Assay

The activity of mitochondrial dehydrogenases within the cell is proportional to cellular proliferation. This property has been utilized to study the effect of various treatments on cell survival and division. Tetrazolium salts like MTT and WST-1 are cleaved to formazan dye by dehydrogenases present within the mitochondria (Stockert et al.,

2018). This results in a colour change which can be read by a microplate reader. Percentage changes in proliferation are calculated with respect to control untreated cells.

Cells were cultured in a 96-well plate (2000 cells/well) and treated with the appropriate chemical. Post incubation, the media was changed and 10µl WST-1 reagent (Sigma Catalogue Number: 5015944001) was added for every 200µl media. The plate was incubated at 37°C, 5%CO_2 for 30mins and readings were taken at 450nm with background subtraction of 655nm using a microplate reader.

4.14 Bicinchoninic Acid (BCA) Assay

Quantification of protein lysates was performed using the Bicinchoninic acid (BCA) assay (Smith et al., 1985). The assay uses the property of reduction of Cu^{2+} to Cu^{+} by proteins in an alkaline environment and consequent chelation of the reduced cuprous ions to amino acid residues. These complexes react with BCA to form a purple-coloured product that increases in intensity with concentration of the protein.

The Pierce BCA protein Assay kit from Invitrogen (Catalogue Number: 23227) has been used in this study. BCA reagents A and B were mixed in a ratio of 1:50. 10µl of the protein sample was added to 190µl of the reagent mixture in a 96-well plate. The plate was incubated at room temperature for 15mins. The plate was then read at 595nm using the BIO-RAD iMark microplate absorbance reader and the concentration of the unknown protein sample was calculated using a standard curve plotted with known concentrations of Bovine serum albumin (BSA).

4.15 Western Blotting

Western blotting is a widely used technique to quantitatively study protein levels and post-translational modifications (Towbin et al., 1979). The procedure involves resolution of a complex protein mixture based on molecular weights using gel electrophoresis. The resolved proteins are then transferred onto a nitrocellulose or PVDF (polyvinylidene fluoride) membrane. The blotted proteins are then probed using antibodies and detected using secondary antibodies conjugated with HRP (Horse radish

peroxidase). Specific protein bands are identified by addition of a peroxide solution and a substrate to HRP, which results in the emission of light. The emitted light is captured by a CCD camera and the intensity of the light produced is directly proportional to the quantity of the protein in the sample. The intensities of the bands of the test protein are compared to a protein whose levels do not change across samples, also known as the loading control.

Culture media was removed completely and cells were washed with cold PBS. The requisite amount of cell lysis buffer (around 500µl of lysis buffer for a packed cell volume of 100µl), was added. The composition of the whole cell lysis buffer used is given in Appendix A1. The cells were incubated in lysis buffer for 30mins on ice and homogenized with a 23-G syringe. The lysates were centrifuged at 14,000rpm for 10mins at 4°C and the supernatants thus obtained were stored at -80° until further use.

Equal quantities of lysates were mixed with 6X Laemmli buffer (composition in Appendix A1) and incubated at 95°C for 15mins. The denatured proteins were loaded on an SDS gel and resolved by electrophoresis. The composition of the acrylamide gel is as follows-

Component	**Volumes**		
	8%	**10%**	**12%**
Autoclaved water	4.6ml	4ml	3.35ml
1.5 M Tris (pH 8.8)	2.5ml	2.5ml	2.5ml
30% Acrylamide	2.7ml	3.3ml	4ml
10% SDS	0.1ml	0.1ml	0.1ml
10% APS	0.1ml	0.1ml	0.1ml
TEMED	10µl	10µl	10µl

Table 4.9: Composition of the resolving gel.

Component	Volumes
Autoclaved water	3.15ml
0.5 M Tris (pH 6.8)	1.25ml
30% Acrylamide	0.5ml
10% SDS	50µl
10% APS	50µl
TEMED	3µl

Table 4.10: Composition of the stacking gel.

Once resolved by electrophoresis, the proteins were transferred onto a nitrocellulose membrane and blocked using 5% milk/3%BSA in Tris buffered saline (pH 7.5) with 0.1% Tween-20 (TBST). The blots were washed thrice (10 mins per wash) in TBST. They were then probed overnight at 4°C using primary antibodies at the appropriate dilutions. The blots were again washed thrice in TBST and secondary antibodies conjugated to HRP were added. The blots were incubated at room temperature for 45mins. The blots were washed thrice and developed using the Pierce ECL western blotting substrate (Invitrogen Catalogue Number: 32209). Blots were imaged using the BIO-RAD ChemiDoc XRS+.

The details of the antibodies used are listed in Appendix A2.

4.16 Flow Cytometry

Flow cytometry uses primary and secondary antibodies conjugated to fluorophores to quantitatively determine the percentage of cells positive for a particular marker in a given cellular pool (McKinnon, 2018). Media was removed completely and the dishes were washed with 1X PBS. Cells were detached from the culture dishes by incubating them with 5mM EDTA in PBS. Cells were spun at 2000rpm and washed with 1X PBS

to free them of remnant media. The cells were then fixed in 2% PFA (in PBS) and incubated for 10mins at room temperature. They were then washed thrice in PBS to remove excess PFA. The fixed cells were permeabilized using 0.1% of the non-ionic detergent, Triton-X100 in PBS and incubated for 10mins at room temperature. After washing in PBS, cells were incubated in blocking reagent (5% FBS in PBS) for 20mins at room temperature to prevent non-specific binding of antibodies. Primary antibodies were then added at the appropriate dilutions (in blocking reagent) and incubated at room temperature for 2h. The cells were then washed thrice in PBS to remove any unbound antibody. The cells were then incubated with secondary antibody at the appropriate dilutions for 45mins at room temperature. Cells were washed thrice in PBS, resuspended in 1ml PBS and staining patterns were analysed by flow cytometry. The FC500 and BD FACS Aria III systems were used for flow cytometry. FlowJo (version 10.7), an open software for analysis of flow cytometry data was used to analyse the data.

4.17 Hoechst Exclusion Assay

The Hoechst exclusion assay is utilized for studying stem-like cells (Hirschmann-Jax et al., 2004). Due to the enhanced efflux ability of CSCs, on account of over-expression of ABC transporters, CSCs efflux the Hoechst dye effectively, resulting in a population with significantly lower Hoechst emission intensities (Hu et al., 2008). This difference in dye-uptake can be quantified by flow cytometry analysis of both Hoechst blue emission maxima (405-450nm) and Hoechst red emission maxima (630-650nm). The population of cells that display low emissions in both the blue and red ranges are deemed to be stem-like. The cells are also treated with verapamil, a blocker of ABC transporters (Zhao et al., 2016). Addition of verapamil allows retention of the Hoechst dye within the cell. Therefore, a comparison of the Hoechst emission patterns in verapamil-treated and untreated cells would provide a true picture of the percentage of the stem-like population.

Culture medium was removed and the cells were washed twice with PBS to remove any remnant media. The cells were detached using 5mM EDTA in PBS. Detached cells were spun at 1500rpm for 5mins and resuspended in Hank's Balanced Salt Solution (Gibco Catalogue Number: 14185). Hoechst 33342 dye (Invitrogen Catalogue Number:

H1399) was added at a concentration of 5µg/ml and the cells were allowed to incubate in a water-bath at 37°C for 2h. Control cells were treated with verapamil (Sigma Catalogue Number: V4629), at a concentration of 2µM, to determine the percentage of cells that constituted the true side-population. The cells were washed twice in HBSS. Propidium iodide (Invitrogen Catalogue Number: P1304MP) was added at a concentration of 1µg/ml to determine the viable cell population. FACS analysis was done using the BD FACS Aria III system.

4.18 Immunofluorescent Staining (for cell lines)

Culture media was removed and cells were washed with PBS. The cells were fixed with 1% PFA (in PBS) and washed with PBS thrice. Permeabilization was done using 0.1% Triton-X100 in PBS for 5mins at room temperature. Non-specific binding of the primary antibody was avoided by blocking. 0.2% fish skin gelatin (FSG) (Sigma Catalogue Number: G7041) diluted in PBS was used for this purpose. FSG was added to the cells and incubated for 20mins at room temperature. Primary antibodies were added at the standardized dilutions in the blocking buffer and incubated overnight at 4°C. The cells were washed thrice with PBS to remove unbound antibody. Secondary antibodies (Alexa Flour 488, Alexa 555 and Alexa 647) were added at the appropriate dilutions made in PBS. Hoechst (Sigma Catalogue Number: 94403) was also used at a dilution of 1:1000 to counterstain the nuclei. The coverslips were incubated at room temperature for 45mins. The cells were washed thrice with PBS and mounted using VECTASHIELD anti-fade mounting media (Vector Labs Catalogue Number: H-1000-10). The slides were imaged using the Zeiss 710 confocal microscope.

4.19 Processing of Tumour Biopsies

The biopsies were collected in PBS and dissociated into single cells. The biopsies were washed twice in PBS and minced well using a scalpel. The finely-chopped tumour pieces were subjected to collagenase type IV (Gibco Catalogue Number: 17104019) treatment at a concentration of 0.2mg/ml under constant agitation for 15mins. The undigested tumour clumps were allowed to settle and the clear liquid (containing

dissociated tumour cells) was collected. The process was repeated on the undigested tumour tissue until adequate number of single cells were obtained.

The study was approved by the Institutional Ethics Committee (IEC) at St. John's Medical College. A copy of the ethical clearance has been included in Appendix A3. The samples were collected with patient consent and all experiments were carried out as per the guidelines. A copy of the subject information sheet and consent form is also provided in Appendices A4 and A5.

4.20 Immunohistochemical Staining

Immunohistochemical staining was performed on clinical specimens to determine the expression and localization of RHOC in cervical tumours. The staining was carried out on paraffin-embedded tissue sections that were fixed in formalin.

The sections were incubated in xylene for deparaffinization and then rehydrated in decreasing ethanol percentages. The antigens were then retrieved by incubating in 10mM citrate buffer (pH 6.0) for 10mins at 85°C. The slides were allowed to cool at room temperature and washed twice in water for 5mins each. Exogenous peroxidase activity was quenched by incubating the slides in 3% hydrogen peroxide in methanol for 15mins. This was followed by two washes in distilled water. Primary antibody was then added onto the sections and they were incubated overnight at 4°C. The antibody used was RHOC (Santa Cruz Biotechnology, Inc., Catalogue Number: SC-26481). The sections were then incubated with biotinylated secondary antibody (Vector Laboratories) followed by streptavidin–HRP complex (Vector Laboratories) at room temperature for 40 min each. The colour was developed using DAB (3,3′-diaminobenzidine, Sigma) and the nuclei were counterstained with haematoxylin. The sections were then dehydrated by immersing them in increasing concentrations of ethanol, and finally xylene. They were mounted and visualised under the Nikon Eclipse Ts2 inverted microscope.

4.21 Immunofluorescent Staining (for sections)

Sections of 7µm thickness were taken from biopsies embedded in OCT compound cryostat embedding medium. The cryosections were incubated in 0.01M citrate buffer at 90°C for 20mins. The slides were allowed to cool to room temperature and the sections were blocked with 3% BSA made in PBS. Primary antibody was added at the appropriate dilutions in the blocking buffer and the sections were incubated overnight at 4°C. This was followed by three PBS washes and incubation with secondary antibody for 45mins at room temperature. Unbound antibody was removed by washing with PBS. Hoechst was added at a dilution of 1:500 and the sections were incubated for another 15mins at room temperature. The slides were mounted with VECTASHIELD anti-fade mounting media and imaged using the Zeiss 710 confocal microscope.

4.22 Antibody-Mediated Inhibition of Proteins

Due to the absence of a chemical inhibitor for RHOC, the antibody-mediated inhibition approach was undertaken. Saponin, a terpenoid that acts as a mild surfactant, was used to create pores in the phospholipid bilayer of the cell membrane, thereby aiding the entry of RHOC-specific antibodies (Behbehani et al., 2014). Once inside the cell, the RHOC antibody binds to its target protein, leading to its consequent degradation. As published earlier by our lab, saponin treatment alone does not lead to significant cell death (Pranatharthi et al., 2019). The method is also seen to successfully reduce levels of the target protein within cells.

Cells were seeded at 70% confluency in DMEM containing 10% FCS. The next day, the media was replaced with DMEM containing 0.0025% saponin (w/v) and 2µg of the desired antibody. The cells were incubated at 37°C, 5% CO_2 for 48h. At the end of 48h, the cells were retrieved and subjected to the required assays.

4.23 Irradiation of Cells

Cells were seeded in DMEM supplemented with 10% FCS in 6-well plates. On the day of irradiation, the media was replaced with 9ml of sterile PBS to create a 1cm water interface between the cells and the air. The linear accelerator was programmed to

deliver the dosage at a depth of 1cm, i.e., at the level of the cells. As published by our lab, several doses of radiation were attempted and 6Gy was found to be the LD_{50} dose for SiHa cells (Pranatharthi et al., 2019). The cells were therefore delivered with a single fraction 6Gy radiation for all experiments. Once the radiation treatment was over, the PBS was replaced with media and the cells were placed in the incubator to be used for various experimental assays.

4.24 Fractionation of Cell Lysates

In order to distinguish nuclear molecular events from cytosolic interactions, the nuclear and cytosolic components were collected separately and studied. A cellular fractionation method based on osmotic lysis was used for this purpose.

Media was removed completely and the cells were washed with PBS. Low osmotic buffer (composition given in Appendix A1) was added (500µl for a 100mm dish) and the cells were observed for disruption of the cell membrane. This approximately takes around 10mins when incubated on ice. Upon complete disruption of the cell membrane, the cytosolic fraction was removed carefully and 500µl of high osmotic buffer (composition given in Appendix A1) was added to the cytosolic fraction to avoid precipitation of proteins. The resulting mixture was spun at 12,000rpm for 15mins and the supernatant collected. This is the cytosolic fraction.

The dish now consists of intact nuclei. The nuclei were washed gently with cold PBS to remove any remnants of the cytosolic fraction. The PBS was removed completely and 500µl of RIPA buffer was added to the nuclei. The dish was incubated on ice for 15mins. After 15mins, the nuclei were collected using a policeman scraper. Syringing was done to ensure shearing of DNA. The nuclear lysate was spun at 12,000rpm for 15mins and the supernatant was collected in another tube. This is the nuclear fraction

4.25 Immunoprecipitation

Immunoprecipitation is used to identify proteins that interact with another target protein (Kaboord and Perr, 2008). The technique utilizes antibodies against the target protein to help “pull-out” protein complexes from protein lysate mixtures. Proteins A and G, sourced from bacteria, have very high affinity to the Fc region of human

immunoglobulins (IgGs). Sepharose/agarose/magnetic beads coated with proteins A or G are therefore used to immobilize antibodies. The magnitude of affinity of Proteins A and G to IgGs vary depending on the type of IgG and must therefore be chosen accordingly. Once the antibody binds to the beads, the antibody-bead conjugates are incubated with the lysate. The antibodies bound to the beads via the Fc region, now bind to the target protein via the Fab region. The beads are then separated from the lysate either by centrifugation or by magnetic separation. The target proteins thus "pulled-out", bring along with them other interacting partners, which may then be analysed to identify proteins that interact with the target protein.

Cells were cultured in DMEM supplemented with 10% FBS. Around 10^7 cells were utilized for each condition. The media was removed completely and the cells were washed with cold PBS. Proteins were cross-linked prior to beginning the procedure, to ensure that the protein-protein interactions are retained throughout (Corgiat et al., 2014; Zhang et al., 2007). Cross linking was done using 5mM DSP (dithiobis succinimidyl propionate) (Invitrogen Catalogue Number: 22585) dissolved in 1%DMSO. DSP comprises of NHS-esters separated by 8 carbon spacer arms. These NHS esters react with primary amines available on proteins, to form stable amide bonds thereby cross-linking the interacting proteins. The DSP slurry (made in PBS) was poured onto the cells and incubated for 30mins at room temperature under slow agitation. The slurry was then removed, and excess DSP was quenched using 25mM Tris buffer (pH 7.4). The Tris buffer was removed completely and the cells were washed with PBS. Fractionation was performed as described in section 4.24.

The nuclear fraction (NF) thus obtained was pre-cleared to remove proteins that non-specifically bind to Protein G, by using ProteinG dynabeads (Invitrogen Catalogue Number: 10003D) equilibrated in lysis buffer. Equilibrated dynabeads (20µl per pull-down) were incubated with 2µg of the desired antibody at room temperature for 10mins and then added to the pre-cleared lysate. IgG was used as the negative control. The proteins were allowed to bind overnight to the antibody-bead complexes under gentle agitation at 4°C. The beads were washed twice with lysis buffer to remove non-specifically binding proteins and incubated at 95°C for 10mins in 20µl of 2X Laemmli buffer. The beads were separated out using the DynaMag (Invitrogen Catalogue Number: 12321D) and the clear supernatant was subjected to further analysis to identify binding partners by either immunoblotting or 2D gel electrophoresis.

4.26 2D Gel Electrophoresis

2D gel electrophoresis is a method used to separate proteins based on two parameters- isoelectric point (the pH at which proteins have a net zero charge) and molecular weight (O'Farrell, 1975). These two properties are unique to proteins, thereby lending high resolution and sensitivity to separation. Here, 2D gel electrophoresis was used to separate complex protein mixtures before subjecting them to mass spectrometry-based identification.

The immunoprecipitated beads stored at -30°C were thawed and incubated with 250µl of elution buffer at room temperature for 30mins. The composition of elution buffer was as follows- urea (7M), thiourea (2M), CHAPS (4%), ampholyte (1%), dithiothreitol (65mM), IPG buffer (GE Healthcare Catalogue Number: 17600440) and bromophenol blue (0.1%). The beads were separated out and the eluted proteins were loaded onto the strip holder carefully, taking care not to introduce any air bubbles during the process. 13cm long IPG strips with a non-linear pH gradient ranging from 3-11 was utilized for the process (GE Healthcare Catalogue Number: 17600375). It was ensured that the pH ranges of the IPG strip and the IPG buffer overlapped. The IPG strip was lowered (gel side down) onto the lysate carefully with the positive end of the strip towards the positive end of the strip holder. After 5mins mineral oil was added over the strip. The lysates were allowed to adsorb onto the strip at room temperature overnight.

The next day, isoelectric focusing was done using the Ettan IPGphor3 system from GE Healthcare. The program used is detailed in **Table 4.11**-

Voltage	Time
300V	1h
500V	1h
500-1000V (gradient)	4h
1000-5000V (gradient)	4h
5000V	3h
500V	overnight

Table 4.11: The program used for isoelectric focusing.

On the next day, the strips were run at 5000V for 30mins to refocus the bands. The mineral oil was removed and the strips were placed (gel side up) in the strip holder. 2ml of Equilibration Buffer I was added and incubated at room temperature for 15mins. Buffer I was removed completely and Equilibration Buffer II was added onto the strip and incubated for another 15mins. Buffers were used from the BIO-RAD 2D gel kit (Catalogue Number: 17600440). The strip was then placed on top of a 10% gel with marker loaded at the positive end. The assembly was then overlaid with low melt agarose. The gel was run and silver staining performed to view the spots. Specific spots were then excised and subjected to MS analysis to identify proteins.

4.27 Staining of Proteins on Gels

Proteins can be detected on polyacrylamide gels using various staining techniques like coomassie and silver staining. These methods have been used to stain proteins for decades due to their compatibility with downstream protein identification techniques like mass spectrometry (Winkler et al., 2007). While coomassie staining has been routinely used to detect proteins in the ranges of 30-50ng (Smejkal, 2004), silver staining is highly sensitive, and is used to detect lower amounts of protein, often upto a fraction of a nanogram (Chevallet et al., 2006). Here, the proteins resolved by 2D gel electrophoresis were detected using coomassie and silver staining procedures.

The proteins separated by 2D gel electrophoresis were first stained by coomassie, followed by silver staining. The gel was fixed in 10% acetic acid and 25% isopropanol for 30mins. The gel was then incubated in staining solution (10% acetic acid, 25% isopropanol, 0.025% Coomassie brilliant blue R-250 (BIO-RAD, Catalogue Number 161-0400)) overnight with gentle agitation. The gel was then destained in 10% acetic acid for a few hours, with regular changes of the destaining solution, until a clear background was obtained. Once destained, the gel was soaked in 30% ethanol for 3h for dehydration. The 30% ethanol was discarded and the gel was soaked in 10% ethanol twice, 5mins each incubation. This was followed by 3 washes in deionized water for 10mins each to gradually rehydrate the gel. The gel was then incubated in Farmer's Reagent Reducer for 15mins at room temperature. It was then washed thrice in deionized water and transferred carefully into another box containing 0.1% silver nitrate and incubated for 45mins. The gel was washed for 30s in deionized water and then transferred to another box. The gel was washed quickly with a small volume of developer and the spots were developed by soaking the gel in a larger volume of developer (enough to immerse the gel), until the desired intensity of staining was achieved. The gel was then soaked in stop solution for 30mins. The gels loaded with lysates from the isotype control and the RHOC pull-down were compared and the unique spots thus identified were excised and subjected to mass spectrometry-based identification of the isolated proteins. The composition of the reagents used are detailed in Appendix A1.

4.28 Mass Spectrometry

Mass spectrometry is a highly sensitive technique used to identify proteins (Siebert et al., 2002). Mass spectrometry involves conversion of the sample into ions and then separating the generated ions based on mass (m) to charge (z) ratio. The ions separated are then passed into an ion detector, to identify the molecule of interest. Initially, the application of mass spectrometry was limited to volatile compounds, but with new ionization techniques like Matrix Assisted Laser Desorption Ionization (MALDI) and Electron Spray Ionization (ESI), mass spectrometry analysis has been extended to a vast range of molecules, including proteins (Domon and Aebersold, 2006). Here, the

immunoprecipitated proteins separated by 2D gel electrophoresis were subjected to mass spectrometry for protein identification.

The excised gel pieces were destained by washing thrice in wash solution (50% acetonitrile and 50mM ammonium bicarbonate). The gel pieces were dehydrated using acetonitrile and rehydrated in reduction solution (10mM DTT and 100mM ammonium bicarbonate). The gel was treated with alkylation solution (50mM iodoacetamide and 100mM ammonium bicarbonate). Post washing, the gel was subjected to trypsin digestion and the extracted peptides were subjected to MS/MS using the Bruker Daltoincs ESI Q-TOF system with the Proxeon EASY-nLC. The data generated was analysed using the MASCOT database to identify the precipitated proteins.

4.29 Chromatin Immunoprecipitation (ChIP) Assay

The ChIP assay is routinely used to study DNA-protein interactions (Gade and Kalvakolanu, 2011). It can be used to investigate dynamic changes in the regulatory proteins that bind to regions on the DNA in response to an external chemical stimulus, differentiation or any other signalling response. Here, ChIP was performed on SiHa-R cells using the Simple ChIP Enzymatic Chromatin IP Kit (CST Catalogue Number: 9003).

10^7 cells were utilized per condition of the ChIP assay. PFA (paraformaldehyde) was used for cross-linking the proteins and DNA. PFA was added to the media to achieve a final concentration of 1%. Cells were incubated at room temperature for 10mins. Excess PFA was quenched using glycine. The cells were washed twice with cold PBS and the buffer was removed completely. 2ml of PBS along with protease inhibitor cocktail was added to the dish and the cells were scraped into the buffer. The cells were spun at 2000g for 5mins at 4°C.

In order to isolate the nuclei, the cells were resuspended in 1ml Buffer A (cold) containing DTT and protease inhibitors. The cells were incubated on ice for 10mins and mixed by inversion every 3mins. The tubes were then spun at 2000g for 5mins at 4°C. The supernatant was removed completely and the pellet was resuspended in 1ml of cold Buffer B containing DTT. The cells were spun at 2000g for 5mins at 4°C. These are the nuclei.

Cell pellets were resuspended in 100µl Buffer B containing DTT. 0.5µl of micrococcal nuclease (MNase) was added per reaction and the tubes were incubated at 37°C for 20mins. The enzyme was inactivated by adding 10µl of 0.5M EDTA and incubating on ice for 2mins. The nuclei were spun down at 16,000g at 4°C for 1min.

In order to shear the DNA, sonication was used. The pellet was resuspended in 100µl ChIP buffer with protease inhibitor cocktail and incubated on ice for 10mins. The nuclei were sonicated in 20s pulses at a frequency of 60Hz, thrice. During the intervals between the sonications, the samples were incubated on ice. The lysates were clarified by spinning at 9400g for 10mins at 4°C. The supernatant is the cross-linked chromatin.

A small part of this chromatin (50µl) was kept aside to be used as input DNA. RNA was digested and the DNA was purified using spin columns. The DNA was run on a 1% TAE gel to ensure that the DNA fragments ranged in sizes between 150-900 bp in length. DNA concentration was determined using the Qubit Fluorimeter.

The samples were diluted such that 500µl of the sample contained 10µg of cross-linked DNA. Protein G dynabeads were incubated with 2µg antibody at room temperature for 10mins to allow binding. Isotype antibodies were used as the negative controls. The samples were gently agitated overnight at 4°C to allow binding of the antibodies to the protein-DNA complexes.

The next day, the beads were washed twice with low salt buffer and once with high salt buffer. The supernatant was completely removed using the DnyaMag and the protein-DNA complexes were eluted in elution buffer. The cross-links were reversed using 6µl of 5M sodium chloride and proteinase K. The eluted DNA was purified using spin columns and quantified using the DNA Qubit High sensitivity assay kit.

Equal amounts of input DNA, IgG purified and DNA pulled down by specific antibodies were tested for promoter enrichment by qPCR analysis. Values thus obtained were normalized against the isotype (IgG) control.

4.30 Luciferase Assay

The Luciferase assay is a highly sensitive technique to measure gene activity (Yun and DasGupta, 2014). It uses a vector with the promoter of the gene of interest placed upstream of the Luciferase gene. Based on experimental conditions, if there are changes in expression to the target gene, regulatory molecules bind to the target promoter and initiate transcription of the luciferase reporter gene, leading to increased amounts of the luciferase enzyme. The amount of luciferase is read by addition of the substrate, luciferin, which results in the production of light, which may be recorded by a luminometer. Since the amount of luciferase enzyme produced is proportional to the activity of the promoter, the amount of light produced by the system is a direct indication of gene activity. Here, the activity of the NANOG promoter was assessed using the Dual Luciferase Reporter Assay system from Promega (Catalogue Number: E1910).

Cells under various treatment conditions were transfected with the pNANOG-Luc plasmid procured from Addgene (Catalogue Number: 25900) and Renilla-Luc. The culture media was removed and the cells were washed with PBS. Passive lysis buffer was added to the cells and the cells were scraped into a tube. The lysates were cleared by spinning at 14,000rpm for 30s. 100µl of Luciferase Assay Reagent II was dispensed into a tube and 20µl of the sample was added. The sample was mixed quickly to ensure homogenization. The Firefly Luciferase reading was recorded using the LUMI luminometer from MicroDigital. 100 µl of Stop and Glo reagent was added to the tubes and mixed gently. A second reading (*Renilla* luciferase) was recorded. Promoter activity was calculated after normalization against the respective experimental controls.

4.31 RNA-Sequencing and Analysis

RNA-sequencing was performed using Illumina paired end sequencing (150x2). The sequenced reads were aligned to the Homo sapiens DRCh38 build genome downloaded from Ensemble database. Tophat was used to align the transcript sequences and Cufflinks was used to create a combined assembly. A Differential Gene Expression (DGE) analysis was performed using the Cuffdiff package. Gene Ontology (GO) analysis was performed using DAVID. Heatmap analysis was done using Clustvis, an

R-based bioinformatic tool. The transcriptomic analysis was performed in replicates of n=2. STRING database (version 11.0) was used to study the interaction networks. Volcano plots were generated using the online tool, Shiny.

4.32 Infinium Human Methylation 850 (EPIC array) and Analysis

DNA was isolated from SiHa-N and SiHa-R cells. Post quantity and quality checks, the DNA was subjected to bisulfite treatment and the Infinium Human Methylation 850 (EPIC array) was performed in duplicates to identify the levels of methylation at various locations in the genome. Briefly, the data generated was pre-processed using SWAN and RnBeads was utilized to visualize the DNA methylation profiles. p-values were calculated by the *limma* package and corrected for multiple testing. Strongly differentially methylated regions with a false discovery rate of <0.05 were taken for further analysis. Heatmaps for differential methylation in SiHa-N and SiHa-R were generated using Clustvis.

4.33 Treatment of Cells with Aloe vera

The gel from fresh Aloe vera leaves was scraped out using a sterile scalpel and the gel was macerated well using a sterile mortar and pestle. The viscous Aloe vera gel was spun down at 4000rpm for 5mins. The supernatant was aliquoted into sterile 1.5ml microcentrifuge tubes at a volume of 1ml each. 1ml of Aloe vera gel weighed 1.71g. The aliquots were stored at -80°C until use. When required, the Aloe vera was thawed out and 464µl of 50% ethanol was added to the tubes (Beya et al., 2012). The tubes were kept on slow rotation for 1h at room temperature. The tubes were spun at 4000rpm for 5mins and the supernatant thus obtained was used for the experiment.

Cells were seeded in DMEM supplemented with 10% FCS at 60% confluency. 25µl of the Aloe vera extract was added per ml of media on the next day. The media was replaced everyday over the next 3 days, with fresh media containing the Aloe vera extract. The cells were retrieved at the end of 72h and subjected to the required assays.

4.34 Statistical Analysis

The mean and standard deviations were computed for the experiments performed in triplicates and the significance was calculated using the t-test. $p<0.05$ was considered significant.

CHAPTER-III

RHOC in Cancer Stem Cell Maintenance

5.1 Introduction

RHOC, a known cytoskeletal regulator, has been implicated in numerous tumour phenotypes across various cancer models. It has been demonstrated to play a significant role in oncogenesis, proliferation, angiogenesis, EMT, intravasation and anoikis resistance (Kamai et al., 2003; Shikada et al., 2003; van Golen et al., 2000a; Wang et al., 2003). The plasticity model of cancer initiation and progression endorses the hypothesis that in order to form metastatic outgrowths, cancer cells must be able to disseminate from the primary tumour, intravasate through the endothelial lining, survive migration in the bloodstream and finally home and colonize at suitable distant sites (Guan, 2015). Since RHOC has been shown to be at the helm of nearly every stage of metastasis, it was envisaged that RHOC could be instrumental in imparting cells with the plasticity required to survive and adapt to these trying conditions.

Over the past few years, reports have indicated a link between RHOC and maintenance of the stem cell population. ALDH, a CSC marker was observed to have an association with RHOC in breast cancer (Rosenthal et al., 2012). Analysis of clinical samples divulged a positive correlation between RHOC and ALDH1. Tumorigenicity assays with limiting numbers of cells in mice exhibited significant loss in tumorigenic potential upon RHOC knockdown in $ALDH^+$ cells, further cementing the association between RHOC and stem-like potential. In head and neck cancers, depletion of RHOC in cell lines was found to result in reduction in expression of stemness markers, and loss of tumoursphere formation ability (Islam et al., 2014). These phenotypes were attributed to activation of the STAT3 pathway via IL-6. In another study, depletion of RHOC was found to result in reduced resistance of aggressive ovarian cancer cell lines A2780-PM and A2780-PTX-PM (Sang et al., 2016). RHOC inhibition was also found to result in decreased expression of CD133 and CD117, known markers for stem-like ability in ovarian cancers. However, there is no report till date that links RHOC to maintenance of stemness characteristics in cervical cancer.

Despite emerging evidence implying a possible link between RHOC and stemness capability, specific details regarding the mechanism behind this observation remain elusive. This chapter presents evidence to prove that RHOC mediates CSC maintenance in the cervical cancer model using clinical specimens, cervical cancer cell lines and xenografts. Utilizing various phenotypic assays, biochemical experiments and high-

throughput approaches, the role of RHOC in enhancing stem-like ability in cervical cancer has been ascertained.

5.2 Results and Discussion

5.2.1 RHOC Over-Expressing Cells Display Superior Efflux Ability

$CD34^+$ cells, one of the first cellular populations to be associated with stem-like ability in blood cancers, have been characterized by their ability to efflux lipophilic dyes (Goodell et al., 1996). This superior effluxing ability was found to be independent of the multi-drug (MDR) efflux system, known to be responsible for chemoresistance of the CSC pool (Hirschmann-Jax et al., 2004). They have instead been attributed to increased expression of ATP-binding cassette reporter genes (Zhou et al., 2001). This subset, defined by its minute size and characteristic appearance in FACS profiles, came to be known as the "side-population" (SP) (Goodell et al., 1996; Goodell et al., 1997; Storms et al., 2000). Isolation of and further experiments on cells comprising the SP pool revealed enhanced tumorigenic ability apart from increased chemoresistance, making abundance of SP cells an important determinant of cancer progression and therapy response (Hirschmann-Jax et al., 2004). Here, RHOC over-expressing SiHa cells (SiHa-R) and cells with the background vector alone (SiHa-N), were subjected to analysis of Hoechst staining profiles to determine alterations in efflux ability upon changes in RHOC expression.

Hoechst staining analysis must be limited to the live-cell population only. The Hoechst staining procedure is known to considerably affect viability, and inclusion of dead cells could result in misjudgment of true efflux abilities (Boesch et al., 2016). Use of a dye that could discriminate cells on the basis of viability was therefore essential. To ensure that only live cells were taken forward for analysis of Hoechst staining, the cells were also stained with propidium iodide. Propidium iodide (PI) is a dye that is impermeable to viable cells, and therefore selectively stains dead cells only (Darzynkiewicz et al., 1997). PI staining is frequently used to study cell death under various experimental conditions (Crowley et al., 2016).

As shown in **Figure 5.1**, two cellular populations were observed upon staining with PI. One population was observed to have very high signal intensity, and were considered to be dead, due to their permeability to propidium iodide. Since live cells do not allow entry of propidium iodide, their emission intensities were expected to be lower. The live cell pool was selected by drawing elliptical gates around the population exhibiting lower emission as depicted in **Figure 5.1**. Further analysis of Hoechst 33342 staining

patterns was limited to this gated population only. Cellular debris (the population seen at the origin), identified by their low scatter properties (Boeck, 2001) were also excluded from the analysis.

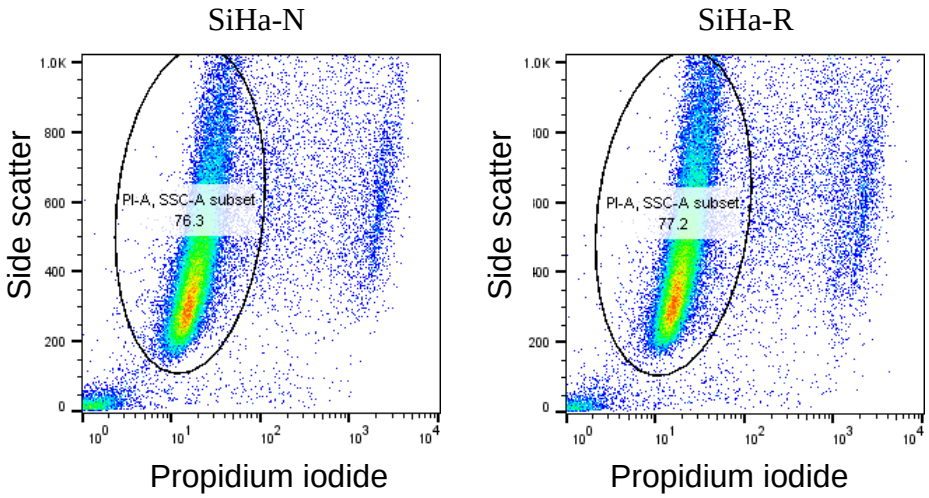

Figure 5.1: Representative FACS plots showing gating of the live cell population. The cells outside the gate were not considered for further analysis due to positive propidium iodide staining.

Cells displaying low Hoechst emissions are considered to have efficient efflux properties and are deemed to be stem-like. On the other hand, cells that were capable of retaining Hoechst for longer periods due to low efflux properties were considered to have reduced stemness characteristics. In order to determine that the observed emission patterns were due to the efficiency/non-efficiency of drug efflux proteins, verapamil, an inhibitor of ABC transporter proteins (Tsuruo et al., 1981), was used to deactivate efflux. Addition of Hoechst 33342 to verapamil-treated cells followed by FACS analysis would reveal the staining pattern expected if all cells retained Hoechst (due to impaired efflux properties). A comparison of Hoechst staining of verapamil treated cells with verapamil non-treated cells must therefore enable determination of the true stem-like pool.

Hoechst 33342 has two distinct emission spectra- one in the range of 405-450nm (Hoechst-blue) and the other spanning 630-650nm (Hoechst-red) (Ellwart and Dormer, 1990). These two emission signals were mapped on a quadrant plot to determine the

cellular population displaying low Hoechst emission. This is represented by cells in quadrant 4 (Q4). Analysis of the Hoechst staining profiles of SiHa-N and SiHa-R cells revealed significant differences between the two. While there was no visible change in the staining profiles between SiHa-N and SiHa-N cells treated with verapamil, SiHa-R cells that were not verapamil treated displayed a significant shift to the left in comparison with the verapamil treated control cells **(Figure 5.2)**. This shift implied that SiHa-R cells were more capable of effluxing the Hoechst dye as compared to SiHa-N cells, which contained the backbone vector alone.

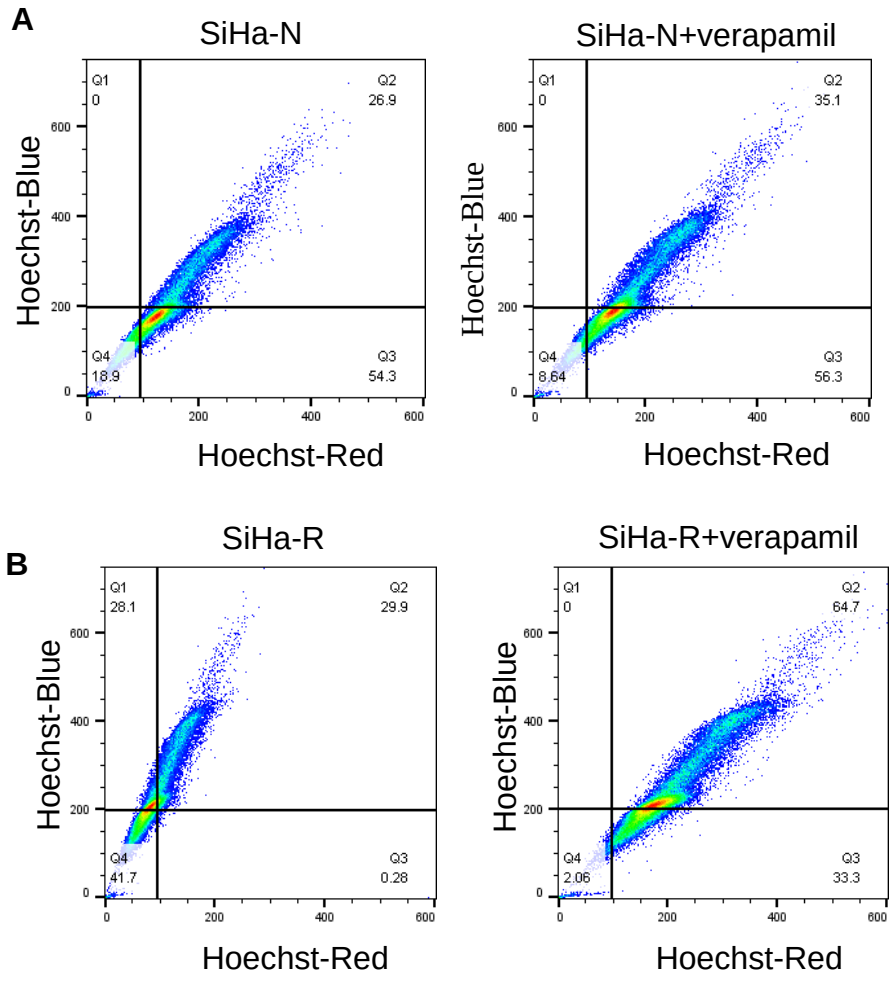

Figure 5.2: Representative FACS plots showing Hoechst 33342 emission profiles for SiHa-N (A), SiHa-R (B) and their respective verapamil-treated controls.

As expected, analysis of the percentage of cells in Q4 (low-Hoechst population) revealed that this population was significantly higher in cells over-expressing RHOC

(SiHa-R) in comparison with SiHa-N cells as represented in **Figure 5.3** (Average percentage of side-population: SiHa-N=9.62%, SiHa-R=30.07%; $p<0.05$). The values were adjusted to accommodate for the percentage of cells seen in Q4 even upon verapamil treatment.

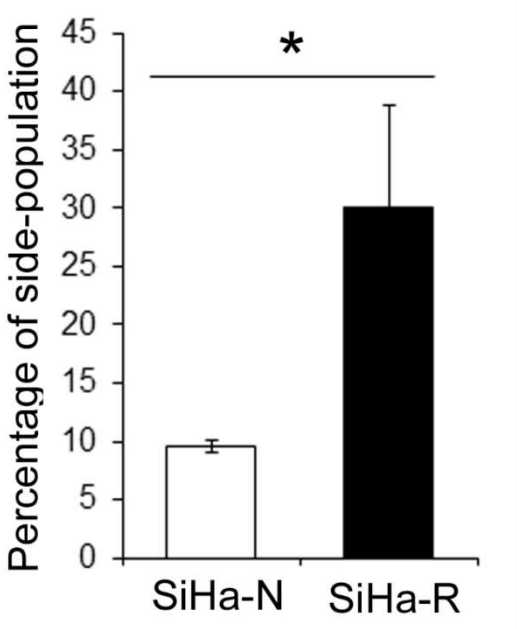

Figure 5.3: Bar graph depicting an increase in percentage of the side-population in SiHa-R cells (n=3, $p<0.05$).

The observation that RHOC over-expression leads to enhanced efflux ability adds weight to the hypothesis that increased RHOC expression enhances stem-like ability. In order to explore this further, cell lines modulated for RHOC expression were subjected to numerous phenotypic assays to investigate a possible link between RHOC expression and stemness capability.

5.2.2 RHOC Alters the Stemness Phenotype in Cervical Cancer Cell Lines

The increased stem-like ability on account of RHOC over-expression was investigated by multiple phenotypic assays. Self-renewal ability is one of the important facets of the CSC sub-population (O'Brien et al., 2010). Therefore, assays that measure the self-renewal phenotype were undertaken to determine the contribution of RHOC to stem-like ability. The clonogenic assay is a method of determining the ability of a single cell

to survive and give rise to clones (defined by a group of more than 50 cells arising from one cell) (Franken et al., 2006). Here, the clonogenic assay was utilized to determine changes in self-renewal ability with modulations in RHOC expression. When subjected to the clonogenic assay, SiHa-R cells were observed to have significantly improved clonogenicity as compared to SiHa-N. SiHa-R were found to form 3.7 times the number of clones formed by SiHa-N cells ($p<0.05$), indicative of enhanced self-renewal capability upon RHOC over-expression **(Figure 5.4)**.

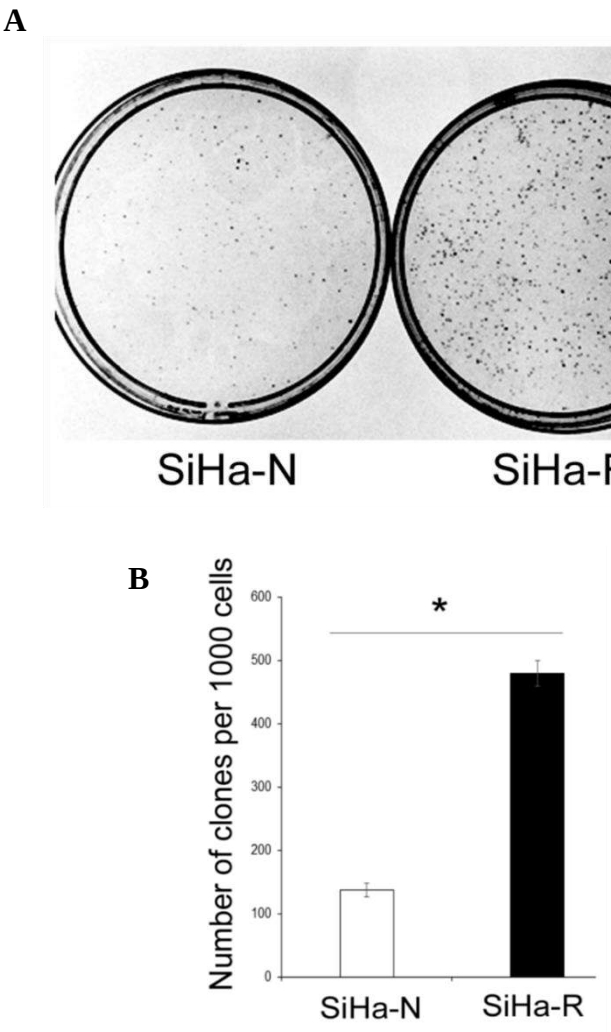

Figure 5.4: (A) Representative image of clones formed by SiHa-N and SiHa-R cells. (B) Graphical representation of the average number of clones formed by SiHa-N and SiHa-R cells ($n=3$, $p<0.05$).

Parallelly, similar studies were undertaken to determine the effect that depletion of RHOC has on cervical cancer cell lines. SiHa cells transfected with RHOC-specific

siRNA were found to result in successful knockdown of the RHOC protein as determined by immunoblotting. **Figure 5.5** is a representative immunoblot of SiHa cells transfected with RHOC siRNA 72h post transfection, with untransfected cells and cells transfected with scrambled siRNA used as negative controls.

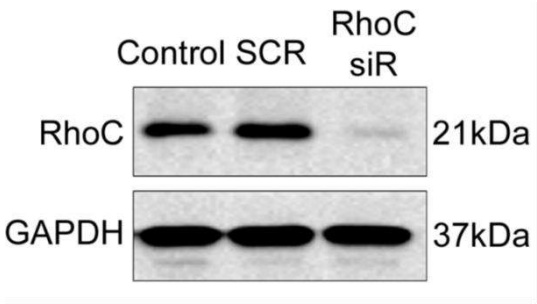

Figure 5.5: Representative western blot image showing knockdown of RHOC in siRNA treated cells (RHOC siR), as compared to scrambled negative control (SCR).

SiHa cells silenced for RHOC via siRNA-mediated inhibition were subjected to the clonogenic assay and the clones formed at the end of 14 days were counted. RHOC inhibition was found to negatively affect self-renewal ability, with RHOC siRNA treated cells (RHOC siR) found to have significantly decreased clonogenicity as compared to the scrambled control (SCR) (SCR=167, RHOC siR=9 colonies; $p<0.05$). **Figure 5.6** depicts the effect of RHOC siRNA transfection on clonogenicity.

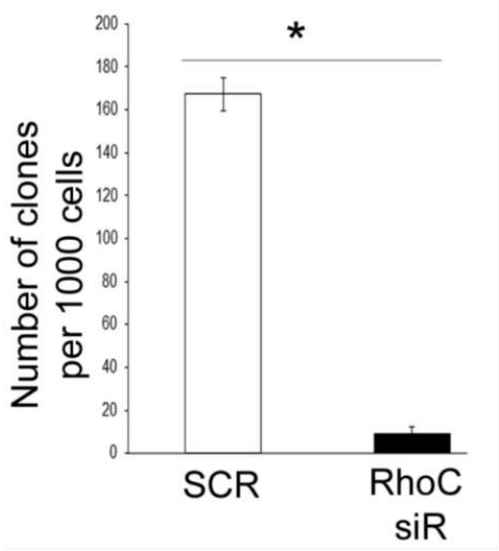

Figure 5.6: Graphical representation of the reduction in clonogenic ability upon RHOC inhibition (n=3, $p<0.05$).

The effect of RHOC depletion on self-renewal ability was also investigated using the CaSki-dnR cell line. CaSki-dnR cells stably over-express the dominant negative form of the RHOC protein. A clonogenic assay was performed on CaSki-dnR cells and CaSki-N cells that harbour the backbone vector alone. CaSki-dnR cells were observed to display loss in clonogenic ability, forming significantly lower number of colonies as compared to CaSki-N cells. **Figure 5.7 (A)** is an image of the colonies formed, while **Figure 5.7 (B)** graphically presents the decreased self-renewal ability of CaSki-dnR cells (CaSki-N=90 colonies, CaSki-dnR=33 colonies; $p<0.05$).

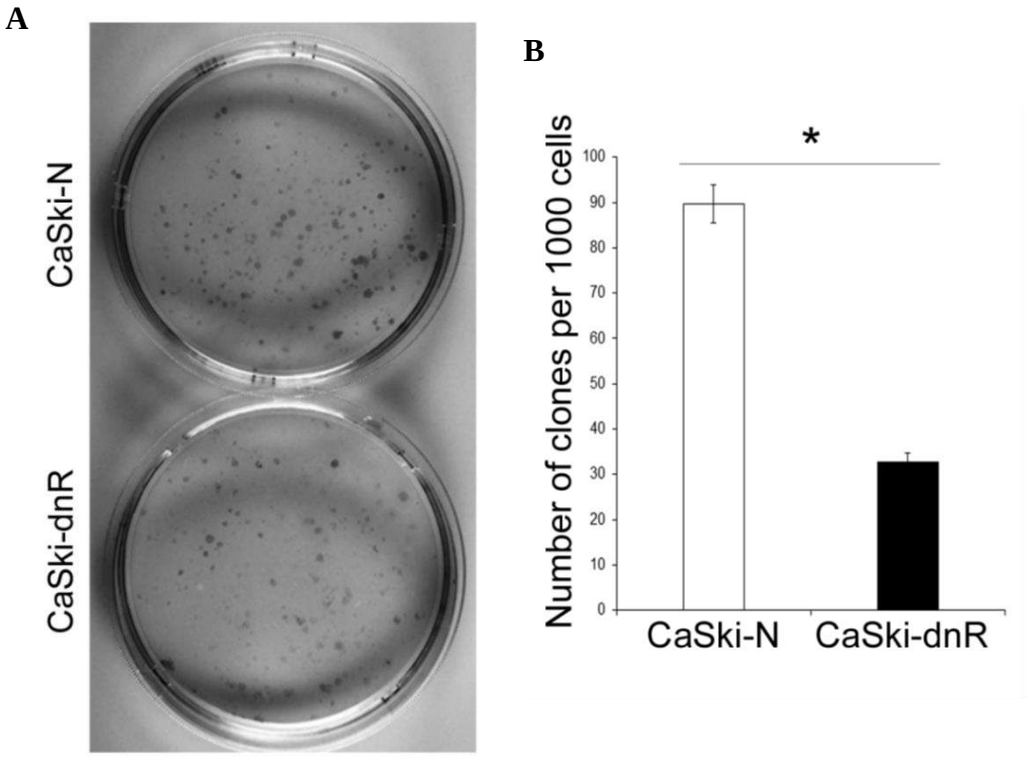

Figure 5.7: (A) Representative image of the clones formed by CaSki-N and CaSki-dnR cells. (B) Graphical representation of the average number of clones formed by CaSki-N and CaSki-dnR cells (n=3, $p<0.05$).

Most epithelial cells are reliant on the extracellular matrix and require basal attachment to allow growth and proliferation (Iyoda and Fukai, 2011). Detachment from this basal layer leads to anoikis, a mode of programmed cell death triggered due to cellular detachment (Frisch and Francis, 1994). However, in order to metastasize to secondary sites, cancer cells must be able to detach from the primary tumour, survive under

anchorage independent conditions, and wade through the bloodstream before homing into distant sites (Frisch et al., 2013). This calls for metastasizing cells to possess increased resistance to anoikis. CSCs, along with self-renewal, are known to have increased resistance to anoikis to facilitate metastatic spread (Ayla and Karahuseyinogluc, 2019). In order to analyze this ability *in-vitro*, cells were grown under ultra-low attachment conditions that induce anoikis. Those cells that had the ability to resist anoikis would survive and proliferate, while those that lacked this property would eventually undergo cell death. FACS analysis was utilized to determine the extent of cell death post culturing under anoikis-inducing conditions. SiHa-N and SiHa-R cells grown under anoikis were assayed for cell death by PI staining followed by FACS. SiHa-R cells were observed to have enhanced anoikis resistance as depicted by increased survival as compared to SiHa-N, upon culturing under anoikis-inducing conditions (SiHa-N=50% average cell death, SiHa-R=33% average cell death; $p<0.05$) (**Figure 5.8)**.

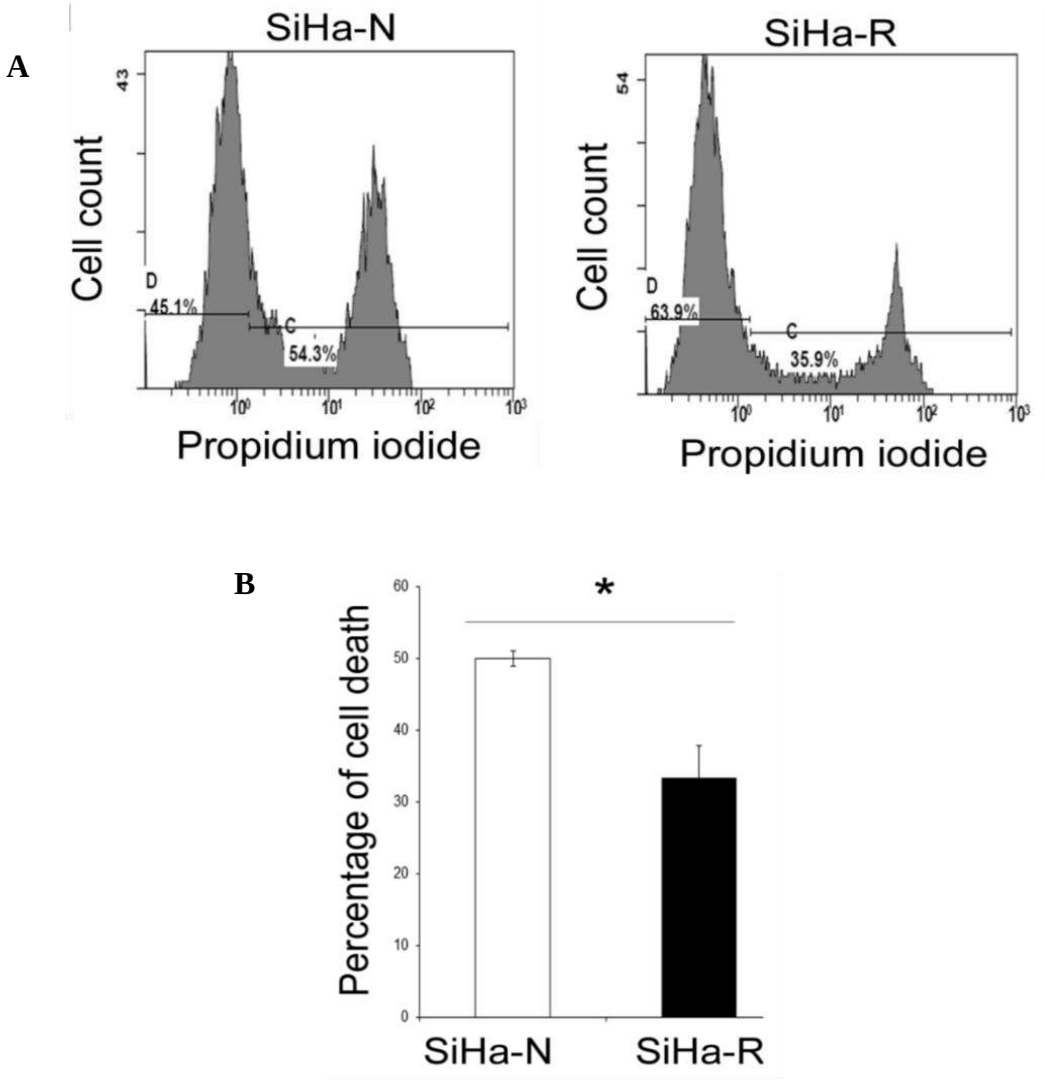

Figure 5.8: (A) Representative FACS plot showing increased propidium iodide staining in SiHa-N cells cultured under anoikis. (B) Bar graph representing the average percentage of cell death seen under anoikis in SiHa-N and SiHa-R cells. SiHa-R were observed to display better survival capability under anoikis (n=3, $p<0.05$).

In order to determine proliferative ability when cultured under anoikis, the size of the spheroidal clusters formed in SiHa-N and SiHa-R cells was compared. It was observed that apart from increased survival, SiHa-R cells also displayed better proliferative potential when cultured under anoikis conditions, as evidenced by the formation of larger spheres (SiHa-N average diameter=61µm, SiHa-R average diameter=193µm; $p<0.05$) **(Figure 5.9)**.

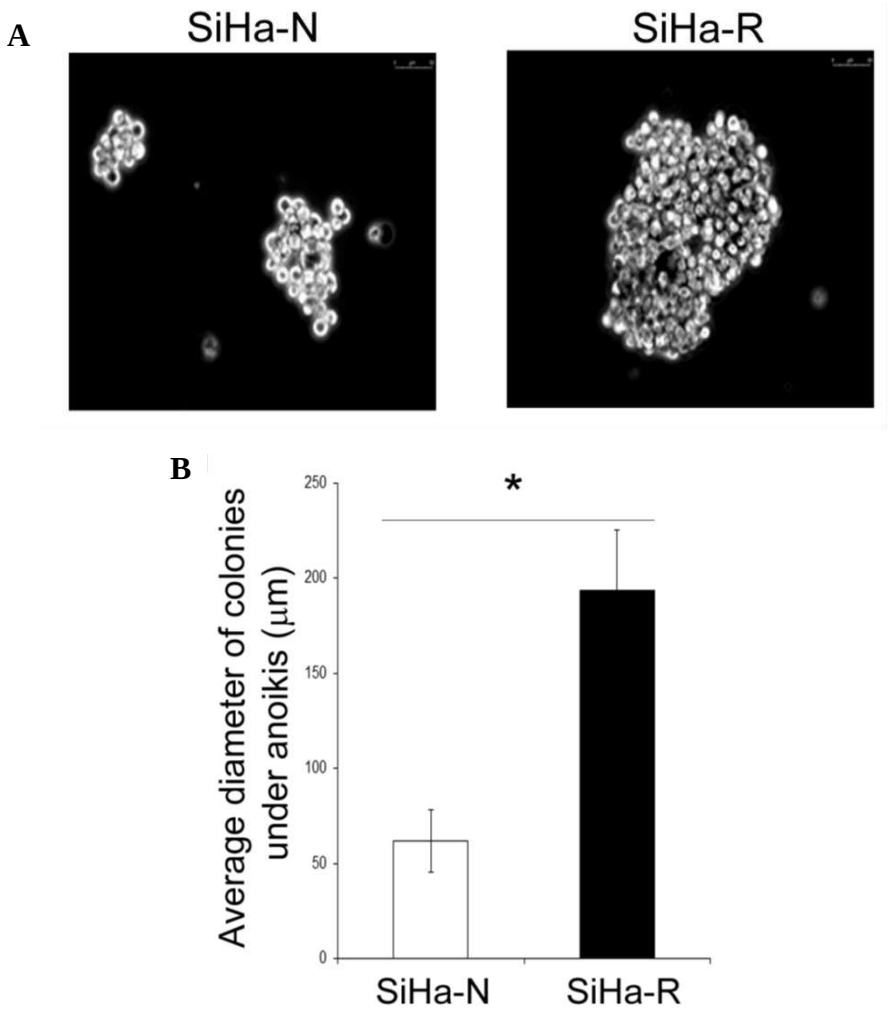

Figure 5.9: (A) Representative image of the colonies formed under anoikis by SiHa-N and SiHa-R cells (scale bars are indicated). (B) Graphical representation of the average diameter of colonies formed under anoikis conditions, with SiHa-R cells forming significantly larger colonies than SiHa-N ($n=3$, $p<0.05$).

Concomitantly, subjection of CaSki-dnR cells to the anoikis assay yielded the opposite result. CaSki-dnR cells were found to form significantly smaller spheres under anoikis in comparison to CaSki-N cells (CaSki-N average diameter=107μm, CaSki-dnR average diameter=38.6μm; $p<0.05$), indicative of loss of proliferative ability under anchorage independent conditions in RHOC compromised cells **(Figure 5.10)**.

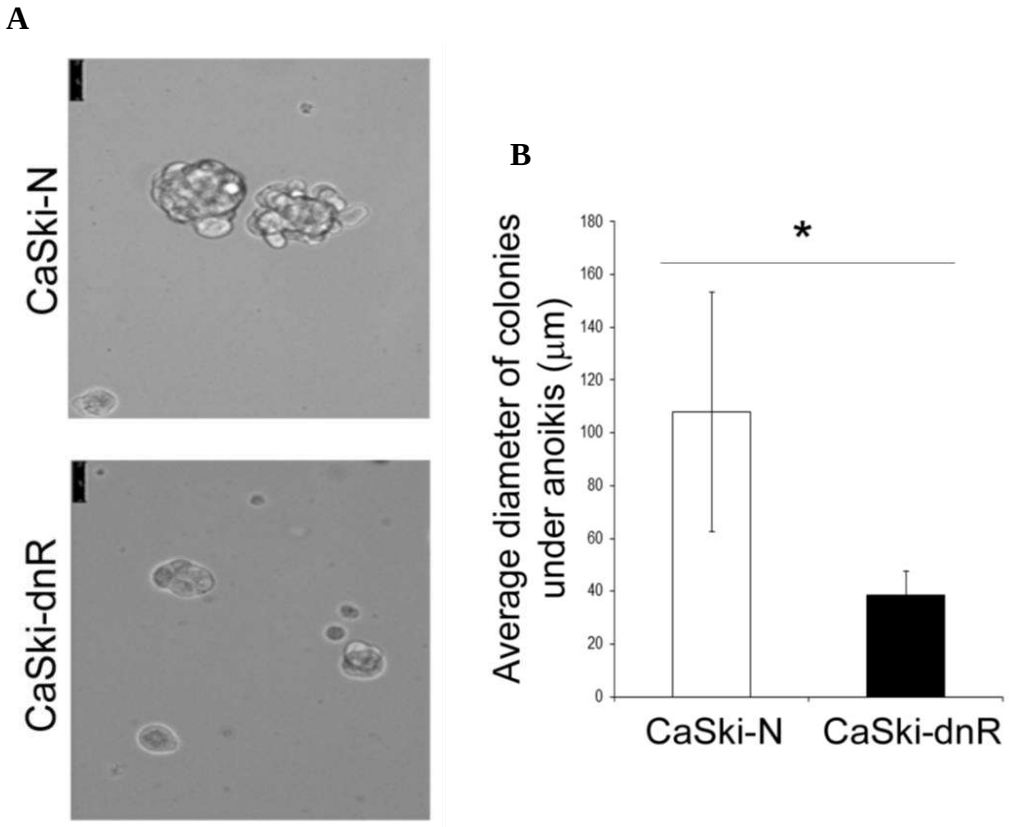

Figure 5.10: (A) Representative images of spheroids formed by CaSki-N and CaSki-dnR cells upon culturing under anoikis conditions. (B) Graphical representation of the average diameter of spheroidal colonies formed by CaSki-N and CaSki-dnR cells (n=3, $p<0.05$).

The soft agar assay was performed to test both clonogenic ability and anchorage independency simultaneously in RHOC modulated cervical cancer cell lines (Borowicz et al., 2014). In this assay, cells are suspended in solid agar media, thereby preventing interaction with neighbouring cells. They are also subjected to conditions that do not provide anchorage ability as they are seeded over a layer of agar, preventing attachment to the surface of the culture dish (Thomson and Meyskens, 1982). SiHa-R cells when subjected to the soft agar assay, exhibited an increase in the number of small (30-50μm), medium (50-100μm) and large sized (greater than 100μm) colonies as compared to SiHa-N ($p<0.05$) indicative of increased self-renewal ability under anoikis conditions **(Figure 5.11)**.

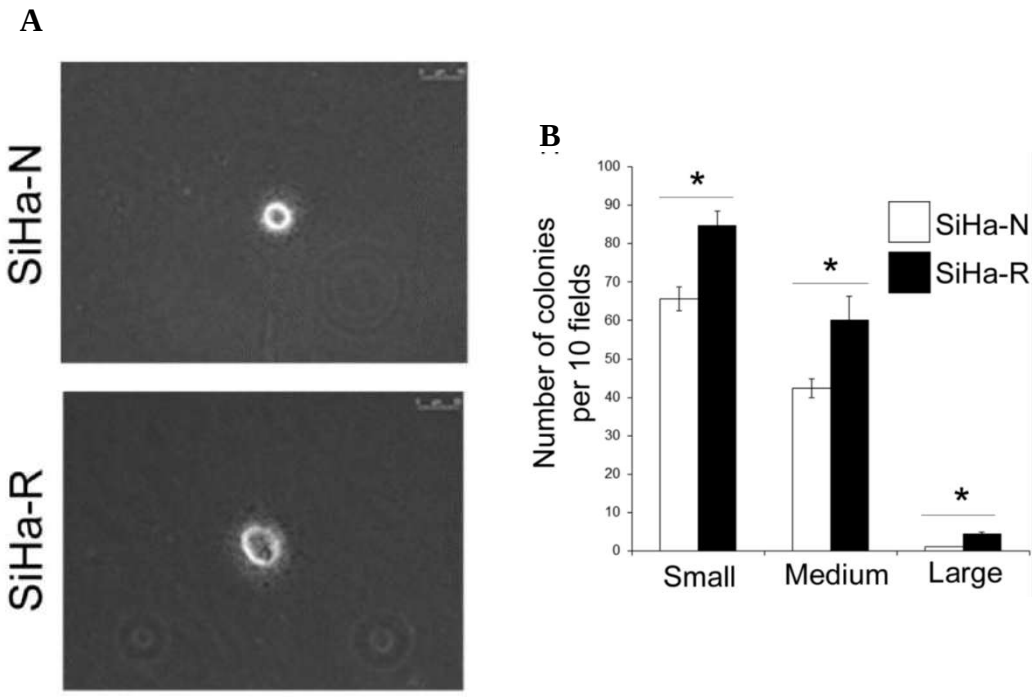

Figure 5.11: (A) Representative images of soft agar colonies formed by SiHa-N and SiHa-R under monolayer conditions. (B) Bar graph representation of the numbers of small, medium and large colonies formed by SiHa-N and SiHa-R cells in the soft agar assay (n=3, $p<0.05$).

Cells when cultured as spheroids are known to exhibit enhanced stem-like properties (Imamura et al., 2020). To determine the stem-like ability of spheroidal cells modulated for RHOC expression, SiHa-N and SiHa-R cells were grown as spheroidal cultures and the stemness capability of the resulting cells was assessed. The soft agar assay performed on spheroidal cultures of SiHa-N and SiHa-R revealed that primary spheroids of SiHa-R had enhanced stem-like ability, with a significant increase in medium and large colonies in SiHa-R cells as compared to SiHa-N cells ($p<0.05$) **(Figure 5.12)**.

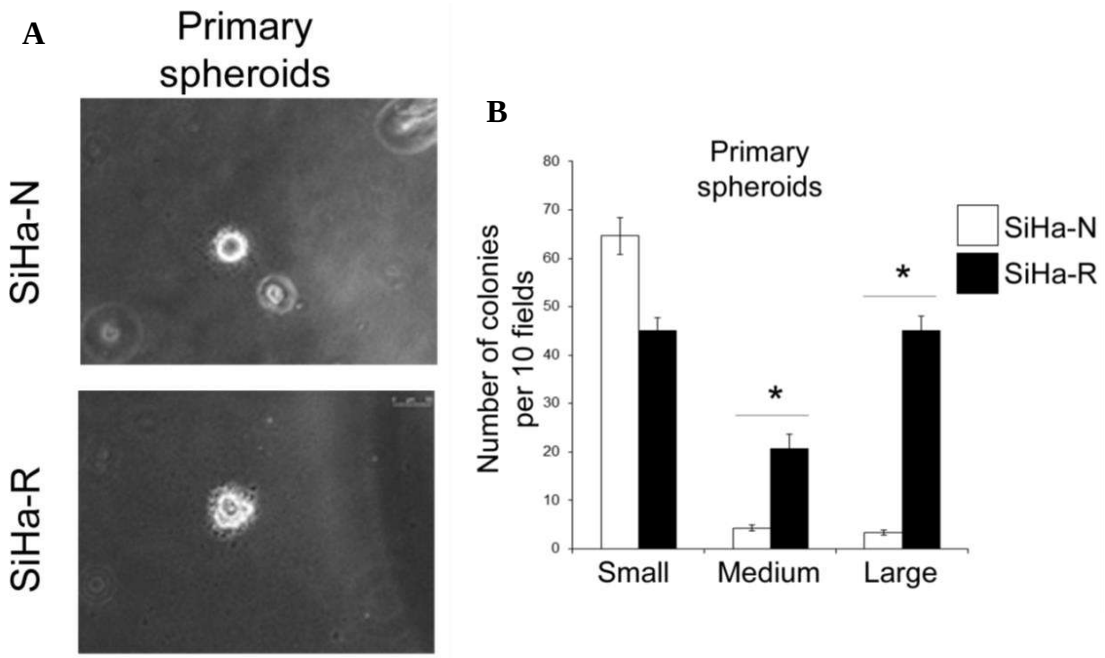

Figure 5.12: (A) Representative images of soft agar colonies formed by SiHa-N and SiHa-R spheroidal cultures. (B) Bar graph representation of the average number of colonies formed by SiHa-N and SiHa-R spheroids in the soft agar assay. (n=3, $p<0.05$).

The primary spheroidal cells were disrupted and regrown in anoikis-inducing conditions to yield secondary spheroids. As shown in **Figure 5.13**, the soft agar assay on secondary spheroidal cells also showed similar results, with SiHa-R cells forming a higher number of medium and large colonies as compared to SiHa-N ($p<0.05$). **Figure 5.13 (A)** is a representative image of the colonies formed by secondary spheroidal cultures of SiHa-N and SiHa-R, while a graphical representation of the average number of colonies formed is depicted in **Figure 5.13 (B)**.

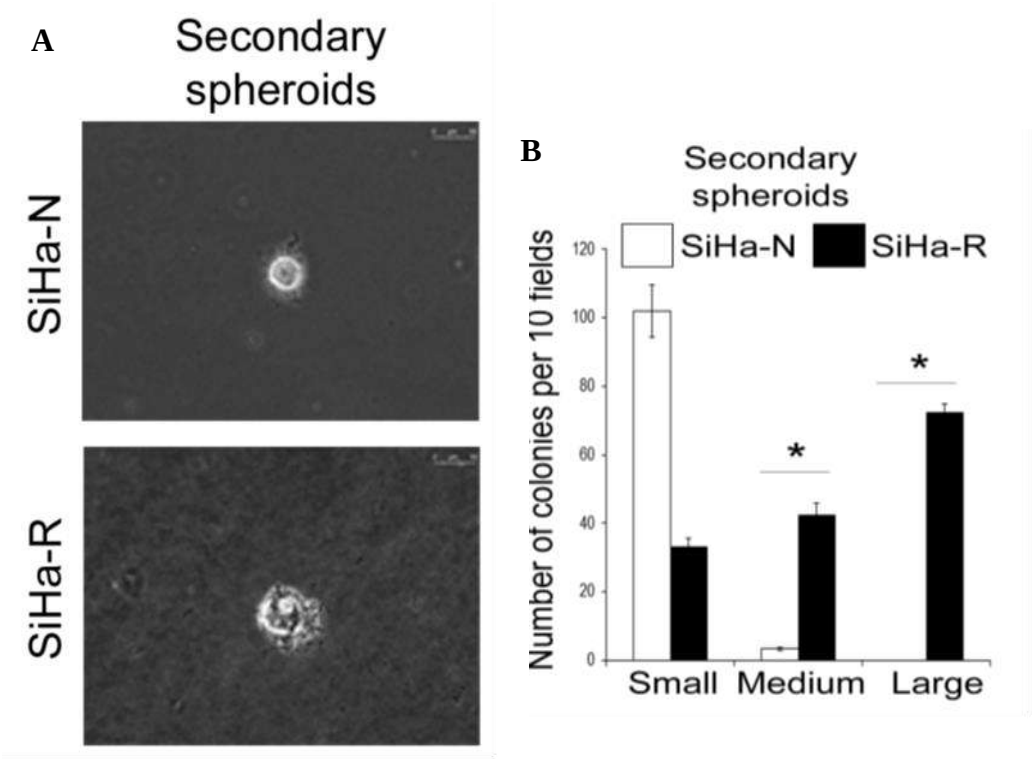

Figure 5.13: (A) Representative images of soft agar colonies formed by SiHa-N and SiHa-R when cultured as secondary spheroids. (B) Graphical representation of average number of colonies formed by secondary spheroidal cultures of SiHa-N and SiHa-R when subjected to the soft agar assay (n=3, $p<0.05$).

Therefore, using multiple phenotypic assays, it was established that cells over-expressing RHOC had enhanced self-renewal ability and anoikis resistance, both hallmark characteristics of stem cells (Cao et al., 2011; Ponti et al., 2005; Reya et al., 2001; Ricci-Vitiani et al., 2007; Yang et al., 2017). Congruently, RHOC depleted cells were proven to display diminished stemness capability as observed in CaSki-dnR and in cells subjected to siRNA-mediated silencing of RHOC. Further studies were directed towards understanding the mechanism by which RHOC alters stemness capability.

5.2.3 RHOC Modulates the Transcriptional Network and Leads to Increased Expression of Genes Involved in Stemness

Since the data presented in sections 5.2.1 and 5.2.2 suggest an association between RHOC and enhanced stemness phenotype, the mechanisms by which RHOC regulates stemness was investigated. In order to establish whether the observed stemness advantage could be attributed to transcriptional up-regulation of genes involved in stemness maintenance, an RNA-seq study was performed on SiHa-N and SiHa-R cells. The RNA-seq experiment aimed to identify the specific genes and the distinct molecular processes associated with stemness which were regulated by RHOC.

The transcriptome of SiHa-N and SiHa-R cells was compared and the genes that were differentially expressed were analyzed. Heatmap and STRING cluster analyses of the RNA-seq data are depicted in **Figure 5.14**. Analysis revealed over-expression of a plethora of genes involved in stemness maintenance, along with survival, proliferation, angiogenesis and signalling in SiHa-R cells (fold change cut-off value=0.5 and 1.5, $p<0.05$). The fold changes of selected genes involved in these processes are depicted as a heatmap generated using ClustVis (Metsalu and Vilo, 2015) in **Figure 5.14 (A)**.

The genes up-regulated in SiHa-R cells were fed into the STRING database (Szklarczyk et al., 2018) to identify the specific pathways that these genes governed. STRING revealed that distinct clusters of genes involved in stemness maintenance, signalling, cell cycle, DNA repair and angiogenesis were up-regulated in RHOC over-expressing cells, indicative of the robust nature of these cells. **Figure 5.14 (B)** depicts the STRING cluster analysis of genes over-expressed in SiHa-R cells.

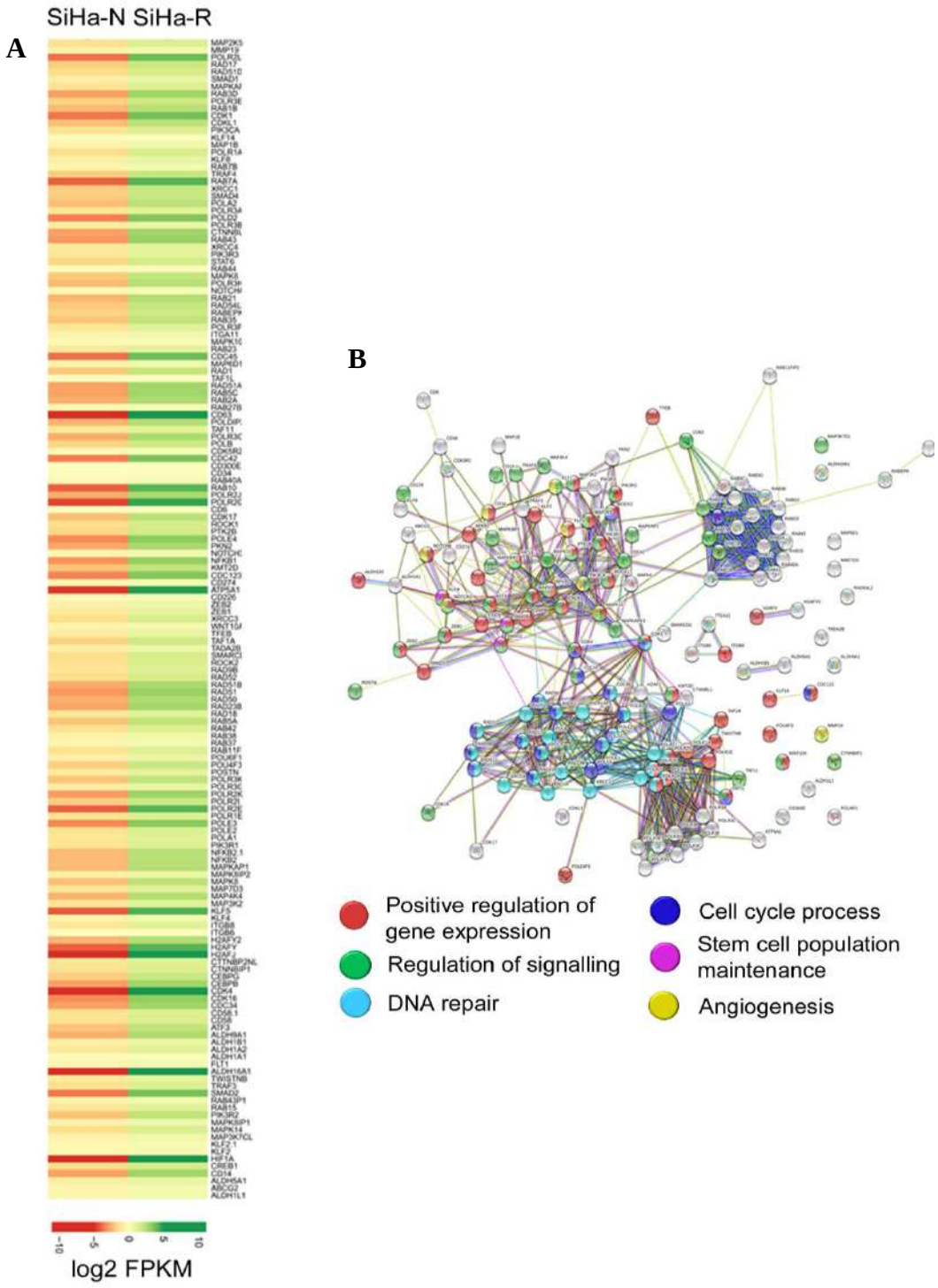

Figure 5.14: (A) Heatmap representation of the differential expression of genes involved in stemness, signalling and DNA repair in SiHa-N and SiHa-R. (B) STRING analysis of RNA-seq data of SiHa-N and SiHa-R cells showing enrichment of processes regulating gene expression, cell cycle, signalling, stem cell maintenance, DNA repair and angiogenesis.

Since analysis of the transcriptome revealed up-regulation of genes involved in stemness maintenance, a few genes were selected and qPCR analysis was performed to determine the fold change in gene expression in SiHa-R cells in comparison to SiHa-N cells. Analysis of the transcript levels validated the RNA-seq data, with stemness genes like *OCT4* (Song et al., 2018; Zeineddine et al., 2014), *SOX2* (Mamun et al., 2018; Song et al., 2016), *NANOG* (Choi et al., 2012; Zhang et al., 2016), *NOTCH1* (Fender et al., 2015; Lee et al., 2016), *NOTCH3* (Leontovich et al., 2018; Ulasov et al., 2019), *ABCG2* (Sasaki et al., 2018; Wee et al., 2016), *ALDH1* (Clark and Palle, 2017; Toledo-Guzman et al., 2018) and *CD49F* (Lopez et al., 2012; Yu et al., 2012) being significantly over-expressed in SiHa-R cells (values normalized against SiHa-N) **(Figure 5.15)**. Expression levels of the gene *GAPDH* was used as the control.

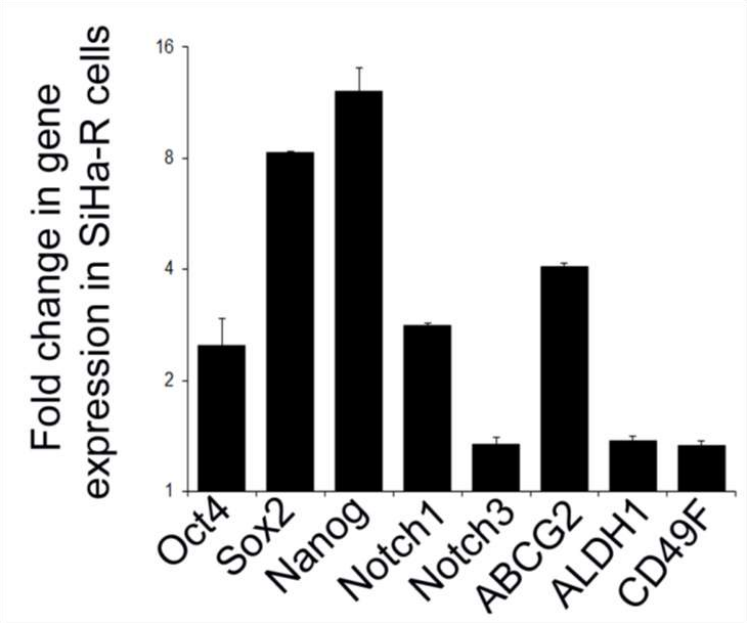

Figure 5.15: qPCR analysis confirms up-regulation of genes regulating stemness maintenance in SiHa-R cells. Gene expression values were normalized to SiHa-N, using GAPDH as the internal control (n=3, $p<0.05$).

In order to determine the effect of RHOC inhibition on gene expression, SiHa cells transfected with RHOC-specific siRNA were subjected to qPCR studies 48h post transfection. Significantly, analysis of the transcript levels of genes involved in maintenance of stemness revealed that RHOC depletion led to a decrease in expression of stemness genes. This observation helped to further establish the link between RHOC

levels and stemness gene expression **(Figure 5.16)**. The gene expression of RHOC siR treated cells was normalized to that of the scrambled negative control (SCR). GAPDH was utilized as the internal control.

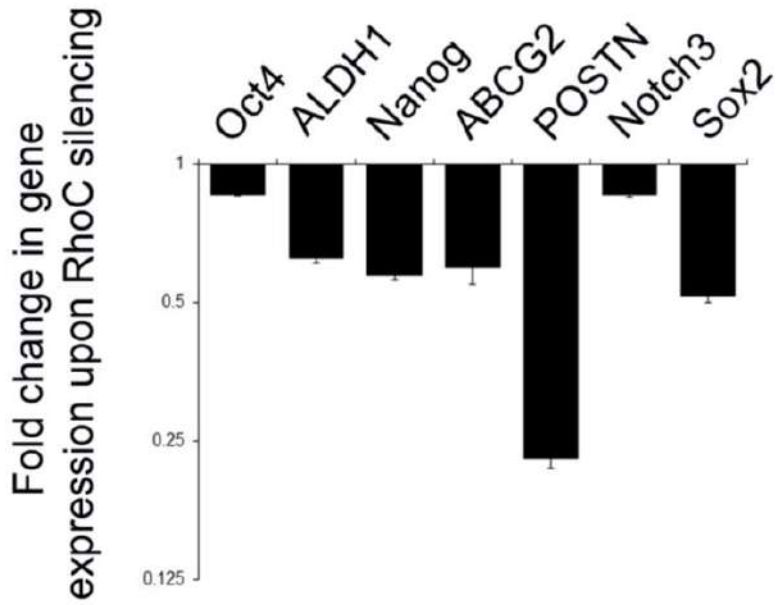

Figure 5.16: siRNA mediated silencing of RHOC leads to decreased expression of stemness genes in SiHa cells as observed by qPCR analysis. Values were normalized to cells treated with scrambled negative control siRNA (SCR). GAPDH was used as the internal control ($n=3$, $p<0.05$).

To ascertain whether the observed changes in gene expression due to modulation of RHOC levels, led to corresponding changes in expression of stemness-related proteins, immunoblotting studies were undertaken. Protein levels of known stemness markers like NANOG, ALDH and CD49F in SiHa-N and SiHa-R cells were assayed. Western blotting analysis revealed up-regulation of NANOG, ALDH and CD49F in SiHa-R cells as compared to SiHa-N **(Figure 5.17)**.

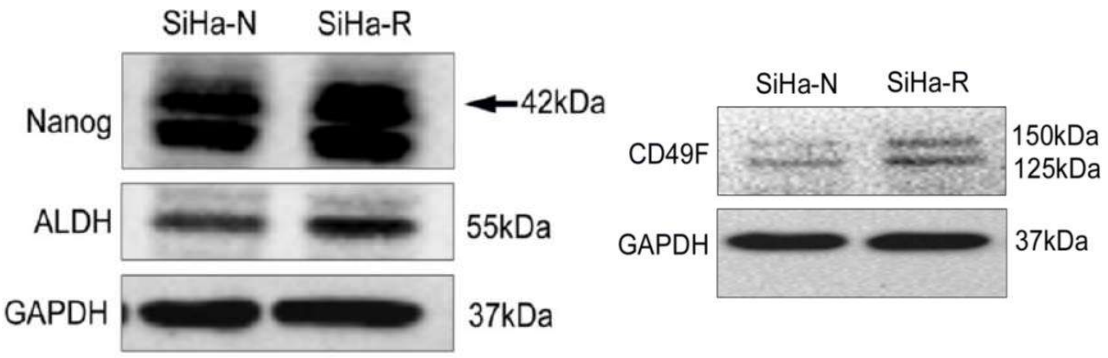

Figure 5.17: Immunoblotting confirms the enrichment of stemness signatures NANOG, ALDH and CD49F in SiHa-R cells (n=3). GAPDH was used as loading control. Representative images are shown.

Parallelly, similar studies were performed on cells depleted for RHOC via siRNA-mediated silencing of RHOC. Knockdown of RHOC was found to result in significant decrease in NANOG, ALDH and CD49F levels as observed by immunoblotting depicted in **Figure 5.18**.

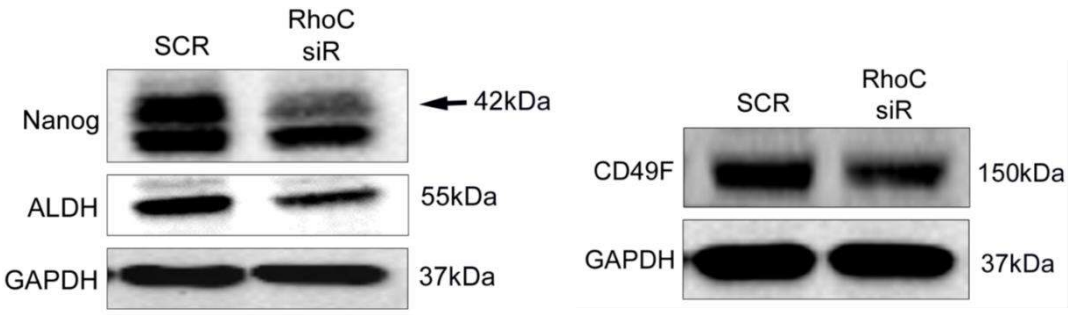

Figure 5.18: A representative western blot image corroborating down-regulation of stemness associated genes in cells knocked down for RHOC 72h post transfection (n=3). Loading levels were verified using GAPDH.

Due to the absence of a chemical inhibitor for RHOC, the antibody-mediated inhibition approach was undertaken (Biocca et al., 1990). Saponin, a terpenoid that acts as a mild surfactant, was used to create pores in the phospholipid bilayer of the cell membrane,

thereby aiding the entry of RHOC-specific antibodies (Jacob et al., 1991). Once inside the cell, the RHOC antibody binds to its target protein, leading to consequent inhibition of downstream effects by interfering with the binding of downstream effector molecules to RHOC (Biocca et al., 1990).

The antibody-mediated inhibition approach was employed to inhibit RHOC in SiHa cells. As shown in **Figure 5.19**, no significant changes were observed in RHOC and CD49F levels in the control (untreated cells), saponin treated cells and cells treated with the isotype control. However, both RHOC and CD49F were found to decrease upon addition of the RHOC antibody, implying a link between RHOC expression and CD49F levels. Interestingly, addition of the RHOC antibody led to significant reduction in the level of RHOC. This indicates that antibody-mediated inhibition could be leading to degradation of the protein and was not limited to mere interference with its functionality. However, the specific mechanism behind this observation is not known and must be investigated.

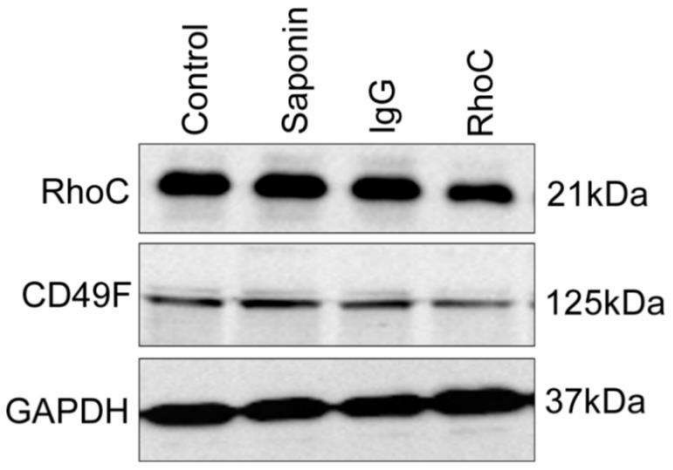

Figure 5.19: Representative immunoblot showing that antibody mediated RHOC inhibition leads to reduction in CD49F levels in SiHa cells (n=3).

The observation that RHOC enhances stemness gene expression was validated using SiHa-N and SiHa-R derived xenografts. As reported earlier by Srivastava et al., tumours originating from SiHa-R cells were larger than SiHa-N tumours (Srivastava et al., 2009). These tumours were further analysed for stemness marker expression by

immunofluorescent staining. Immunofluorescent analysis of xenograft sections derived from SiHa-N and SiHa-R tumours revealed a significant increase in expression of NANOG and CD49F in sections derived from SiHa-R xenografts, thus confirming the association between RHOC and increased stemness marker expression. **Figure 5.20** depicts representative immunofluorescent images from SiHa-N and SiHa-R xenografts analysed for NANOG and CD49F levels. These observations suggest that RHOC regulates the expression of stemness genes in cervical cancer cell lines.

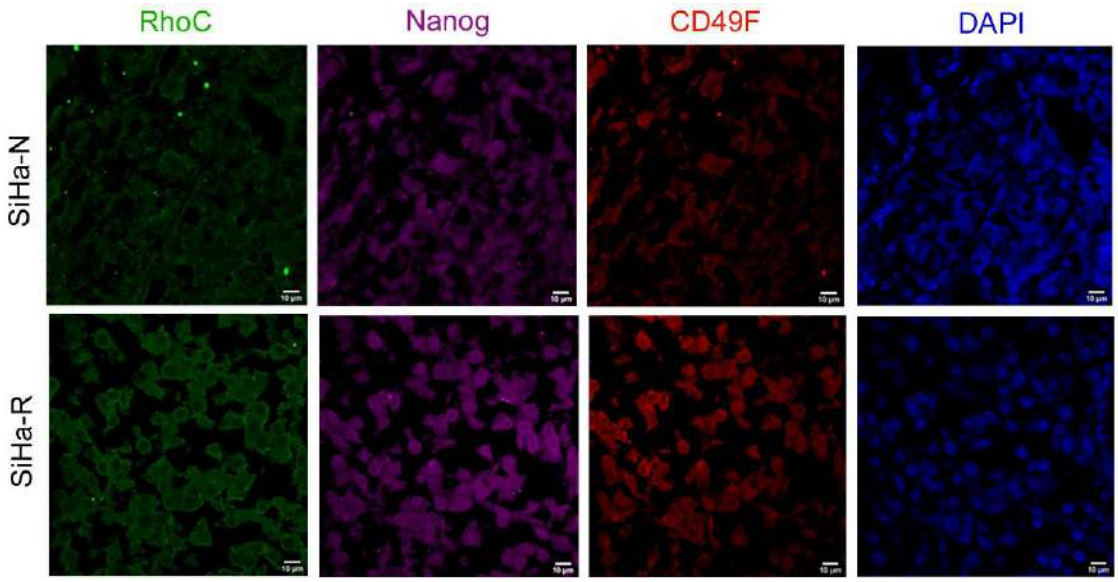

Figure 5.20: Immunofluorescent analysis of SiHa-N and SiHa-R xenograft sections show an increase in NANOG and CD49F, along with RHOC, in SiHa-R xenografts (scale bars are indicated).

In order to confirm that expression of CD49F was indeed affected by RHOC and leads to consequent modulation of stemness ability, SiHa cells over-expressing RHOC were subjected to siRNA-mediated CD49F silencing and consequent phenotypic assays. **Figure 5.21** shows the efficiency of knockdown of CD49F post siRNA inhibition.

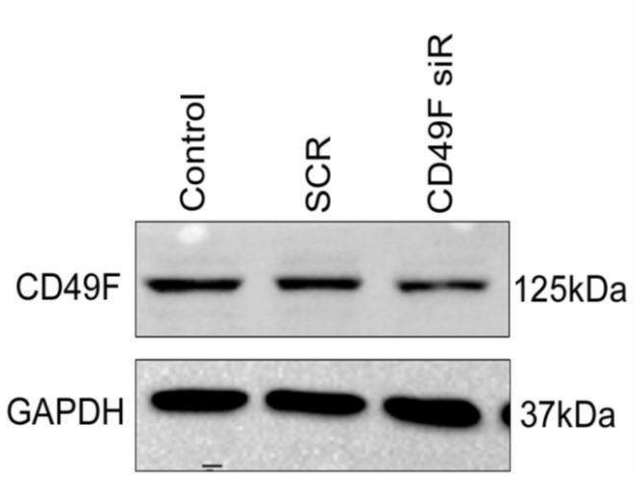

Figure 5.21: Representative immunoblot indicating reduction in CD49F levels upon siRNA mediated silencing of CD49F (n=3).

Next, SiHa-R cells depleted for CD49F were tested for changes in self-renewal ability. siRNA mediated knockdown of CD49F in SiHa-R cells was found to lead to reversal of the gain of stemness phenotype associated with SiHa-R cells. CD49F silencing in SiHa-R cells (CD49F siR) resulted in decreased clone formation as compared to control SiHa-R cells, and SiHa-R cells treated with the scrambled siRNA (SCR). **Figure 5.22 (A)** depicts an image of the clones formed, with significant reduction observed upon CD49F silencing (Average number of clones- Control=314, SCR=280 and CD49F siR=134; $p<0.05$). **Figure 5.22 (B)** is a graphical representation of the same.

A

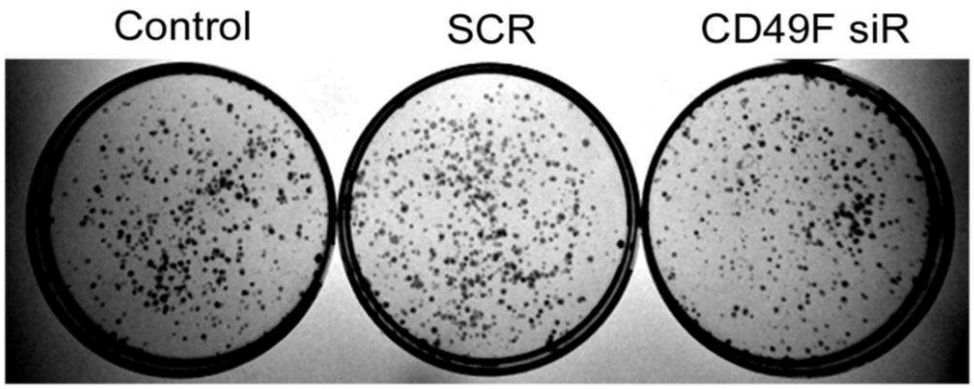

B

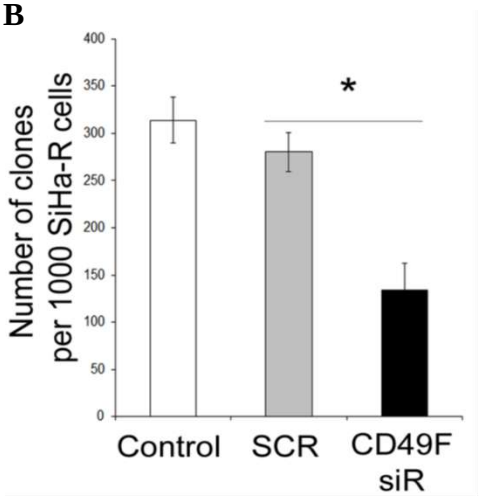

Figure 5.22: (A) Representative image of the clones formed by untreated SiHa-R cells (control), SiHa-R cells treated with scrambled siRNA (SCR) and SiHa-R cells knocked down for CD49F (CD49F siR). (B) Bar graph representation of the average number of clones formed by SiHa-R cells upon CD49F silencing (n=3, $p<0.05$).

Conversely, the changes in self-renewal ability upon over-expression of CD49F in cells compromised for functional RHOC (CaSki-dnR) was assessed. The soft agar assay carried out on CaSki-dnR cells transfected with the CD49F over-expressing plasmid (Addgene Catalogue Number: 53352), was observed to result in partial regaining of the stemness capability lost on account of the dominant negative form of RHOC expressed in these cells. Transient over-expression of CD49F in CaSki-dnR cells was observed to result in an increase in the number of medium and large colonies as compared to control CaSki-dnR cells ($p<0.05$) as shown in **Figure 5.23**.

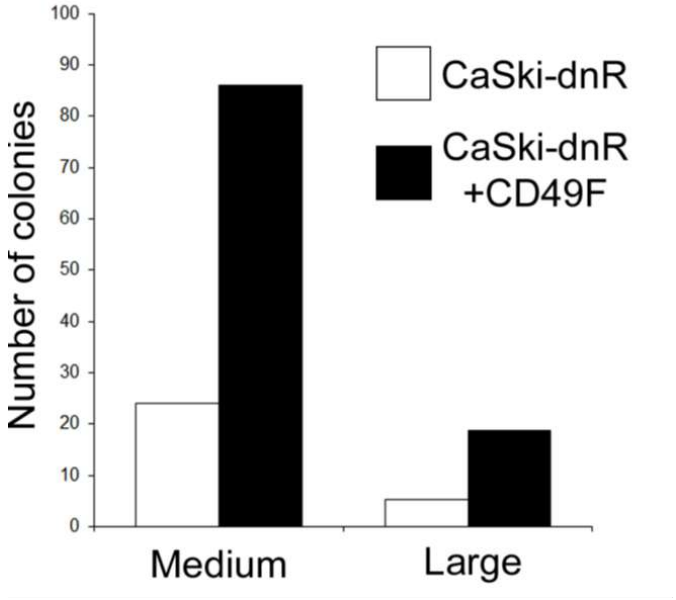

Figure 5.23: Graphical representation of the average number of colonies formed per 10 fields depicting regain of stemness phenotype in RHOC compromised cells (CaSki-dnR) upon over-expression of CD49F (n=2).

Together, these data illustrate that the stemness associated functions of RHOC in cervical cancer cells are predominantly mediated via transcriptional regulation of stemness genes and divulge specific molecular targets that are transcriptionally modulated as a consequence of alterations in RHOC expression.

5.2.4 Clinical Sample-Derived Cells Expressing the Stemness Markers NANOG and CD49F Co-Express RHOC

Transcriptomic and biochemical experiments on cervical cancer cell lines modulated for RHOC expression, revealed that increased RHOC expression was associated with positive regulation of transcriptional machinery of genes associated with stemness. In order to establish that RHOC is involved in stemness maintenance in cervical cancer, patient-derived tumour cells were analysed for the expression patterns of RHOC in conjunction with known markers for stemness- NANOG and CD49F (Lopez et al., 2012; Organista-Nava et al., 2016).

Flow cytometric analysis of patient-derived tumour cells showed that a population of these cells were positive for NANOG. These percentages ranged from 2% to 25.3%. FACS plots for the same are depicted in **Figure 5.24 (A)**. Within this NANOG positive pool, a considerable number of cells were found to be RHOC positive. Analysis of the NANOG positive pool revealed that an average of 66.04% of cells harbouring NANOG, were also positive for RHOC. This is depicted in **Figure 5.24 (B)**.

A similar analysis was performed to determine the association between CD49F and RHOC in clinical samples. Patient-derived tumour cells were stained for CD49F and subjected to FACS analysis. The percentage of CD49F positive cells ranged from 3.3% to 47.4%. FACS plots are shown in **Figure 5.25 (A)**. Further analysis of the CD49F positive pool revealed that an average of 66.72% of these cells had RHOC in them. This is graphically depicted in **Figure 5.25 (B)**.

Together, these data show that a majority of the tumour cells that were positive for stemness markers NANOG and CD49F, were also marked by RHOC expression. This overlap in expression indicates that RHOC expression is associated with stem-like tumour cells in clinical specimens too.

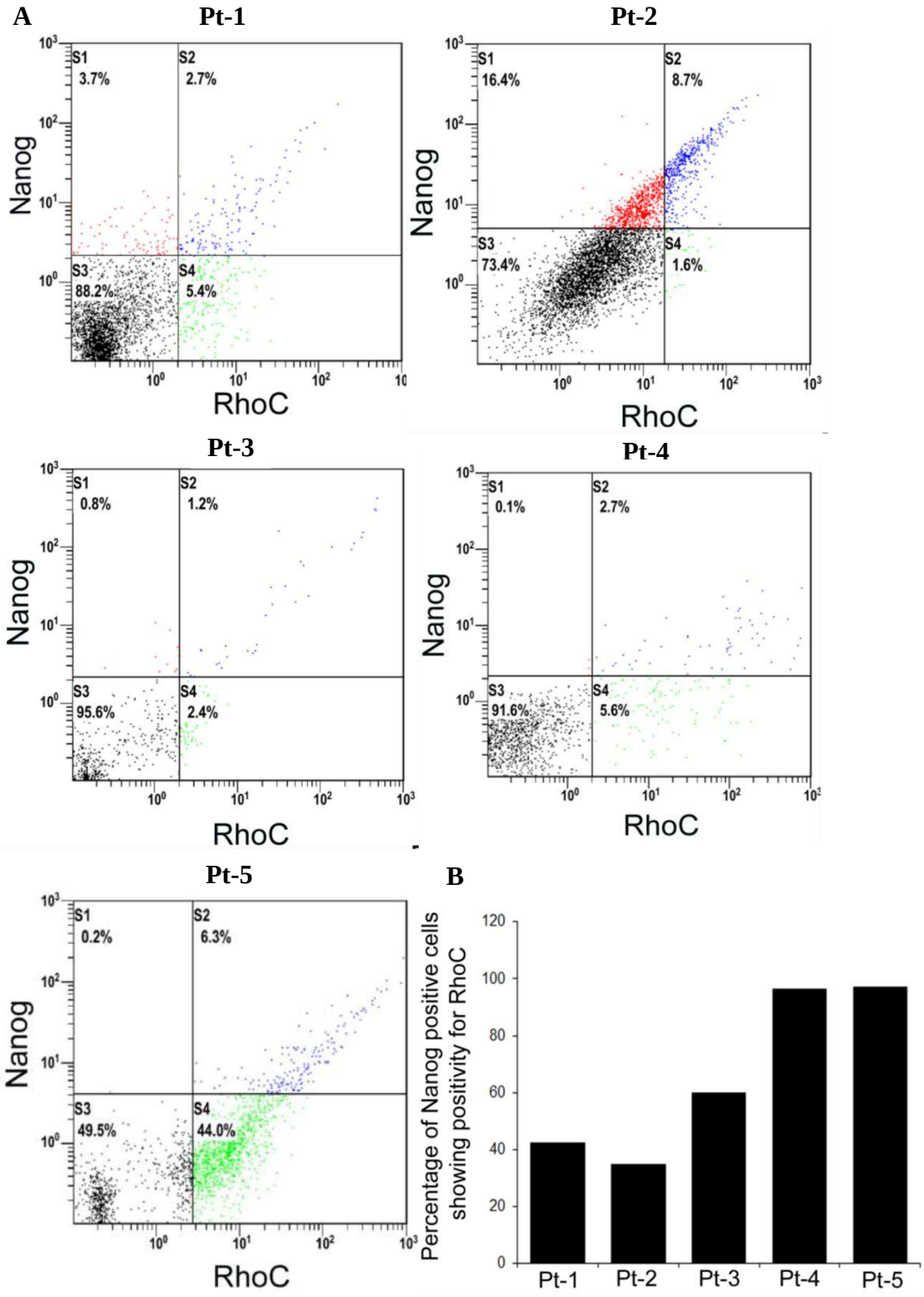

Figure 5.24: (A) FACS quadrant plots showing dual positive cell population for RHOC and NANOG in patients Pt-1, Pt-2, Pt-3, Pt-4 and Pt-5. (B) Bar graph representation of the percentage of $NANOG^{+}$ cells exhibiting positivity for RHOC.

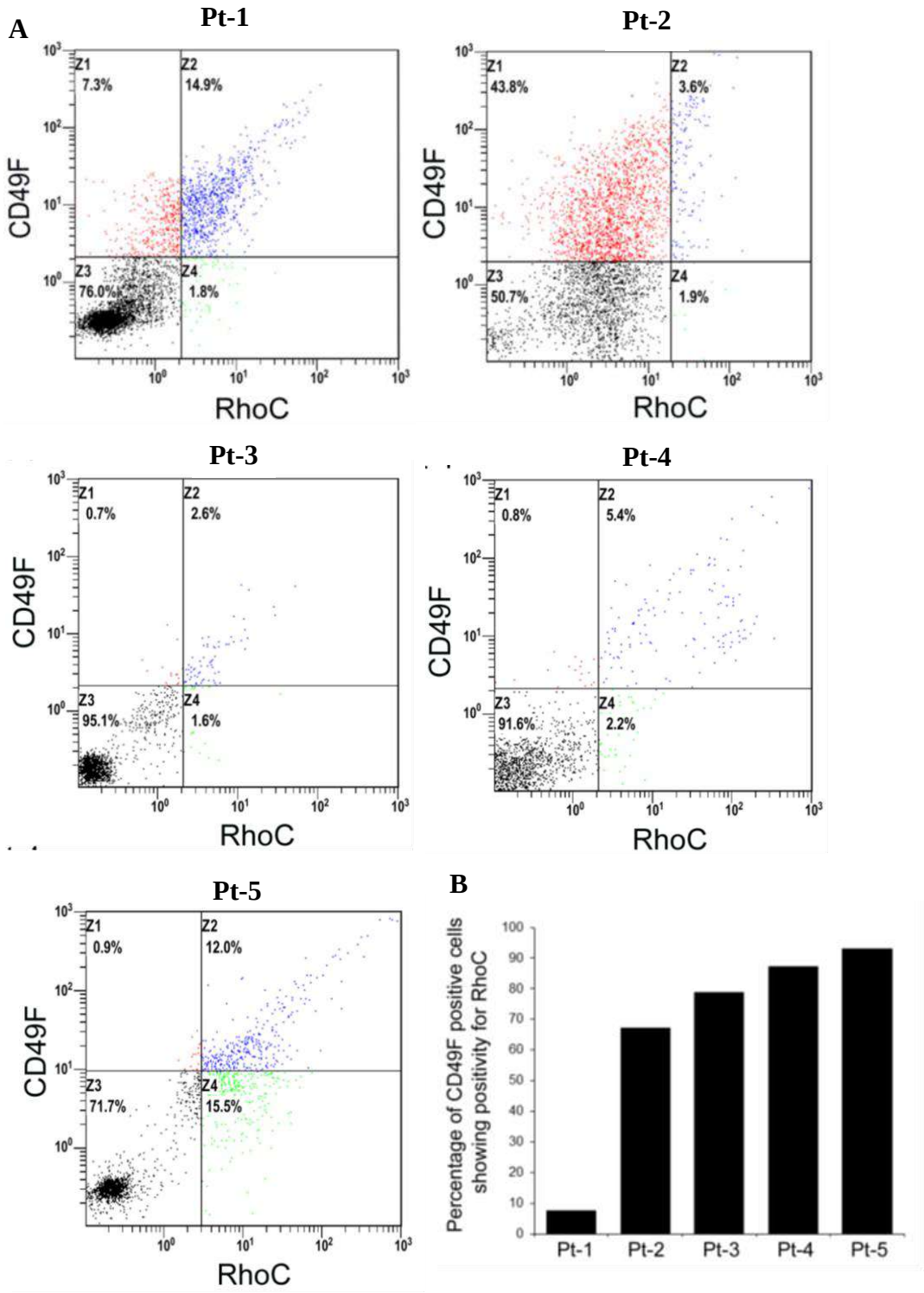

Figure 5.25: (A) Representative FACS quadrant plot showing dual positive cell population for RHOC and CD49F in patients Pt-1, Pt-2, Pt-3, Pt-4 and Pt-5. (B) Bar graph representation of the percentage of $CD49F^{+}$ cells exhibiting positivity for RHOC.

Clinical data accrued for these patients was analysed to determine the aggressiveness and extent of progression of the disease. Incidentally, all these patients presented with metastatic lesions. Details regarding the sites of metastasis are enumerated in **Table 5.1**. The observation that the clinically-derived specimens showing co-expression of RHOC with stemness markers had metastatic lesions, implies that RHOC-driven stemness could be responsible for progression of the disease.

Patient Code	Metastasis (Yes/No)	Metastatic site
Pt-1	Yes	Bilateral common iliac, External iliac and obturator nodes.
Pt-2	Yes	Left external iliac and left obturator node.
Pt-3	Yes	Bilateral obturator and right common iliac. Two Paraaortic lymph nodes.
Pt-4	Yes	Common iliac and obturator nodes.
Pt-5	Yes	Common iliac and obturator nodes.

Table 5.1: Clinical description of patients Pt-1 to Pt-5.

In addition to FACS analysis, immunofluorescent staining of clinically derived sections was undertaken to determine the expression pattern of RHOC, NANOG and CD49F. As shown in **Figures 5.26** and **5.27**, immunofluorescent analysis of clinical sections revealed that while RHOC was present in most tumour cells, pockets of cells that showed significant over-expression of the protein, were also enriched for NANOG and CD49F, indicating that RHOC marked for cells that expressed the stemness markers NANOG and CD49F.

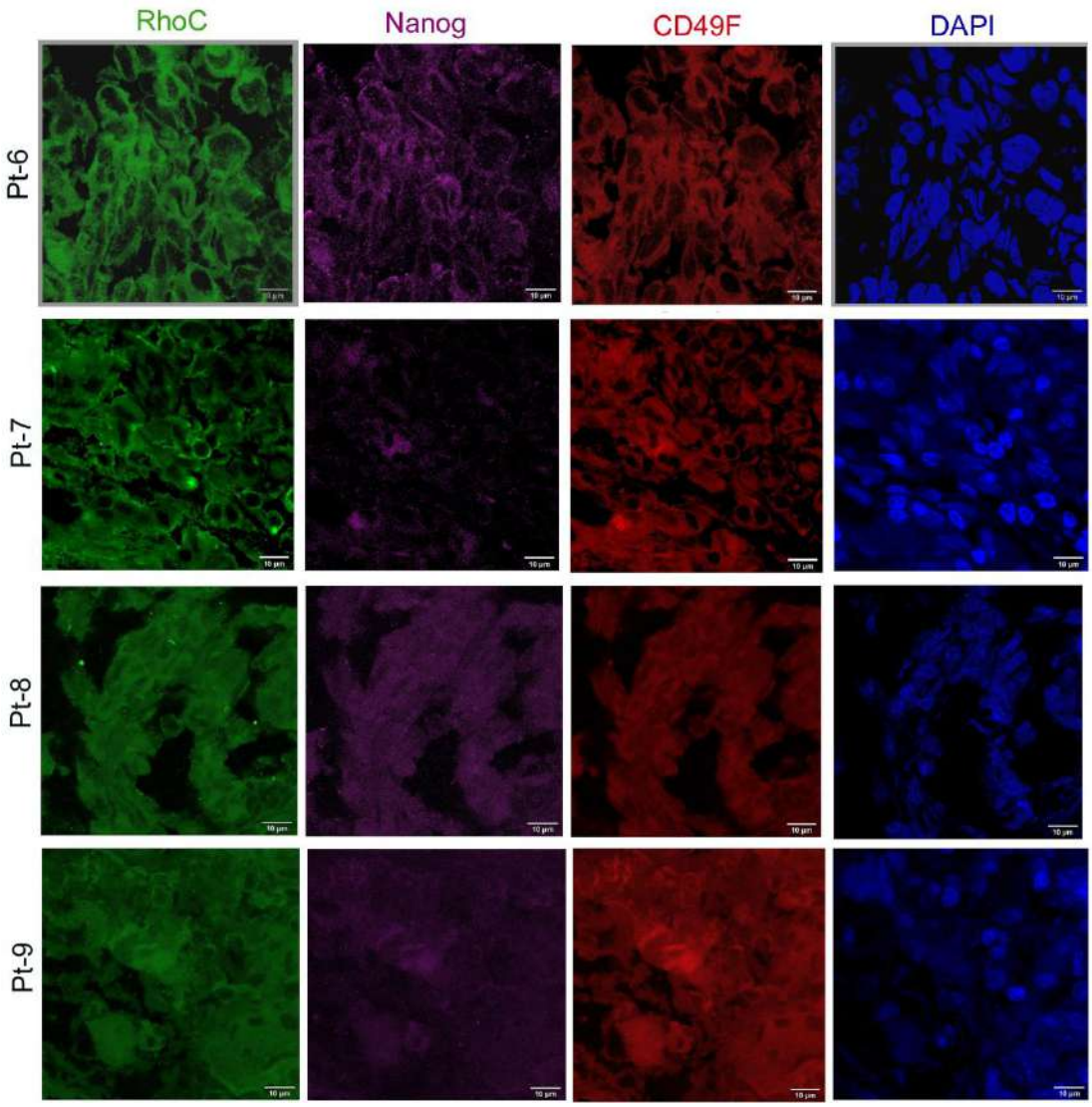

Figure 5.26: Confocal microscopy images of immunofluorescent staining of clinical sections (Pt-6 – Pt-9) with RHOC, NANOG and CD49F showing that cells with high RHOC have increased NANOG and CD49F expression. Scale bars are indicated.

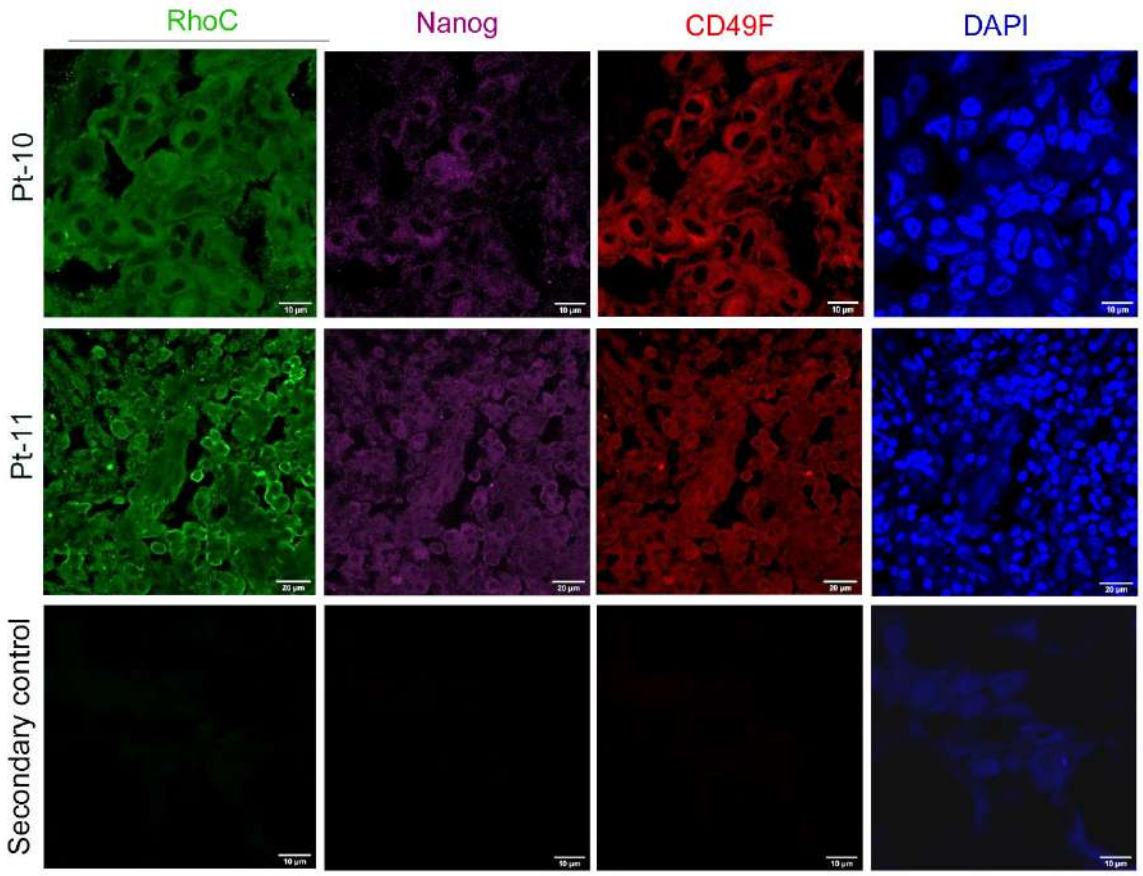

Figure 5.27: Confocal microscopy images of immunofluorescent staining of clinical sections (Pt-10 and Pt-11) with RHOC, NANOG and CD49F showing that pockets of cells with high RHOC have increased NANOG and CD49F expression. Representative images of secondary control are also shown.

The observation that RHOC expression is elevated in NANOG and CD49F marked cervical cancer cells confirms that RHOC is associated with increased stem-like ability. Although these and previous findings link the role of RHOC with stemness phenotype (Islam et al., 2014; Rosenthal et al., 2012), the overall mechanism by which it regulates stemness is not well understood. Further chapters investigate the mechanistic behind these observations.

5.3 Conclusion

In order to address the hypothesis that RHOC aids maintenance of stem cells in cervical cancer, cell lines in which levels of RHOC were artificially modulated were assayed for phenotypic stemness characteristics. RHOC over-expressing cells were observed to have enhanced efflux properties as observed by reduced retention of the Hoechst dye in these cells, a characteristic of the chemo-resistant CSC pool.

Since self-renewal is a hallmark of CSCs, RHOC over-expressing cells, and cells depleted of RHOC or expressing the dominant negative form of the protein, were subjected to clonogenic and soft agar assays. Over-expression of RHOC was found to result in gain of self-renewal property as evidenced by an increase in the number and size of colonies formed by these cells. RHOC knockdown on the other hand, was observed to result in diminished stemness capability.

RHOC was also found to enhance survival under anoikis conditions, with RHOC over-expression resulting in decreased cell death and formation of larger colonies under ultra-low attachment conditions. Contrarily, cells expressing dominant-negative RHOC were found to form significantly smaller colonies, indicative of loss of anoikis resistance.

RNA-sequencing was performed on RHOC over-expressing SiHa-R cells to determine the specific genes that contributed to the phenotypic advantage displayed by these cells. Data analysis revealed significant up-regulation of a host of genes involved in stemness, survival, angiogenesis, cell division and cell signalling. qPCR and western blotting revealed up-regulation of stemness genes NANOG, ALDH, CD49F, OCT4, SOX2 and ABCG2, amongst several others, thereby confirming the RNA-seq data. Concomitantly, siRNA and antibody-mediated inhibition of RHOC was observed to reverse this effect.

Further, SiHa-R xenografts were observed to display enhanced expression of NANOG and CD49F, confirming that RHOC over-expression leads to robust stemness signatures. Finally, FACS-based analysis and confocal microscopy of patient-derived cells revealed co-expression of RHOC in cells positive for NANOG and CD49F, indicating the presence of RHOC in stem-like cells.

Therefore, the data in Chapter 3 establishes that RHOC via regulation of the transcriptional network, leads to up-regulation of genes involved in stemness, resulting in the heightened stemness advantage observed in cells over-expressing the RHOC protein.

CHAPTER-IV

RHOC Expression Regulates Response to Radiation Therapy

6.1 Introduction

Conventional forms of therapy, particularly radiation, cause DNA damage, thereby halting cell division (Radford, 1985; Sugimura, 2002). This assault leads to reduced cell proliferation and tumour regression (Baskar et al., 2014). However, these approaches mainly target the rapidly proliferating differentiated tumour bulk (Hu, 2017; Ogawa et al., 2013). Due to this, quiescent CSCs remain largely unaffected, enabling them to repopulate over time, eventually resulting in relapse of the disease (Clarke and Fuller, 2006).

Research has attributed this inherent resistance of CSCs to increased activation of DNA damage checkpoints, enhanced DNA repair abilities, increased ability to efflux cytotoxic drugs and the up-regulation of enzymes that aid detoxification of chemotherapeutic drugs from within the cell (Phi et al., 2018). It has therefore become imperative to identify a molecular target that is at the crux of this process, and could possibly be used to sensitize CSCs to chemoradiation therapy.

Both homologous recombination (HR) and non-homologous end joining (NHEJ) mechanisms have been discerned to play crucial roles in eliciting DNA damage response (Iliakis, 2009; Jeggo et al., 2011). Various signalling pathways have been reported to be involved in contributing to CSCs and their evasive mechanisms post radiation treatment (Schulz et al., 2019). Primarily, CSCs are known to generate an augmented DNA damage response, enabling them to repair DNA damaged by ionizing radiation, thereby allowing them to efficiently overcome the cytotoxic effects of radiation therapy (Abad et al., 2020; Valencia-Gonzalez et al., 2019).

In the previous chapter, the contribution and mechanism of RHOC in maintenance of stemness in cervical cancer cell lines, xenografts and clinical specimens has been elucidated. This chapter investigates whether RHOC contributes towards radiation-induced DNA repair, and if depletion of this protein could lead to successful sensitization of cells to radiation therapy.

6.2 Results and Discussion

6.2.1 RHOC Regulates Radiation Response in Cervical Cancer Cell Lines

CSCs are known to be equipped with mechanisms that promote efficient DNA repair, thus aiding evasion to radiation therapy (Abad et al., 2020; Valencia-Gonzalez et al., 2019). Since it has been ascertained in Chapter 3 that RHOC is associated with maintenance of the CSC pool, the possible contribution of RHOC towards radiation-induced DNA repair was investigated.

If RHOC did indeed play a role in response to DNA damage, it was hypothesised that radiation treatment would lead to up-regulation of RHOC. To determine changes in levels of RHOC with radiation treatment, SiHa cells were exposed to radiation and the level of RHOC was analysed by western blotting. As expected, immunoblotting analysis of SiHa cells subjected to radiation treatment, revealed significant up-regulation of RHOC 24h post radiation as compared to the non-irradiated control (NR). The dose of radiation utilized was optimized at 6Gy, as previous work in the lab (Pranatharthi et al., 2019) indicated that 6Gy radiation was the LD_{50} dosage. **Figure 6.1** is an image of the immunoblot showing elevated levels of RHOC upon radiation in SiHa cells.

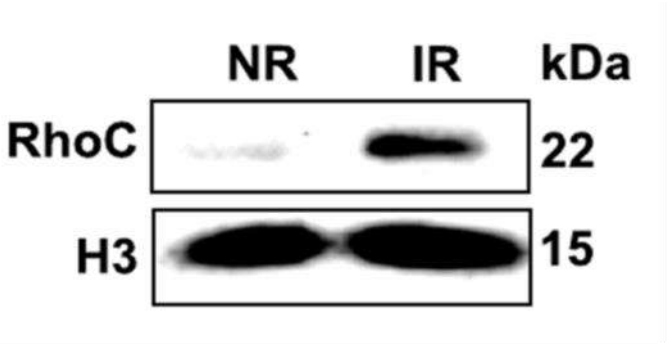

Figure 6.1: Representative immunoblotting image depicting increased RHOC levels in irradiated SiHa cells. Histone3 was used as the loading control (n=3).

To identify changes in viability of cells post radiation assault in the background of RHOC over-expression, the clonogenic assay was utilized. SiHa-N and SiHa-R cells were irradiated and then subjected to the clonogenic assay. At the end of 14 days, the number of clones formed by each cell type was considered to be an indicator of their ability to survive radiation treatment. As depicted in **Figure 6.2**, SiHa-R cells were

observed to form a significantly larger number of clones as compared to SiHa-N cells, confirming the superior self-renewal ability of these cells post radiation treatment.

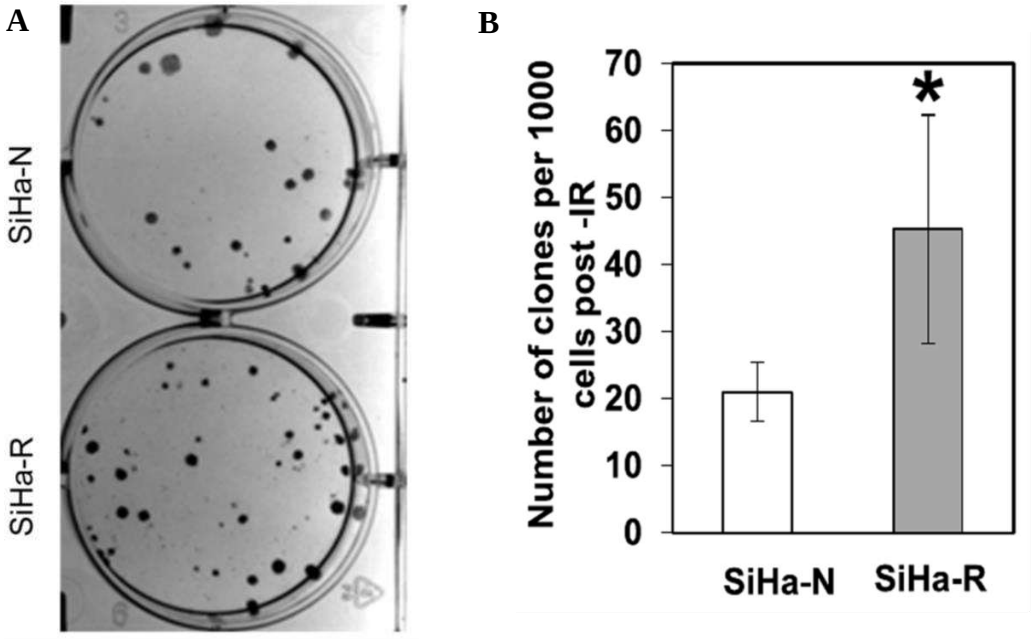

Figure 6.2: (A) Representative image of clones formed by SiHa-N and SiHa-R cells post irradiation. (B) Graphical representation of the increased self-renewal ability of SiHa-R cells post radiation treatment (n=3, $p<0.05$).

The clonogenic assay indicated that over-expression of RHOC aided cell survival post irradiation. Further studies were taken up to investigate the effect of inhibition of RHOC on survival after radiation treatment. If RHOC over-expression offered protection to radiation, it was envisaged that RHOC inhibition could lead to the opposite effect. To test this, SiHa cells transfected with RHOC-specific siRNA were irradiated and assayed for cell death by staining with Annexin V, followed by FACS analysis. Annexin V is a marker that is frequently used to analyse apoptotic populations on the basis of membrane integrity (Vermes et al., 2000; Vermes et al., 1995). Antibodies against Annexin V bind to phosphatidyl serine residues that appear on the outer surface of the cytoplasmic membrane of apoptotic cells due to flipping of the cell membrane, a precursor of apoptosis (Segawa and Nagata, 2015).

FACS analysis to determine the percentage of cells positive for Annexin V after treatment with 6Gy radiation revealed an increase in the percentage of pre-apoptotic cells in RHOC knocked down cells (RHOC) as compared with the scrambled negative control (SCR). This is shown graphically in **Figure 6.3**.

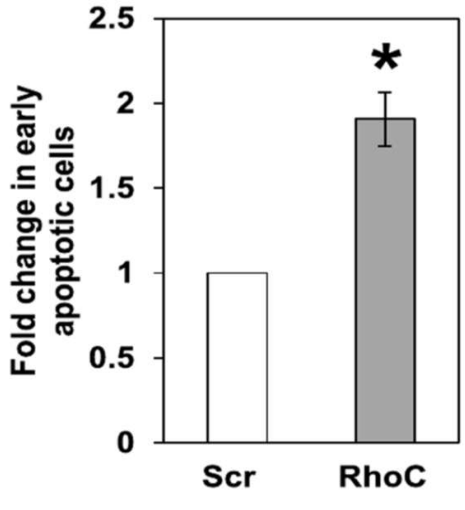

Figure 6.3: Bar graph representation of percentage of apoptotic cells (Annexin V positive) in RHOC siRNA treated (RHOC) and scrambled (SCR) control as evaluated by FACS analysis (n=3, $p<0.05$).

These data imply a possible association between RHOC and survival ability of cervical cancer cells post radiation treatment. Further studies were undertaken to delve into the molecular mechanisms behind this observation.

6.2.2 RHOC Expression Results in Increased Expression of Proteins Involved in DNA Repair

Phenotypic assays revealed that RHOC facilitated increased survival of cells post radiation assault. Since CSCs are known for their robust DNA repair machinery and enhanced DNA damage response, RNA-seq data of SiHa-N and SiHa-R was examined to determine the status of DNA repair machinery upon RHOC over-expression. DAVID analysis of RNA-seq data revealed that various biological processes like cell cycle progression, cell proliferation and double-stranded break repair were significantly enriched in SiHa-R cells **(Figure 6.4)**.

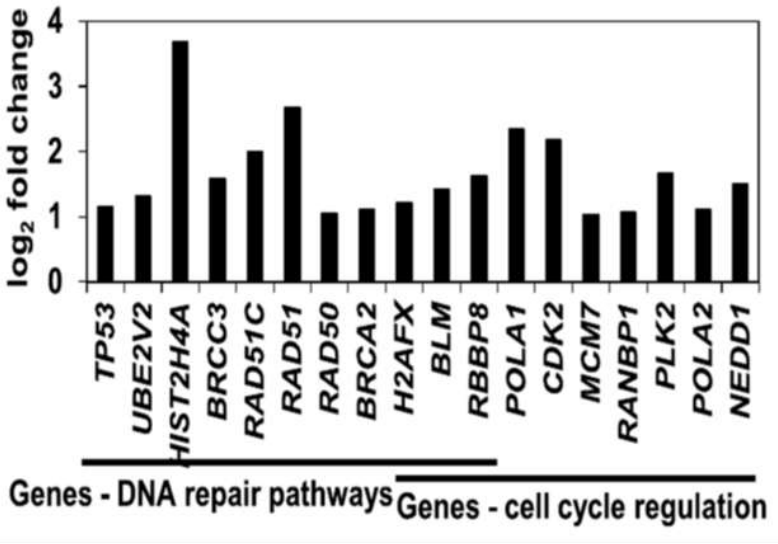

Figure 6.4: Bar graph representation of biological processes up-regulated in SiHa-R cells as revealed by RNA-seq data.

Further analysis of the specific genes involved in these processes revealed that genes like *RAD50* and *BRCA2*, which have important functions in DNA repair (Rojowska et al., 2014; Yoshida and Miki, 2004), and genes involved in progression of the cell cycle like *CDK2* and *POLA2* (Bacevic et al., 2017; Simbulan-Rosenthal et al., 1998) were elevated in SiHa-R cells. The level of enrichment of genes in SiHa-R cells that contribute towards DNA repair and cell cycle progression as seen in the RNA-seq data are depicted in **Figure 6.5**.

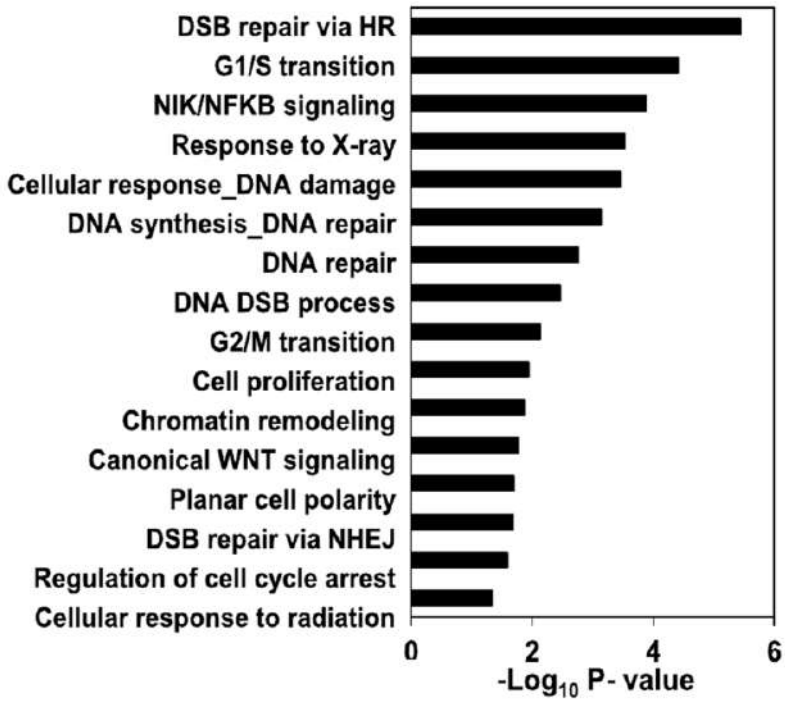

Figure 6.5: Graphical representation of fold changes of genes involved in DNA repair and cell cycle regulation in SiHa-R as exhibited by the RNA-seq data (values normalized against SiHa-N).

This observation of up-regulation in DNA repair markers was validated by qPCR. Transcript analysis of the DNA repair genes *RAD50*, *BRCA2* and *NBS1* showed increased expression of these genes in SiHa-R cells as compared to SiHa-N, thus validating these findings. **Figure 6.6** is a graphical representation of the fold increase in expression of DNA repair genes in SiHa-R cells, using GAPDH as control.

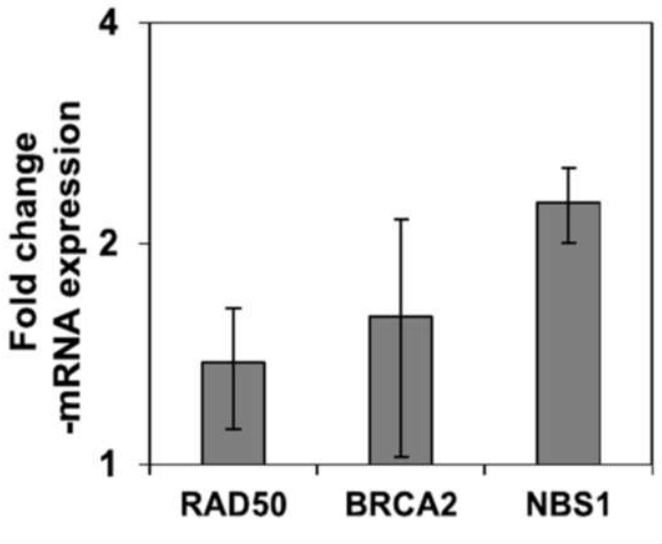

Figure 6.6: Transcript levels of genes involved in DNA repair in SiHa-R cells, with values normalized against SiHa-N (n=3, $p<0.05$). GAPDH was used as the internal control.

Phosphorylation of Ser139 of H2Ax is one of the early events of DNA repair (Ivashkevich et al., 2012; Rogakou et al., 1999), and helps recruit DNA repair proteins to the site of the double-strand break (DSB). It also aids in activation of cell cycle checkpoints (Mah et al., 2010; Podhorecka et al., 2010). Therefore, the level of pH2Ax was assayed by immunofluorescent staining of SiHa-N and SiHa-R cells, 30mins post radiation treatment to determine differences in DNA repair activation upon RHOC over-expression. As shown in **Figure 6.7**, immunofluorescent staining revealed considerable increase in pH2Ax foci formation in SiHa-R cells upon radiation**,** indicative of increased activation of DNA repair machinery upon radiation in cells over-expressing RHOC.

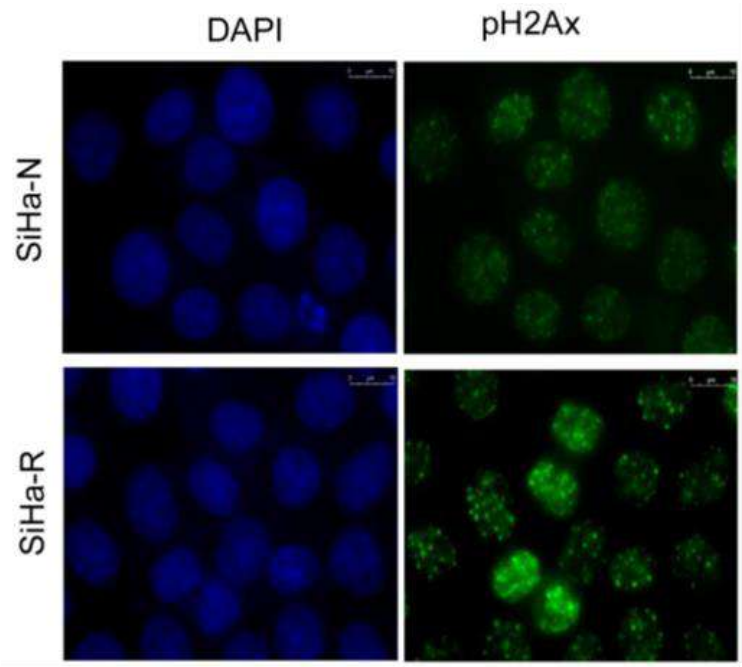

Figure 6.7: Representative immunofluorescent image showing increased formation of pH2Ax foci in SiHa-R cells upon irradiation (n=3). Scale bars are indicated.

Immunoblot analysis was also performed to confirm the above observation. Analysis of the difference in levels of pH2Ax in SiHa-N and SiHa-R cells upon radiation revealed that pH2Ax was indeed up-regulated in SiHa-R cells in comparison with SiHa-N cells as depicted in **Figure 6.8**.

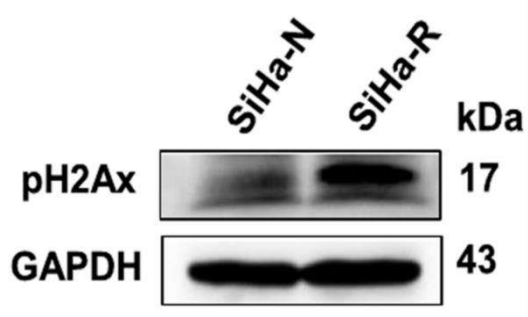

Figure 6.8: Representative immunoblot image of pH2Ax levels in irradiated SiHa-N and SiHa-R cells (n=3). GAPDH was used as loading control.

The DNA repair proteins MRE11, RAD50 and NBS1, that constitute the MRN complex, play crucial roles in detection of DSBs and their consequent repair via NHEJ and HR mechanisms (Lamarche et al., 2010). The expression levels of these proteins were therefore analysed in SiHa-N and SiHa-R cells to investigate whether the DNA repair machinery in SiHa-R cells was enhanced in comparison to SiHa-N. Immunoblot analysis was carried out on SiHa-N and SiHa-R cells post radiation treatment. This revealed significant increase of MRE11 and RAD50 in SiHa-R cells, indicative of the robust DNA repair machinery existent in these cells as depicted in **Figure 6.9**.

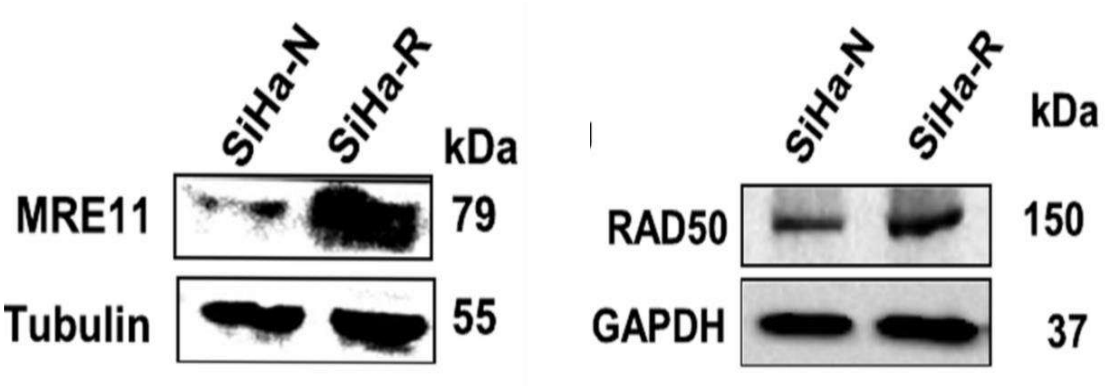

Figure 6.9: Representative immunoblot images of DNA repair proteins, MRE11 and RAD50 in SiHa-N and SiHa-R cells (n=3). GAPDH was used as loading control.

Parallel studies were carried out in CaSki-dnR cells depleted of functional RHOC. Immunoblotting was performed on these cells to determine the status of DNA repair machinery in the absence of functional RHOC. As shown in **Figure 6.10**, immunoblot analysis revealed significant reduction of RAD50 in CaSki-dnR cells in comparison to CaSki-N.

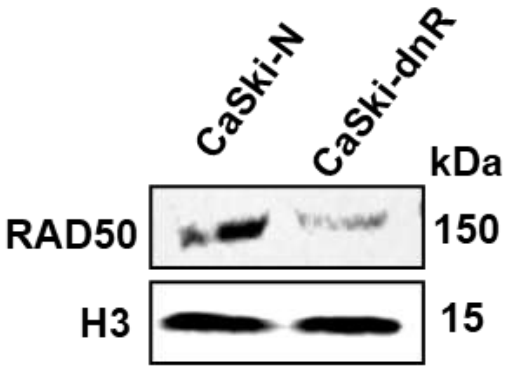

Figure 6.10: Representative immunoblot depicting a decrease in RAD50 levels in CaSki-dnR cells (n=3). Histone3 (H3) was used as the loading control.

In order to further confirm that RHOC regulated DNA damage response, levels of DNA repair proteins were assayed in SiHa-N and SiHa-R derived xenografts. Xenografts derived from SiHa-N and SiHa-R cells (Srivastava et al., 2009) were subjected to immunofluorescent staining to determine the levels of DNA repair proteins in these tumours. As shown in **Figure 6.11**, immunofluorescent analysis confirmed elevated levels of pH2Ax, MRE11 and RAD50 proteins in SiHa-R xenografts.

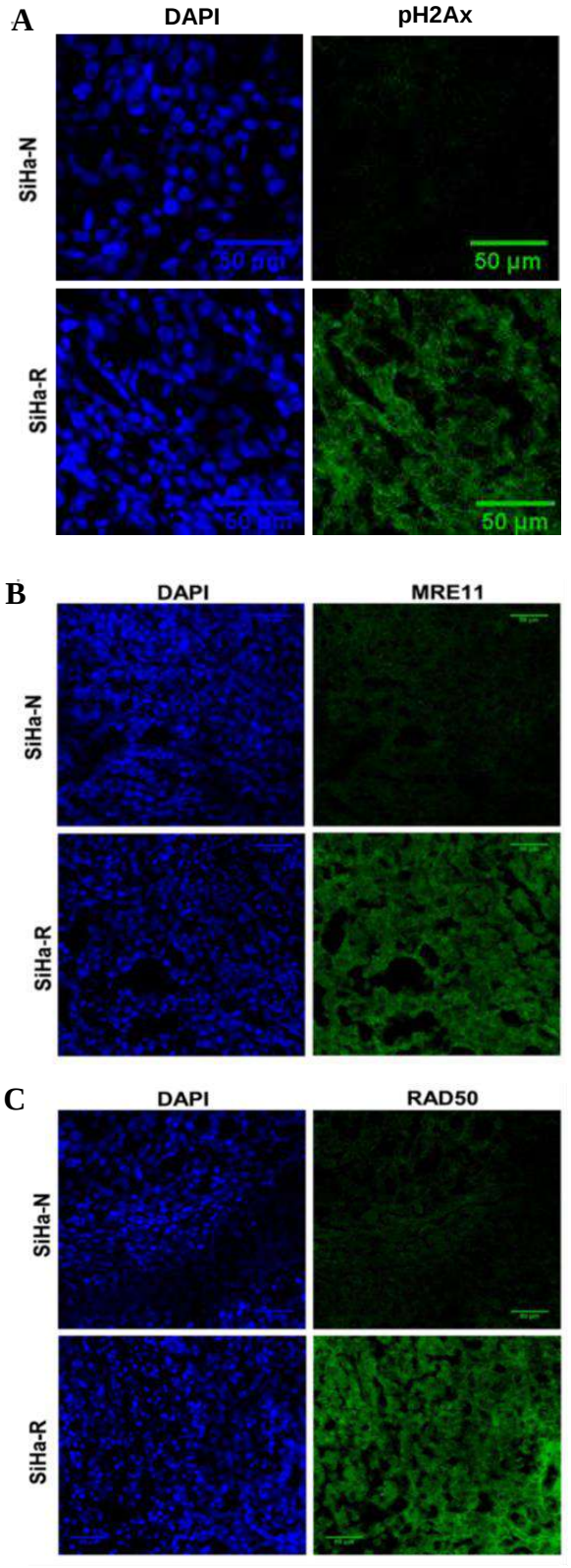

Figure 6.11: Representative immunofluorescent images of pH2Ax (A), MRE11 (B) and RAD50 (C) in SiHa-N and SiHa-R derived xenografts. Scale bars are indicated.

These observations imply that the survival advantage observed in SiHa-R cells post radiation, could be attributed to RHOC's contribution in mediating DNA damage response by transcriptionally up-regulating DNA repair machinery.

6.2.3 Antibody-Mediated RHOC Inhibition Leads to Sensitization of Clinical Sample-Derived Cells to Radiation Treatment

The data thus far implies that RHOC transcriptionally up-regulates DNA repair proteins, thus equipping cells with robust DNA repair machinery to combat the detrimental effects of radiation therapy. This prompted examination of the effect of RHOC depletion on cell survival post radiation assault in clinical samples. FACS-based analysis of cell death following antibody-mediated inhibition of RHOC and irradiation revealed that RHOC inhibition successfully sensitized tumour cells to radiation therapy. As shown in **Figure 6.12**, propidium iodide staining to determine cell death revealed that RHOC antibody treated cells (RHOC) resulted in a greater percentage of cell death in patients Pt-15 and Pt-16, post radiation treatment, in comparison with IgG treated control cells. However, two out of four samples did not show any change in survival (Pt-17 and Pt-18). It must be noted that some tumours may not over-express RHOC. Inhibition of RHOC in such tumours may not lead to sensitization of cells to radiation treatment. The observed lack of increased cell death upon RHOC depletion in some clinical specimens, could be attributed to this.

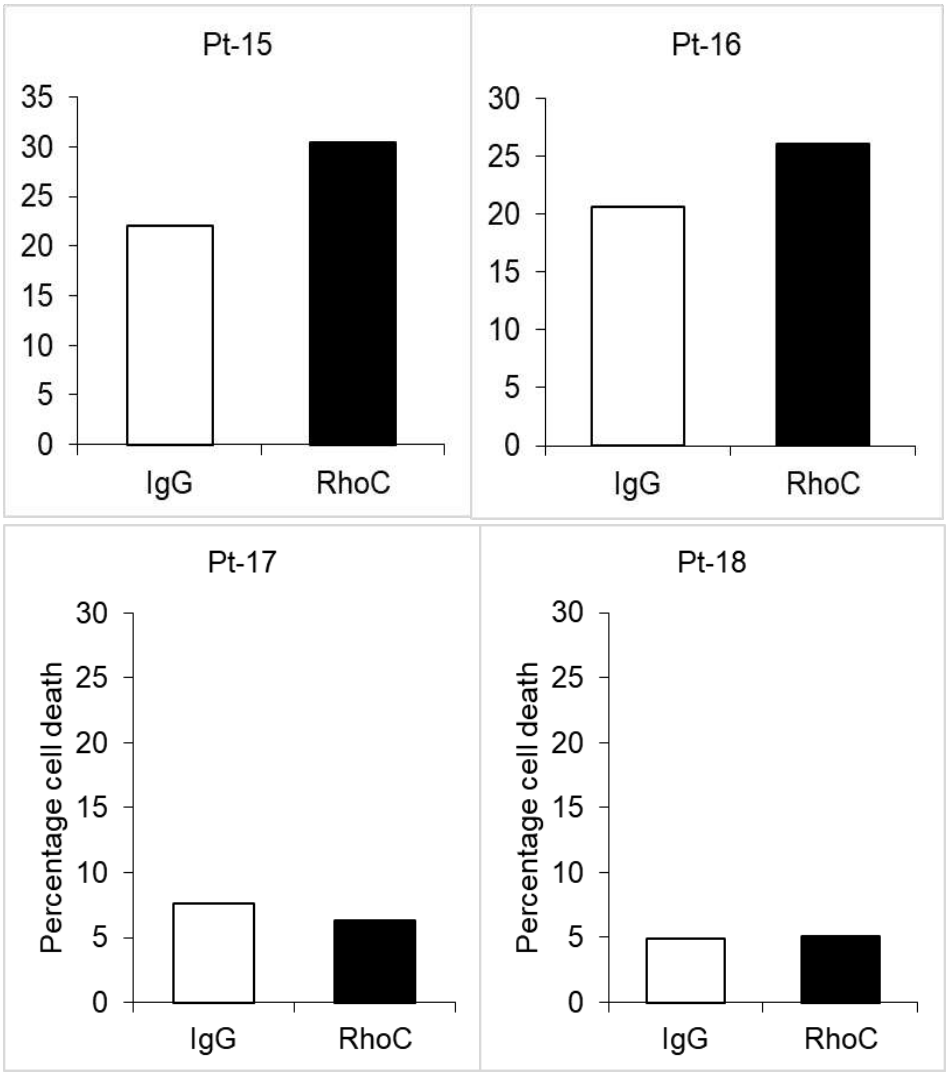

Figure 6.12: Bar graph representation of the percentage of dead cells in clinical samples as observed by propidium iodide staining followed by FACS analysis. Antibody-mediated RHOC inhibition was observed to sensitize patient-derived cells to radiation treatment in comparison to IgG treated control cells in patients Pt-15 and Pt-16, while no significant change was observed in patients Pt-17 and Pt-18.

Therefore, the data thus far establishes that RHOC enhanced stem-like abilities, elevated stemness signatures and also mediated DNA damage induced repair, thus aiding resistance to treatment interventions. Further chapters explore the possible mechanisms behind these observations in detail.

6.3 Conclusion

Evidence demonstrating the strong relationship between RHOC and maintenance of stem-like characteristics, led to the hypothesis of a possible link between RHOC and enhanced DNA damage response. Investigations carried out to this effect revealed that RHOC over-expression resulted in decreased sensitivity to radiation treatment, while knockdown of RHOC reversed this effect.

Further experiments revealed that RHOC transcriptionally up-regulates molecules involved in various aspects of DNA repair, thereby resulting in better cell survival post irradiation. RNA-seq and biochemical experiments revealed up-regulation of key players of DNA damage response like pH2Ax, MRE11 and RAD50 in RHOC over-expressing cells, with RHOC depletion leading to consequent reduction in levels of these proteins.

Finally, antibody-mediated inhibition of RHOC in cells derived from patient biopsies appeared to result in sensitization of cells to radiation, as evidenced by increased cell death in RHOC inhibited cells. These data indicate that RHOC could serve as an important therapeutic target that could help sensitize the resilient CSC pool to therapy. Experiments carried out in the lab to decipher the molecular intricacies behind this process unearthed ROCK2, a RHOC effector, as an important target in mediating response to radiation (Pranatharthi et al., 2019).

CHAPTER-V

RHOC Regulates the Expression of Stemness Genes CD49F and ALDH via the ERK Signalling Pathway

7.1 Introduction

RHOC has been shown to regulate tumour progression via various pathways. Proliferation, invasion and migration of colorectal cancer cells has been demonstrated to be controlled by actin remodelling through the RHOC/FAK pathway (Zeng et al., 2018b). RHOC has also been implicated in regulating EMT, proliferation, angiogenesis and anoikis resistance by Notch1 signalling in cancer of the cervix (Srivastava et al., 2009). The TGF-β-RHOC axis has been found to be important in progression of cervical cancer. Experimental evidence suggested that RHOC was essential for TGF-β mediated EMT in cervical cancer, with cells depleted of RHOC being unable to undergo successful EMT post TGF-β stimulation (He et al., 2015). Interestingly, RHOC was found to play a pertinent role in regulation of angiogenesis by modulating vascular migration, proliferation and permeability through VEGF signalling (Hoeppner et al., 2015). In melanomas, RHOC has been demonstrated to regulate invasive ability via PI3K/Akt signalling independent of its downstream effector, ROCK (Ruth et al., 2006). Importantly, the MAPK signalling pathway emerged as a significant downstream event of RHOC activation in inflammatory breast cancer, with both the p38 and ERK arms of MAPK being found to be involved in the regulation of invasion, migration and angiogenesis in IBC (van Golen et al., 2002).

In this chapter, efforts were made to tease out the specific signalling pathway involved in CSC maintenance in cervical cancer. Despite the availability of ample evidence of contribution of the TGF-β and NF-κβ pathways in CSC regulation, this study did not find a significant role for these signalling mechanisms in the RHOC context. However, ERK signalling emerged as an important mediator of CSC maintenance, by enhancing the expression of CD49F and ALDH1 through its downstream transcription factor, E2F1 in RHOC over-expressing cells.

7.2 Results

7.2.1 ERK Signalling is Activated in RHOC Over-Expressing Cells

Detailed analysis of the RNA-seq data was undertaken to delineate the possible signalling pathways downstream of RHOC responsible for stemness maintenance in cervical cancer. Gene ontology (GO) analysis for biological processes of genes up-regulated in SiHa-R, using the DAVID tool (Fold change cut-off=1.5, $p<0.05$) was carried out to identify the specific processes elevated in cells over-expressing RHOC.

As shown in **Figures 7.1 and 7.2**, GO analysis revealed enrichment of a substantial number of genes involved in numerous biological processes such as stem cell population maintenance, cell cycle, cell proliferation, NF-κβ, and ERK/MAPK signalling pathways in SiHa-R cells. **Figure 7.1** depicts the most common biological processes identified in SiHa-R cells based on the significance level of the genes up-regulated in SiHa-R. **Figure 7.2** depicts the biological processes that had the greatest number of genes up-regulated in SiHa-R cells.

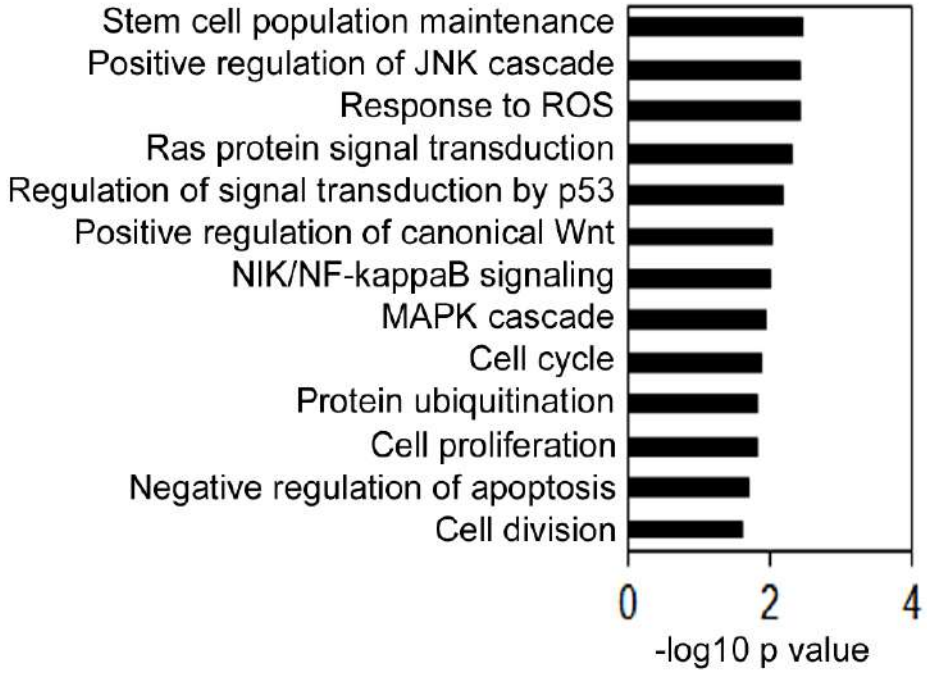

Figure 7.1: Bar graph representation of the biological processes enriched in SiHa-R cells as observed by GO analysis of the transcriptome data, based on significance (n=2, $p<0.05$).

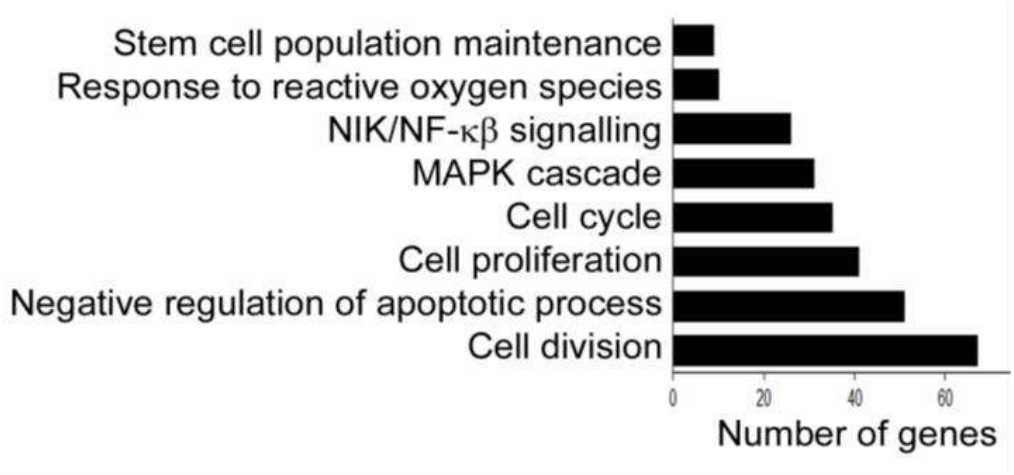

Figure 7.2: Graphical representation of the number of genes involved in various signalling pathways that were over-expressed in SiHa-R cells (n=2, $p<0.05$).

Studies have shown that RHOC regulates angiogenesis, migration, metastasis and invasion through the MAPK pathway, controls oncogenic transformation via NF-κβ and promotes EMT by activation of the TGF-β-RHOC axis (Cammarano and Minden, 2001; Iiizumi et al., 2008; Liu et al., 2007; Lu et al., 2016; van Golen et al., 2002). In the present study, the involvement of these signalling mechanisms as RHOC effector pathways in stemness maintenance was investigated.

NF-κβ signalling emerged as one of the pathways that were up-regulated as per the transcriptomic data. Dimerization of p-65 is one of the main events governing activation of NF-κβ mediated transcription (Giridharan and Srinivasan, 2018). Here, differences in nuclear levels of p-65 upon modulation in RHOC expression was investigated to determine the involvement of NF-κβ signalling in SiHa-R cells. As shown in **Figure 7.3**, p-65 levels were found to remain unaltered upon RHOC over-expression.

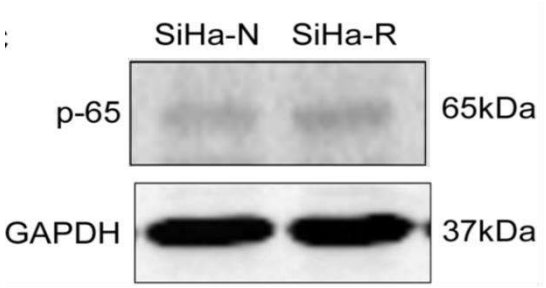

Figure 7.3: Representative immunoblot image of p-65 levels in SiHa-N and SiHa-R cells, with GAPDH as loading control (n=2).

The converse approach of RHOC inhibition was also undertaken to understand the extent of involvement of RHOC in NF-κβ signalling. To this effect, immunoblotting of p-65 was performed on SiHa cells transfected with RHOC-specific siRNA (RHOC siR) and cells transfected with scrambled control (SCR) 72h post transfection. As shown in **Figure 7.4**, immunoblot analysis revealed that levels of p-65 remained unchanged upon depletion of RHOC in comparison with cells treated with scrambled control.

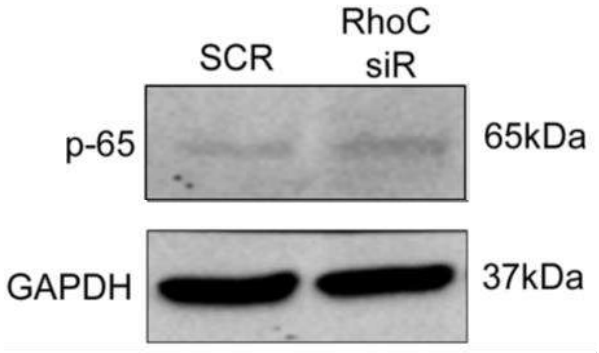

Figure 7.4: Representative immunoblot image of SiHa cells transfected with scrambled negative control (SCR) and RHOC siRNA (RHOC siR) and probed for p-65 (n=2). Lysates were prepared 72h post GAPDH was used as loading control.

To investigate the contribution of RHOC towards activation of TGF-β signalling, levels of SMAD4 upon changes in RHOC expression were assayed. SMAD4, the core mediator of TGF-β signalling, is responsible for initiation of transcription of target

genes (Zhao et al., 2018). Immunoblotting was therefore performed on lysates of SiHa-N and SiHa-R to determine changes in levels of SMAD4 upon RHOC over-expression. SiHa-N and SiHa-R cells subjected to immunoblotting revealed no significant changes to SMAD4 levels with increased RHOC expression as depicted in **Figure 7.5**.

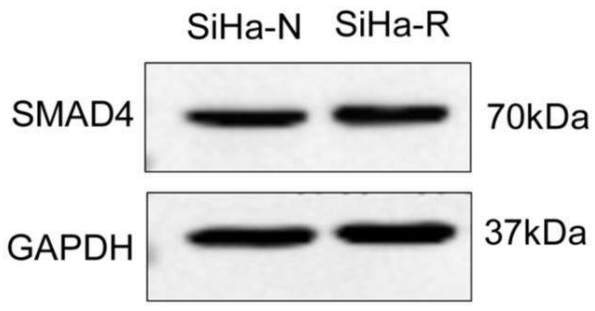

Figure 7.5: Representative immunoblot image of SMAD4 levels in SiHa-N and SiHa-R cells, with GAPDH serving as the loading control (n=2).

SMAD4 levels were also probed in SiHa cells subjected to siRNA-mediated silencing of RHOC to evaluate the effect of RHOC depletion on TGF-β activation. Immunoblotting analysis showed that RHOC silencing resulted in no significant change in nuclear SMAD4 levels in SiHa cells as shown in **Figure 7.6**.

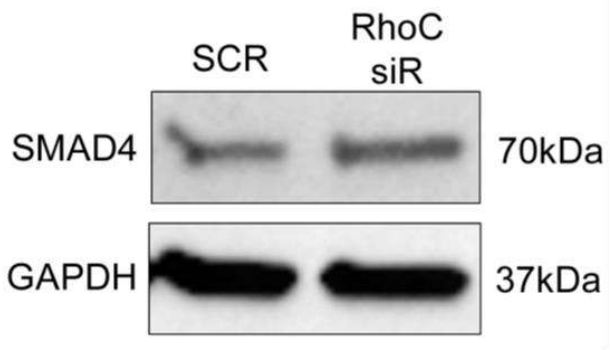

Figure 7.6: Representative immunoblot image of SMAD4 levels upon RHOC knockdown (RHOC siR) in comparison with scrambled siRNA (SCR) (n=2). GAPDH was utilized as the loading control.

These results were indicative that RHOC may not have significant control over TGF-β signalling. However, scientific evidence suggests that TGF-β mediated signalling works via RHOC to result in EMT in cervical cancer cell lines (He et al., 2015).

On the contrary, activation of the MAPK/ERK signalling pathway, was found to undergo major alterations with variations in RHOC levels. Phosphorylation of ERK1/2 is indicative of activation of ERK signalling (Guo et al., 2020; Wortzel and Seger, 2011). To investigate the possible contribution of RHOC towards activation of the ERK pathway, SiHa cells depleted for RHOC were assessed for levels of phosphorylated forms of ERK1/2 (p-ERK1/2). Immunoblotting studies carried out on RHOC siRNA treated SiHa cells (RHOC siR) revealed that silencing of RHOC led to significant reduction in both p-ERK1/2 and ERK1/2 levels in comparison with scrambled control (SCR) as depicted in **Figure 7.7**.

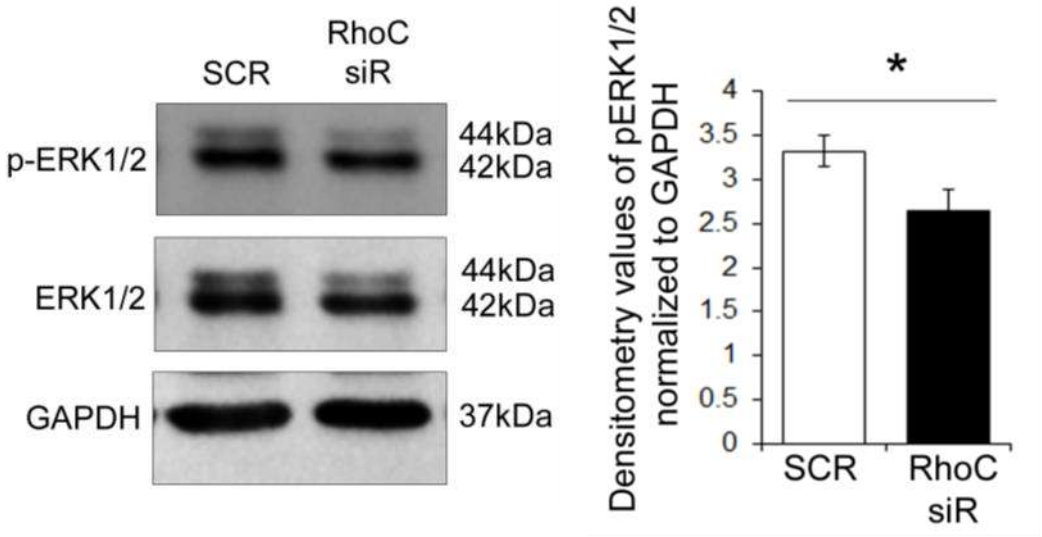

Figure 7.7: Western blotting shows decreased levels of ERK1/2 and p-ERK1/2 in cells treated with RHOC siRNA (RHOC siR) (n=3). Representative images are depicted, with GAPDH serving as the loading control. Densitometry values are also represented with p-ERK1/2 intensity values normalized to GAPDH.

Therefore, the ERK pathway emerges as the signalling mechanism that is activated downstream of RHOC in SiHa cells. Further investigations were carried out to define the role of the ERK pathway in RHOC-mediated stemness maintenance.

7.2.2 RHOC Regulates Stemness Maintenance by Transcriptional Up-Regulation of Stemness Factors CD49F And ALDH1 via ERK Signalling

To further elucidate the role of ERK signalling in regulation of stemness downstream of RHOC, clonogenicity and molecular expression assays for stemness genes were conducted on SiHa-R cells post ERK pathway inactivation. PD184352, a highly selective inhibitor of MKK1 and MKK2, was used for this purpose (Allen et al., 2003). Treatment of SiHa cells at various concentrations of PD184352 to determine the most effective concentration of the inhibitor proved that PD184352 effectively reduced phosphorylation of ERK1/2 at concentrations of 0.5µM and above **(Figure 7.8)**. Therefore, all further experiments were performed at a concentration of 0.5µM.

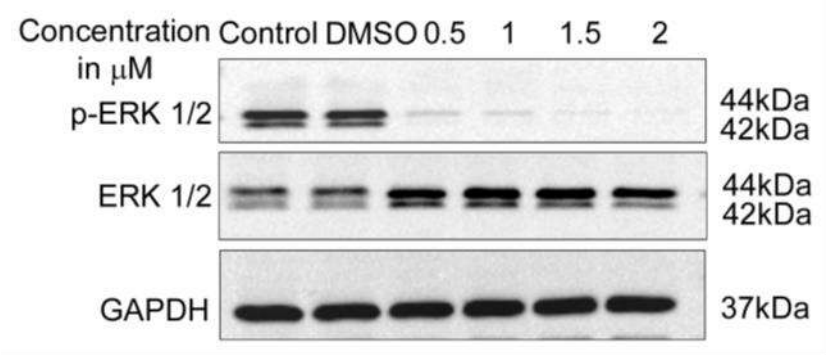

Figure 7.8: Representative western blot depicting diminished p-ERK1/2 levels upon PD184352 treatment of SiHa cells (n=3), with GAPDH serving as the loading control.

In order to determine the contribution of ERK signalling in maintenance of self-renewal capability in SiHa-R cells, SiHa-R cells treated with PD184352 were subjected to the clonogenic assay. Treatment of SiHa-R with PD184352 at a concentration of 0.5µM was found to remarkably compromise the clonogenicity gained upon RHOC over-expression. As shown in **Figure 7.9**, SiHa-R cells treated with PD184352 formed significantly lower number of clones in comparison with the vehicle control, DMSO (Average number of colonies- Control=142, DMSO=120, PD184352=30; $p<0.05$). This indicated that inhibition of the ERK pathway led to partial abrogation of the gain in self-renewal ability observed upon RHOC over-expression.

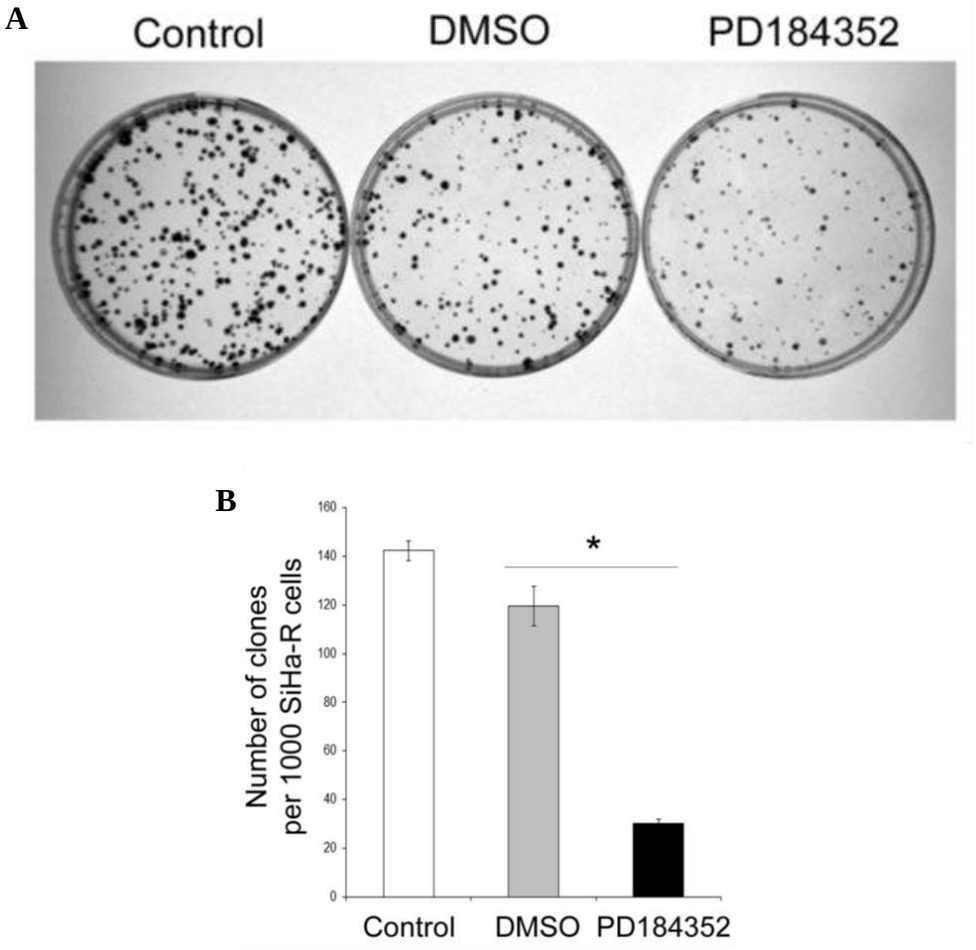

Figure 7.9: (A) Representative image showing decreased clonogenicity upon PD184352 treatment of SiHa-R. (B) Bar graph representation of the average number of clones formed by SiHa-R cells, showing a decrease upon PD184352 treatment, as compared with vehicle control (DMSO) (n=3, $p<0.05$).

To identify the specific genes affected by ERK signalling downstream of RHOC, gene expression of SiHa-R cells subjected to PD184352 treatment was studied. Expression patterns of *ALDH1*, *CD49F*, *ABCG2*, *POSTN* and *NANOG* were analysed in SiHa-R cells treated with the ERK inhibitor. Transcript level analysis of stemness genes in SiHa-R cells revealed a modest, but significant reduction in expression of *CD49F* and *ALDH1* upon ERK inhibition as shown in **Figure 7.10**.

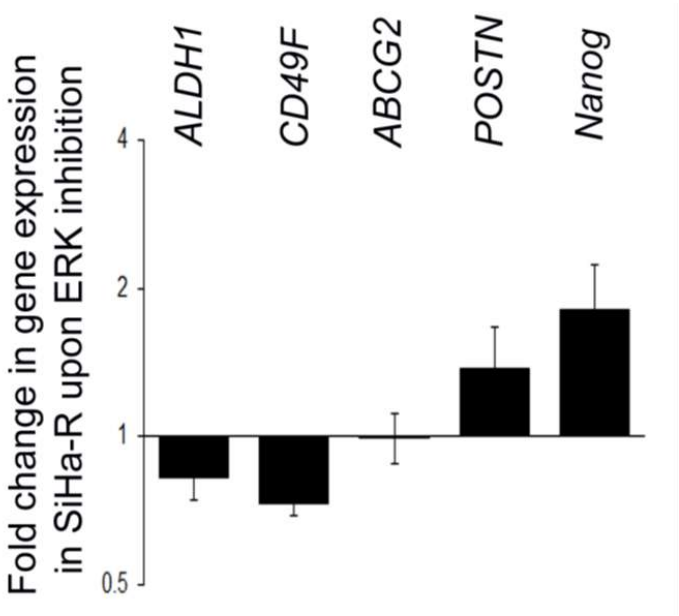

Figure 7.10: qPCR analysis shows a reduction in transcript levels of specific stemness markers in SiHa-R cells upon treatment with the ERK pathway inhibitor (PD184352). Average values of gene expression obtained post normalization with the vehicle control (DMSO) have been plotted. AICDA was used as the internal control (n=3, $p<0.05$).

Interestingly, *POSTN* and *NANOG* showed an increase in expression upon PD184352 treatment. This observation is in agreement with a report in the year 2014, which suggested that activation of ERK signalling could suppress renewal of embryonic stem cells (Hamilton and Brickman, 2014). Significantly, the expression of *NANOG* has been found to be up-regulated upon ERK inhibition (Martello et al., 2013).

Parallelly, immunoblotting studies were carried out to further confirm this observation. SiHa-R cells blocked for active ERK signalling were probed for the expression status of CD49F, ALDH, SOX2 and NANOG. PD184352 treatment in SiHa-R cells was observed to result in down-regulation of CD49F and ALDH levels, whereas expression of SOX2 and NANOG remained unchanged as depicted in **Figure 7.11**.

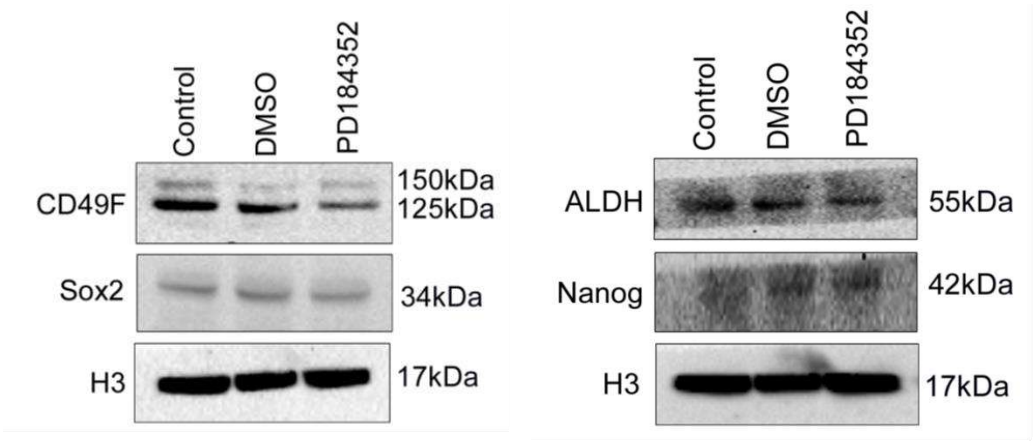

Figure 7.11: Representative immunoblot image shows a decrease in CD49F and marginal decrease in ALDH levels upon ERK pathway inhibition (PD184352) in SiHa-R cells, with no change in SOX2 and NANOG in comparison with the vehicle control (DMSO) (n=3). H3 was used as the loading control.

These data together confirm that the ERK pathway contributes to stemness maintenance by transcriptional up-regulation of CD49F and ALDH1. Interestingly, however, though RHOC was observed to regulate the expression of a plethora of genes involved in stemness maintenance, including those involved in pluripotency, ERK signalling was observed to contribute towards changes in expression levels of CD49F and ALDH1 alone. No significant change was observed upon blocking ERK activation in NANOG and SOX2 expression, which are known pluripotency factors (Chambers and Tomlinson, 2009; Fong et al., 2008).

7.2.3 E2F1 is the Transcription Factor Downstream of ERK Signalling That Promotes Up-Regulation Of CD49F and ALDH1

In order to identify the specific ERK-dependent transcription factor responsible for induction of stemness gene expression in a RHOC-high background, immunofluorescent staining was performed on a range of transcription factors known to be dependent on ERK activation for their localization/activation. Activation of the transcription factors ATF2, CREB and c-EBPα have previously been favourably linked to ERK signalling (Ouwens et al., 2002; Ross et al., 2004; Xiao et al., 2010). **Figure**

7.12 shows the array of transcription factors that were studied in SiHa-N and SiHa-R cells.

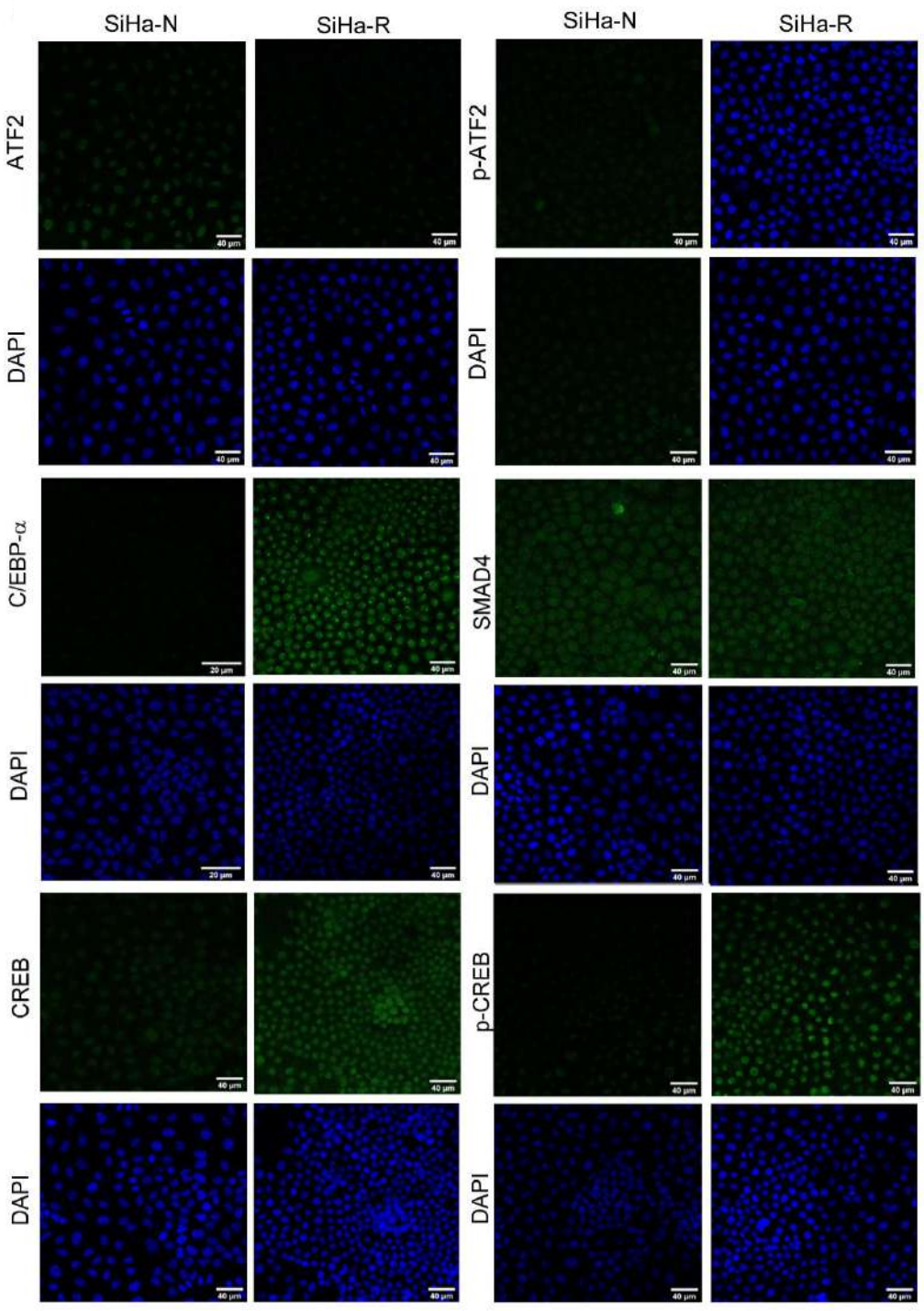

Figure 7.12: Representative immunofluorescent images depicting the levels and localization of various transcription factors in SiHa-N and SiHa-R cells (n=3). Scale bars are indicated.

Amongst the transcription factors analysed, c-EBPα was observed to undergo significant up-regulation in SiHa-R cells. As shown in **Figure 7.13**, E2F1 was also observed to undergo considerable changes in expression and localization upon RHOC over-expression. RHOC over-expression was seen to result in a remarkable increase in nuclear E2F1 levels, as observed by immunofluorescent staining of E2F1 in SiHa-R cells.

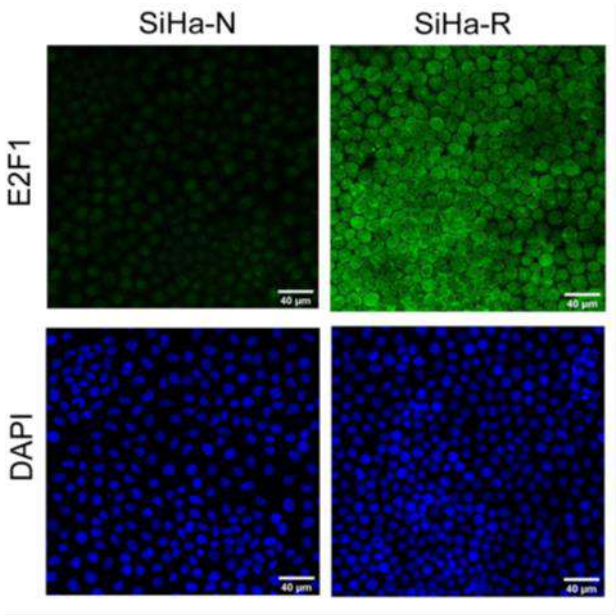

Figure 7.13: Immunofluorescent analysis reveals significant increase in E2F1 levels in SiHa-R cells, in comparison with SiHa-N cells (n=3). Scale bars are indicated.

Analysis of the transcription factors revealed up-regulation of c-EBPα and E2F1 in SiHa-R cells as compared to SiHa-N. In order to verify if the observed changes are reversed upon RHOC depletion, SiHa cells were transfected with RHOC siRNA and immunofluorescent staining was performed for c-EBPα and E2F1 in RHOC siR and SCR (cells transfected with scrambled control siRNA) cells. As shown in **Figure 7.14**, no significant change was observed in either expression or localization of c-EBPα upon RHOC knockdown.

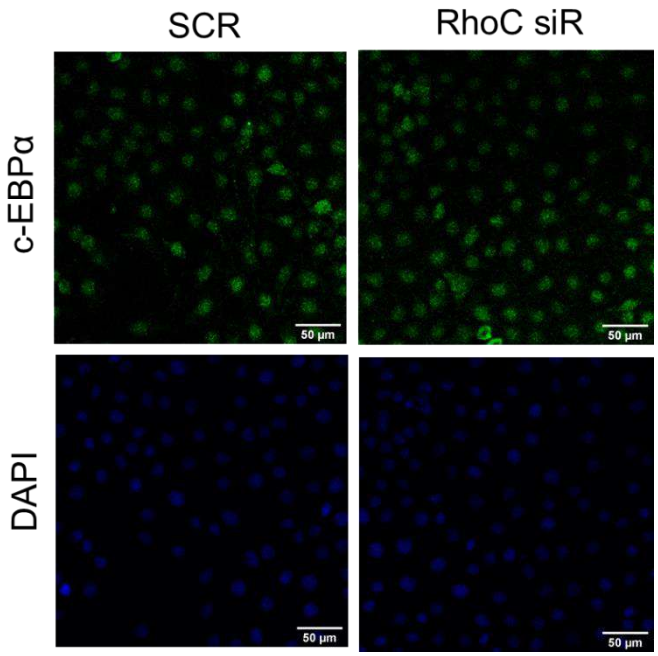

Figure 7.14: Representative immunofluorescent images of c-EBPα in SiHa cells upon RHOC siRNA transfection. No change was observed in c-EBPα levels on RHOC silencing in comparison with the scrambled control (SCR) (n=3).

However, RHOC siRNA transfection was observed to result in a significant decrease in nuclear E2F1, as shown in **Figure 7.15**, implying a possible role for RHOC in nuclear localization of E2F1.

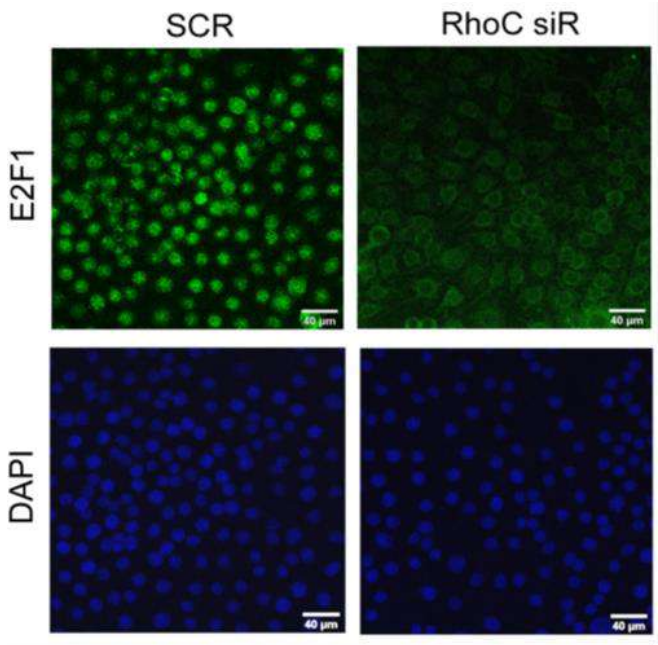

Figure 7.15: siRNA mediated knockdown of RHOC was observed to result in nuclear depletion of E2F1 (n=3) (scale bars are indicated).

Immunoblotting further confirmed this observation. Analysis of the E2F1 levels in SiHa-N and SiHa-R cells by western blotting revealed a significant increase in E2F1 in SiHa-R cells as compared to SiHa-N as depicted in **Figure 7.16**.

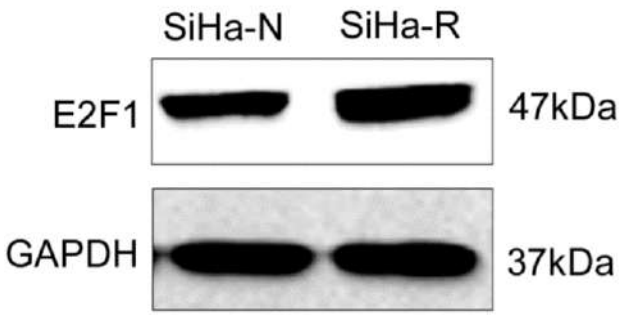

Figure 7.16: Immunoblotting verifies the up-regulation of E2F1 in RHOC over-expressing cells (SiHa-R) in comparison with SiHa-N (n=3). GAPDH was used as the loading control.

Parallel western blotting investigations were undertaken on SiHa cells subjected to siRNA mediated RHOC knockdown. Transfection of SiHa cells with RHOC-specific siRNA was observed to result in reduction in E2F1 levels in comparison with the scrambled control (SCR), as shown in **Figure 7.17**.

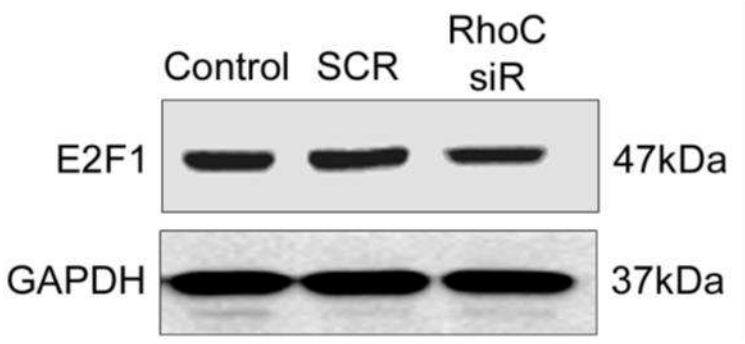

Figure 7.17: Representative immunoblot images of RHOC siRNA treated (RHOC siR) cells display a down-regulation in E2F1 levels in comparison with scrambled control (SCR) 72h post transfection (n=3). GAPDH was utilized as loading control.

Numerous reports have linked E2F1 to active ERK signalling (Korotayev et al., 2008; Meng and Ghosh, 2014). In order to establish whether this change in E2F1 expression and localization is a result of ERK signalling, nuclear levels of E2F1 were assessed in SiHa-R cells upon ERK pathway inactivation. Immunofluorescent staining to determine changes in localization of E2F1 in SiHa-R cells upon PD184352 treatment, revealed that deactivation of ERK signalling led to significant decrease in nuclear E2F1 levels as compared to the vehicle control (DMSO) **(Figure 7.18)**.

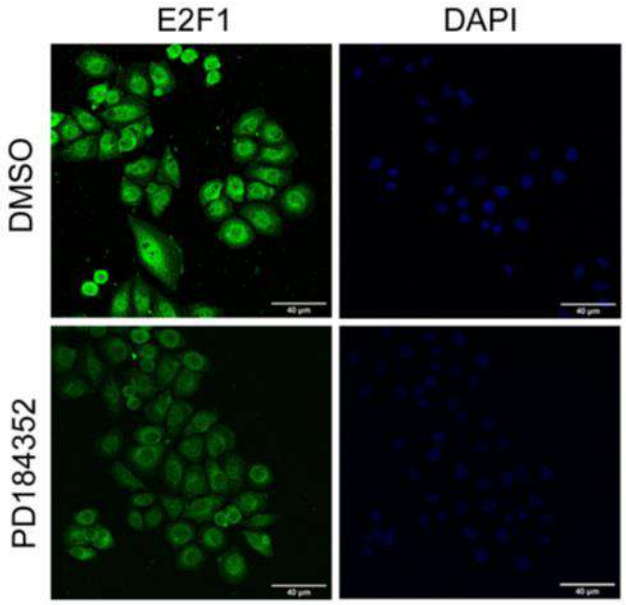

Figure 7.18: Immunofluorescent analysis verifies reduction in nuclear E2F1 upon ERK pathway inhibition (PD184352) in SiHa-R cells, in comparison with vehicle control (DMSO) (n=3). (scale bars are indicated)

To further confirm this, SiHa-N and SiHa-R cells were subjected to cellular fractionation to isolate nuclear and cytosolic components of each cell type separately. Fractionated lysates of SiHa-R cells treated with PD184352 were analysed for E2F1 levels by immunoblotting. As depicted in **Figure 7.19**, determination of E2F1 levels by western blotting also revealed significant reduction in nuclear E2F1, thereby confirming depletion of nuclear E2F1 upon ERK signalling in SiHa-R cells. Histone 3 (H3) was used as the loading control for the nuclear fraction (NF), whereas the cytosolic protein tubulin was utilized as the loading control for the cytosolic fraction (CF) (Herrmann et al., 2017).

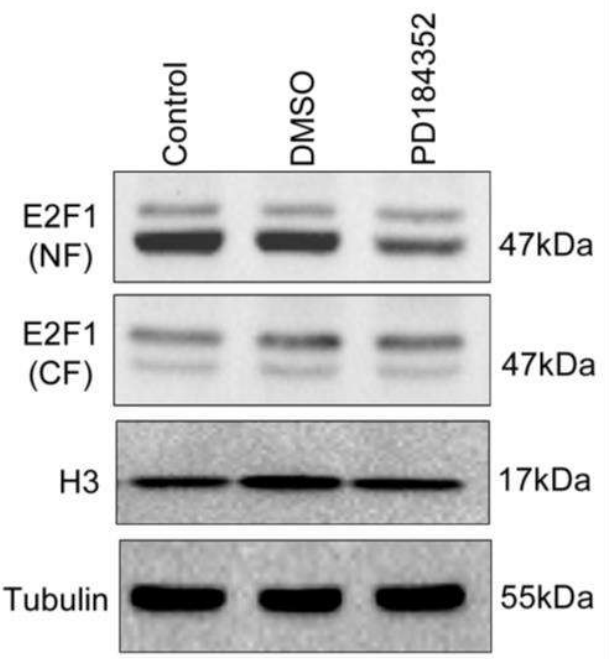

Figure 7.19: Representative western blotting image of fractionated lysates shows clear down-regulation of nuclear E2F1 levels (E2F1 (NF)) in SiHa-R cells upon ERK inhibition (PD184352), in comparison with vehicle control (DMSO) (n=3). No significant difference was observed in cytosolic E2F1 (E2F1 (CF)) levels. Histone3 (H3) and tubulin were used as loading controls for nuclear and cytosolic fractions respectively.

Data thus far indicates a possible link between levels of nuclear E2F1 and ERK signalling in RHOC over-expressing cells. In order to determine the specific genes regulated by E2F1 in RHOC over-expressing cells via ERK signalling, SiHa-R cells were subjected to siRNA-mediated inhibition of E2F1 and the expression of target stemness genes was analysed. Firstly, immunoblotting was performed to ascertain the efficiency of E2F1 siRNA transfection by comparing the E2F1 levels of transfected cells (E2F1 siR) with scrambled negative control (SCR). As depicted in **Figure 7.20**, western blotting confirmed the depletion of E2F1 in siRNA transfected cells.

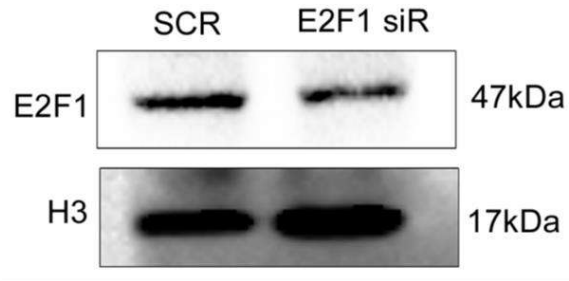

Figure 7.20: Representative immunoblot image shows successful knockdown of E2F1 upon siRNA mediated silencing (n=3). H3 was used as the loading control.

Post confirmation of successful knockdown of E2F1, SiHa-R cells were depleted of E2F1 and the resulting effect on stemness gene expression was analysed. qPCR analysis to determine transcript levels of genes in E2F1 knocked down SiHa-R cells revealed significant reduction in *CD49F* and *ALDH1* as shown in **Figure 7.21**. Importantly, as observed in the case of PD184352 mediated inhibition of ERK signalling in SiHa-R cells, mRNA levels of *NANOG* and *SOX2* remained unaltered upon E2F1 silencing.

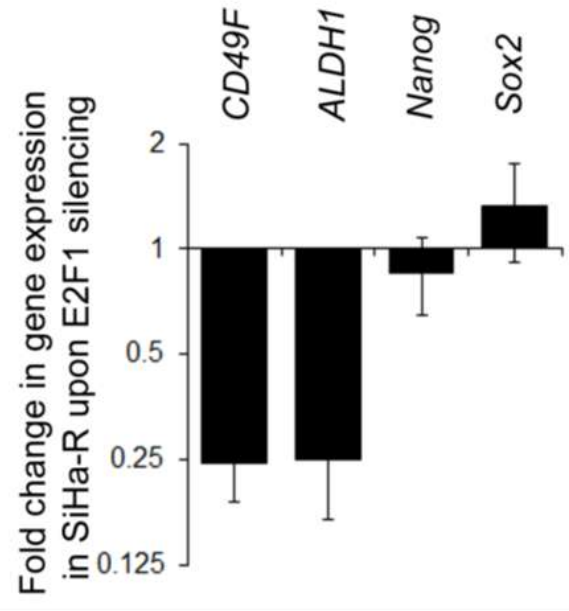

Figure 7.21: Bar graph representation of significant decrease in CD49F and ALDH1 transcripts in SiHa-R cells upon E2F1 siRNA treatment (n=3, $p<0.05$). Values were normalized against gene expression data from scrambled siRNA (SCR) treated cells, with AICDA as internal control.

Immunoblotting further confirmed reduction in CD49F and ALDH levels upon E2F1 siRNA transfection. As shown in **Figure 7.22**, SiHa-R cells transfected with E2F1 specific siRNA was observed to result in decreased CD49F and ALDH levels as compared to cells transfected with the scrambled negative control (SCR).

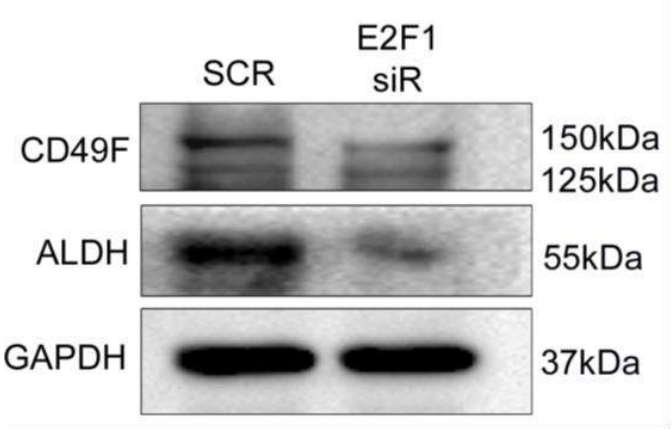

Figure 7.22: Immunoblotting verifies reduction in CD49F and ALDH levels upon E2F1 knockdown (E2F1 siR) in comparison with scrambled control (SCR) (n=3), with GAPDH as loading control. Representative image is shown.

Collectively, these data allude favourably to the hypothesis that RHOC via ERK signalling results in E2F1-mediated transcriptional activation of stemness genes CD49F and ALDH1. However, it must be noted that not all the stemness genes investigated in this study were under the control of the RHOC-ERK signalling axis. Specifically, modulations to the ERK pathway were observed to result in no significant changes to genes related to maintenance of pluripotency.

7.3 Conclusion

Transcriptomic data analyses revealed up-regulation of various pathways including MAPK and NF-κβ signalling in SiHa-R cells. However, further investigations revealed that RHOC-ERK signalling had the largest impact on RHOC-mediated CSC regulation. RHOC was found to activate the ERK pathway leading to up-regulation of factors that regulate stemness ability. Inhibition of this pathway was observed to lead to reduction in stemness capability, as proven both phenotypically and through molecular expression analyses, that revealed diminished levels of CD49F and ALDH. Interestingly, factors that regulate pluripotency, like NANOG and SOX2 were found to remain unaltered upon ERK inhibition in SiHa-R cells.

Further, the RHOC-ERK axis was found to be driven by the transcription factor E2F1, with inhibition of ERK signalling resulting in decreased nuclear levels of E2F1 in the background of RHOC over-expression. As observed by ERK inhibition, E2F1 depletion was found to result in a similar reduction of the stemness markers CD49F and ALDH in SiHa-R cells, with no effect on pluripotent markers. These observations confirm that RHOC leads to activation of the ERK pathway, which supports the stemness phenotype of RHOC over-expressing cells via regulation of expression of cytosolic stemness proteins through its downstream effector E2F1.

Importantly, this signalling arm was found to regulate only extracellular and cytosolic stemness-related factors, with minimal effect on the core genes involved in maintenance of pluripotency like NANOG and SOX2. However, since RHOC has been found to regulate both extracellular CD markers involved in stemness regulation as well as core transcriptional activators of pluripotency, it was hypothesised that RHOC could be operating through two parallel arms- one cytoplasmic signalling axis that mediates regulation of expression of cytosolic proteins, and another alternate mechanism that governs core regulatory networks that control pluripotency. The following chapters attempt to identify this alternate mechanism.

CHAPTER -VI

Nuclear RHOC Interacts with WDR5 and Enhances Stem-Like Ability by Activating the Expression of Stemness Genes

8.1 Introduction

Epigenetic alterations are emerging as important events governing cancer progression and response to therapy (Sharma et al., 2010). Changes in DNA methylation profiles and histone modifications have been associated with accessibility of transcriptional regulators to the genome (Bannister and Kouzarides, 2011; Karlic et al., 2010; Razin and Cedar, 1991).

Differentiation and dedifferentiation mechanisms are tightly regulated by epigenetic modifications. A slight tip in this intricately maintained balance can result in triggering "reprogramming" processes that significantly alter self-renewal capabilities (Munoz et al., 2012). Histone modifications have been associated with changes in the gene expression profile (Bannister and Kouzarides, 2011). Over the years, cumulative evidence suggests that these versatile marks are closely linked to cancer progression and response to therapy (Zhao and Shilatifard, 2019). Alterations to histones can be of varied types including methylation, acetylation, phosphorylation, sumoylation and many others (Biswas and Rao, 2018). The resultant effect on gene expression is dependent on the type and site of modification.

Histone modifications have been associated with poor outcomes in various cancer models. In head and neck cancer, histone deacetylation (HDAC) inhibition has been observed to lead to shrinking of the CSC pool (Giudice et al., 2013). In agreement with this finding, HDAC inhibitors designed specifically for HDAC1 and HDAC7 were observed to successfully target CSCs in ovarian and breast cancers (Witt et al., 2017). Significantly, colorectal cancer has been found to be heavily reliant on modifications to histone proteins. Various types of histone methylations, acetylations and phosphorylations have been associated with progression of colorectal cancers (Qin et al., 2020). Histone methylation and acetylation at various sites have been observed to regulate breast cancer progression based on the type of histone modification and the site of alteration (Zhuang et al., 2020).

Rho GTPases have been linked to tumour progression in various models, but none so far have been associated with epigenetic modulations in the cancer context. Until date, there has been only one report that associates a Rho GTPase with chromatin structure. MgcRacGAP has been linked with maintenance of CENP-A, an epigenetic mark that

ensures genomic stability at the centromeric region of chromosomes, and aids segregation of DNA during cell division (Lagana et al., 2010).

This chapter explores the nuclear role of RHOC and proposes significant novel contributions of the protein to chromatin remodelling via interactions with nuclear proteins. RHOC expression was observed to result in changes in the level of trimethylation of Histone3 at the fourth lysine residue via its interaction with WDR5. It has been shown using mass spectrometry, phenotypic assays, expression profiling and luciferase reporter assays that RHOC interacts with WDR5 at the NANOG promoter and results in changes in H3K4me3 levels, consequently regulating stemness capability.

8.2 Results and Discussion

8.2.1 RHOC Over-Expression Leads to Global Up-Regulation of Gene Expression and Transcriptionally Active Chromatin

Since data presented in Chapter 5 indicated that classical pluripotent factors like NANOG, OCT4 and SOX2 were unaffected by ERK signalling, efforts were directed towards deciphering alternate mechanisms by which RHOC could regulate these molecules.

Cancer progression is often a result of complex integration between signalling and epigenetic mechanisms (Wainwright and Scaffidi, 2017). Analysis of the RNA-seq data revealed that 70% of the genes in SiHa-R cells were up-regulated. This implied global up-regulation of the transcriptional network in RHOC over-expressing cells. **Figure 8.1** is a pie chart that illustrates the differential gene expression status of SiHa-R cells in comparison with SiHa-N, clearly indicative of its transcriptionally enhanced status.

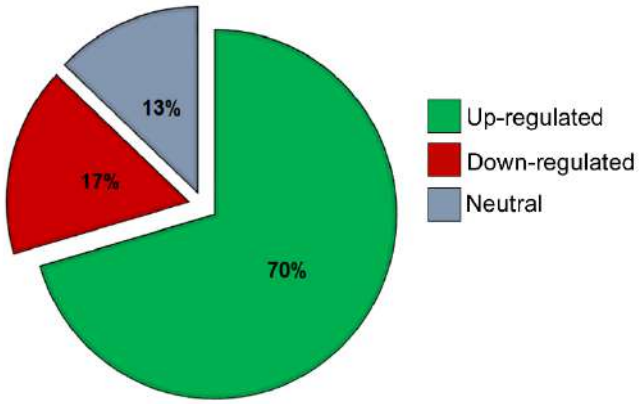

Figure 8.1: Pie-chart depicting up-regulation of 70% of the genes in SiHa-R cells as revealed by the RNA-seq data.

To provide an overview of the changes in gene expression induced by RHOC over-expression, volcano plots that depict both significance and fold changes were generated using the online software, Shiny (https://paolo.shinyapps.io/ShinyVolcanoPlot/). As shown in **Figure 8.2**, the volcano plot clearly illustrates preferential up-regulation of genes in SiHa-R cells as compared to SiHa-N.

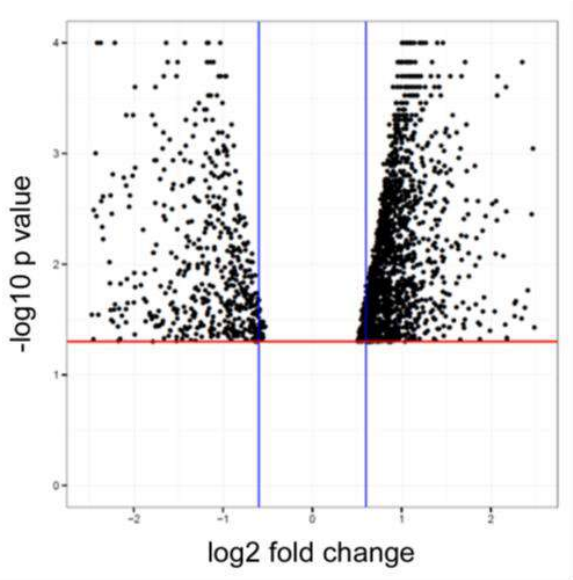

Figure 8.2: A volcano plot depicting distribution of the fold change in gene expression showing a clear transcriptional advantage in SiHa-R cells (fold change cut-off value=1.5 for up-regulated genes and 0.5 for down-regulated genes, $p<0.05$).

The RNA-seq data was further analysed to determine the specific genes that were positively regulated in SiHa-R cells and the extent of their up-regulation. **Figure 8.3** is a heatmap displaying fold changes of the top 3000 genes that exhibited significant changes in gene expression on account of RHOC over-expression. The heatmap generated shows that a majority of the genes were up-regulated in SiHa-R cells, with a relatively much smaller number showing increased expression in SiHa-N cells (fold change cut-off value=0.5 and 1.5, $p<0.05$). These data are indicative of the transcriptional advantage endowed on cells by virtue of over-expression of the RHOC protein.

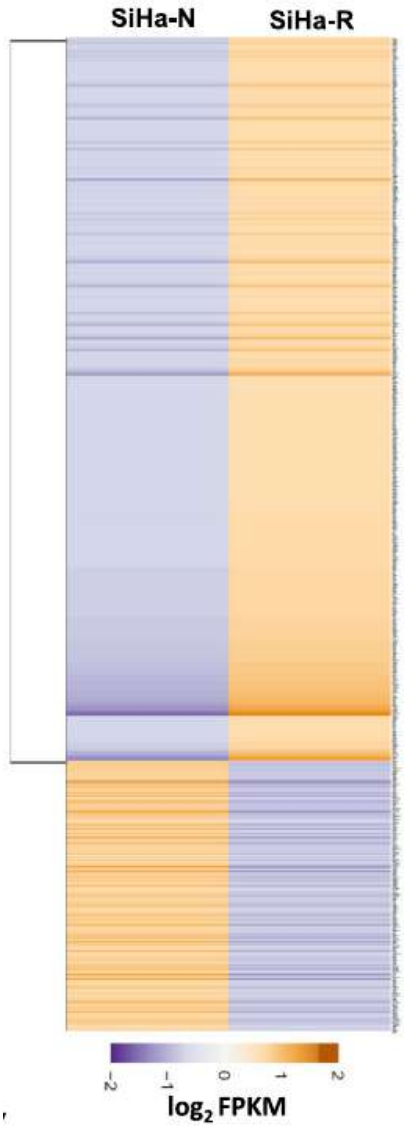

Figure 8.3: Clustvis-enabled heatmap analysis showing the transcriptionally elevated status of SiHa-R cells (n=2, $p<0.05$).

Analysis of the transcriptomic data revealed global up-regulation of gene expression in SiHa-R cells. Such widespread changes in gene expression cannot be attributed to a single signalling pathway alone, leading to the deduction that there could be more than one mechanism at play under the helm of RHOC.

Epigenetic alterations are known to dictate organization of the chromatin (Jones and Wolffe, 1999). Structure of the chromatin, in turn is known to affect gene expression on a global scale (Li et al., 2007). It was therefore hypothesised that RHOC over-

expression might be resulting in epigenetic alterations to the DNA, which modify chromatin organization, eventually leading to global changes in gene expression.

Interestingly, in line with this hypothesis, several genes with well-defined nuclear functions were found to be over-expressed in SiHa-R cells. Cytoplasmic component (CC) analysis of the transcriptome data using the DAVID online tool was used to determine the cellular compartment in which the up-regulated genes operate. **Figure 8.4** is a graphical depiction of the CC analysis which revealed that a majority of the transcripts over-expressed in SiHa-R had distinct nuclear functions.

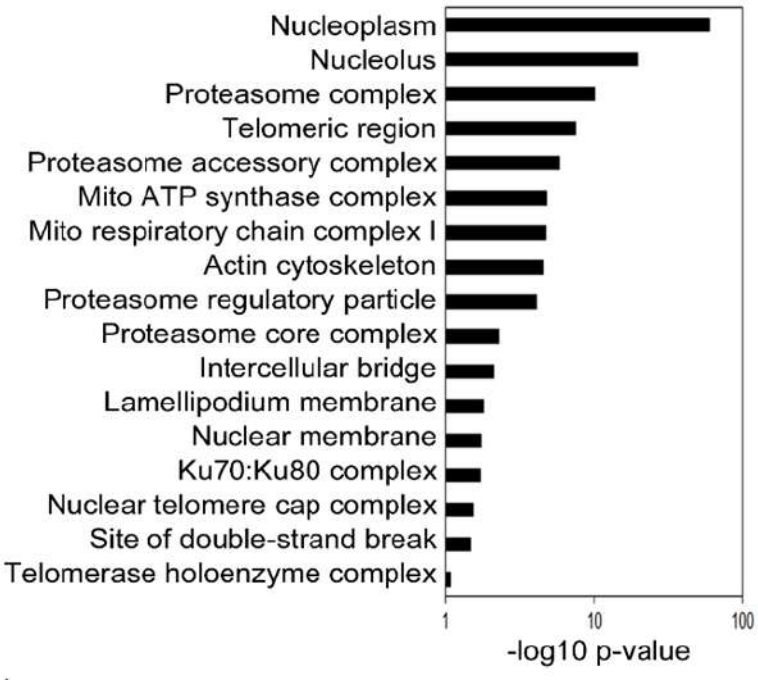

Figure 8.4: Bar graph representing localization of the up-regulated gene products in SiHa-R as observed by cytosolic component (CC) analysis using DAVID, with the localization being found to be largely nuclear.

The up-regulated genes were further studied to determine their specific molecular functions. Analysis revealed that a large number of the genes that were over-expressed in SiHa-R had well-established epigenetic functions. The cohort of epigenetic genes up-regulated in SiHa-R and their fold changes are represented by a heatmap in **Figure 8.5**.

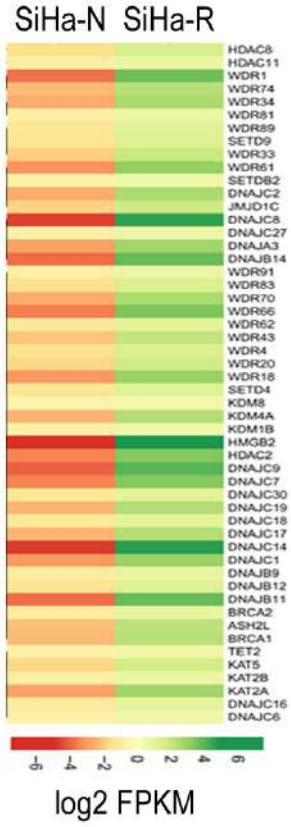

Figure 8.5: Heatmap representation of the up-regulated genes in SiHa-R known to be involved in epigenetic modifications.

It is known that accessibility of DNA to transcription factors is primarily mediated by DNA demethylation and histone modifications (Cusack et al., 2020; Heberle and Bardet, 2019). However, no study has so far reported a link between RHOC and epigenetic modifications of DNA. It was therefore intriguing to explore whether RHOC, with its contribution to multiple tumour phenotypes, globally alters the transcriptional landscape by regulating mechanisms that epigenetically modify DNA.

8.2.2 RHOC Expression and Association with Chromatin Openness

Our lab has earlier reported a nuclear role for RHOC by demonstrating its involvement in DNA repair in conjunction with ROCK2 (Pranatharthi et al., 2019). However, no study thus far has deciphered the molecular events governed by nuclear RHOC. Further studies were therefore taken up to explore this aspect in detail.

Experiments were conducted to determine localization of RHOC in patient-derived tumour sections. Immunohistochemical analysis revealed an interesting expression pattern for RHOC. As shown in **Figure 8.6**, intense nuclear expression of RHOC was observed in spindle-shaped motile cells at the leading edge of the tumour bordering the stroma (indicated with black arrows), while non-motile cells away from the border had diffused RHOC expression in the cytoplasm.

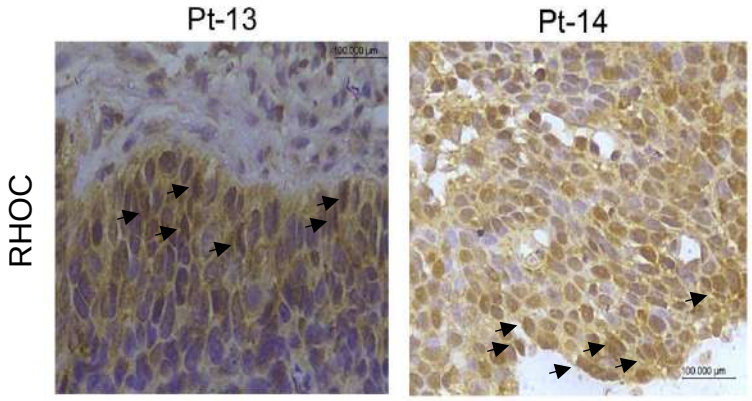

Figure 8.6: Representative images of nuclear RHOC expression in clinical specimens as observed by immunohistochemical staining of RHOC. (scale bars are indicated)

Spindle-shaped cells present at the tumour stroma junction are representative of highly invasive tumours undergoing EMT (Friedl and Alexander, 2011). Importantly, the EMT process has been associated with gain of stemness properties (Jolly et al., 2015; Mani et al., 2008), suggesting that the cells at the invasive front may be stem-like. The presence of nuclear RHOC in these cells therefore suggests that RHOC may be an important factor in driving the aggressive nature of these cells via nuclear functions.

Stem-like cells are known to have open, easily accessible chromatin (Gaspar-Maia et al., 2010). Since RHOC has been shown to be associated with the stemness phenotype, it was interesting to explore the role of RHOC in chromatin remodelling. Experiments were therefore designed to investigate the link between RHOC and chromatin compactness. Immunofluorescent staining of RHOC along with the nuclear stain, DAPI in patient-derived tumour sections, revealed that a pocket of cells displayed nuclear expression of RHOC, while cytoplasmic staining was observed in the neighbouring cells as shown in **Figure 8.7**. Interestingly, cells with nuclear localization of RHOC displayed less intense staining of the chromatin with DAPI. Compactness of the

chromatin has been inversely linked to the propensity for DAPI uptake (Mascetti et al., 2001). This implies that cells expressing nuclear RHOC have relatively open chromatin that may be easily accessible to transcriptional modulators.

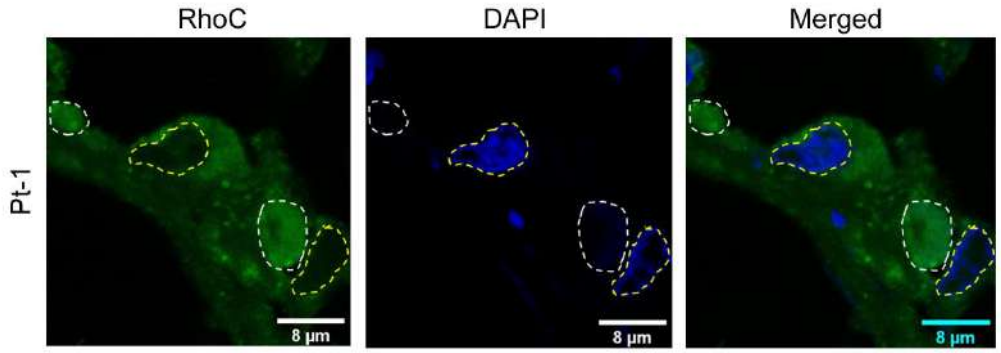

Figure 8.7: Representative confocal images of patient-derived tumour sections showing that cells with high nuclear RHOC (marked with white dotted lines) have faint DAPI staining, whereas cells with largely cytosolic localization of RHOC display intense DAPI staining (marked by yellow dotted lines).

8.2.3 Mass Spectrometry Analysis to Identify Nuclear Binding Partners of RHOC

The data presented so far sets forth evidence to show that RHOC is expressed in the nuclei of tumour cells. Notably however, RHOC does not have a DNA binding domain. Thus, it is likely that the nuclear functions of RHOC are carried out by RHOC's interaction with other nuclear proteins that are known to interact with DNA. Studies were thus designed to identify the nuclear binding partners of RHOC.

In order to unearth the proteins that interact with RHOC in the nucleus, investigations were performed on the nuclear fraction of SiHa-R cells. To ensure clean fractionation of cellular components without any spill-over from non-targeted compartments, western blotting was performed to determine the levels of the cytosolic protein tubulin, and the nuclear protein histone3 (H3) in the fractionated lysates (Herrmann et al., 2017). As shown in **Figure 8.8**, the nuclear fraction showed clear enrichment in levels of H3, with absence of tubulin, whereas the cytosolic fraction displayed elevated tubulin levels accompanied with absence of H3, indicative of successful fractionation.

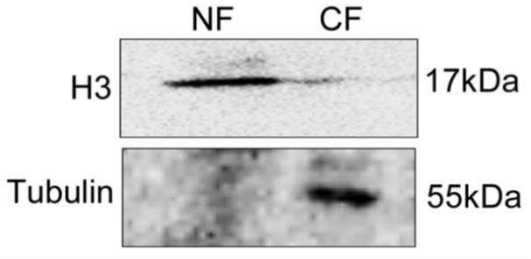

Figure 8.8: Representative western blot image showing presence of H3 in the nuclear fraction (NF) only, and tubulin in the cytosolic fraction (CF) only, indicating clean fractionation of cytosolic and nuclear compartments (n=3).

After confirming that fractionated lysates had the desired cellular components only, proteins in the nuclear fraction of SiHa-R cells were cross-linked and immunoprecipitated using the RHOC antibody, along with the isotype control (IgG). The pulled-down proteins were then subjected to 2D gel electrophoresis and silver staining. The silver-stained gels were compared and spots specific to the RHOC pull-down were excised and analysed by mass spectrometry to identify possible nuclear binding partners of RHOC. **Figure 8.9** is an image of the silver-stained gels.

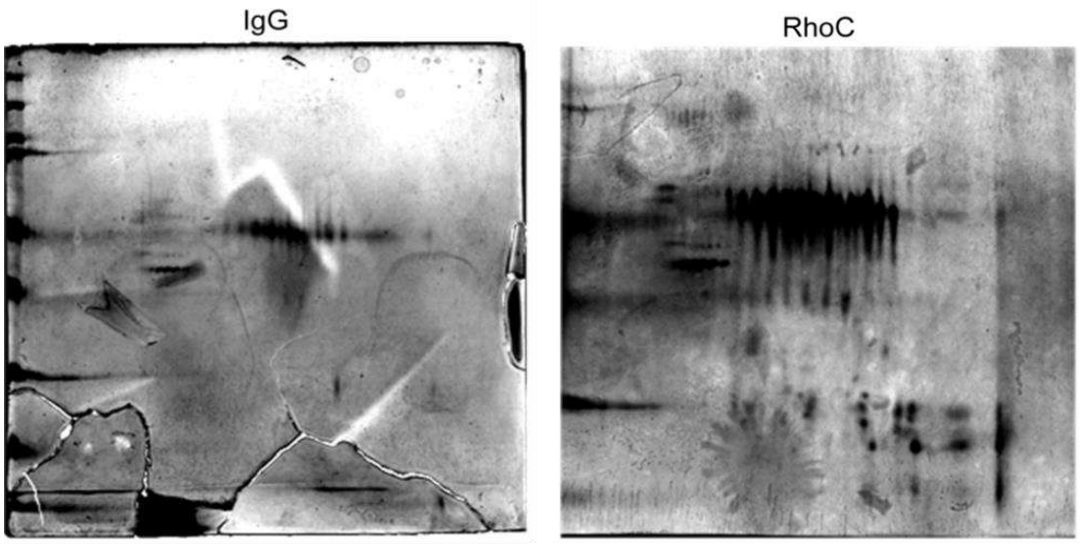

Figure 8.9: Representative gel image of proteins immunoprecipitated from the nuclear fraction of SiHa-R cells using the RHOC antibody, separated by 2D gel electrophoresis and subjected to silver staining to reveal specific spots unique to the RHOC pull-down. These spots were excised and analysed by mass spectrometry to identify the interacting proteins (n=2).

Mass spectrometry (MS) is a highly robust technique that over the past few decades, has emerged as an indispensable tool to identify proteins (Baldwin, 2004). MS is capable of identifying proteins both from single bands/spots excised from gels or from complex protein mixtures, and has a sensitivity of detection in the femtomolar range (Carr et al., 1996). If complex protein mixtures must be analysed, MS is very often preceded by multi-dimensional HPLC, which allows initial separation by chromatography (Washburn et al., 2001). Here, 2D gel electrophoresis was used to separate out the immunoprecipitated proteins. The spots unique to the RHOC pull-down were excised and subjected to MS analysis.

Mass spectrometry data obtained using the Bruker Daltoincs ESI Q-TOF system was analysed using the protein identification software, MASCOT. Detailed analysis of the data revealed possible nuclear targets of RHOC. WDR5 was one of the important nuclear binding targets of RHOC that was unearthed during this process. **Figure 8.10** shows the spectral peaks obtained. The amino acid residues overlapping with the WDR5 protein sequence are coloured in red.

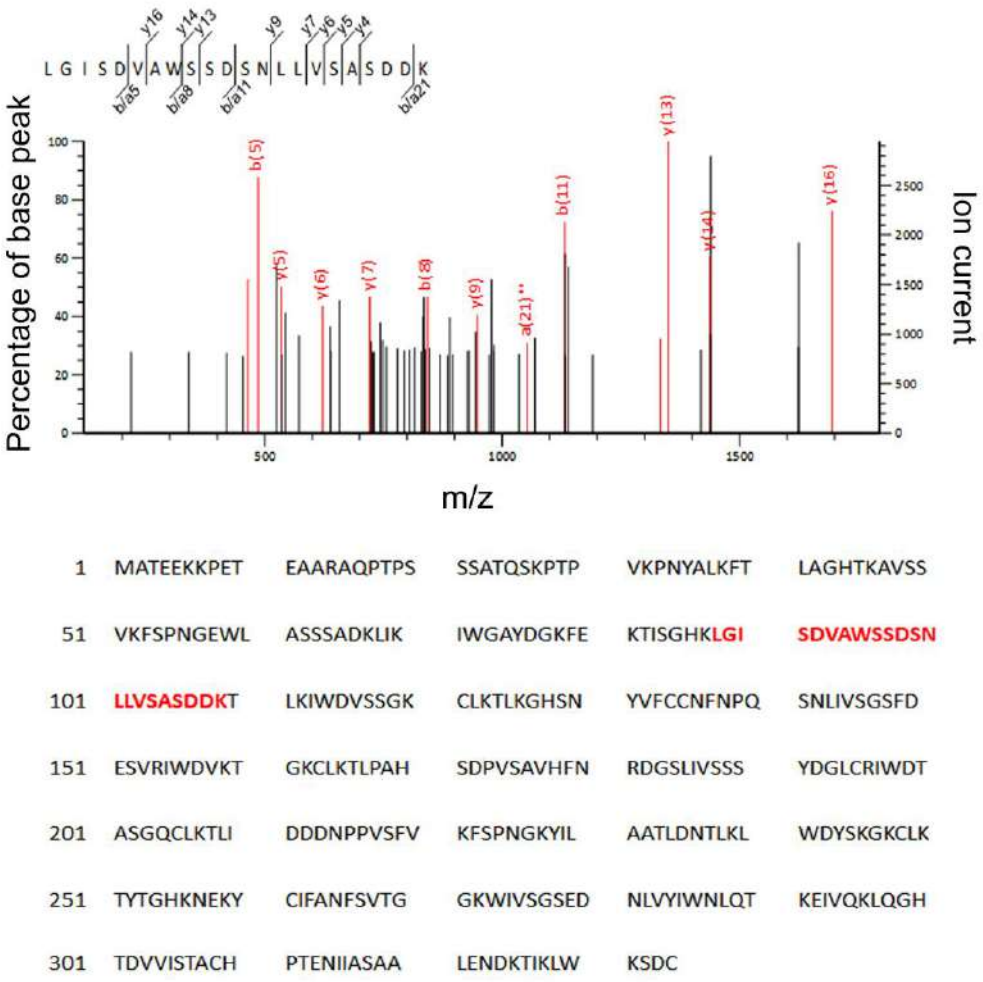

Figure 8.10: Results of the mass spectrometry analysis with residues shown in red indicating an overlap with the amino acid sequence for WDR5.

8.2.4 WDR5 and RHOC Interact Within the Nucleus in Cervical Cancer Cell Lines

WDR5 (WD40 repeat protein 5), is a histone modifier that promotes methylation of histones by acting as a scaffold that holds the multi-subunit complex composed of the retinoblastoma-binding protein-5 (RbBP5) and the absent, small, homeotic disks-2-like (ASH2L) proteins (Dou et al., 2006; Odho et al., 2010). This complex regulates the activity of histone lysine methyltransferases like KMTs, MLLs (mixed lineage leukemia) and SET (Su(var)3-9, Enhancer-of-zeste and Trithorax) proteins (Avdic et al., 2011; Zhang et al., 2012). Specifically, WDR5 is known to cause methylation of histone3 proteins at lysine residues (Ruthenburg et al., 2006).

WDR5 has been implicated in numerous cancer phenotypes in various models. For instance, WDR5 has been shown to interact with c-Myc to regulate initiation, proliferation and progression of pancreatic ductal adenocarcinoma (Carugo et al., 2016). In prostate cancer, WDR5, in association with H3T11P, regulates proliferation and resistance to castration therapy (Kim et al., 2014). Similarly, proliferative and chemo-resistant attributes of bladder cancer have been found to be governed by WDR5 expression (Chen et al., 2015b). Significantly, WDR5 inhibition was found to reduce metastatic spread in breast cancer, and sensitize colon cancer cells to radiation therapy, indicative of its role in supporting aggressive cancer phenotypes (Neilsen et al., 2018; Punzi et al., 2019). As discussed previously, RHOC is also known to be associated with regulation of myriad phenotypes across cancer models. Therefore, the discovery that WDR5 could potentially bind to nuclear RHOC to carry out downstream epigenetic events that support cancer progression was significant.

In order to validate the data obtained from mass spectral analysis, immunofluorescent staining for both RHOC and WDR5 was performed on cells over-expressing RHOC. Analysis of the immunofluorescent staining revealed that WDR5 interacted with RHOC within the nuclei of SiHa-R cells. Confocal microscopy revealed co-localization of RHOC and WDR5, as represented by white pixels in **Figure 8.11**.

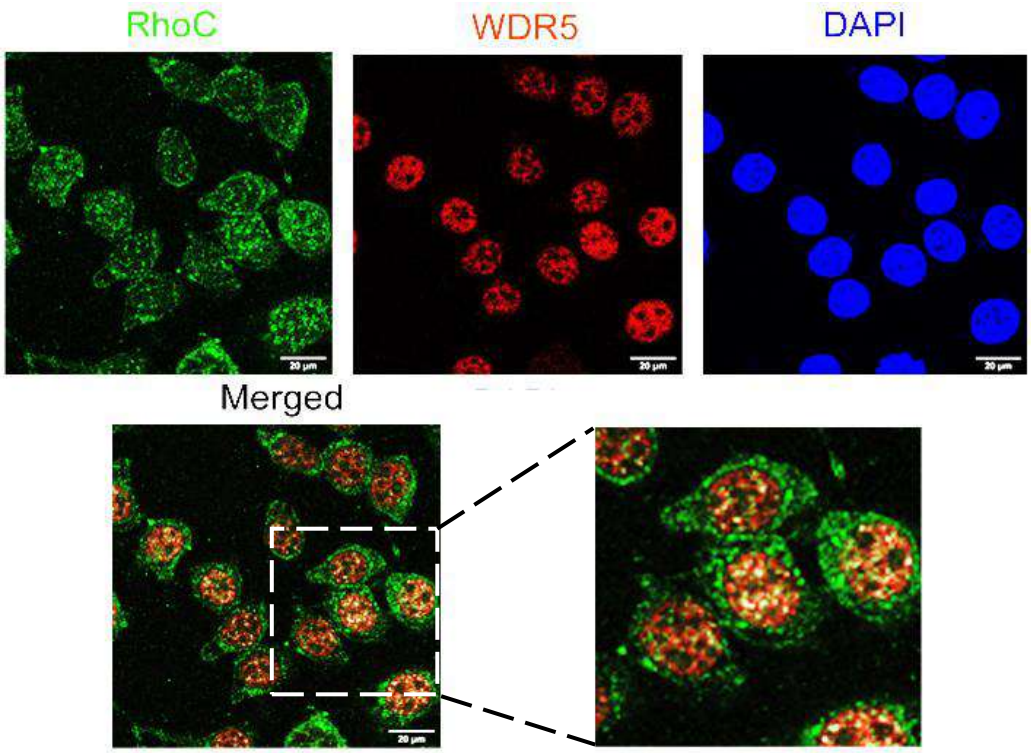

Figure 8.11: Confocal imaging confirms interaction of RHOC and WDR5 in SiHa-R nuclei (n=3). Representative images are shown. (scale bars are indicated).

To further confirm the observed interaction, immunoprecipitation assays were carried out. Nuclear lysates of SiHa-R were immunoprecipitated using the RHOC antibody and probed for WDR5. As shown in **Figure 8.12**, immunoblotting of the precipitated proteins indicated an interaction between RHOC and WDR5. Western blotting of the precipitated complexes depicted the presence of RHOC in the RHOC IP lane, indicative of successful RHOC pull-down. The RHOC IP lane also showed positive detection of WDR5 implying that RHOC and WDR5 interact within the nuclei in SiHa-R cells.

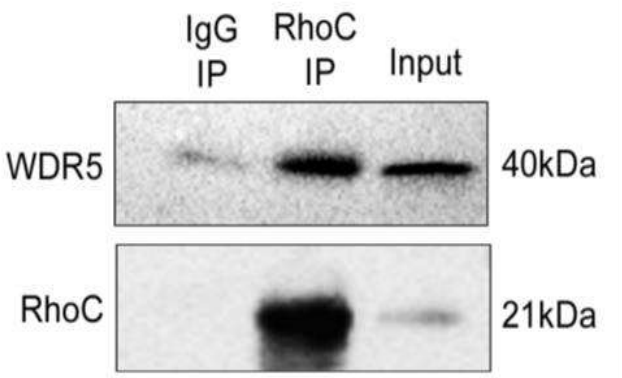

Figure 8.12: Representative immunoblot image showing detection of WDR5 and RHOC in nuclear SiHa-R lysates pulled down with the RHOC antibody (n=3).

To further confirm this finding, a reverse co-IP with WDR5 was performed on the nuclear fraction in SiHa-R cells. The pulled-down complexes were subjected to immunoblotting studies to determine the presence of RHOC in the complexes precipitated by the WDR5 antibody. As depicted in **Figure 8.13**, a positive band in the WDR5 IP lane, suggested successful pull-down of WDR5. Further probing of these blots with the RHOC antibody revealed detection of a band for RHOC in the WDR5 IP confirming the interaction of RHOC and WDR5.

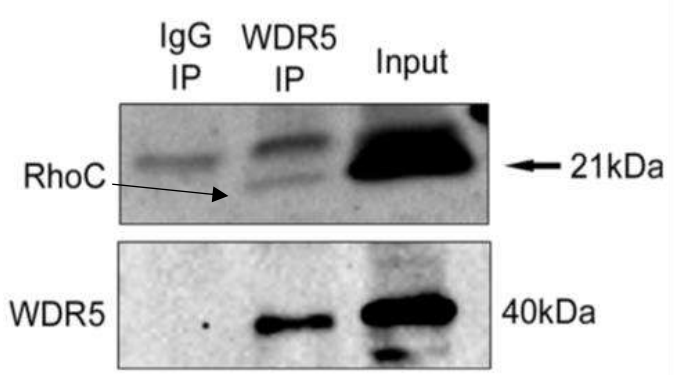

Figure 8.13: Representative immunoblot image showing positive detection of RHOC and WDR5 in nuclear lysates of SiHa-R upon WDR5 pull down (n=3).

Taken together, the mass spectrometry data, immunofluorescent staining and immunoblotting of RHOC IP and WDR5 IP complexes establish that RHOC interacts with WDR5 within the nuclei of SiHa cells over-expressing the RHOC protein.

8.2.5 The RHOC-WDR5 Complex Modulates H3K4 Trimethylation in Cervical Cancer Cell Lines

Once the formation of the RHOC-WDR5 complex was established, the contribution of RHOC towards WDR5 activity was scrutinized. H3K4me3, an active transcriptional mark is associated with poor prognosis in cancer patients (Li et al., 2018). H3K4me3 alteration is mediated by WDR5 and the SET1/COMPASS proteins (Cruz et al., 2018; Howe et al., 2016). The level of this modification was therefore used as a measure of WDR5 activity.

To confirm that WDR5 does indeed regulate the H3K4me3 modification in cervical cancer cell lines, SiHa cells were knocked down for WDR5 and the consequent effect on H3K4me3 modification was assayed. As shown in **Figure 8.14**, WDR5 siRNA-mediated knockdown was seen to result in a remarkable reduction in WDR5 levels as compared to the scrambled control (SCR), indicative of successful knockdown of WDR5 upon transfection with WDR5 siRNA. Analysis of H3K4me3 levels revealed marginal reduction in H3K4me3 upon WDR5 silencing, as compared with SCR **(Figure 8.14)**.

Pixel count analysis of the H3K4me3 signal was performed to quantitatively compare H3K4me3 levels between WDR5 siR treated cells and cells treated using the scrambled control (SCR) shown in **Figure 8.15**. Signal intensity was quantified in 10 random cells from each field and the average pixel counts were plotted. As shown in **Figure 8.15**, analysis revealed that the observed reduction was indeed significant ($p= 2.0508X10^{-5}$).

It must be noted that western blot analysis to study changes in levels of H3K4me3 were attempted multiple times. However, since the H3K4me3 antibody procured was compatible only with immunofluorescent staining, conclusive results could not be obtained using the immunoblotting technique.

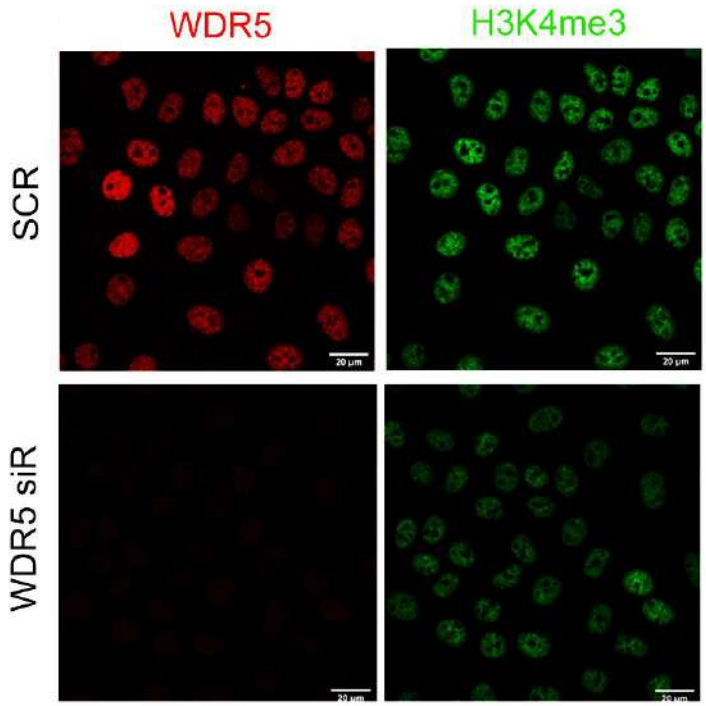

Figure 8.14: Knockdown of WDR5 in SiHa cells leads to successful reduction in H3K4me3 levels, as compared to scrambled negative control (SCR) (n=3). The cells were fixed and stained 72h post transfection. Representative images are shown. (scale bars are indicated).

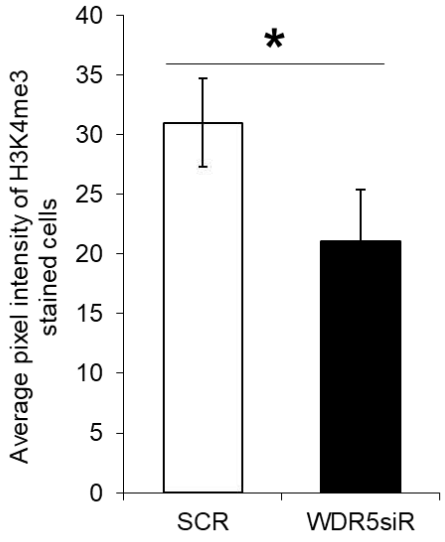

Figure 8.15: Graphical representation of the densitometry analysis performed on H3K4me3 staining in SiHa cells knocked down for WDR5 and those treated with the negative scrambled control (SCR) (n=3, $p<0.05$).

To determine whether RHOC plays a role in WDR5-mediated H3K4me3 modification, changes in the level of H3K4me3 with modulations in RHOC expression were investigated. RHOC was inhibited using siRNA in SiHa cells and the resulting effect on trimethylation of H3K4 was evaluated. siRNA mediated knockdown of RHOC in SiHa cells was seen to result in substantial decrease in H3K4me3 levels as shown in **Figure 8.16**. This observation suggested that RHOC could play a prominent role in aiding H3K4me3 modifications.

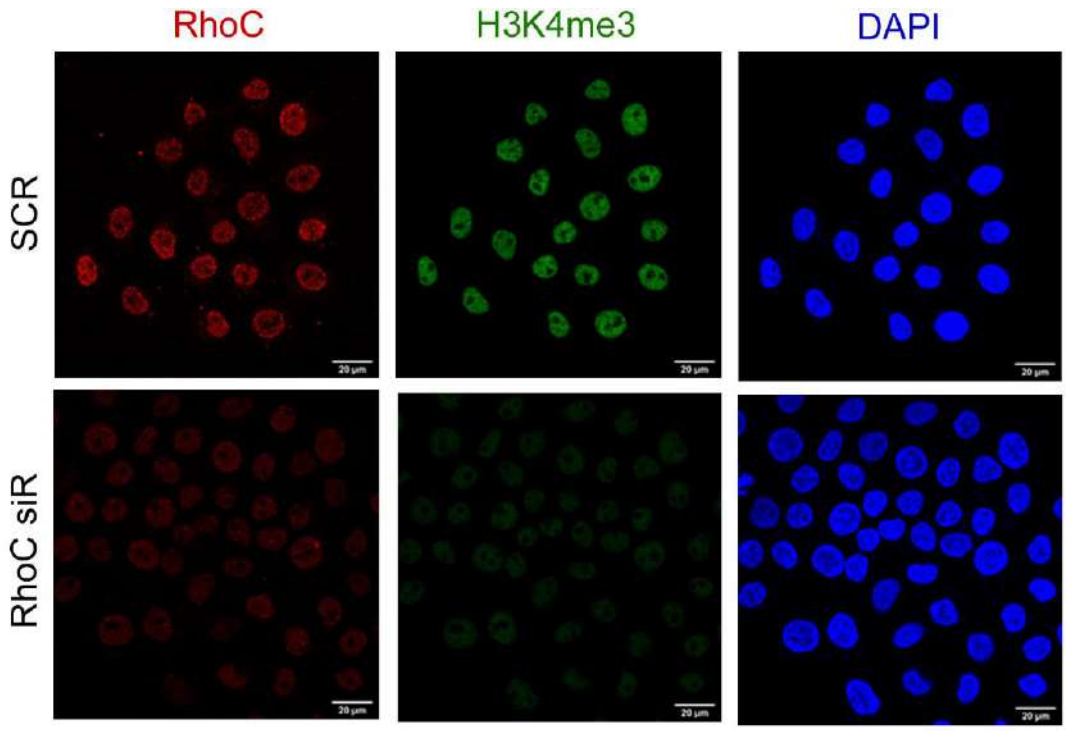

Figure 8.16: siRNA mediated silencing of RHOC resulted in a corresponding decrease in H3K4me3 levels as compared to scrambled control (SCR) (n=3). Immunofluorescence staining was carried out 72h post transfection. Representative images are shown. (scale bars are indicated)

The above data suggests that RHOC and WDR5 contribute to H3K4me3 modifications. In order to ascertain that WDR5 was indeed the downstream effector of RHOC in this context, WDR5 was knocked down in a RHOC-high background and the consequent effect on H3K4 methylation was assessed. Immunofluorescent analysis indicated that silencing of WDR5 in SiHa-R cells led to decreased H3K4me3 levels as shown in **Figure 8.17.** This substantiated the claim that disruption of the RHOC-WDR5 complex had a detrimental effect on WDR5 activity, and consequently on H3K4me3 levels.

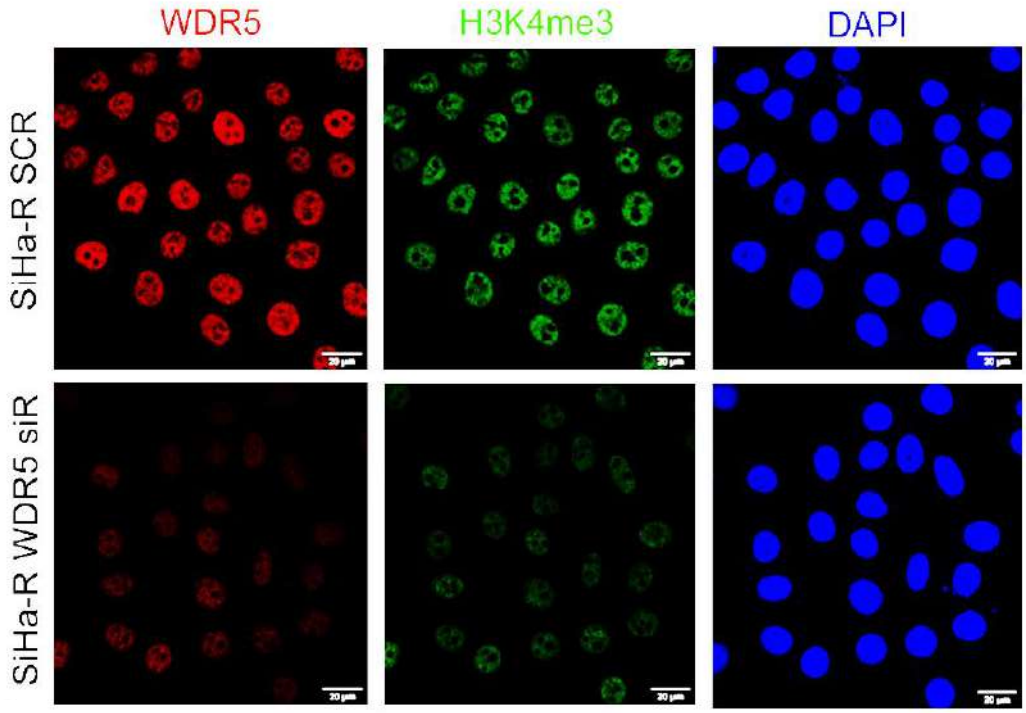

Figure 8.17: Representative image showing reduction in WDR5 and consequent decrease in H3K4me3 levels in SiHa-R cells upon WDR5 knockdown (n=2). Cells were stained 72h post transfection. (scale bars are indicated)

8.2.6 The RHOC-WDR5 Complex Regulates Stem-Like Ability in RHOC Over-Expressing Cells and Transcriptionally Activates NANOG by Binding to Its Promoter

The data thus far indicates that the RHOC-WDR5 complex is instrumental in bringing about trimethylation of H3K4, a mark of actively transcribing genes. Further experiments were carried out to determine the involvement of this complex in stemness maintenance.

Phenotypic assays were undertaken to investigate the effect of WDR5 inhibition on cells endowed with enhanced stemness capability on account of RHOC over-expression. SiHa-R cells silenced for WDR5 were assayed for self-renewal and anoikis resistance capabilities through the soft agar colony formation assay. Analysis of the number of colonies formed revealed that WDR5 knockdown abrogated the augmented stemness ability of SiHa-R cells. WDR5 siRNA treated SiHa-R cells were observed to form significantly lower numbers of medium and large colonies as shown in **Figure**

8.18 ($p<0.05$). These observations implied that WDR5 and RHOC crosstalk could be important in the context of stemness maintenance.

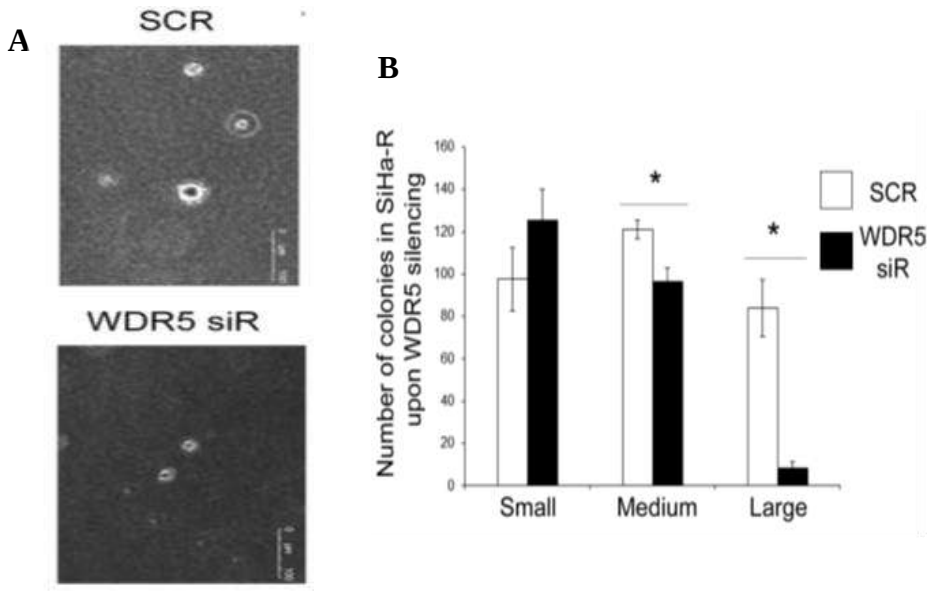

Figure 8.18: (A) Representative soft agar colony images of SiHa-R cells treated with scrambled siRNA (SCR) and WDR5 specific siRNA (WDR5 siR) (n=3). SiHa-R cells were transfected with WDR5 siRNA and seeded for the soft agar assay 72h after transfection. (B) Bar graph representation of the number of colonies formed by SiHa-R cells upon WDR5 siRNA treatment. WDR5 silencing was observed to result in loss of colony forming ability in SiHa-R cells (n=3, $p<0.05$).

Since the soft agar assay indicated a possible role for WDR5 in maintenance of the heightened stem-like features of SiHa-R cells, the specific gene targets that WDR5 could transcriptionally modulate were assessed. To evaluate the effect of the RHOC-WDR5 complex on expression of stemness signatures in SiHa-R cells, transcript levels of key stemness genes were analysed in SiHa-R cells post transfection with WDR5 siRNA. As shown in **Figure 8.19**, qPCR analysis revealed decreased expression of *NANOG*, *ABCG2*, *POSTN*, *OCT4*, *ALDH1* and *CD49F* upon WDR5 depletion in SiHa-R cells, with *NANOG* in particular being highly depleted in comparison with the scrambled negative control (fold change=0.288, $p<0.05$).

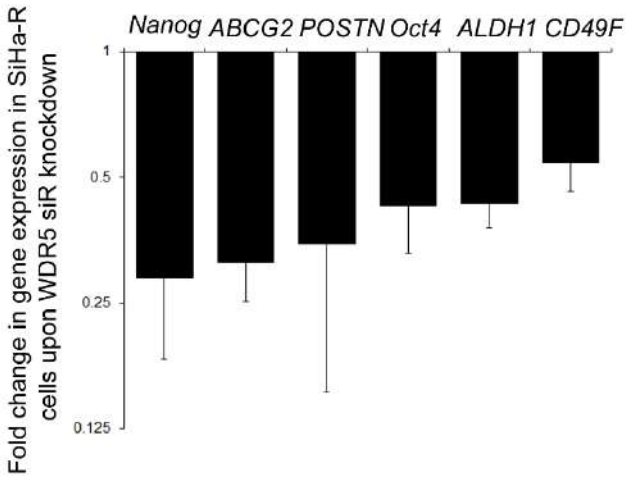

Figure 8.19: qPCR analysis depicts a reduction in mRNA levels of genes involved in stemness maintenance in SiHa-R cells knocked down with WDR5 siRNA (n=3, $p<0.05$).

Immunoblotting studies were also carried out to determine the effect of WDR5 on the protein levels of genes involved in stemness maintenance. As depicted in **Figure 8.20**, western blotting of lysates of SiHa-R cells depleted of WDR5, revealed decreased expression of NANOG, SOX2 and ALDH in comparison with the scrambled negative control (SCR), indicative of a prominent role for WDR5 in stemness gene expression in SiHa-R cells.

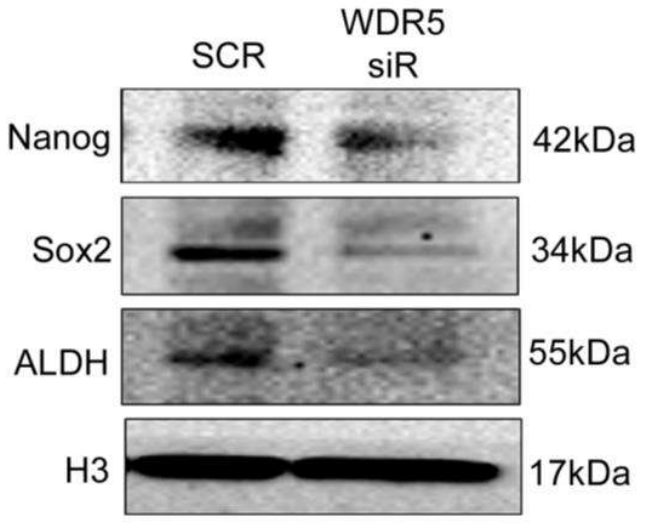

Figure 8.20: Immunoblot analysis confirms reduction in NANOG, SOX2 and ALDH upon WDR5 silencing (WDR5 siR), in comparison with scrambled control (SCR) (n=3). Lysates were prepared from cells that had been transfected with WDR5 siRNA for 72h. Representative images are shown.

WDR5 has previously been shown to bring about self-renewal via H3K4me3 modification of genes involved in embryonic stem cell reprogramming (Ang et al., 2011). It was therefore investigated whether the RHOC-WDR5 complex results in increased stemness ability by supporting transcriptional activation of *NANOG*. Towards this aim, two sets of primers spanning two halves of the *NANOG* promoter were designed for ChIP-qPCR studies. A diagrammatic representation of the *NANOG* promoter indicating the regions of the promoter spanned by the primers is shown in **Figure 8.21**.

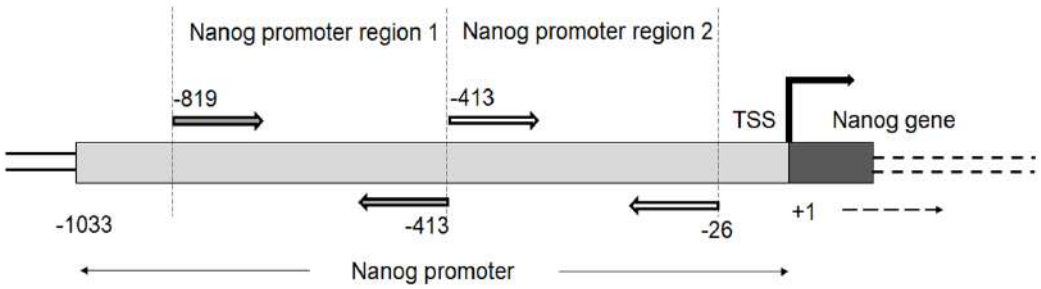

Figure 8.21: Schematic representation of the regions of the *NANOG* promoter spanned by the two sets of primers.

To investigate whether RHOC and WDR5 regulate transcription of *NANOG* by directly binding to the promoter region of the *NANOG* gene, ChIP was performed with RHOC and WDR5 antibodies on SiHa-R DNA. The DNA thus pulled down by RHOC and WDR5 antibodies was analysed for enrichment of the *NANOG* promoter by qPCR. ChIP-qPCR analysis revealed enrichment of the *NANOG* promoter in both RHOC and WDR5 pull-downs in comparison with the isotype control as shown in **Figure 8.22**. This confirms that the RHOC-WDR5 complex does indeed bind to the promoter region of the *NANOG* gene. Additionally, it was observed that the binding of RHOC was higher at the proximal end of the promoter, whereas WDR5 bound to both distal and proximal ends evenly.

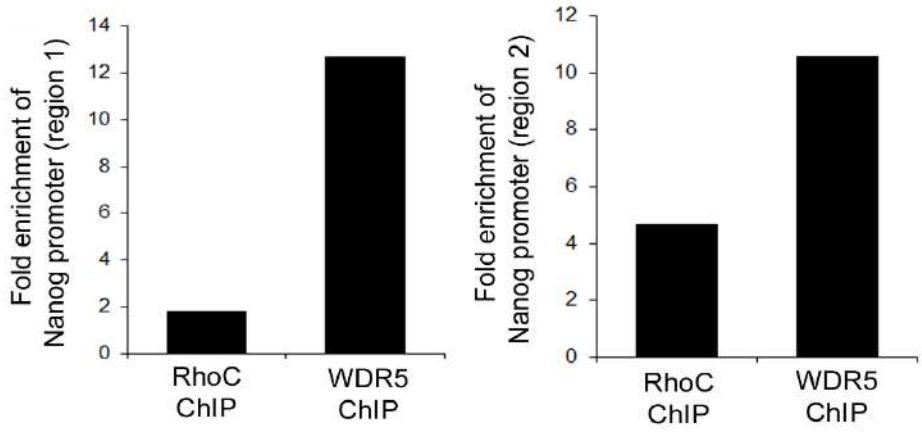

Figure 8.22: ChIP-qPCR with RHOC and WDR5 antibodies, show occupation of both halves of the *NANOG* promoter by RHOC and WDR5 (n=2).

The ChIP-qPCR assay proved that both RHOC and WDR5 bind to promoter sequences of the *NANOG* gene. To determine whether this binding results in positive regulation of *NANOG* transcription, a luciferase-based reporter assay was carried out. Cells were transfected with the pNANOG-Luc plasmid which had the luciferase gene controlled by the *NANOG* promoter as the insert. The luciferase activity thus measured would be proportional to activity of the *NANOG* promoter. The assay was performed under various conditions of modulations in expression of RHOC and WDR5, consequently providing evidence of the extent of change in activity of the *NANOG* promoter upon alterations in levels of RHOC and WDR5. As shown in **Figure 8.23**, transient over-expression of RHOC in SiHa cells utilizing the wild-type RHOC plasmid (wtR) was

seen to result in increased *NANOG* promoter activity in comparison with the backbone vector alone (pcDNA3) ($p<0.05$).

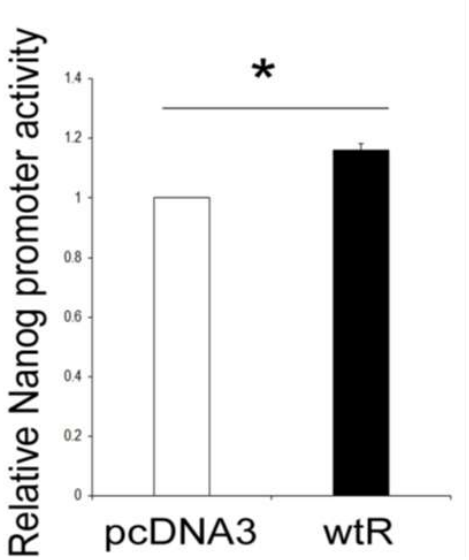

Figure 8.23: Bar graph representation of increase in *NANOG* promoter activity upon transient transfection of the RHOC over-expressing plasmid (wtR) in comparison with the backbone alone (pcDNA3) ($n=3$, $p<0.05$). Cells were analysed for *NANOG* promoter activity 72h post transfection with the respective plasmids.

Conversely, the effect of siRNA mediated knockdown of RHOC on *NANOG* promoter activity was also assayed. **Figure 8.24** indicates that depletion of RHOC in SiHa cells resulted in partial, but significant decrease in activity of the *NANOG* promoter. This implied that decrease in RHOC levels directly affected *NANOG* expression by compromising *NANOG* promoter activity.

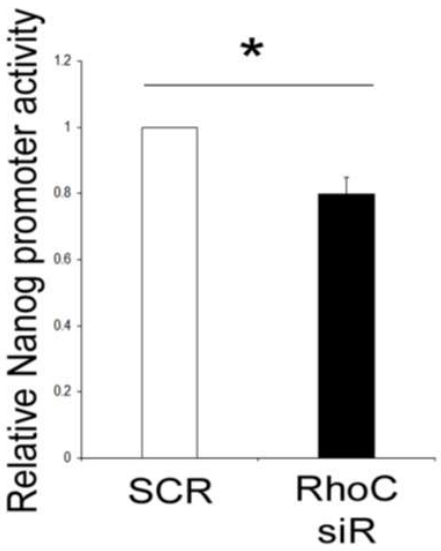

Figure 8.24: Bar graph showing decrease in *NANOG* promoter activity upon siRNA mediated RHOC knockdown (RHOC siR) after 72h of transfection in comparison with scrambled negative control (SCR) (n=3, $p<0.05$).

In addition to RHOC knockdown, the effect of WDR5 silencing on *NANOG* promoter activity was investigated. *NANOG-Luc* promoter assay on SiHa cells inhibited for WDR5 using siRNA also revealed significant reduction in activity of the *NANOG* promoter in comparison to scrambled control as shown in **Figure 8.25**.

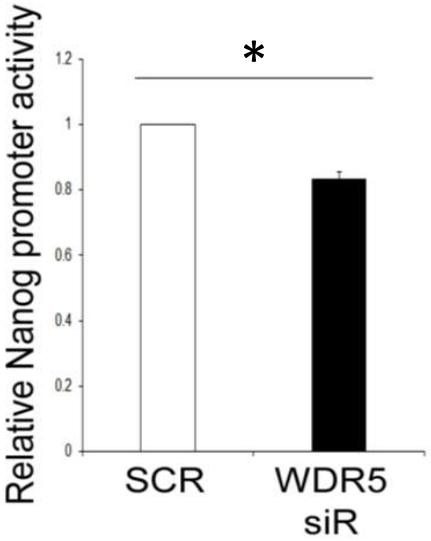

Figure 8.25: Bar graph depicting decrease in *NANOG* promoter activity upon WDR5 silencing (WDR5 siR) in comparison with scrambled control (SCR) (n=3, $p<0.05$). Cells had been transfected for 72h prior to the Luc assay.

These observations support the finding that the RHOC-WDR5 complex regulates *NANOG* expression, and that a disjunction of this interaction led to reduced *NANOG* expression and consequent diminishing of the stemness phenotype conferred by RHOC.

The data enumerated thus far suggests that RHOC and WDR5 interact to result in increased expression of stemness genes in cervical cancer cell lines. To test whether this holds true in patients too, clinically derived sections were assessed for RHOC-WDR5 interaction. **Figure 8.26** depicts immunofluorescent staining of RHOC and WDR5 in patient-derived tumour sections. Immunofluorescent analysis showed co-localization of RHOC and WDR5 in clinical sections too, as indicated by yellow pixels. However, it was noted that cells in the tumour section showed mostly cytoplasmic interaction of RHOC and WDR5, as compared to cell lines where the interaction was largely nuclear. This may be indicative of formation of the complex in the cytoplasm before being translocated to the nucleus. However, this hypothesis needs to be investigated further.

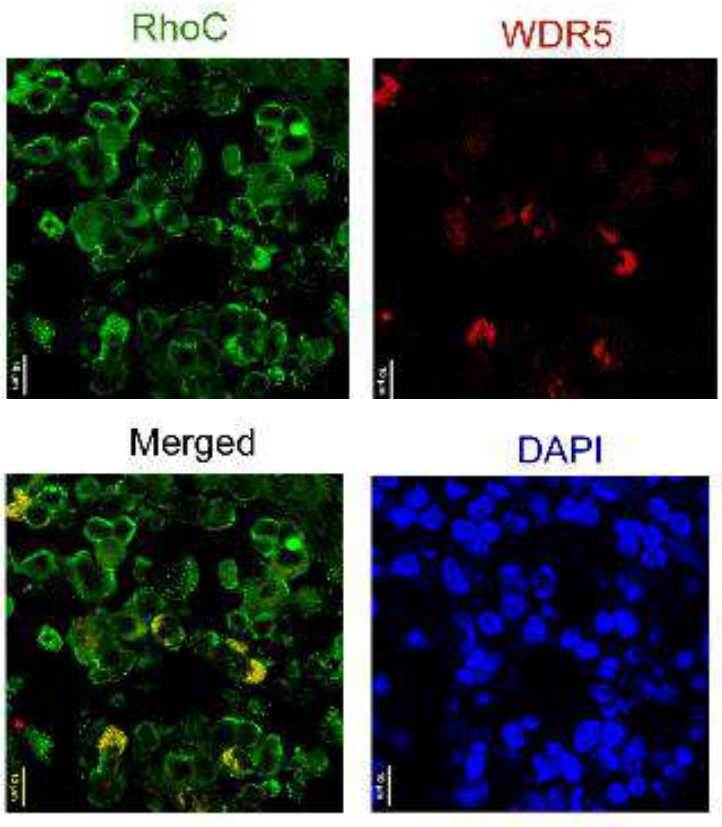

Figure 8.26: Representative immunofluorescent image showing co-localization of RHOC and WDR5 in a patient derived tumour section (Pt-11).

Collectively, these data confirm that RHOC interacts with WDR5 to result in elevated stemness characteristics by increasing expression of stemness genes like NANOG and SOX2, via trimethylation of H3K4.

8.3 Conclusion

While cytosolic functions of RHOC are well-known, here a novel nuclear function of RHOC has been reported. The presence of RHOC in the nucleus of tumour cells prompted further investigations into this finding. Immunoprecipitation of nuclear lysates of SiHa-R cells using the RHOC antibody and mass spectrometry to identify pulled-down proteins revealed that WDR5 is a nuclear binding partner of RHOC. This observation was confirmed by immunofluorescent analysis which exhibited co-localization of RHOC and WDR5 both in SiHa-R cells and in clinically derived tumour sections.

H3K4me3, a modification known to be regulated by the WDR5/SET complex of proteins, was used as a measure of WDR5 activity. H3K4me3 levels were observed to fluctuate proportionally to RHOC expression. Additionally, depletion of WDR5 in SiHa-R cells was observed to result in a consequent decrease in H3K4me3 levels, confirming that both RHOC and WDR5 are essential to bring about trimethylation of H3K4 residues.

H3K4me3 is an active mark of transcription. It was therefore envisaged that the increased expression of stemness genes in SiHa-R could be abrogated by WDR5 inhibition. As expected, WDR5 knockdown resulted in decreased stem-like ability, both phenotypically and by inhibition of stemness gene expression.

Further analysis revealed that the RHOC-WDR5 complex alters *NANOG* expression by binding to the promoter region. ChIP-qPCR and Luciferase promoter activity assays confirmed that the RHOC-WDR5 complex binds to and activates the *NANOG* promoter.

Together, these data establish that RHOC interacts with the nuclear protein WDR5 and alters its activity. Further, this chapter demonstrates the role of the RHOC-WDR5 complex in stemness maintenance by proving that it physically binds to and up-regulates expression of the *NANOG* gene.

CHAPTER -VII

RHOC Mediates Active DNA Demethylation to Enhance the Expression of Stemness Genes

9.1 Introduction

Both histone modifications and DNA methylation contribute towards epigenetic regulation of gene expression (Chen et al., 2013; Dawson and Kouzarides, 2012; Jin et al., 2011). DNA methylation involves covalent addition of a methyl group onto the 5^{th} carbon atom of the cytosine ring (Robertson, 2005). While a majority of DNA methylation events occur at CpG sites, instances of non-CpG methylations have also been reported (Lister et al., 2009).

DNA methylation has been largely linked to gene silencing and chromatin compactness (Choy et al., 2010; Wade, 2001). Methylation of DNA is known to trigger recruitment of Methyl-CpG binding proteins that in turn initiate reorganization of the chromatin, resulting in decreased chromatin accessibility (Newell-Price et al., 2000).

DNA methylation plays a critical role in development, regulating embryonic differentiation patterns in mammals (Greenberg and Bourc'his, 2019; Smith and Meissner, 2013). Apart from normal developmental processes, alterations in DNA methylation patterns have been associated with cancer initiation and progression in various tumour models (Baylin et al., 2000; Issa, 2000). Hypermethylation of tumour suppressors and genes involved in DNA repair have been reported to mediate cancer progression and alter response to therapy (Baylin, 2005; Lahtz and Pfeifer, 2011; Locke et al., 2019). On the other hand, hypomethylation of DNA has been linked to global reorganization of chromatin structure and consequent triggering of oncogenic events (Ehrlich, 2009; Hoffmann and Schulz, 2005; Sheaffer et al., 2016).

Since RHOC over-expression has been shown to be associated with global transcriptional up-regulation and open chromatin, it was envisaged that RHOC could result in genomic reorganization by altering DNA methylation patterns. This chapter explores the possible contribution of RHOC to DNA hypomethylation that could result in the observed plastic nature of cells over-expressing the RHOC protein.

9.2 Results and Discussion

9.2.1 RHOC Over-Expression Results in Global DNA Demethylation

Chapter 6 elucidated the link between RHOC and H3K4 trimethylation via interaction with WDR5. Apart from histone modifications, chromatin accessibility is also governed by the extent of DNA methylation (Guo et al., 2016). Various studies have shown that methylation of DNA and chromatin compactness are inversely related (Choy et al., 2010; Kass et al., 1997; Robertson, 2002).

Hypomethylated DNA has often been associated with increased transcriptional accessibility, consequently promoting cancer progression (Feinberg and Vogelstein, 1983; Fraga et al., 2004). This loss in methylation has been reported to be global, with decreased DNA methylation observed in both intronic and coding regions of DNA (Feinberg and Tycko, 2004). Since the data presented in the previous chapter implies that tumour cells expressing nuclear RHOC display open chromatin, the association of RHOC with DNA methylation levels was explored.

5mC a mark of methylated DNA (Schubeler, 2015) was utilized to study the extent of DNA methylation in cells manipulated for RHOC expression. In mammals, methylation occurs at the cytosine residues of DNA (Lister et al., 2009). Further, it has been observed that the covalent addition of methyl groups occurs mostly at CpG dinucleotides (Jin et al., 2011). However, in some cases the methylated cytosine may be followed by an adenine (A), thymidine (T) or another cytosine (C) moiety (Lister et al., 2009). The level of 5mC is therefore a direct indication of DNA methylation and was used to study changes in DNA methylation in cervical cancer cell lines modulated for RHOC expression, in order to determine the impact of RHOC on DNA methylation levels.

As shown in **Figure 9.1**, flow cytometry revealed a significant reduction in the percentage of 5mC positive cells upon RHOC over-expression. SiHa-R cells were observed to have significantly lower levels of DNA methylation in comparison with SiHa-N as represented in **Figure 9.2**, an observation that was in consonance with the proposed hypothesis of RHOC resulting in decreased methylation of DNA moieties.

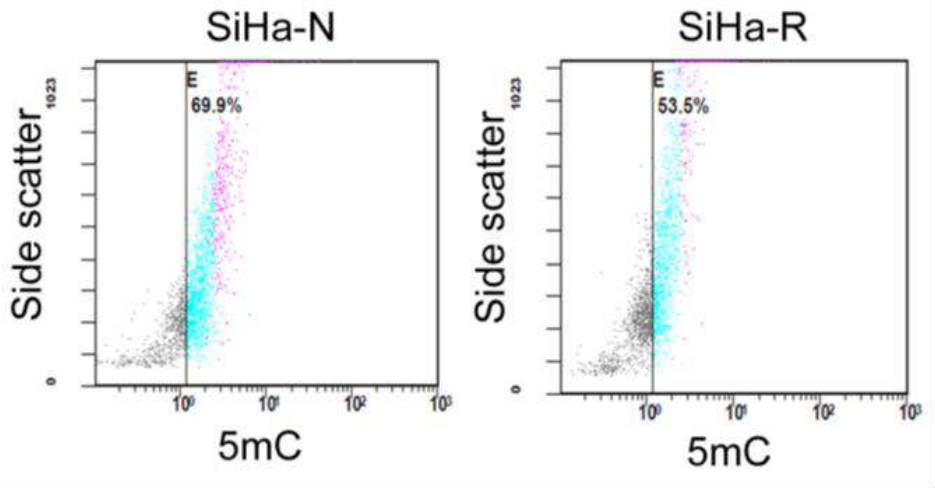

Figure 9.1: Representative FACS plot showing decrease in 5mC levels in SiHa-R in comparison with SiHa-N.

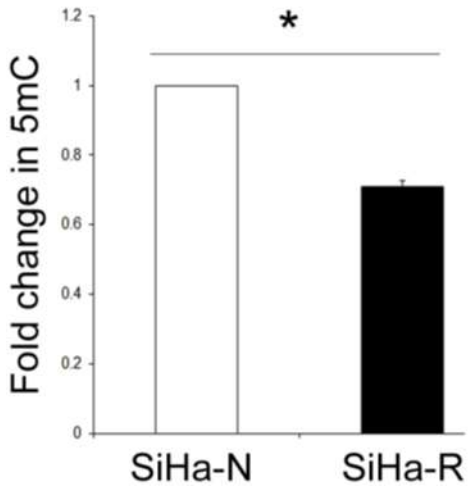

Figure 9.2: Bar graph representation of fold reduction in 5mC positive cells in SiHa-R, represented by fold decrease over SiHa-N (n=3, $p<0.05$).

To determine if RHOC levels were in fact linked to methylation of DNA, SiHa cells were knocked down for RHOC and the resulting effect on 5mC levels was studied. SiHa cells were transfected with RHOC siRNA for a period of 72h and then assayed for 5mC by flow cytometry. As shown by the FACS plots in **Figure 9.3**, RHOC siRNA treated

SiHa cells were observed to have increased levels of 5mC in comparison with scrambled negative control (SCR), thus implying a possible connection between RHOC expression and DNA hypomethylation. **Figure 9.4** is a bar graph representation of the same. It may be noted however, that the increase in 5mC levels though significant, was not starkly different between RHOC siRNA treated cells and the scrambled control. This could be attributed to variable efficiency of transfection. Additionally, long-term inhibition of RHOC may be necessary to bring about a more marked change in DNA methylation levels, as opposed to the 72h transfection period.

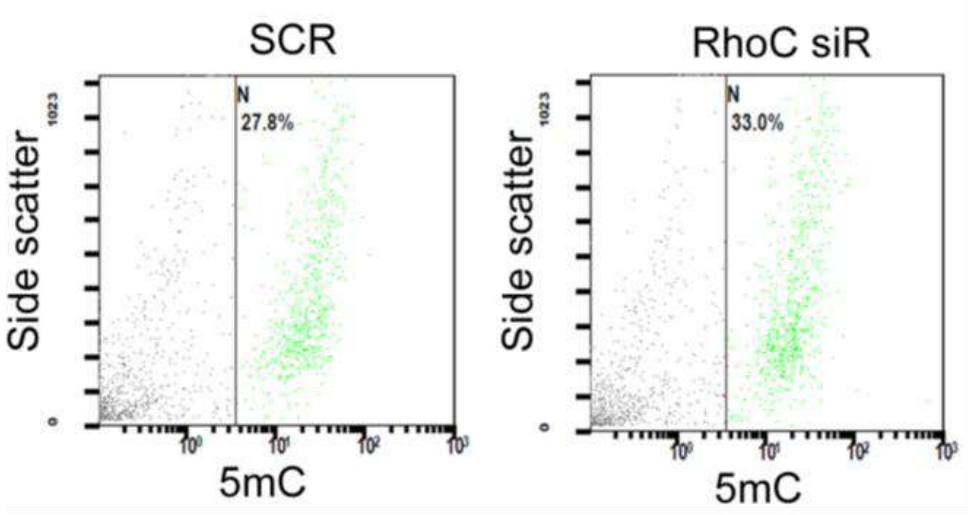

Figure 9.3: Representative FACS plot showing increased 5mC upon siRNA mediated RHOC knockdown in SiHa cells (n=3).

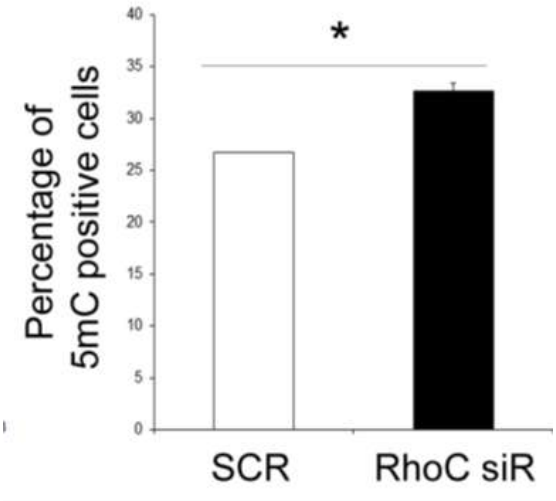

Figure 9.4: Bar graph representation of average percentage of 5mC positive cells, showing increase in 5mC positivity upon RHOC knockdown (RHOC siR) in comparison with scrambled control cells (SCR) (n=3, $p<0.05$).

Endonuclease treatment of DNA is also used to study differences in DNA methylation (Bird and Southern, 1978). The inability of methylation-sensitive enzymes to digest DNA at sites that are methylated is utilized to draw conclusions regarding the extent of DNA methylation. One such enzyme that has been used to study DNA methylation patterns is *Hpa*II (Waalwijk and Flavell, 1978). *Hpa*II recognizes the sequence -CCGG- but is unable to cut the DNA stretch if the second cytosine of the recognition sequence is methylated. Therefore, *Hpa*II, (which cuts DNA at unmethylated CpG sites only) was utilized to determine overall DNA methylation levels of SiHa-N and SiHa-R cells.

Genomic DNA from SiHa-N and SiHa-R cells was isolated and subjected to *Hpa*II digestion. The digested products were run on a gel, and the extent of digestion of DNA was determined by measuring the decrease in intensity of the DNA bands upon digestion by densitometry. The fold change in intensity of digested products in comparison with the undigested control was calculated. As shown in **Figure 9.5**, gel electrophoresis and densitometry analysis revealed extensive digestion of SiHa-R DNA (as observed by fainter bands than undigested DNA) in comparison with SiHa-N DNA. This was indicative of the hypomethylated status of DNA in these cells.

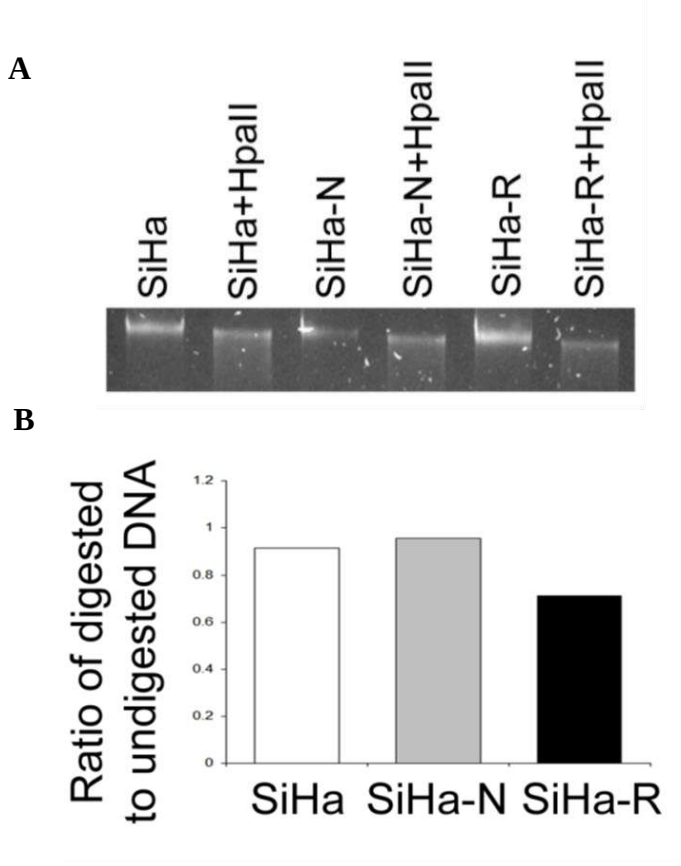

Figure 9.5: (A) Representative gel image showing increased digestion of SiHa-R DNA upon treatment with the methylation sensitive restriction enzyme *Hpa*II (n=2). (B) Bar graph representation of the ratio of digested DNA to undigested DNA revealing more extensive digestion of SiHa-R DNA by *Hpa*II, indicative of its demethylated status (n=2).

The FACS and restriction enzyme digestion data imply a possible link between DNA hypomethylation and RHOC expression. To further interrogate the specific sites that were hypomethylated on account of RHOC over-expression, the Infinium Human Methylation 850 (EPIC array) was performed on SiHa-N and SiHa-R cells. The data generated was first assessed for the overall status of DNA methylation in SiHa-N and SiHa-R cells.

Figure 9.6 is a volcano plot of the methylation levels of genes along with their respective p-values. The methylation values of SiHa-N were used as control, and $\log_2$ values of +1 and -1 served as cut-offs. The plot indicates that genes in SiHa-R cells were hypomethylated, with a larger number of genes with decreased DNA methylation

(higher number of events below -1). This substantiated the claim of demethylated DNA in cells with RHOC over-expression.

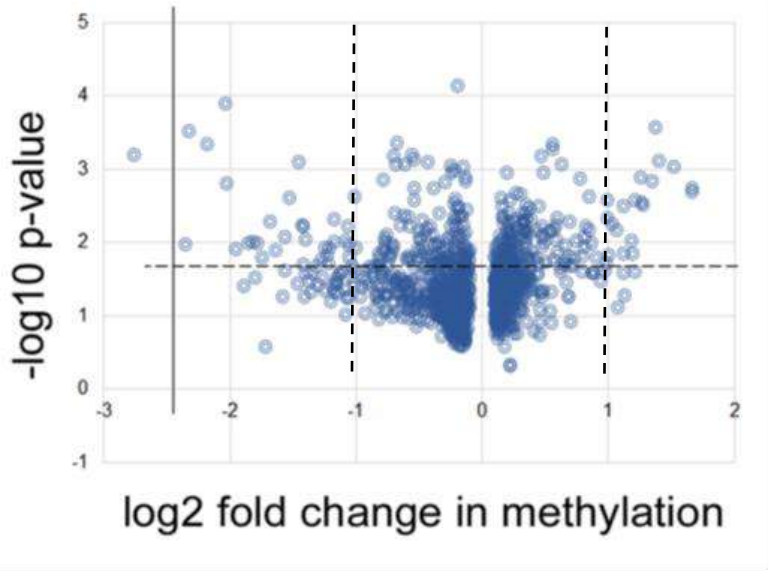

Figure 9.6: Volcano plot showing preferential decrease in methylation levels of SiHa-R cells as seen by the Illumina 850K methylation array data ($p<0.05$). The cut-off values are indicated by vertical dotted lines.

Further analysis revealed that this hypomethylation was distributed across the genome. The DNA in both promoter regions and as well as sites within genes were found to be demethylated in SiHa-R cells. **Figure 9.7** is a heatmap representing the fold change in methylation values between SiHa-N and SiHa-R cells. **Figure 9.7 (A)** is a representation of the fold change in methylation of promoter DNA, with negative methylation values being represented by darker shades of blue. The heatmap shows a larger number of promoter sites with hypomethylated DNA in SiHa-R cells. Similar analysis of regions within genes revealed decreased methylation in SiHa-R DNA. **Figure 9.7 (B)** is a heatmap representing the extent of DNA methylation within coding regions. Green represents hypomethylated DNA, while red represents DNA with increased methylation. All methylation values of SiHa-R were normalized against methylation values of SiHa-N DNA (methylation cut-off value=0.5 and 1.5, $p<0.05$).

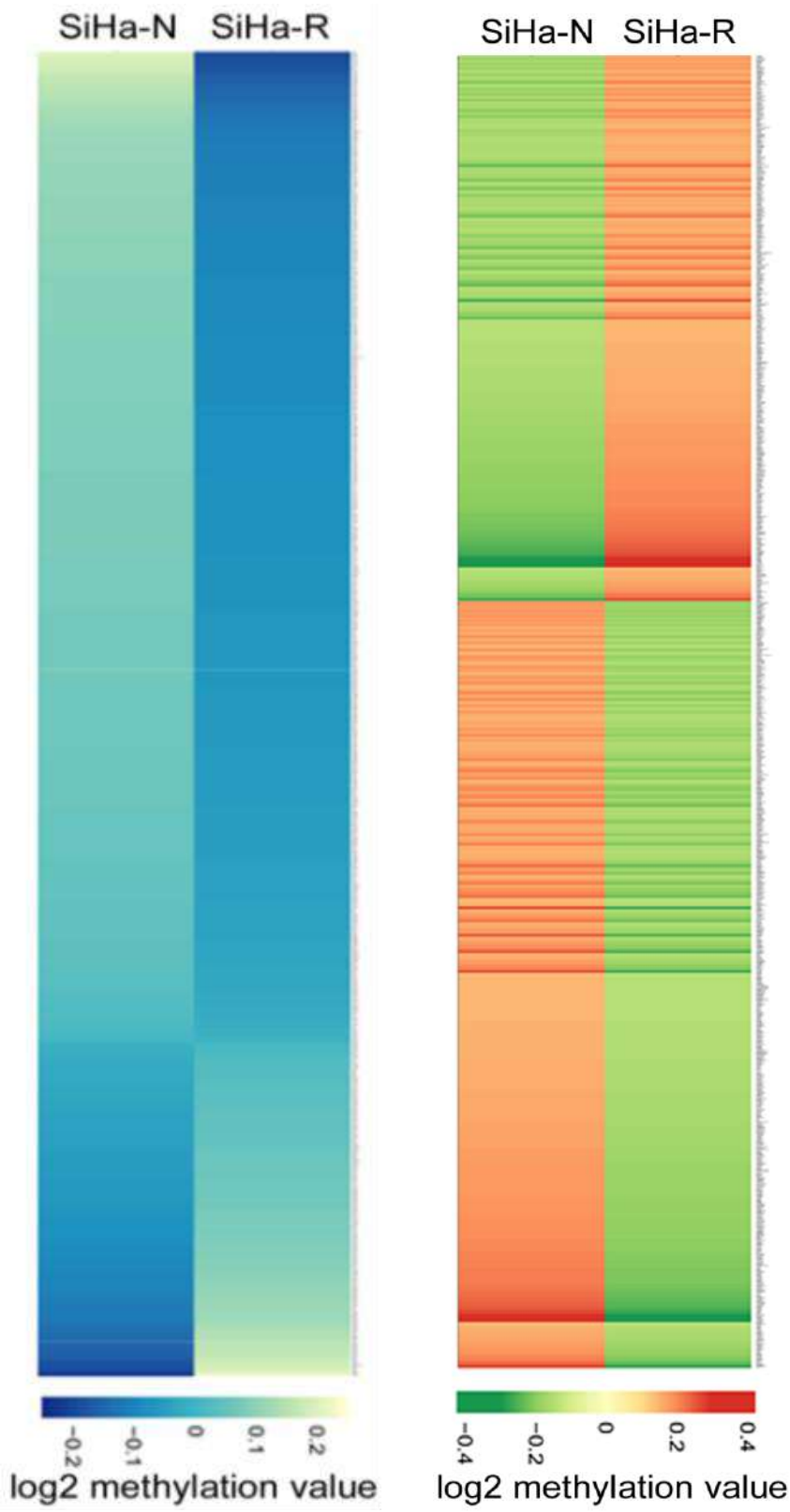

Figure 9.7: Heatmap representation of the mean methylation values of promoter sites (A) and regions within genes (B) showing decreased methylation levels in SiHa-R DNA as compared to SiHa-N (n=2, $p<0.05$).

Further analysis was undertaken to identify methylation patterns across genes involved in stemness maintenance, signalling and epigenetic modifications in RHOC modulated cells. As expected, scrutiny of methylation levels across SiHa-N and SiHa-R DNA revealed decreased methylation of genes governing maintenance of stemness, signalling events and epigenetic modifications in SiHa-R cells. These changes have been represented by heatmaps in **Figure 9.8**. In **Figures 9.8 (A)** and **9.8 (C)**, green signifies decreased methylation, whereas red is indicative of increased methylation levels. The heatmaps clearly display decreased methylation levels of stemness genes and epigenetic modifiers in SiHa-R cells. The heatmap in **Figure 9.8 (B)** represents genes involved in signalling, with colours ranging from dark blue to yellow signifying increasing levels of methylation towards the yellow. The heatmap in **Figure 9.8 (B)** therefore implies decreased methylation of genes involved in signalling pathways in SiHa-R cells.

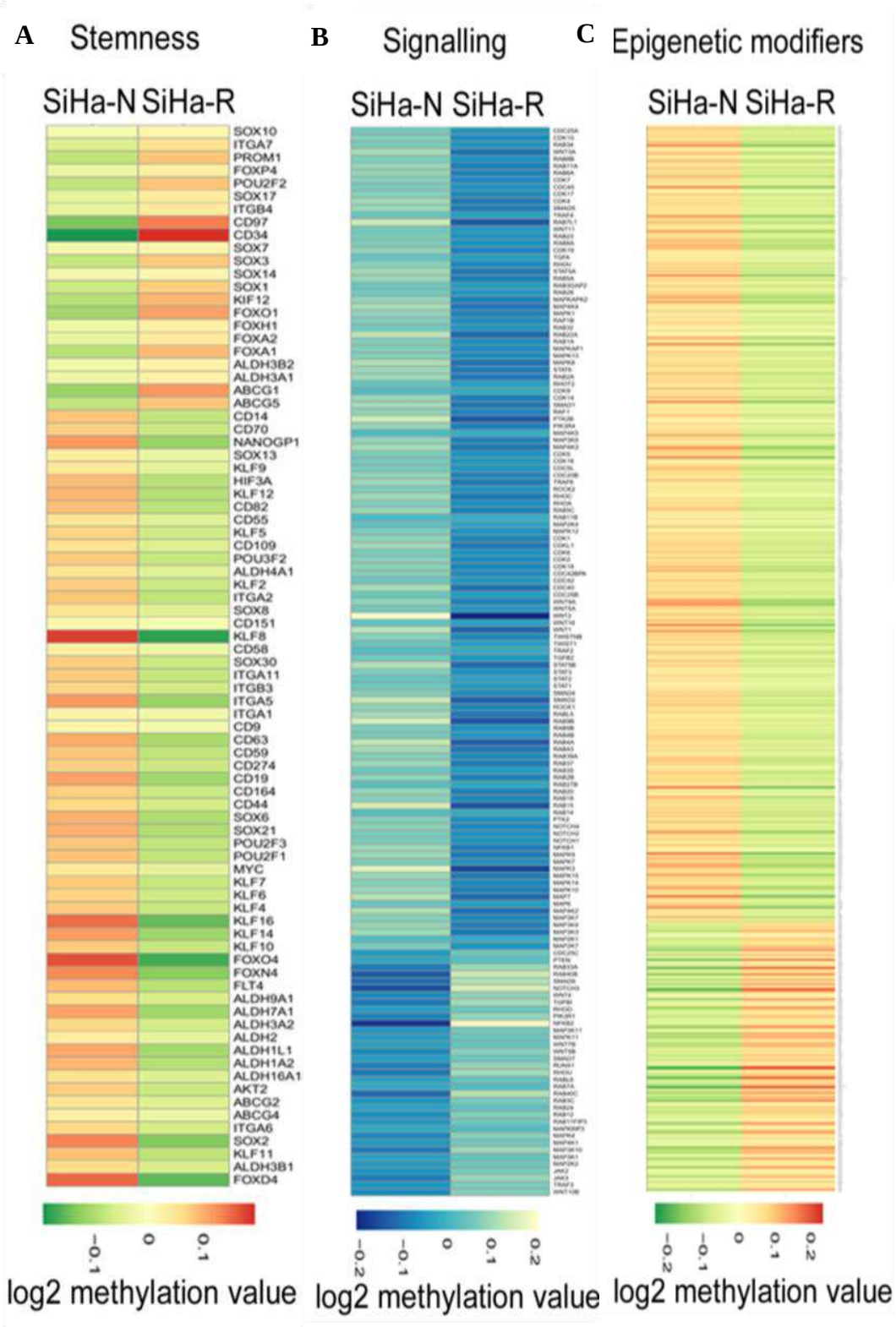

Figure 9.8: Heatmap representation of methylation levels of genes associated with stemness (A), signalling (B) and epigenetics (C) showing decreased average methylation values in SiHa-R.

Figure 9.9 gives an overview of relative methylation levels at various locations in the genome. The first track of the plot depicts the position of the chromosomes and the second track depicts the position of RefSeq genes across the chromosomes, with the height of the green peaks corresponding to the mean gene count. The third track displays the methylation scores in SiHa-R relative to SiHa-N. Using the methylation value of SiHa-N as the baseline, the difference in methylation between SiHa-N and SiHa-R cells ($SiHa\text{-}R_{methylation}$-$SiHa\text{-}N_{methylation}$) was calculated. The regions of the genome that generated a positive value had increased methylation in SiHa-R cells in comparison to SiHa-N cells. These regions are denoted by vertical red lines above the axis. Genomic locations that were hypomethylated in SiHa-R cells as compared to SiHa-N cells generated negative values and are represented by vertical blue lines below the axis.

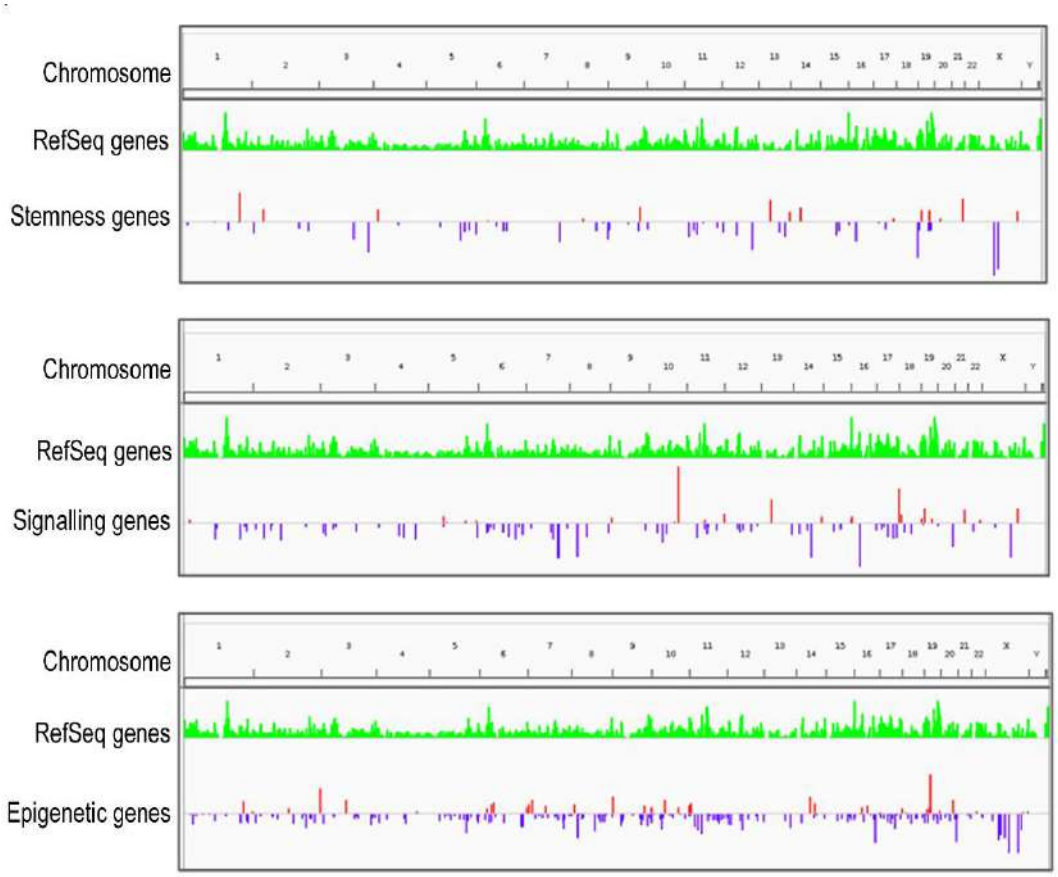

Figure 9.9: Genome-wide methylation pattern analysis showed reduced methylation levels of genes involved in stemness, signalling and epigenetic modulations in SiHa-R DNA in comparison to SiHa-N (down-regulation represented by vertical blue lines below the axis and up-regulation depicted by vertical red lines above the axis).

As shown in **Figure 9.9**, genomic locations housing genes that played major roles in maintenance of the stemness phenotype, signalling networks and chromosomal modifications were found to be largely hypomethylated in SiHa-R cells. This observation was in agreement with the hypothesis that RHOC is associated with decreased DNA methylation and increased chromosomal accessibility.

These data substantiate the claim that RHOC over-expressing cells exhibit global transcriptional up-regulation on account of extensive DNA demethylation. Further investigations were carried out to determine the specific molecular target involved in demethylation of DNA in the background of RHOC over-expression.

9.2.2 TET2 is the Modulator of DNA Demethylation in RHOC Over-Expressing Cells

Demethylation of DNA can occur either passively (loss of methylation marks during DNA replication) or actively (replacement of 5mC with cytosine via demethylases). TET enzymes (ten eleven translocation dioxygenases) are responsible for active loss of DNA methylation and are known to be deregulated in various types of cancer (Kamdar et al., 2019; Zhou et al., 2019). TET enzymes carry out demethylation of DNA by oxidizing 5mC to intermediate products that are recognized by break-excision repair (BER) proteins. The oxidized cytosine is then replaced with unmethylated cytosine by the BER machinery, consequently leading to loss of methylation marks along DNA (Rasmussen and Helin, 2016).

In order to tease out the molecular mechanism behind the hypomethylated status of DNA in RHOC over-expressing cells, the level of TET enzymes was investigated in SiHa-R cells. Transcriptomic data analysis showed significant up-regulation of TET2 in SiHa-R cells (fold change=1.68, $p<0.02$), whereas TET1 was found to be down-regulated (fold change=0.195) and TET3 depicted no significant change (fold change=0.7) as shown in **Figure 9.10**.

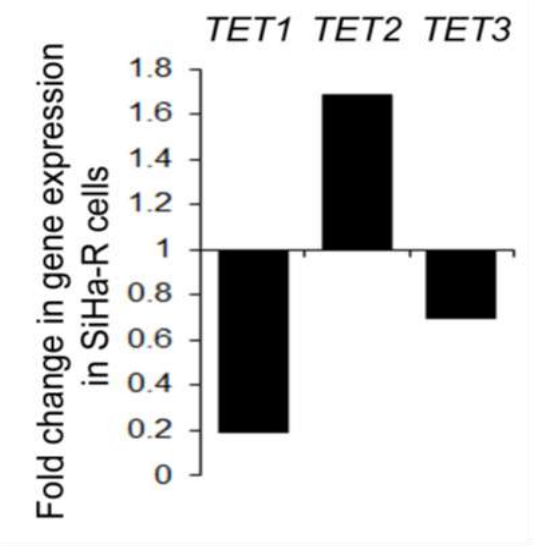

Figure 9.10: Bar graph showing significant increase in TET2 transcripts, and not TET1 and TET3, in SiHa-R cells (normalized against SiHa-N), as revealed by the RNA-seq data.

Parallelly, the status of TET2 expression upon RHOC inhibition was investigated. qPCR analysis of TET2 transcripts in SiHa cells subjected to RHOC siRNA-mediated silencing was undertaken. As shown in **Figure 9.12**, RHOC depletion resulted in lower levels of TET2 as compared to the scrambled negative control (SCR) ($p<0.05$).

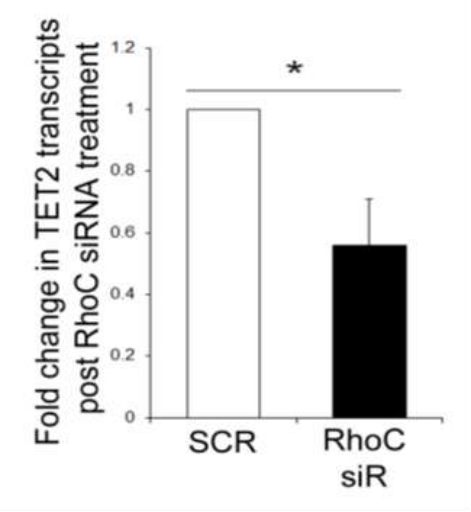

Figure 9.11: qPCR analysis depicts decrease in TET2 mRNA levels upon siRNA-mediated RHOC knockdown (RHOC siR) in comparison with scrambled control (SCR) ($n=3$, $p<0.05$). GAPDH was used as the internal control.

A similar analysis was carried out at the protein level by immunoblotting. Immunoblot analysis of SiHa cells transfected with RHOC siRNA (RHOC siR) also showed decreased TET2 levels in comparison with scrambled control (SCR) as shown in **Figure 9.12** (p=0.041).

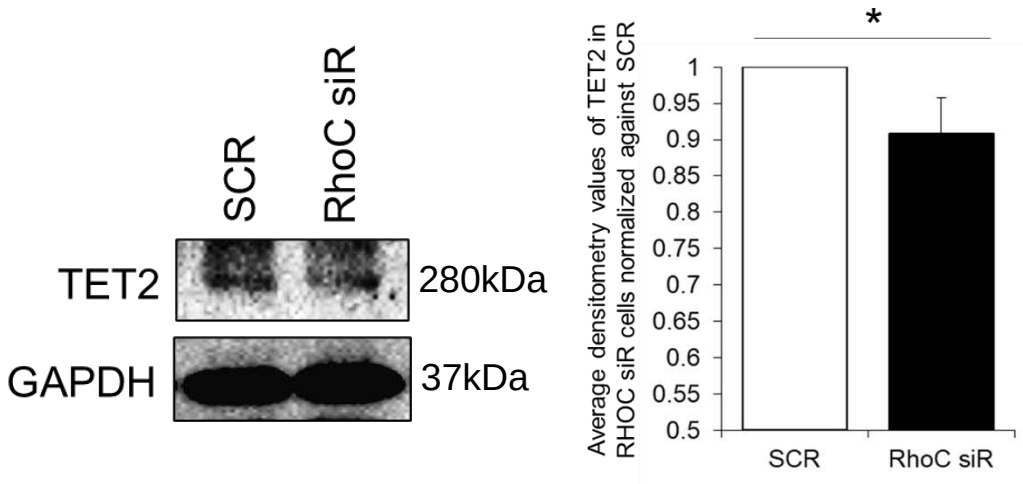

Figure 9.12: Representative immunoblot analysis of TET2 in SiHa cells transfected with RHOC siRNA (RHOC siR) and scrambled control (SCR). GAPDH was used as the loading control (n=3, $p<0.05$). Densitometry values are also shown.

To further validate the association between RHOC and TET2 expression, immunofluorescent staining of TET2 was performed on SiHa-N and SiHa-R cells. As shown in **Figure 9.13**, immunofluorescent analysis confirmed over-expression of the protein in SiHa-R cells in comparison with SiHa-N.

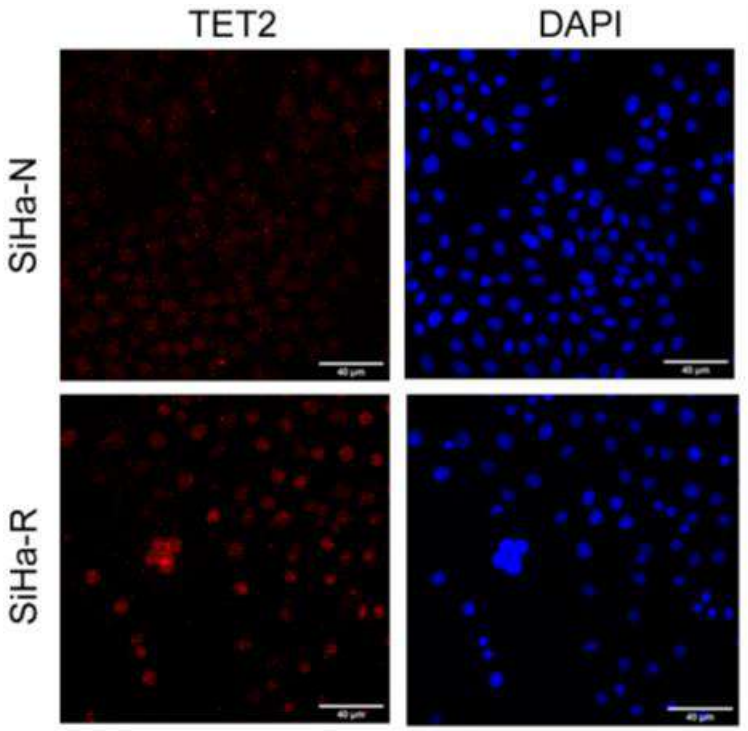

Figure 9.13: Immunofluorescent analysis of TET2 confirms up-regulation in SiHa-R cells (n=3). (scale bars are indicated)

Ensuing confirmation of the association between RHOC and TET2 expression, the involvement of TET2 in RHOC induced stemness was investigated. In order to achieve this, SiHa-R cells subjected to TET2 knockdown were analysed for stemness capability. **Figure 9.14** shows successful depletion of TET2 levels upon TET2 siRNA transfection.

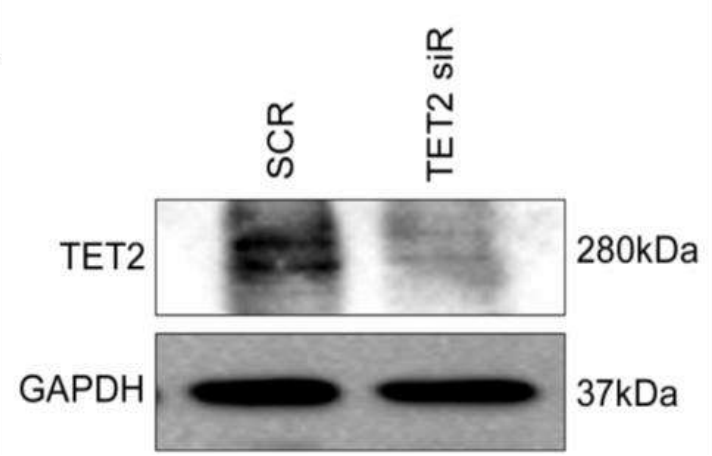

Figure 9.14: Representative western blot image to show successful knockdown of TET2 upon transfection with TET2 siRNA (n=3).

SiHa-R cells inhibited for TET2 were assessed phenotypically for changes in stemness capability. The soft agar assay showed that TET2 depletion led to successful abrogation of the stemness advantage imparted to SiHa-R. SiHa-R cells knocked down for TET2 displayed reduced colony formation ability when subjected to the soft agar assay as depicted in **Figure 9.15**, with the number of medium and large-sized colonies formed in SiHa-R cells decreasing significantly upon TET2 siRNA silencing.

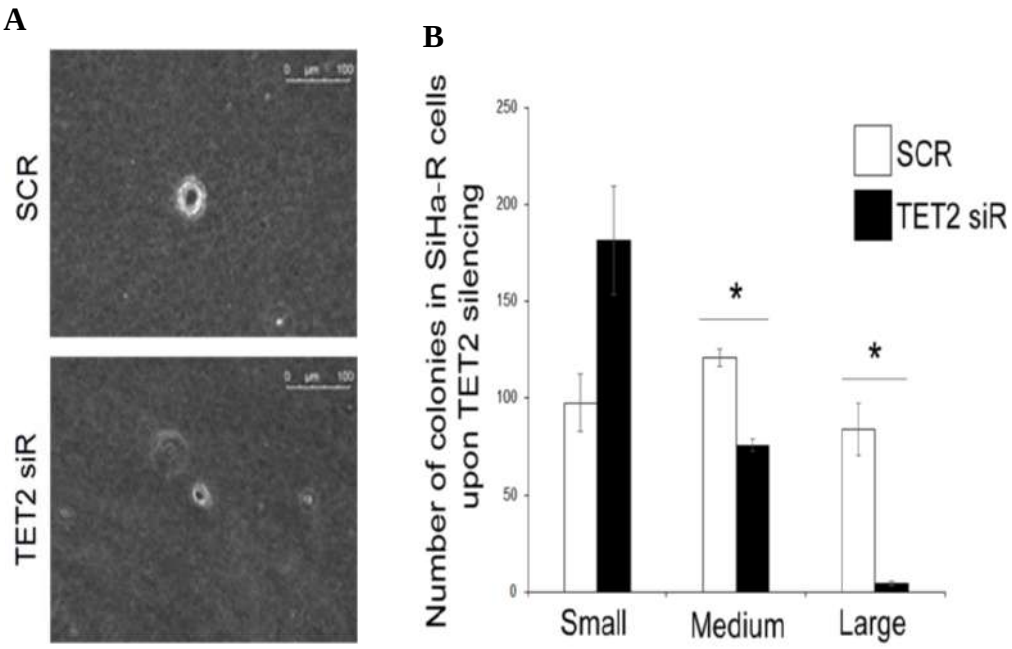

Figure 9.15: (A) Representative image of colonies formed in the soft agar assay by SiHa-R cells transfected with scrambled siRNA (SCR) and TET2 specific siRNA (TET2 siR). (B) Bar graph representation depicting the average number of colonies formed by SiHa-R cells upon TET2 silencing, shows that reduction in TET2 levels leads to successful abrogation of the stemness advantage possessed by SiHa-R cells (n=3, $p<0.05$).

To determine the specific stemness genes that were affected by TET2 inhibition, transcript levels of markers for stemness in SiHa-R cells knocked down for TET2 were investigated. qPCR analysis revealed significant reduction in expression of *ABCG2*, *NANOG*, *OCT4*, *ALDH1*, *SOX2*, *CD49F* and *NOTCH3* in TET2 siRNA treated SiHa-R cells in comparison with scrambled control (SCR) as shown in **Figure 9.16**.

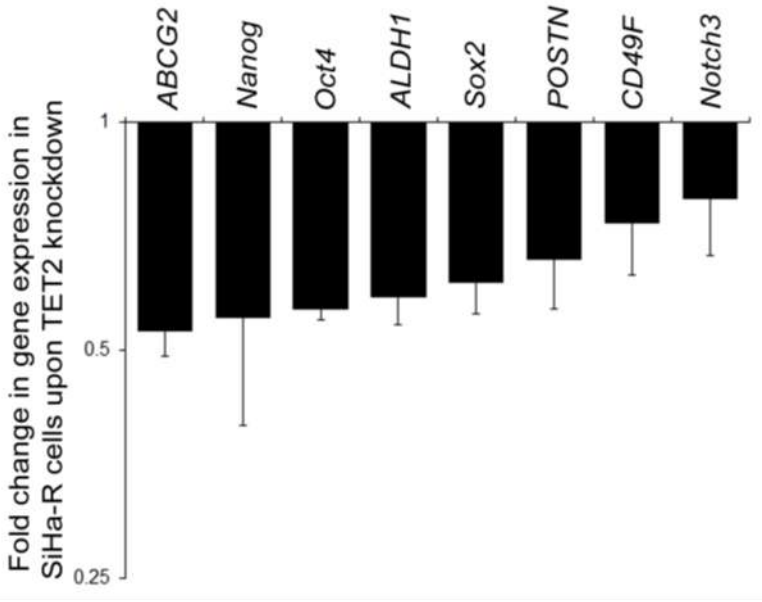

Figure 9.16: qPCR analysis reveals decrease in transcript levels of stemness genes upon TET2 knockdown in SiHa-R cells 72h post transfection (n=3, $p<0.05$). Values were normalized against the scrambled control (SCR). AICDA was used as the internal control.

Immunoblotting corroborated this observation. Western blotting analysis of SiHa-R cells depleted for TET2 by siRNA-mediated silencing revealed reduction in CD49F, POSTN, ALDH and SOX2 levels as compared with SiHa-R cells treated with scrambled control **(Figure 9.17)**.

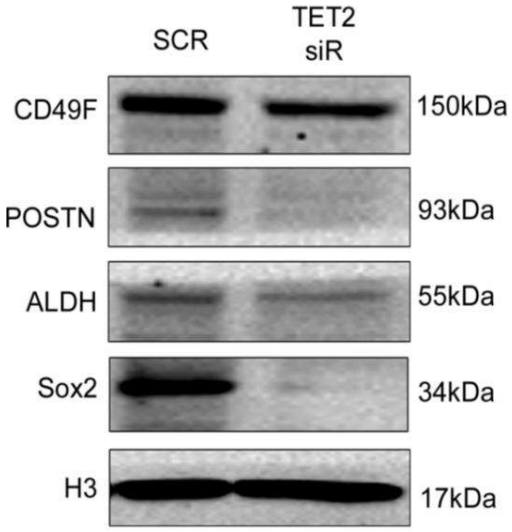

Figure 9.17: Immunoblotting confirms down-regulation of stemness genes in SiHa-R upon TET2 silencing (n=3). Representative images are shown. H3 was used as the loading control.

To confirm that TET2 was indeed the molecule downstream of RHOC that mediates DNA demethylation, the levels of 5mC were checked in SiHa-R cells treated with TET2 siRNA. FACS analysis revealed significant increase in cells with positive staining for 5mC in TET2 siRNA transfected cells, indicating increased DNA methylation in SiHa-R cells depleted of TET2 as compared to the scrambled negative control (SCR) **(Figure 9.18)**.

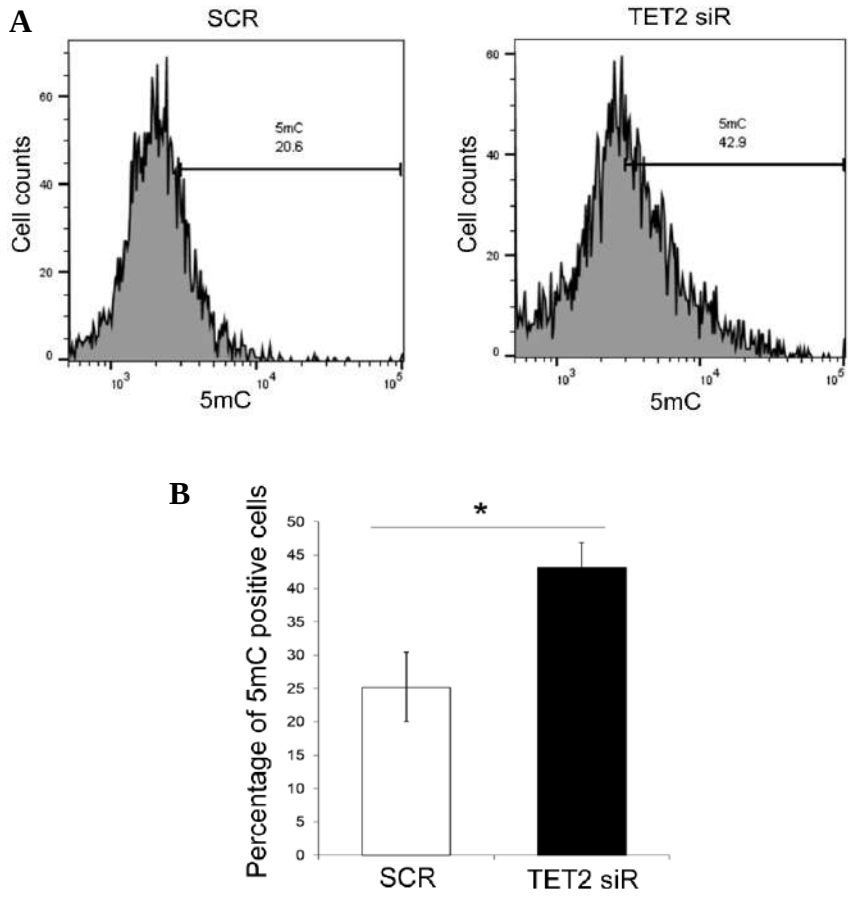

Figure 9.18: (A) Representative FACS plot showing the percentage of 5mC positive cells in TET2 siRNA and SCR cells. (B) Bar graph representation of the increase in 5mC positive cells in SiHa-R cells upon TET2 siRNA treatment (n=3, $p<0.05$).

Taken together, these data suggest that RHOC via TET2 mediates DNA demethylation and results in transcriptional activation leading to stemness advantage in RHOC over-expressing cells.

9.3 Conclusion

Previous chapters have described RHOC's role in maintenance of stemness via ERK signalling and histone modifications. Here, the contribution of RHOC towards demethylated, actively transcribing DNA was investigated.

FACS analysis of the DNA methylation mark, 5mC, revealed the hypomethylated status of cells over-expressing RHOC, which was reversed upon RHOC depletion. The EPIC array further confirmed this, with global DNA demethylation patterns observed in SiHa-R cells, spanning both stemness maintenance and signalling processes.

The observed hypomethylated DNA in SiHa-R was found to be a result of active demethylation by the TET2 molecule. TET2, a dioxygenase, found to be over-expressed in SiHa-R cells, was demonstrated to be involved in the up-regulation of genes involved in maintenance of stemness characteristics, thereby resulting in enhanced self-renewal abilities. Inhibition of TET2 was found to result in gain of DNA methylation, consequently abolishing the stemness advantage conferred on SiHa-R cells, as observed by both phenotypic assays and molecular expression studies.

This chapter therefore exemplifies that RHOC over-expression is associated with global DNA demethylation as substantiated by the EPIC array data. Further, TET2 has been identified as the molecule responsible for hypomethylated DNA and the accompanying stemness characteristics observed in a RHOC-high background.

CHAPTER -VIII

Combinatorial Treatment of Aloe vera and Atorvastatin Sensitizes SiHa Cells to Radiation

10.1 Introduction

Concurrent chemoradiation therapy (CRT) is the gold standard of treatment for locally advanced carcinoma of the cervix (Morris et al., 1999; Rose et al., 1999; Whitney et al., 1999). However, radiation in combination with cisplatin has been observed to result in only a marginal increase in survival, with an improvement of around 10% in 5-year survival rates, as compared to radiotherapy alone (Bernier et al., 2004).

Cancer of the cervix is largely treated with brachytherapy, a technique that helps deliver high doses of radiation to the tumour, with minimal effect to surrounding tissues (Mahantshetty et al., 2019). This encompasses placing radioactive sources (or radioactive seeds) within the tumour, that help deliver a concentrated radiation dose to the primary tumour. However, possible metastatic outgrowths in the para-aortic and pelvic lymph nodes receive only a fraction of the delivered dose owing to their distance from the radioactive seed planted at the tumour site. (Banerjee et al., 2014). To overcome this drawback, brachytherapy is often used in combination with external beam radiation therapy. However, external beam radiation therapy is associated with various comorbidities (Viswanathan et al., 2014). For instance, patients treated with pelvic radiation may present with chronic radiation proctitis resulting in rectal bleeding, prolonged diarrhoea and various other gastrointestinal complications (Nout et al., 2011). External beam radiation has also seen to result in chronic radiation cystitis that leads to genitourinary side-effects including bladder dysfunction, urinary incontinence and vaginal stenosis (Saibishkumar et al., 2006). Higher doses of radiation in combination with chemotherapeutic drugs tend to disrupt the bone marrow environment leading to hematologic toxicity, making patients susceptible to infections (Mauch et al., 1995). Though rare, radiation treatment can result in weakening of the bone structure and ulceration of the skin (Morris et al., 1999; Schmeler et al., 2010).

In addition to long-term side effects, it has been noted that not all cancer cells are susceptible to radiation therapy. CSCs have been found to evade CRT owing to their increased efflux ability (Dean, 2009) and enhanced DNA repair mechanisms (Arnold et al., 2020; Bao et al., 2006), leading to resistance to therapy and relapse of the disease. The limited range of brachytherapy, the toxicities associated with external beam radiation and the acquisition of radiation resistance properties warrant the need for an effective radiosensitizer that may help increase the efficacy of radiation therapy,

preferably at lower doses, resulting in decreased side-effects and improved quality of life post CRT.

Naturally occurring compounds are rapidly gaining traction as potential anti-carcinogenic compounds. They have been proven to have considerable effect on preventing initiation, reducing proliferation, affecting differentiation patterns, metastatic abilities and angiogenic properties of tumours (Nobili et al., 2009). Emerging role of many of these molecules is being explored for a possible therapeutic role in cancer. These molecules are relatively more economical and hypothesised to be less toxic. Various phytochemicals like curcumin (Harini et al., 2019; Kim et al., 2006), resveratrol (found in red grapes) (Athar et al., 2009), quercetin (found in apples) (Lamson and Brignall, 2000) and many others have been shown to have anti-cancerous effects.

Aloe vera (*Aloe barbadensis miller*), a succulent, evergreen shrub has been used for treating skin ailments for centuries (Surjushe et al., 2008). However, recent evidence points to its possible role in cancer therapy. Aloe vera has been proven to reduce proliferative potential of breast and cervical cancer cells (Hussain et al., 2015). Aloe vera has also been observed to suppress angiogenesis and consequently tumour growth in mice (Kocik et al., 2014). Aloe vera and cisplatin (a conventional chemotherapeutic drug), worked synergistically leading to better efficacy even at lower doses of the drug (Hussain et al., 2015). Aloe vera has also been observed to activate the immune system, thereby helping clear tumour cells (Cathcart and Stebbing, 2016) and cancer-causing viruses like the herpes simplex virus (Kim et al., 1999). Further, studies have also indicated that Aloe vera extracts modulated the Wnt and NOTCH pathways in colorectal cancer (Peng et al., 2019), while another report proved that Aloe vera stimulates apoptosis in colorectal cancer cell lines (Cheng and Dong, 2018; Li et al., 2018).

Therefore, in this chapter, the possible use of Aloe vera as an effective radiosensitizer in combination with atorvastatin (a pan GTPase inhibitor previously shown to inhibit RHOC), has been explored.

10.2 Results and Discussion

10.2.1 Effect of Aloe vera on Cell Survival

Aloe vera has been previously shown to result in reduced proliferation of breast, colorectal and cervical cancer cell lines (Hussain et al., 2015; Peng et al., 2019). Here, using varying doses of the Aloe vera extract at different time points, an attempt has been made to study possible effects of Aloe vera on survival of SiHa cells.

One of the crucial factors that determine the stability of bioactive compounds is the solvent used for their extraction (Thouri et al., 2017). Various methods of Aloe vera extraction have been previously attempted in the lab. Aloe vera was extracted using solvents like dimethylsulfoxide (DMSO) and ethanol (EtOH) and their effect on cell proliferation in combination with imatinib was studied in the Chronic Myelogenous Leukemia (CML) model. Data from the lab indicated that the ethanolic extracts of Aloe vera led to sensitization of cells to imatinib as compared to extracts obtained using DMSO. Therefore, ethanolic extracts were used for this study.

To determine the effect of ethanolic Aloe vera extracts on SiHa cells, they were treated with various volumes of the extract and changes in cell survival were assayed. The WST assay revealed no significant change in cell survival with respect to the vehicle control (EtOH) over 3 different volumes of the extract (a=25µl, b=50µl and c=100µl per ml of media). The assay was performed at the end of 24h. As shown in **Figure 10.1**, no significant change was noted in survival when compared with the vehicle control.

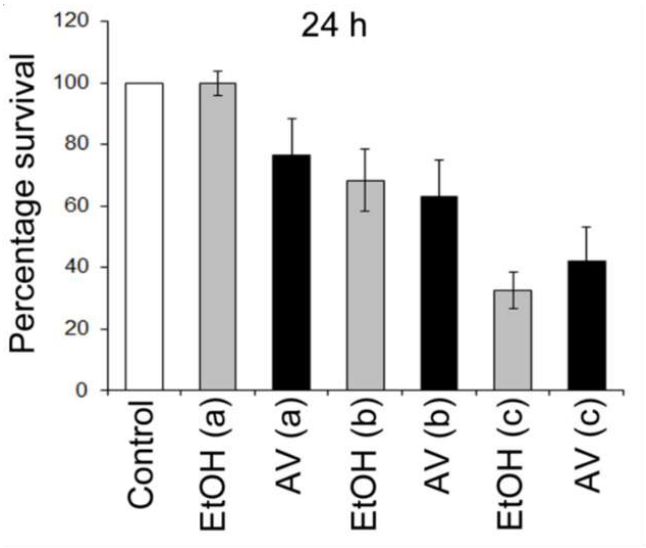

Figure 10.1: Bar graph representation of percentage survival of SiHa cells when treated with varying volumes of Aloe vera extract for 24h (n=3).

However, it was observed that increasing volumes of the extract led to decreased cell survival. Since similar levels of cytotoxicity were seen in cells treated with the respective vehicle controls, the observed decrease in cell survival was attributed to the toxic nature of ethanol, and not seen as an effect of Aloe vera alone. Since using the Aloe vera extract at higher volumes would lead to cell death due to increased cytotoxic effects of the vehicle (EtOH), further experiments were carried out using the lowest concentration of 25µl of the extract per ml of media.

In order to determine if Aloe vera had an effect on proliferation of SiHa cells when incubated for longer durations, the WST assay was performed on SiHa cells at 48h and 72h time points. Similar results with no change in cell survival in comparison with the vehicle control were observed at 48h and 72h time points **(Figure 10.2)**. This indicated that Aloe vera extracts did not alter proliferative capacity of SiHa cells.

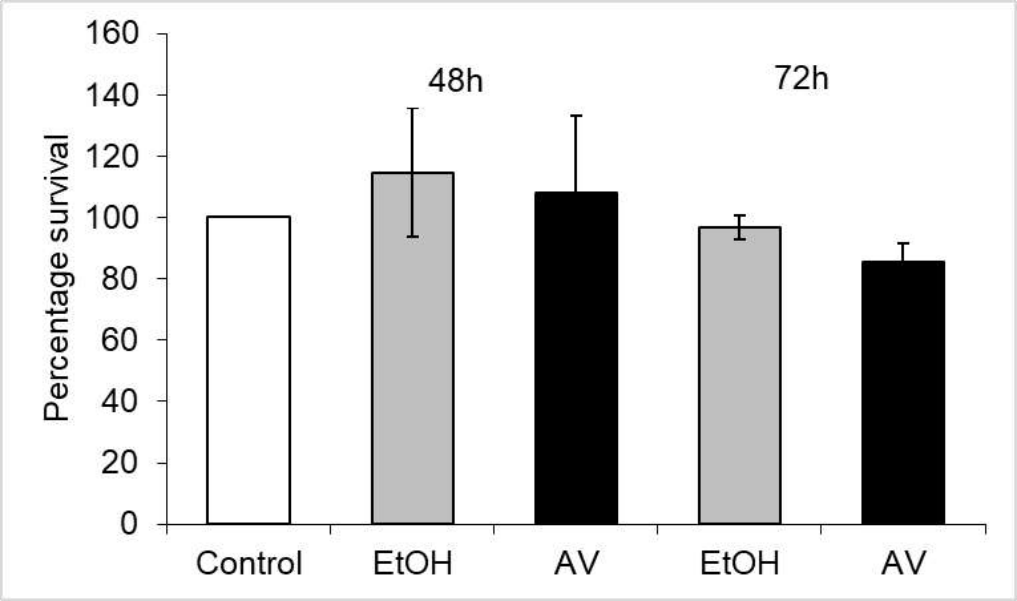

Figure 10.2: Bar graph representation of percentage survival of SiHa cells when treated with Aloe vera extract for 48h and 72h (n=3).

These results indicated that treatment of cells with Aloe vera alone does not induce cell death. This was contrary to previous reports that implied a role for Aloe vera in reducing proliferation of HeLa cells (Hussain et al., 2015). Further experiments were performed to determine the effect of Aloe vera on cell cycling profiles.

10.2.2 Effect of Aloe vera on Cell Cycle Profiles

The WST assay revealed no significant change in survival of SiHa cells upon addition of Aloe vera. To determine if Aloe vera alters the cycling patterns of SiHa cells, the cell cycle profile of Aloe vera treated cells was analysed. SiHa cells were treated with Aloe vera extracts along with the respective control (EtOH), and fixed in methanol post 24h of incubation. The cells were then stained with propidium iodide and the percentage of cells in each phase of the cell cycle was determined by flow cytometry.

Representative FACS plots of cell cycle profiles are shown in **Figure 10.3**. Gates D, E and F represent cells in the G1, S and G2/M phases of the cell cycle respectively. This distinction is based on the emission intensities of propidium iodide, which is proprtional to the DNA content present within the cell (Crowley et al., 2016). Since DNA content varies as cells progress through each phase of the cell cycle (Darzynkiewicz, 2012), this feature has been utilized to determine the percentage of cells in each cycling phase. The resulting percentages were compared with the vehicle control (EtOH) to determine the variations in cycling profiles upon addition of Aloe vera. As shown graphically in **Figure 10.4**, no significant changes were observed in cycling profiles upon Aloe vera treatment.

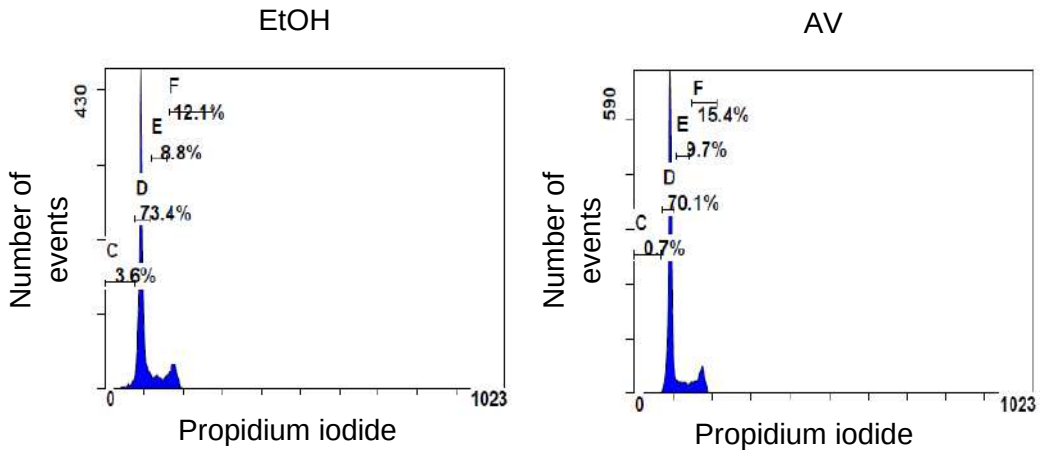

Figure 10.3: Representative FACS plots depicting the percentage of cells in each phase of the cell cycle upon Aloe vera addition (AV) and the respective vehicle control (EtOH).

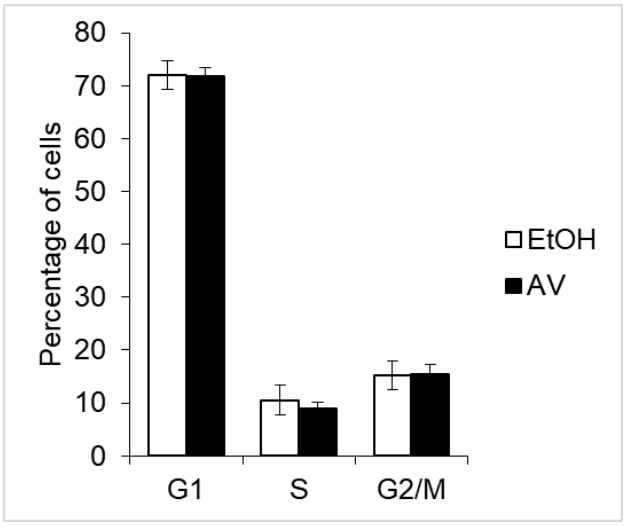

Figure 10.4: Graphical representation of percentage of cells in each phase of the cell cycle upon Aloe vera treatment (AV) and its corresponding vehicle control (EtOH). No significant change in cycling profiles was observed upon Aloe vera addition (n=3).

10.2.3 Effect of Aloe vera on Self-Renewal Capability and EMT

Thus far, it has been observed that Aloe vera had no significant effect on survival and cycling profiles of SiHa cells. In order to verify whether Aloe vera affects self-renewal and proliferative abilities over prolonged incubations, phenotypic assays were performed to determine the effect of Aloe vera on self-renewal abilities over extended periods of time.

The clonogenic assay was performed with SiHa cells and the effect of Aloe vera on clonogenicity was investigated. As shown in **Figure 10.5**, Aloe vera led (AV) to reduced formation of clones in comparison with the untreated and vehicle (EtOH) controls. The bar graph depicted in **Figure 10.6** indicates that this reduction was indeed significant ($p<0.05$).

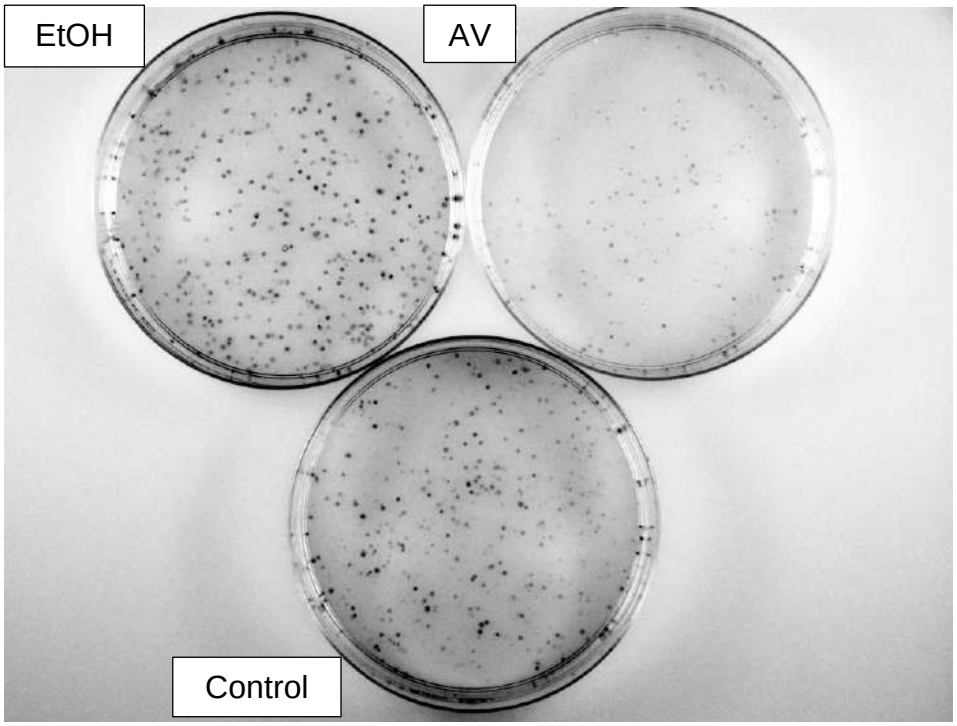

Figure 10.5: Representative image of reduction in clones formed by SiHa cells upon treatment with Aloe vera (AV), in comparison with vehicle control (EtOH).

.

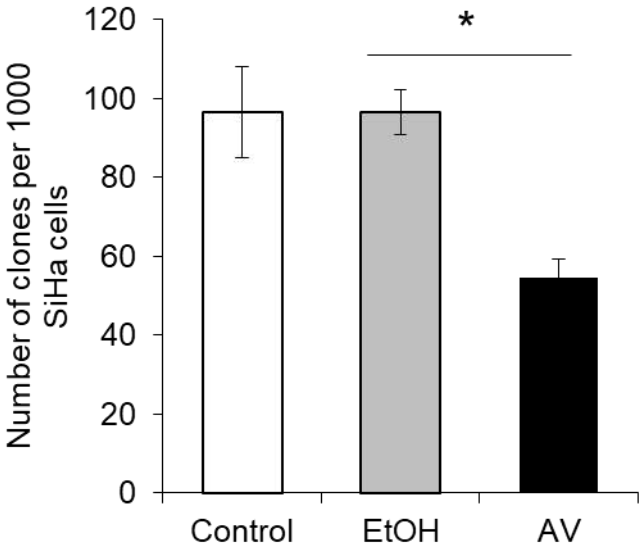

Figure 10.6: Graphical representation of reduction in clonogenic ability of SiHa cells when treated with Aloe vera extracts (n=3, $p<0.05$).

Since Aloe vera was observed to reduce self-renewal potential, it was investigated whether this was achieved by alterations in expression of genes involved in stemness maintenance. For this purpose, spheroidal cultures of SiHa cells were used. Cells grown as spheroids are known to have enhanced stem-like abilities (Cheng et al., 2013; Imamura et al., 2020; Liao et al., 2014). Therefore, the effect of Aloe vera treatment on aggressive spheroidal cells with enhanced self-renewal potential was assessed. qPCR analysis revealed that transcript levels of the stemness marker *POSTN* decreased significantly upon Aloe vera addition. On the other hand, no reduction was observed in expression of *NANOG*, *OCT4* and *ALDH*, while *CD49F* showed marginal reduction in expression upon Aloe vera treatment. The changes in transcript levels are depicted as a bar graph in **Figure 10.7**.

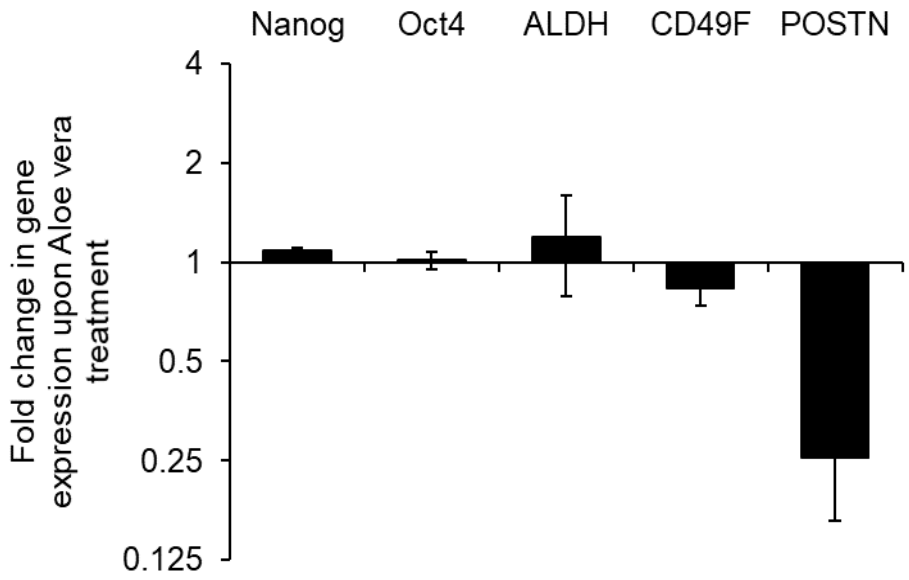

Figure 10.7: qPCR analysis showing changes in patterns of expression of stemness markers upon 48h of Aloe vera treatment. The fold changes were calculated with respected to the vehicle control (n=3, $p<0.05$). GAPDH was used as the internal control.

The decrease in POSTN was validated by immunofluorescent staining. SiHa cells were treated with Aloe vera extracts and the respective vehicle controls (EtOH) for 72h. They were then stained for POSTN and the difference in expression of POSTN was analysed. **Figure 10.8** shows a clear reduction in POSTN expression in Aloe vera treated SiHa cells in comparison with the vehicle control.

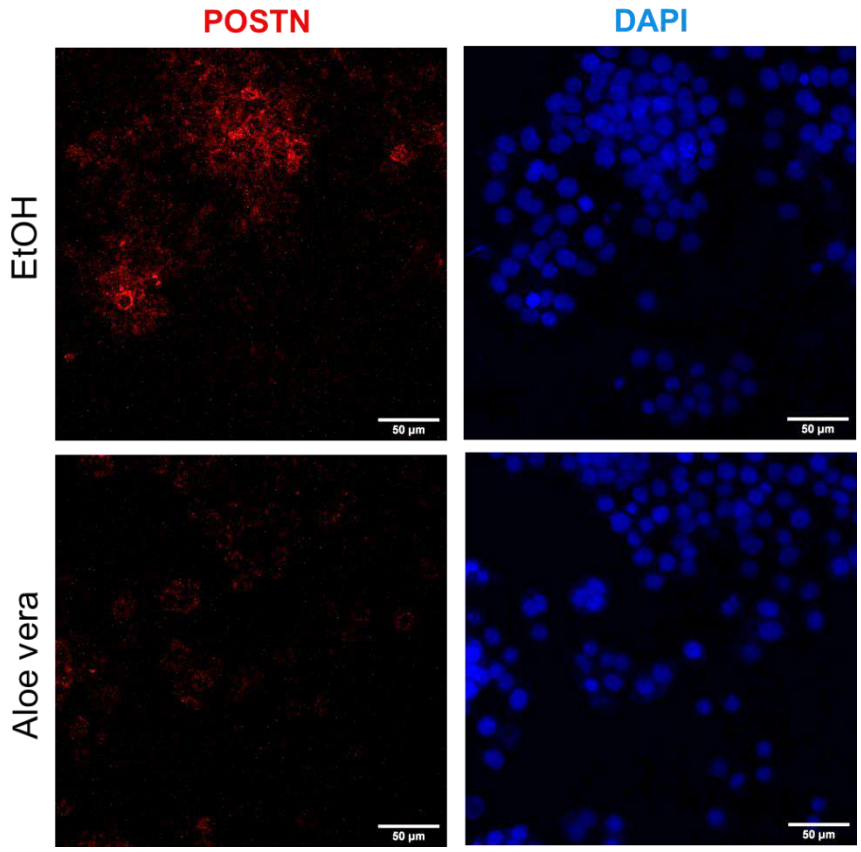

Figure 10.8: Representative confocal images of immunofluorescent analysis of changes in levels of POSTN in SiHa cells upon treatment with Aloe vera. Cells treated with the vehicle (EtOH) were used as the control. Scale bars are indicated. (n=2)

This was further confirmed by western blotting. SiHa cells were treated with Aloe vera extracts and the respective vehicle control (EtOH) for 72h. Immunoblotting analyses revealed a significant reduction in POSTN expression upon treatment with Aloe vera as depicted in **Figure 10.9**.

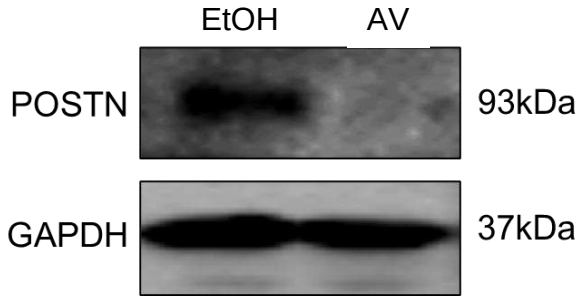

Figure 10.9: Representative immunoblot image of POSTN levels in SiHa cells upon Aloe vera treatment (AV) in comparison with the vehicle control (EtOH) (n=3). GAPDH was used as the loading control.

These observations indicate that Aloe vera affects long-term proliferative capacity and leads to reduced expression of the stemness marker POSTN. POSTN, largely recognised as a stromal factor, is known to promote maintenance of cancer stem-cells by regulating interactions between cancer cells and their environment (Wang and Ouyang, 2012; Zeng et al., 2018a). Though its increased expression has been mostly linked to tumour-associated fibroblasts (TAFs) (Yu et al., 2018), POSTN has also been shown to be elevated within cancer cells. Studies have demonstrated increased expression and secretion of POSTN in glioblastoma CSCs, resulting in alteration of the stem-cell niche (Zhou et al., 2015). Multiple studies have associated POSTN expression with increased metastasis, promotion of stem-like ability and acquisition of EMT traits (Bao et al., 2004; Gonzalez-Gonzalez and Alonso, 2018; Kyutoku et al., 2011; Lambert et al., 2015; Nakazawa et al., 2018; Wang et al., 2013; Zhong et al., 2019).

As treatment of SiHa cells with Aloe vera extracts was observed to result in pronounced reduction of POSTN, and since POSTN has been associated with the gain of mesenchymal characteristics, alterations in mesenchymal properties upon Aloe vera treatment were explored. In order to study changes in EMT, variations in the level of fibronectin was analysed. Fibronectin is a well-established marker of the mesenchymal phenotype and has been associated with increased metastasis in various tumour models (Akiyama et al., 1995; Zeisberg and Neilson, 2009). Additionally, since EMT promotes migratory and invasive properties (Pearson, 2019; Son and Moon, 2010), cancer cells that are highly motile must have increased actin polymerization and a well-defined actin

cytoskeleton (Yamaguchi and Condeelis, 2007). Therefore, modulations in the actin cytoskeleton post treatment with Aloe vera extracts was also examined by staining the cells with phalloidin. Phalloidin is a cyclic peptide that binds to actin filaments (Mahaffy and Pollard, 2008), a property which has been utilized to study the assembly of actin filaments (Ballestrem et al., 1998).

SiHa cells were treated with Aloe vera extracts for 72h. The cells were then fixed and changes in the level of fibronectin and actin cytoskeleton formation was analysed by immunofluorescent staining of cells treated with Aloe vera. As depicted in **Figure 10.10**, immunofluorescent analysis revealed a marked reduction in fibronectin levels in Aloe vera treated cells in comparison with the vehicle control. Additionally, while control SiHa cells (treated with the vehicle alone) were found to have a dense network of actin filaments along with the presence of spindle-shaped cells indicative of high motility, the actin cytoskeleton was found to have undergone disassembly in cells treated with Aloe vera as shown in **Figure 10.10**.

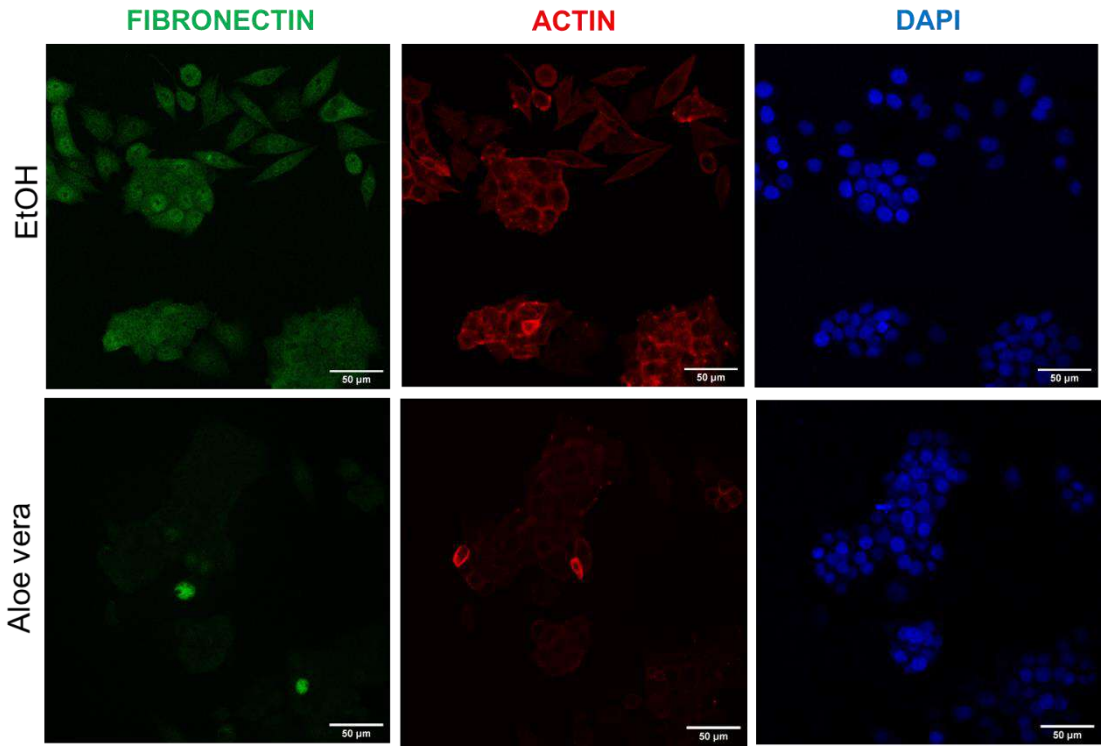

Figure 10.10: Representative immunofluorescent images of fibronectin and actin cytoskeleton staining of SiHa cells treated with Aloe vera extracts. SiHa cells treated the vehicle (EtOH) was used as the control. Scale bars are indicated. (n=2)

Therefore, treatment of cells with Aloe vera was found to result in decreased POSTN expression, which consequently resulted in loss of mesenchymal properties of SiHa

cells, as evidenced by decreased fibronectin and actin levels. The mesenchymal phenotype has been previously associated with increased stemness capability (Jolly et al., 2015; Mani et al., 2008; Shibue and Weinberg, 2017). The observation that treatment of cells with Aloe vera compromises long-term self-renewal ability, could therefore be explained by the highly apparent loss of mesenchymal phenotype in these cells. Since Aloe vera treatment has been linked to loss of stem-like ability, further studies were directed towards determining the effect of Aloe vera extracts as a sensitizer to existing modes of cancer therapy.

10.2.4 Effect of Aloe vera in Combination with Atorvastatin in Sensitization of SiHa Cells to Radiation

Since Aloe vera was observed to result in reduction of long-term self-renewal ability of SiHa cells, it was investigated whether Aloe vera in combination with radiation therapy could lead to increased cell death. SiHa cells were pre-treated with Aloe vera extracts for 24h before being irradiated at 6Gy. The cells were then assayed for cell death 48h after radiation.

Microscopic evaluation of cells revealed no change in cellular morphology of cells treated with Aloe vera followed by radiation treatment. **Figure 10.11** depicts a representative image of SiHa cells treated with vehicle control (EtOH) and Aloe vera 48h after irradiation.

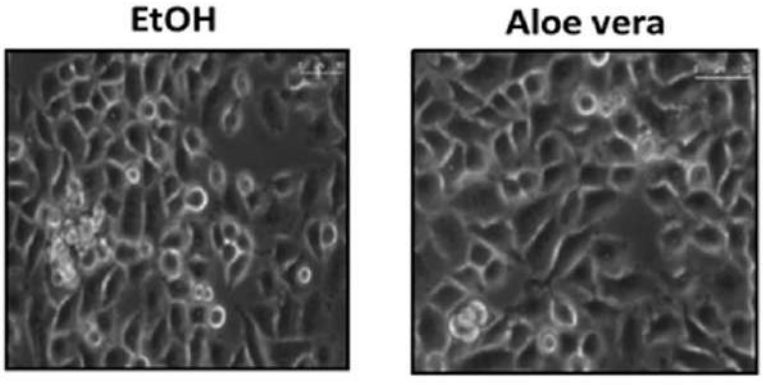

Figure 10.11: Representative light microscope images of SiHa cells treated with vehicle control (EtOH) and Aloe vera, at 48h post-radiation treatment.

The extent of cell death in these cells was analysed by FACS. Propidium iodide (PI) staining was performed to determine the population of dead cells. As depicted in

Figures 10.12 and **10.13**, FACS analysis revealed no significant changes in cell survival upon pre-treatment with Aloe vera in irradiated cells.

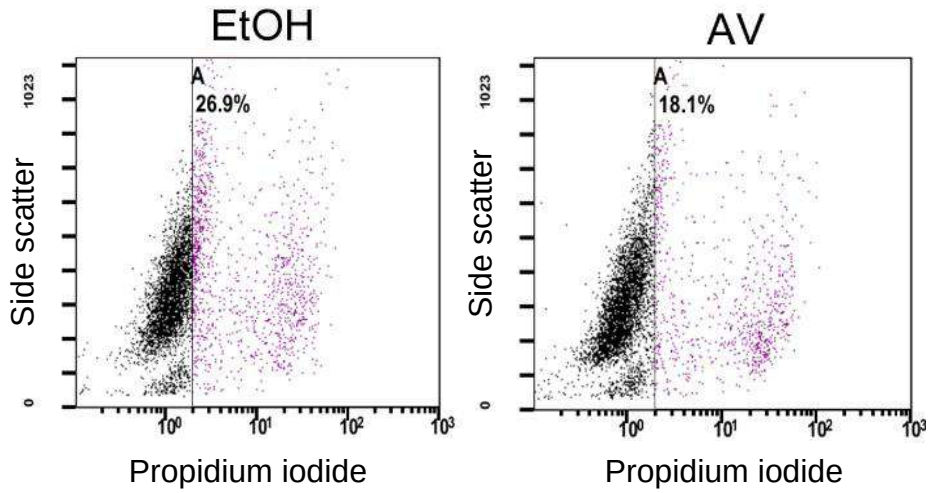

Figure 10.12: Representative FACS plots of SiHa cells treated with vehicle control (EtOH) and Aloe vera. Cells that positively stained for propidium iodide are depicted in purple.

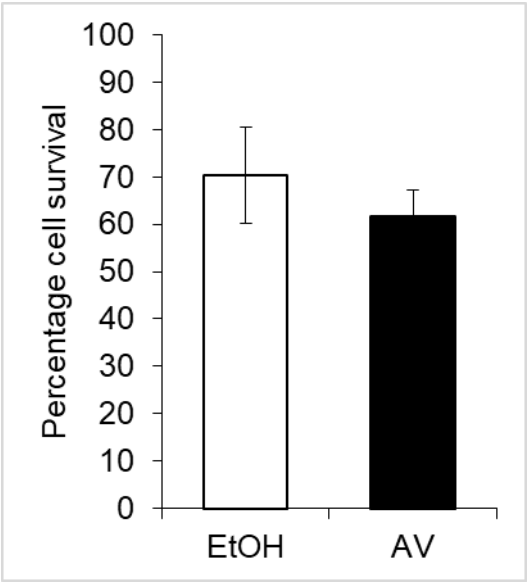

Figure 10.13: Graphical representation of percentage of live cells after Aloe vera treatment and irradiation. No significant change in survival was observed upon Aloe vera treatment (n=3).

As seen earlier in section 10.2.3, Aloe vera treatment led to significant reduction in transcript levels of *POSTN*. RHOC depletion on the other hand, led to reduction in

levels of expression of a range of stemness genes (Section 5.2.3). It was therefore envisaged that simultaneous inhibition of RHOC, coupled with Aloe vera treatment may lead to considerable impairment of stemness ability and consequent increased sensitivity to radiation.

In the work presented so far, RHOC has been shown to be associated with enhanced stem-like ability. Previously published data from the lab indicates RHOC's critical role in orchestrating DNA repair post radiation treatment (Pranatharthi et al., 2019). Therefore, a RHOC-specific inhibitor could be utilized as a radiosensitizer to eliminate the radio-resistant pool of cells within the tumour. Due to the lack of an inhibitor specifically for RHOC, atorvastatin, a pan inhibitor for RhoGTPases has been used.

Atorvastatin, a commonly used drug to prevent cardiovascular disease in individuals with abnormally high cholesterol levels (Shepherd et al., 1995), is a competitive inhibitor of HMG-CoA reductase and blocks cholesterol synthesis by preventing the conversion of HMG-CoA to mevalonate (Endo et al., 1976). Rho GTPases require prenylation for their activity (Collisson et al., 2002). The CAAX motif present at the carboxy terminus of Rho GTPases (Roberts et al., 2008), specifically supports addition of a farnesyl or geranylgeranyl group to the protein (Ridley, 2013; Wennerberg and Der, 2004). Since both farnesylpyrophosphate (FPP) and geranylgeranylpyrophosphate (GPP) are precursors of cholesterol (Nes, 2011), inhibition of the cholesterol synthesis pathway results in reduced activity of proteins that require post-translational addition of these groups for their functionality (Collisson et al., 2003). Since RHOC has been shown to be involved in regulating DNA repair (Pranatharthi et al., 2019), the effect of atorvastatin in combination with Aloe vera on survival of irradiated cells was scrutinized.

SiHa cells were pre-treated for 24h with atorvastatin (10µM) and Aloe vera extracts. They were then irradiated and cell survival was assayed at the end of 48h. **Figure 10.14** depicts light microscope images of SiHa cells treated with Aloe vera, atorvastatin and the respective vehicle controls 48h post irradiation. Atorvastatin treated cells were observed to lose their ability to adhere to the culture dish. This was attributed to the role of Rho GTPases in maintenance of membrane integrity and cytoskeletal organization (Maddala et al., 2004), which was lost upon treatment with atorvastatin. Interestingly, simultaneous treatment of cells with Aloe vera and atorvastatin coupled with radiation

proved to be highly lethal to SiHa cells. As shown in **Figure 10.14**, light microscope images of SiHa cells treated with both Aloe vera and atorvastatin taken 48h post radiation were indicative of cell death, as seen by a large number of non-refractive cells in the treated pool.

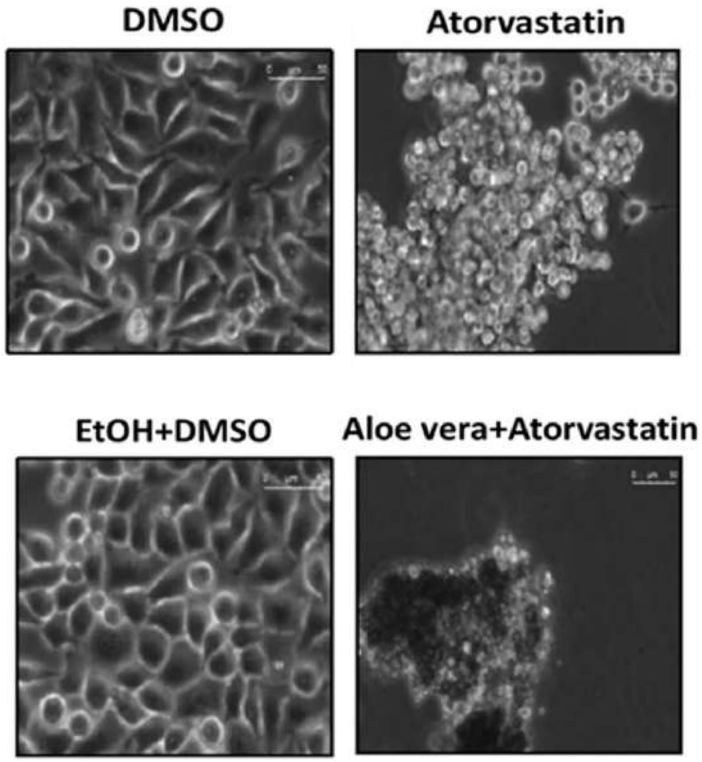

Figure 10.14: Representative light microscope images of SiHa cells pre-treated with Aloe vera and atorvastatin, taken 48h after radiation treatment. SiHa cells treated with atorvastatin and DMSO (vehicle control) are also shown. Scale bars are indicated.

To determine the extent of cell death, these cells were stained with propidium iodide (PI) and subjected to flow cytometry. FACS analysis revealed that pre-treatment of SiHa cells with a combination of Aloe vera and atorvastatin resulted in significant decrease in survival upon radiation in comparison with the vehicle control (EtOH+DMSO). **Figure 10.15** depicts the FACS plots and **Figure 10.16** is a bar graph of the same.

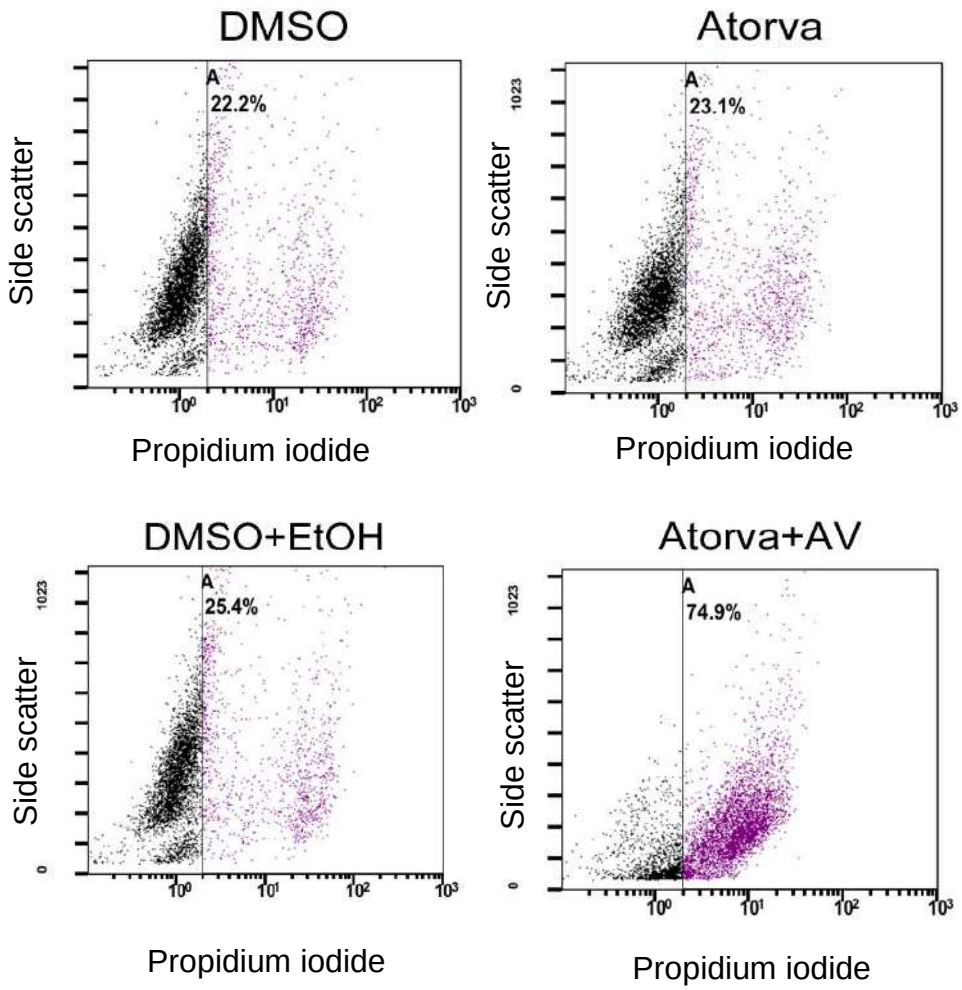

Figure 10.15: Representative FACS plots showing the percentage of dead cells upon treatment with a combination of Aloe vera and atorvastatin (Atorva) along with the respective vehicle controls followed by radiation treatment.

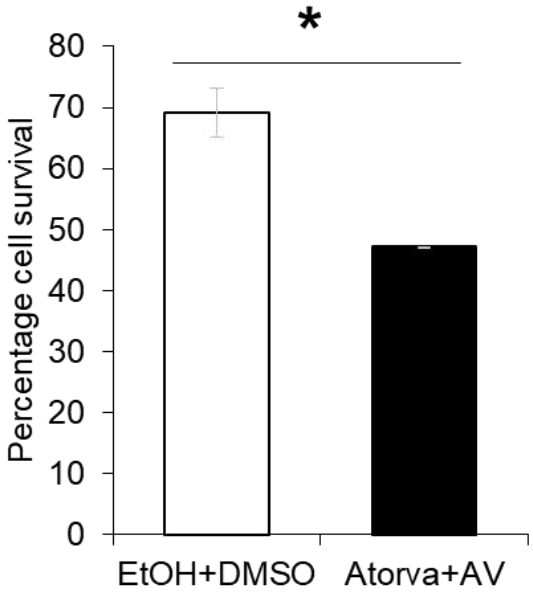

Figure 10.16: Graphical representation of cell survival upon combinatorial treatment of SiHa cells with atorvastatin and Aloe vera extracts (Atorva+AV) in comparison with vehicle control (EtOH+DMSO), followed by radiation (n=3, $p<0.05$).

These results indicate that combinatorial treatment of SiHa cells with both Aloe vera and atorvastatin lead to sensitization of SiHa cells to radiation. Importantly, treatment of cells with Aloe vera alone did not lead to significant changes in cell survival post radiation. This could be attributed to the observation that Aloe vera treatment leads to reduction of transcript levels of *POSTN* only, while most other stemness markers remain unchanged.

Additionally, treatment of cells with atorvastatin alone did not increase sensitivity of SiHa cells to radiation, whereas section 6.2.1 clearly demonstrates increase in apoptotic cells upon RHOC-specific knockdown via siRNA treatment. This indicates that pan Rho GTPase inhibition is not as effective at increasing sensitivity to radiation as compared to targeted knockdown of RHOC, thereby re-emphasizing the link between RHOC and radiation response. However, dual impairment of self-renewal pathways by combined Aloe vera and atorvastatin treatment was found to significantly sensitize SiHa cells to radiation treatment.

10.3 Conclusion

This chapter attempted to gain a broad understanding of the effect of Aloe vera on cervical cancer cell lines. Unlike previous studies that reported anti-proliferative properties of Aloe vera, here survival, proliferation and cell cycle profiles indicated no significant changes upon treatment with Aloe vera. However, since Aloe vera was reported to play an important role in reversing various phenotypes of cancer progression, its effect on long term self-renewal was investigated.

Clonogenicity assays revealed significant reduction in self-renewal capability of SiHa cells upon Aloe vera addition. qPCR analysis also revealed a marked reduction in transcript levels of *POSTN* and *CD49F* upon addition of Aloe vera to spheroidal SiHa cells, with POSTN in particular undergoing a massive reduction. Owing to POSTN's role in facilitating EMT, markers of the mesenchymal phenotype were assayed post Aloe vera treatment. Both fibronectin and actin, known to play crucial roles in EMT and migration, were found to be depleted upon treatment with Aloe vera extracts, implying a possible role for Aloe vera in halting epithelial to mesenchymal transition, a prerequisite for metastasis.

Next, the effect of Aloe vera in combination with atorvastatin, a pan Rho inhibitor, on radiation treatment was studied. Significantly, combinatorial treatment of cells with Aloe vera and atorvastatin led to sensitization of cells to radiation, with a prominent increase observed in the percentage of dead cells. This implied sensitization of cancer cells by Aloe vera and atorvastatin to radiation.

This paves the way for possible reduction of the radiation doses currently employed, without compromising on survival rates. However, these data are preliminary and further *in vitro* experiments need to be performed to identify the specific mechanisms by which Aloe vera brings about the observed effects. *In vitro* data must also be complemented with studies in mice to identify possible systemic effects of Aloe vera on preventing cancer progression.

CHAPTER -IX

Conclusion

11.1 Conclusion

Monumental advancements have been made over the past few decades towards comprehending cancer progression and devising effective treatment modalities to tackle the disease. However, current forms of therapy (primarily chemo-radiation), while being capable of eliminating the rapidly proliferating tumour bulk, have minimal detrimental effect on a sub-population of tumour cells that later came to be known as CSCs (Pattabiraman and Weinberg, 2014; Yang and Wechsler-Reya, 2007). CSCs have since been identified to play a crucial role in metastasis and relapse (Chang, 2016). Efforts have therefore been directed towards understanding this elusive population primarily responsible for poor prognosis. This study explores the role of RHOC as a key contributor to CSC maintenance.

RHOC has been previously shown to regulate stemness in head and neck, breast and ovarian cancers (Islam et al., 2014; Rosenthal et al., 2012). This work puts forward evidence that RHOC regulates cervical CSCs. The novel findings of this work include- a) Establishment of a link between RHOC and maintenance of cervical CSCs b) The identification of a population of cells co-expressing RHOC along with NANOG and CD49F, in patient-derived cervical cancer specimens c) Regulation of stemness gene expression by RHOC via both ERK signalling and modulation of the epigenetic machinery d) Association of RHOC with the epigenetic modulators WDR5 and TET2 resulting in open, easily accessible chromatin e) Combinatorial treatment of SiHa cells with Aloe vera extracts and atorvastatin increases sensitivity to radiation.

To unravel the association between RHOC and stemness, cells that were artificially modulated for RHOC expression were analysed for stemness capability. RHOC over-expressing cells were observed to have enhanced effluxing abilities, a feature typical of CSCs. *In-vitro* phenotypic studies confirmed the association between stemness and RHOC, with cells modulated for RHOC expression displaying varying self-renewal potentials. RHOC over-expression was observed to result in increased stem-like ability, whereas knockdown of RHOC led to abrogation of the stemness phenotype. This was tested using various approaches including the clonogenic, soft agar and anoikis resistance assays.

To understand the specific stemness targets regulated by RHOC expression, RNA-seq studies were carried out on SiHa-N and SiHa-R (a RHOC over-expressing cell line)

cells. Consistent with the phenotypic data, bioinformatic analysis of the transcriptome revealed up-regulation of a plethora of genes involved in stemness maintenance, proliferation and various signalling pathways in SiHa-R cells. qPCR and western blotting analysis confirmed this finding, with stemness markers like NANOG, POSTN, CD49F, ALDH1 and several others showing increased expression in SiHa-R cells, and subsequent down-regulation upon RHOC depletion. SiHa-R xenografts, which were found to be larger than SiHa-N (Srivastava et al., 2009), were also analysed for the expression of these stemness markers. As envisaged, immunofluorescent staining revealed up-regulation of NANOG and CD49F in SiHa-R xenografts as compared to SiHa-N.

Clinical specimens were also analysed to verify these findings. Expression analysis of RHOC and key stemness genes, NANOG and CD49F, in patient-derived samples revealed co-expression of NANOG/RHOC and CD49F/RHOC in RHOC-high expressing tumour cells. Interestingly, clinical feature analysis revealed that all clinical samples subjected to FACS analysis presented with metastasis in the iliac lymph nodes. Several studies have previously shown that RHOC is associated with increased instances of metastatic tumours (Clark et al., 2000; Ikoma et al., 2004; Lang et al., 2017). Therefore, in this context, the above observations may be indicative of a link between RHOC, stemness marker expression and progression of the disease.

Since RHOC-high cells were observed to have a stem-like phenotype, the association between RHOC and resistance to radiation was explored. Analysis of the RNA-seq data revealed enrichment of genes regulating cell cycle, survival and DNA repair in SiHa-R cells (Pranatharthi et al., 2019). Immunofluorescent staining and immunoblotting procedures confirmed this finding, with proteins involved in DNA repair- pH2Ax, BRCA2 and MRE11 (Bian et al., 2019; Lowndes and Toh, 2005), found to be elevated in SiHa-R. Immunofluorescent analysis of xenograft sections also revealed a similar up-regulation of the DNA repair machinery in SiHa-R xenografts. Finally, depletion of RHOC in SiHa cells was found to increase the percentage of apoptotic cells upon radiation. This was further confirmed in clinical specimens, where antibody-based inhibition of RHOC was observed to lead to sensitization of tumour cells to radiation therapy. These findings further strengthen the hypothesis that RHOC over-expression results in a robust stem-like pool capable of evading radiation-induced cell death.

Since the RNA-seq data implied increased expression of genes involved in signalling pathways linked to cancer progression, the specific signalling pathway that regulated stemness maintenance in the background of RHOC over-expression was investigated. ERK signalling was identified as the possible signalling mechanism that controlled stem-like ability in RHOC-high cells. Numerous reports have linked the ERK cascade with differentiation, proliferation, migration and survival (Dhillon et al., 2007; Garcia-Gomez et al., 2018). Deregulation of this pathway, either via mutations or by changes in activation, have been associated with poor progression in multiple cancers (Deschenes-Simard et al., 2014; Kohno and Pouyssegur, 2006; McCubrey et al., 2007).

Here, inhibition of the ERK pathway was observed to result in significant decrease in stem-like ability of SiHa-R cells. qPCR and western blotting experiments confirmed that blocking ERK signalling led to decreased expression of the stemness genes, CD49F and ALDH1 in cells over-expressing RHOC. Further, E2F1 was identified as the transcription factor downstream of the ERK pathway that led to increased expression of stemness markers. Reports have previously shown that activation of E2F1 by the ERK pathway is associated with poor cancer progression (Riverso et al., 2017). E2F1 is known to regulate therapy resistance (Yan et al., 2014), metastasis (Hollern et al., 2019), invasion and migration (Liang et al., 2016) in various cancers like that of the colon (Fang et al., 2020), breast (Hollern et al., 2019), kidney (Ma et al., 2013), prostate (Chun et al., 2019) and skin (Riverso et al., 2017). In this study, both RHOC silencing and ERK inhibition were individually observed to result in a decrease in nuclear levels of E2F1, implying that RHOC-mediated ERK signalling might be responsible for nuclear localization of E2F1. Further, knockdown of E2F1 resulted in decreased transcript levels of CD49F and ALDH1 in SiHa-R cells, a pattern that overlapped with the expression profile obtained upon ERK inhibition. Therefore, it was concluded that RHOC over-expression enhances stem-like features of cervical cancer cell lines by activation of the ERK signalling cascade, that resulted in increased expression of stemness genes by increasing nuclear localization of E2F1. However, it must be noted that only CD49F and ALDH1 were observed to be significantly affected by ERK activation, whereas core regulators of pluripotency like NANOG, OCT4 and SOX2 remained unaltered. Therefore, further experiments were undertaken to decipher the mechanisms by which RHOC could be regulating these stemness factors.

RNA-seq data suggested an alteration of the global transcriptional network upon RHOC over-expression. Further, a captivating analysis of RHOC expression pattern and chromatin compactness revealed that RHOC was highly expressed in the nuclear compartment of cells with less compact (open) chromatin. The observation that RHOC resulted in global up-regulation of the transcriptome, and the existence of nuclear RHOC, prompted investigations into a possible epigenetic role for RHOC. It was therefore hypothesized that RHOC over-expression modulates chromatin, resulting in increased expression of genes regulating various biological processes including stemness, radio-resistance and metastasis.

As RHOC is devoid of a DNA binding domain, the potential nuclear binding partners of RHOC were investigated. MS analysis of proteins co-precipitated with RHOC from the nuclear fraction, unveiled WDR5 as a prominent binding partner of RHOC. WDR5 has been previously implicated in colon cancer progression by aiding resistance to radiation-induced DNA damage (Neilsen et al., 2018), and by facilitating the EMT process in breast cancer (Punzi et al., 2019). WDR5 has a significant role in chromatin modification and is known to result in methylation of H3 at lysine 4, an active transcriptional mark (Santos-Rosa et al., 2002). Therefore, changes in the levels of H3K4me3 upon modulation in RHOC expression were assessed.

As expected, H3K4me3 levels were found to be elevated in SiHa-R cells, and diminished upon RHOC inhibition. Additionally, knockdown of WDR5 was observed to result in abrogation of RHOC-induced stemness phenotype. This was also accompanied with decreased expression of stemness genes, particularly NANOG. Consistent with this finding, ChIP-qPCR analysis established binding of both RHOC and WDR5 to the NANOG promoter. The NANOG promoter reporter assay further confirmed this observation, with activity of the NANOG promoter being found to change proportionally to RHOC and WDR5 levels. Finally, co-expression of RHOC and WDR5 was also observed in patient-derived samples. However, it is important to note that the exact mechanistic of translocation of RHOC to the nucleus is not understood. Details pertaining to the possible triggers that result in shuttling of RHOC between the cytosolic and nuclear compartments are being currently explored in the lab.

Apart from histone modifications, methylation of DNA is also known to regulate gene expression patterns (Gyorffy et al., 2015). DNA methylation is widely linked to gene

silencing and repression of gene expression (Fukushige and Horii, 2013). To investigate the association between RHOC expression and methylation status of DNA, the EPIC methylation array was carried out on SiHa-N and SiHa-R cells. Analysis of this data revealed that increased RHOC expression led to genome-wide DNA hypomethylation. Specifically, genes belonging to stemness and signalling clusters were found to be hypomethylated.

Active demethylation involves oxidation of 5-methylcytosine (5mC) to 5-hydroxymethylcytosine (5hmC). The 5hmC is then replaced with 5C by break-excision repair mechanisms, eventually resulting in decreased 5mC levels (Tahiliani et al., 2009; Wu and Zhang, 2017). Analysis of 5mC upon modulations in levels of RHOC divulged an inverse relationship between the two. A decrease in percentage of cells positive for 5mC was observed with increased RHOC expression, whereas RHOC knockdown led to the opposite effect. These findings support the rationale that RHOC over-expression results in demethylation of DNA, resulting in increased expression of stemness genes, along with genes associated with DNA repair and cell signalling.

Experiments were undertaken to probe the possible mechanism behind RHOC-mediated DNA demethylation. Active DNA demethylation is moderated by the TET, BER and AID/APOBEC families (Bhutani et al., 2011). Detailed analysis of the transcriptome data between SiHa-N and SiHa-R revealed up-regulation of the DNA demethylase, TET2. Mutational inactivation of TET2 has been previously associated with the initiation of haematological malignancies (Moran-Crusio et al., 2011), while on the other hand, TET2-positive cells have been found to mark for slow-cycling-cancer cells (SCCCs), associated with chemoresistance and recurrence in various solid tumour models like melanomas, glioblastomas and colorectal cancer (Puig et al., 2018). Therefore, the association between RHOC-induced DNA demethylation and TET2 was explored further.

The observed over-expression of TET2 was validated by immunofluorescent analysis of TET2 in SiHa-R cells. Additionally, TET2 expression was found to be diminished upon RHOC depletion, as proven by qPCR and western blotting. To determine the link between TET2 and the stemness advantage conferred by RHOC, phenotypic assays were undertaken on RHOC over-expressing cells that were depleted of TET2. It was observed that TET2 knockdown was capable of abrogating the gain of stemness

phenotype observed due to RHOC over-expression, with TET2 silencing resulting in reduced colony formation ability. Transcript analysis by qPCR also revealed decreased expression of stemness genes in SiHa-R cells knocked down for TET2. These results indicated that RHOC via TET2 led to increased demethylation of DNA and enhanced stemness capability.

Taken together, this work confirms the role of RHOC in the maintenance of stemness in cervical cancer by positively regulating the expression of stemness genes via modifications to the DNA, thereby assigning a novel epigenetic role to RHOC. Previous studies have associated RHOC-mediated ERK signalling with invasion, motility, metastasis and angiogenesis in breast and prostate cancers (Iiizumi et al., 2008; van Golen et al., 2002). Here, a significant link has been drawn between RHOC-activated ERK signalling and stemness maintenance in cervical cancer. The ERK pathway was found to regulate the expression of prominent stemness markers like CD49F and ALDH in cells over-expressing RHOC.

Therefore, the regulatory mechanisms governed by RHOC appear to be two-pronged. It may be concluded that RHOC regulates stemness status by both epigenetic modifications and cytoplasmic signalling mechanisms. It is interesting to note that the expression of the core network of genes (OCT4, SOX2 and NANOG), responsible for maintenance of the embryonic stem cell (ESC) pool (Zhao et al., 2017), was influenced by epigenetic modulations governed by RHOC, but was unaffected by the ERK pathway. On the other hand, expression of the surface marker CD49F and the cytosolic protein ALDH was found to be regulated both epigenetically and by cytoplasmic ERK signalling. These findings may be indicative of the presence of parallel regulatory mechanisms that control stemness gene expression, and further investigations must be performed to understand the molecular underpinnings of this process.

This work also encompassed the investigation of naturally derived extracts as anti-cancer agents. Previously, studies have reported that Aloe emodin, a compound purified from Aloe vera leaves, was an effective anti-tumour molecule in various tumour models including bladder, colon, neuroectodermal, cervical, gastric and many others (Pecere et al., 2000; Sanders et al., 2017). However, studies have indicated that natural whole plant extracts are more effective than purified components that work in isolation (Rasoanaivo et al., 2011). Crude extracts have been observed to work in synergy with other

associated components leading to better cellular uptake and a consequent increase in effectiveness (Gilbert and Alves, 2003). Therefore, this study explores the effect of crude Aloe vera extracts as an anti-cancer agent.

It was observed that while treatment of SiHa cells with Aloe vera alone did not lead to significant changes to short-term survival and cell cycle profiles, it resulted in marked reduction of long-term survival and self-renewal abilities. Transcript analysis of stemness markers revealed significant reduction in the expression of POSTN, a gene known for its association with promoting the stem-like phenotype and acquisition of mesenchymal traits in cancer (Wang et al., 2013). EMT has previously been linked to the stem-like phenotype in cancers (Wang et al., 2015). On similar lines, it was observed that along with a reduction in the stemness-related gene POSTN, treatment of SiHa cells with Aloe vera resulted in significant down-regulation of fibronectin and the actin cytoskeleton, both of which are linked with EMT and increased migratory and invasive phenotype (Li et al., 2017; Yamaguchi and Condeelis, 2007; Yamazaki et al., 2005). Thus, while Aloe vera did not change proliferation and cell cycling profiles, it was observed to result in significant reduction of self-renewal and loss of the EMT phenotype.

Since this work has proven RHOC's contribution towards the stemness phenotype, the effect of Aloe vera extracts in conjunction with atorvastatin (a pan inhibitor of RHO GTPases) on radiation was scrutinized. Atorvastatin has been previously used to successfully inhibit RHOC in head and neck cancers (Islam et al., 2013). Treatment of cells with atorvastatin was observed to result in a reduction in the active form of RHOC by preventing isoprenylation, a post-translational modification essential for its biological activity (Collisson et al., 2003; Islam et al., 2013). Intriguingly, it was found that pre-treatment of SiHa cells with a combination of Aloe vera and atorvastatin resulted in a remarkable decrease in cell survival post radiation treatment, while solitary treatment with either Aloe vera or atorvastatin alone did not lead to any significant change in survival. Data presented here indicates that treatment with Aloe vera resulted in significant loss of EMT and stemness phenotype. The work also highlights RHOC's contribution towards maintenance of stemness in cervical cancer. In conjunction with this, numerous reports have implicated RHOC in proliferation, migration and invasive abilities across tumour models. Therefore, simultaneous deregulation of pathways involved in maintenance of the stem-like phenotype, promotion of EMT, migration and

invasion, by combinatorial treatment with Aloe vera and atorvastatin, could have resulted in the observed loss in the ability of cervical cancer cells to resist radiation therapy

11.2 Summary

This work vehemently confirms RHOC's role in stemness maintenance in tumour cells and proposes the testing of novel drugs against RHOC on patient-derived tumour xenografts. However, RHOC is a cytoplasmic protein, making live-sorting of RHOC-high cells a difficult endeavour. Efforts are ongoing in the lab to establish an assay that would allow isolation of viable RHOC-high cells from patient-derived tumours, and subject them to tumorigenicity assays for suitable drug development.

Development of inhibitors specific to RHOC could help reduce incidences of metastasis and relapse. Interestingly, RV001, a vaccine that targets RHOC over-expressing metastatic cells thereby deterring metastasis, is currently under trial in prostate cancer patients (Schuhmacher et al., 2020). Also, RHOC with an important contribution to CSC maintenance, has immense potential to be developed as a biomarker that would help identify tumours with metastatic potential, thereby predicting response to therapy. Additionally, since this work establishes that RHOC regulates maintenance of cervical CSCs via epigenetic and signalling mechanisms, inhibition of this protein could result in potential sensitization of CSCs to modes of treatment currently employed at the clinic.

Further, RNA-seq data of SiHa-N and SiHa-R cells revealed differential expression of a cohort of miRNAs. These included miR 210, miR 100 and miR 4435, which are known to regulate survival under hypoxic conditions (Grosso et al., 2013), tumorigenesis (Qin et al., 2015) and progression of cancer (Zhu et al., 2020) respectively. Therefore, specific targeting of these miRNAs could help alleviate the adverse RhoC-driven phenotype of cancers.

Additionally, it was observed that combinatorial treatment of cells with Aloe vera extracts and atorvastatin led to increased cell death upon radiation. This implies sensitization of cervical cancer cells to radiation when pre-treated with a combination of Aloe vera and atorvastatin, paving the way for a possible reduction in radiation dosage, thereby lowering the long-term side effects associated with radiation therapy. However, these results must be supplemented with studies in mice and further *in vitro* investigations must be taken up to understand the molecular mechanisms behind this observation in detail.

Overall, this work establishes RHOC's central role in regulation of the stemness phenotype in cervical cancer and assigns it with a novel function as an epigenetic regulator in cervical cancer, that is capable of globally controlling the transcriptional framework of a cancer cell. These observations herald the use of RHOC as a prognostic biomarker, and emphasize the importance of the development of inhibitors specific to RHOC, that could serve as sensitizers of the resistant CSC pool, making them more amenable to current forms of therapy. Further, the work proposes that the use of Aloe vera extracts along with the widely-used statin drug, atorvastatin, sensitizes cervical cancer cells to radiation, and studies should be undertaken to explore its possible use as an adjunctive therapy to effectively treat the disease.

12.0 REFERENCES

1) Abad, E., Graifer, D., and Lyakhovich, A. (2020). DNA damage response and resistance of cancer stem cells. Cancer Lett *474*, 106-117.
2) Abel, E. V., Kim, E. J., Wu, J., Hynes, M., Bednar, F., Proctor, E., Wang, L., Dziubinski, M. L., and Simeone, D. M. (2014). The Notch pathway is important in maintaining the cancer stem cell population in pancreatic cancer. PLoS One *9*, e91983.
3) Aceto, N., Bardia, A., Miyamoto, D. T., Donaldson, M. C., Wittner, B. S., Spencer, J. A., Yu, M., Pely, A., Engstrom, A., Zhu, H., *et al.* (2014). Circulating tumor cell clusters are oligoclonal precursors of breast cancer metastasis. Cell *158*, 1110-1122.
4) Akiyama, S. K., Olden, K., and Yamada, K. M. (1995). Fibronectin and integrins in invasion and metastasis. Cancer Metastasis Rev *14*, 173-189.
5) Al-Hajj, M., Wicha, M. S., Benito-Hernandez, A., Morrison, S. J., and Clarke, M. F. (2003). Prospective identification of tumorigenic breast cancer cells. Proc Natl Acad Sci U S A *100*, 3983-3988.
6) Aldea, C., Alvarez, C. P., Folgueira, L., Delgado, R., and Otero, J. R. (2002). Rapid detection of herpes simplex virus DNA in genital ulcers by real-time PCR using SYBR green I dye as the detection signal. J Clin Microbiol *40*, 1060-1062.
7) Allen, L. F., Sebolt-Leopold, J., and Meyer, M. B. (2003). CI-1040 (PD184352), a targeted signal transduction inhibitor of MEK (MAPKK). Semin Oncol *30*, 105-116.
8) Ang, Y. S., Tsai, S. Y., Lee, D. F., Monk, J., Su, J., Ratnakumar, K., Ding, J., Ge, Y., Darr, H., Chang, B., *et al.* (2011). Wdr5 mediates self-renewal and reprogramming via the embryonic stem cell core transcriptional network. Cell *145*, 183-197.
9) Arbyn, M., Weiderpass, E., Bruni, L., de Sanjose, S., Saraiya, M., Ferlay, J., and Bray, F. (2020). Estimates of incidence and mortality of cervical cancer in 2018: a worldwide analysis. Lancet Glob Health *8*, e191-e203.
10) Arnold, C. R., Mangesius, J., Skvortsova, II, and Ganswindt, U. (2020). The Role of Cancer Stem Cells in Radiation Resistance. Front Oncol *10*, 164.

11) Athar, M., Back, J. H., Kopelovich, L., Bickers, D. R., and Kim, A. L. (2009). Multiple molecular targets of resveratrol: Anti-carcinogenic mechanisms. Arch Biochem Biophys *486*, 95-102.

12) Audia, J. E., and Campbell, R. M. (2016). Histone Modifications and Cancer. Cold Spring Harb Perspect Biol *8*, a019521.

13) Avdic, V., Zhang, P., Lanouette, S., Groulx, A., Tremblay, V., Brunzelle, J., and Couture, J. F. (2011). Structural and biochemical insights into MLL1 core complex assembly. Structure *19*, 101-108.

14) Ayla, S., and Karahuseyinogluc, S. (2019). Cancer Stem Cells, Their Microenvironment and Anoikis. Crit Rev Oncog *24*, 27-34.

15) Bacevic, K., Lossaint, G., Achour, T. N., Georget, V., Fisher, D., and Dulic, V. (2017). Cdk2 strengthens the intra-S checkpoint and counteracts cell cycle exit induced by DNA damage. Sci Rep *7*, 13429.

16) Bahena-Ocampo, I., Espinosa, M., Ceballos-Cancino, G., Lizarraga, F., Campos-Arroyo, D., Schwarz, A., Garcia-Lopez, P., Maldonado, V., and Melendez-Zajgla, J. (2016). miR-10b expression in breast cancer stem cells supports self-renewal through negative PTEN regulation and sustained AKT activation. EMBO Rep *17*, 1081.

17) Baldwin, M. A. (2004). Protein identification by mass spectrometry: issues to be considered. Mol Cell Proteomics *3*, 1-9.

18) Ballestrem, C., Wehrle-Haller, B., and Imhof, B. A. (1998). Actin dynamics in living mammalian cells. J Cell Sci *111 (Pt 12)*, 1649-1658.

19) Bannister, A. J., and Kouzarides, T. (2011). Regulation of chromatin by histone modifications. Cell Res *21*, 381-395.

20) Bao, S., Ouyang, G., Bai, X., Huang, Z., Ma, C., Liu, M., Shao, R., Anderson, R. M., Rich, J. N., and Wang, X. F. (2004). Periostin potently promotes metastatic growth of colon cancer by augmenting cell survival via the Akt/PKB pathway. Cancer Cell *5*, 329-339.

21) Bao, S., Wu, Q., McLendon, R. E., Hao, Y., Shi, Q., Hjelmeland, A. B., Dewhirst, M. W., Bigner, D. D., and Rich, J. N. (2006). Glioma stem cells promote radioresistance by preferential activation of the DNA damage response. Nature *444*, 756-760.

22) Baskar, R., Dai, J., Wenlong, N., Yeo, R., and Yeoh, K. W. (2014). Biological response of cancer cells to radiation treatment. Front Mol Biosci *1*, 24.

23) Baylin, S. B. (2005). DNA methylation and gene silencing in cancer. Nat Clin Pract Oncol *2 Suppl 1*, S4-11.

24) Baylin, S. B., Belinsky, S. A., and Herman, J. G. (2000). Aberrant methylation of gene promoters in cancer---concepts, misconcepts, and promise. J Natl Cancer Inst *92*, 1460-1461.

25) Becker, J. S., Nicetto, D., and Zaret, K. S. (2016). H3K9me3-Dependent Heterochromatin: Barrier to Cell Fate Changes. Trends Genet *32*, 29-41.

26) Behbehani, G. K., Thom, C., Zunder, E. R., Finck, R., Gaudilliere, B., Fragiadakis, G. K., Fantl, W. J., and Nolan, G. P. (2014). Transient partial permeabilization with saponin enables cellular barcoding prior to surface marker staining. Cytometry A *85*, 1011-1019.

27) Ben-Porath, I., Thomson, M. W., Carey, V. J., Ge, R., Bell, G. W., Regev, A., and Weinberg, R. A. (2008). An embryonic stem cell-like gene expression signature in poorly differentiated aggressive human tumors. Nat Genet *40*, 499-507.

28) Bernier J, Domenge C, Ozsahin M, Matuszewska K, Lefèbvre JL, Greiner RH, Giralt J, Maingon P, Rolland F, Bolla M, Cognetti F, Bourhis J, Kirkpatrick A and van Glabbeke M. (2004). Postoperative irradiation with or without concomitant chemotherapy for locally advanced head and neck cancer. N Engl J Med. *19*, 1945-52.

29) Banerjee R and Kamrava M. (2014). Brachytherapy in the treatment of cervical cancer: a review. Int J Womens Health. *6*, 555-64.

30) Beya, W., Davidson, B., and Erlwanger, K. H. (2012). The effects of crude aqueous and alcohol extracts of Aloe vera on growth and abdominal viscera of suckling rats. Afr J Tradit Complement Altern Med *9*, 553-560.

31) Bhutani, N., Burns, D. M., and Blau, H. M. (2011). DNA demethylation dynamics. Cell *146*, 866-872.

32) Bian, L., Meng, Y., Zhang, M., and Li, D. (2019). MRE11-RAD50-NBS1 complex alterations and DNA damage response: implications for cancer treatment. Mol Cancer *18*, 169.

33) Biocca, S., Neuberger, M. S., and Cattaneo, A. (1990). Expression and targeting of intracellular antibodies in mammalian cells. EMBO J *9*, 101-108.

34) Bird, A. P., and Southern, E. M. (1978). Use of restriction enzymes to study eukaryotic DNA methylation: I. The methylation pattern in ribosomal DNA from Xenopus laevis. J Mol Biol *118*, 27-47.

35) Birnie, R., Bryce, S. D., Roome, C., Dussupt, V., Droop, A., Lang, S. H., Berry, P. A., Hyde, C. F., Lewis, J. L., Stower, M. J., *et al.* (2008). Gene expression profiling of human prostate cancer stem cells reveals a pro-inflammatory phenotype and the importance of extracellular matrix interactions. Genome Biol *9*, R83.

36) Biswas, S., and Rao, C. M. (2018). Epigenetic tools (The Writers, The Readers and The Erasers) and their implications in cancer therapy. Eur J Pharmacol *837*, 8-24.

37) Bockhorn, M., Jain, R. K., and Munn, L. L. (2007). Active versus passive mechanisms in metastasis: do cancer cells crawl into vessels, or are they pushed? Lancet Oncol *8*, 444-448.

38) Boeck, G. (2001). Current status of flow cytometry in cell and molecular biology. Int Rev Cytol *204*, 239-298.

39) Boesch, M., Wolf, D., and Sopper, S. (2016). Optimized Stem Cell Detection Using the DyeCycle-Triggered Side Population Phenotype. Stem Cells Int *2016*, 1652389.

40) Bonecchi, R., Galliera, E., Borroni, E. M., Corsi, M. M., Locati, M., and Mantovani, A. (2009). Chemokines and chemokine receptors: an overview. Front Biosci (Landmark Ed) *14*, 540-551.

41) Bonnet, D., and Dick, J. E. (1997). Human acute myeloid leukemia is organized as a hierarchy that originates from a primitive hematopoietic cell. Nat Med *3*, 730-737.

42) Borowicz, S., Van Scoyk, M., Avasarala, S., Karuppusamy Rathinam, M. K., Tauler, J., Bikkavilli, R. K., and Winn, R. A. (2014). The soft agar colony formation assay. J Vis Exp, e51998.

43) Cammarano, M. S., and Minden, A. (2001). Dbl and the Rho GTPases activate NF kappa B by I kappa B kinase (IKK)-dependent and IKK-independent pathways. J Biol Chem *276*, 25876-25882.

44) Cao, L., Zhou, Y., Zhai, B., Liao, J., Xu, W., Zhang, R., Li, J., Zhang, Y., Chen, L., Qian, H., *et al.* (2011). Sphere-forming cell subpopulations with

cancer stem cell properties in human hepatoma cell lines. BMC Gastroenterol *11*, 71.

45) Carr, K. M., Bittner, M., and Trent, J. M. (2003). Gene-expression profiling in human cutaneous melanoma. Oncogene *22*, 3076-3080.

46) Carr, S. A., Huddleston, M. J., and Annan, R. S. (1996). Selective detection and sequencing of phosphopeptides at the femtomole level by mass spectrometry. Anal Biochem *239*, 180-192.

47) Carugo, A., Genovese, G., Seth, S., Nezi, L., Rose, J. L., Bossi, D., Cicalese, A., Shah, P. K., Viale, A., Pettazzoni, P. F., *et al.* (2016). In Vivo Functional Platform Targeting Patient-Derived Xenografts Identifies WDR5-Myc Association as a Critical Determinant of Pancreatic Cancer. Cell Rep *16*, 133-147.

48) Cathcart, P., and Stebbing, J. (2016). Aloe vera, a natural cancer soother? Lancet Oncol *17*, 421.

49) Chaffanet, M., Gressin, L., Preudhomme, C., Soenen-Cornu, V., Birnbaum, D., and Pebusque, M. J. (2000). MOZ is fused to p300 in an acute monocytic leukemia with t(8;22). Genes Chromosomes Cancer *28*, 138-144.

50) Chaffer, C. L., Brueckmann, I., Scheel, C., Kaestli, A. J., Wiggins, P. A., Rodrigues, L. O., Brooks, M., Reinhardt, F., Su, Y., Polyak, K., *et al.* (2011). Normal and neoplastic nonstem cells can spontaneously convert to a stem-like state. Proc Natl Acad Sci U S A *108*, 7950-7955.

51) Chaffer, C. L., Marjanovic, N. D., Lee, T., Bell, G., Kleer, C. G., Reinhardt, F., D'Alessio, A. C., Young, R. A., and Weinberg, R. A. (2013). Poised chromatin at the ZEB1 promoter enables breast cancer cell plasticity and enhances tumorigenicity. Cell *154*, 61-74.

52) Chaffer, C. L., and Weinberg, R. A. (2011). A perspective on cancer cell metastasis. Science *331*, 1559-1564.

53) Chambers, I., and Tomlinson, S. R. (2009). The transcriptional foundation of pluripotency. Development *136*, 2311-2322.

54) Chang, J. C. (2016). Cancer stem cells: Role in tumor growth, recurrence, metastasis, and treatment resistance. Medicine (Baltimore) *95*, S20-S25.

55) Chen, C., Cao, F., Bai, L., Liu, Y., Xie, J., Wang, W., Si, Q., Yang, J., Chang, A., Liu, D., *et al.* (2015a). IKKbeta Enforces a LIN28B/TCF7L2 Positive

Feedback Loop That Promotes Cancer Cell Stemness and Metastasis. Cancer Res *75*, 1725-1735.

56) Chen, Q. W., Zhu, X. Y., Li, Y. Y., and Meng, Z. Q. (2013). Epigenetic regulation and cancer (review). Oncol Rep *31*, 523-532.

57) Chen, X., Xie, W., Gu, P., Cai, Q., Wang, B., Xie, Y., Dong, W., He, W., Zhong, G., Lin, T., and Huang, J. (2015b). Upregulated WDR5 promotes proliferation, self-renewal and chemoresistance in bladder cancer via mediating H3K4 trimethylation. Sci Rep *5*, 8293.

58) Cheng, C., and Dong, W. (2018). Aloe-Emodin Induces Endoplasmic Reticulum Stress-Dependent Apoptosis in Colorectal Cancer Cells. Med Sci Monit *24*, 6331-6339.

59) Cheng, N. C., Chen, S. Y., Li, J. R., and Young, T. H. (2013). Short-term spheroid formation enhances the regenerative capacity of adipose-derived stem cells by promoting stemness, angiogenesis, and chemotaxis. Stem Cells Transl Med *2*, 584-594.

60) Cheng, Y., He, C., Wang, M., Ma, X., Mo, F., Yang, S., Han, J., and Wei, X. (2019). Targeting epigenetic regulators for cancer therapy: mechanisms and advances in clinical trials. Signal Transduct Target Ther *4*, 62.

61) Chevallet, M., Luche, S., and Rabilloud, T. (2006). Silver staining of proteins in polyacrylamide gels. Nat Protoc *1*, 1852-1858.

62) Chiba, S. (2006). Notch signaling in stem cell systems. Stem Cells *24*, 2437-2447.

63) Choi, S. C., Choi, J. H., Park, C. Y., Ahn, C. M., Hong, S. J., and Lim, D. S. (2012). Nanog regulates molecules involved in stemness and cell cycle-signaling pathway for maintenance of pluripotency of P19 embryonal carcinoma stem cells. J Cell Physiol *227*, 3678-3692.

64) Choy, J. S., Wei, S., Lee, J. Y., Tan, S., Chu, S., and Lee, T. H. (2010). DNA methylation increases nucleosome compaction and rigidity. J Am Chem Soc *132*, 1782-1783.

65) Chun, J. N., Cho, M., Park, S., So, I., and Jeon, J. H. (2019). The conflicting role of E2F1 in prostate cancer: A matter of cell context or interpretational flexibility? Biochim Biophys Acta Rev Cancer *1873*, 188336.

66) Clark, D. W., and Palle, K. (2017). Aldehyde dehydrogenases in cancer stem cells: potential as therapeutic targets. Ann Transl Med *4*, 518.

67) Clark, E. A., Golub, T. R., Lander, E. S., and Hynes, R. O. (2000). Genomic analysis of metastasis reveals an essential role for RhoC. Nature *406*, 532-535.

68) Clarke, M. F., and Fuller, M. (2006). Stem cells and cancer: two faces of eve. Cell *124*, 1111-1115.

69) Clement, V., Sanchez, P., de Tribolet, N., Radovanovic, I., and Ruiz i Altaba, A. (2007). HEDGEHOG-GLI1 signaling regulates human glioma growth, cancer stem cell self-renewal, and tumorigenicity. Curr Biol *17*, 165-172.

70) Collisson, E. A., Carranza, D. C., Chen, I. Y., and Kolodney, M. S. (2002). Isoprenylation is necessary for the full invasive potential of RhoA overexpression in human melanoma cells. J Invest Dermatol *119*, 1172-1176.

71) Collisson, E. A., Kleer, C., Wu, M., De, A., Gambhir, S. S., Merajver, S. D., and Kolodney, M. S. (2003). Atorvastatin prevents RhoC isoprenylation, invasion, and metastasis in human melanoma cells. Mol Cancer Ther *2*, 941-948.

72) Cook, A. M., Li, L., Ho, Y., Lin, A., Stein, A., Forman, S., Perrotti, D., Jove, R., and Bhatia, R. (2014). Role of altered growth factor receptor-mediated JAK2 signaling in growth and maintenance of human acute myeloid leukemia stem cells. Blood *123*, 2826-2837.

73) Corgiat, B. A., Nordman, J. C., and Kabbani, N. (2014). Chemical crosslinkers enhance detection of receptor interactomes. Front Pharmacol *4*, 171.

74) Crowley, L. C., Scott, A. P., Marfell, B. J., Boughaba, J. A., Chojnowski, G., and Waterhouse, N. J. (2016). Measuring Cell Death by Propidium Iodide Uptake and Flow Cytometry. Cold Spring Harb Protoc *2016*.

75) Cruz, C., Della Rosa, M., Krueger, C., Gao, Q., Horkai, D., King, M., Field, L., and Houseley, J. (2018). Tri-methylation of histone H3 lysine 4 facilitates gene expression in ageing cells. Elife *7*.

76) Cusack, M., King, H. W., Spingardi, P., Kessler, B. M., Klose, R. J., and Kriaucionis, S. (2020). Distinct contributions of DNA methylation and histone acetylation to the genomic occupancy of transcription factors. Genome Res *30*, 1393-1406.

77) Dalerba, P., Dylla, S. J., Park, I. K., Liu, R., Wang, X., Cho, R. W., Hoey, T., Gurney, A., Huang, E. H., Simeone, D. M., *et al.* (2007). Phenotypic

characterization of human colorectal cancer stem cells. Proc Natl Acad Sci U S A *104*, 10158-10163.

78) Darzynkiewicz, Z. (2012). Critical aspects in analysis of cellular DNA content. Curr Protoc Cytom *Chapter 7*, Unit 7 2.

79) Darzynkiewicz, Z., Juan, G., Li, X., Gorczyca, W., Murakami, T., and Traganos, F. (1997). Cytometry in cell necrobiology: analysis of apoptosis and accidental cell death (necrosis). Cytometry *27*, 1-20.

80) Das, P. K., Pillai, S., Rakib, M. A., Khanam, J. A., Gopalan, V., Lam, A. K. Y., and Islam, F. (2020). Plasticity of Cancer Stem Cell: Origin and Role in Disease Progression and Therapy Resistance. Stem Cell Rev Rep *16*, 397-412.

81) Dawson, M. A., and Kouzarides, T. (2012). Cancer epigenetics: from mechanism to therapy. Cell *150*, 12-27.

82) Dean, M. (2009). ABC transporters, drug resistance, and cancer stem cells. J Mammary Gland Biol Neoplasia *14*, 3-9.

83) Deschenes-Simard, X., Kottakis, F., Meloche, S., and Ferbeyre, G. (2014). ERKs in cancer: friends or foes? Cancer Res *74*, 412-419.

84) Dhillon, A. S., Hagan, S., Rath, O., and Kolch, W. (2007). MAP kinase signalling pathways in cancer. Oncogene *26*, 3279-3290.

85) Dick, J. E., Bhatia, M., Gan, O., Kapp, U., and Wang, J. C. (1997). Assay of human stem cells by repopulation of NOD/SCID mice. Stem Cells *15 Suppl 1*, 199-203; discussion 204-197.

86) Domon, B., and Aebersold, R. (2006). Mass spectrometry and protein analysis. Science *312*, 212-217.

87) Doorbar, J. (2013). The E4 protein; structure, function and patterns of expression. Virology *445*, 80-98.

88) Dou, Y., Milne, T. A., Ruthenburg, A. J., Lee, S., Lee, J. W., Verdine, G. L., Allis, C. D., and Roeder, R. G. (2006). Regulation of MLL1 H3K4 methyltransferase activity by its core components. Nat Struct Mol Biol *13*, 713-719.

89) Duan, S., Yuan, G., Liu, X., Ren, R., Li, J., Zhang, W., Wu, J., Xu, X., Fu, L., Li, Y., *et al.* (2015). PTEN deficiency reprogrammes human neural stem cells towards a glioblastoma stem cell-like phenotype. Nat Commun *6*, 10068.

90) Ehrlich, M. (2009). DNA hypomethylation in cancer cells. Epigenomics *1*, 239-259.

91) El Helou, R., Wicinski, J., Guille, A., Adelaide, J., Finetti, P., Bertucci, F., Chaffanet, M., Birnbaum, D., Charafe-Jauffret, E., and Ginestier, C. (2014). Brief reports: A distinct DNA methylation signature defines breast cancer stem cells and predicts cancer outcome. Stem Cells *32*, 3031-3036.

92) Ellwart, J. W., and Dormer, P. (1990). Vitality measurement using spectrum shift in Hoechst 33342 stained cells. Cytometry *11*, 239-243.

93) Endo, A., Kuroda, M., and Tanzawa, K. (1976). Competitive inhibition of 3-hydroxy-3-methylglutaryl coenzyme A reductase by ML-236A and ML-236B fungal metabolites, having hypocholesterolemic activity. FEBS Lett *72*, 323-326.

94) Eun, K., Ham, S. W., and Kim, H. (2017). Cancer stem cell heterogeneity: origin and new perspectives on CSC targeting. BMB Rep *50*, 117-125.

95) Fang, Z., Lin, M., Li, C., Liu, H., and Gong, C. (2020). A comprehensive review of the roles of E2F1 in colon cancer. Am J Cancer Res *10*, 757-768.

96) Fares, J., Fares, M. Y., Khachfe, H. H., Salhab, H. A., and Fares, Y. (2020). Molecular principles of metastasis: a hallmark of cancer revisited. Signal Transduct Target Ther *5*, 28.

97) Faried, A., Faried, L. S., Kimura, H., Nakajima, M., Sohda, M., Miyazaki, T., Kato, H., Usman, N., and Kuwano, H. (2006). RhoA and RhoC proteins promote both cell proliferation and cell invasion of human oesophageal squamous cell carcinoma cell lines in vitro and in vivo. Eur J Cancer *42*, 1455-1465.

98) Feinberg, A. P., and Tycko, B. (2004). The history of cancer epigenetics. Nat Rev Cancer *4*, 143-153.

99) Feinberg, A. P., and Vogelstein, B. (1983). Hypomethylation distinguishes genes of some human cancers from their normal counterparts. Nature *301*, 89-92.

100) Fender, A. W., Nutter, J. M., Fitzgerald, T. L., Bertrand, F. E., and Sigounas, G. (2015). Notch-1 promotes stemness and epithelial to mesenchymal transition in colorectal cancer. J Cell Biochem *116*, 2517-2527.

101) Ferrer, A. I., Trinidad, J. R., Sandiford, O., Etchegaray, J. P., and Rameshwar, P. (2020). Epigenetic dynamics in cancer stem cell dormancy. Cancer Metastasis Rev *39*, 721-738.

102) Fidler, I. J. (1970). Metastasis: quantitative analysis of distribution and fate of tumor emboli labeled with 125 I-5-iodo-2'-deoxyuridine. J Natl Cancer Inst *45*, 773-782.

103) Folkman, J., and Moscona, A. (1978). Role of cell shape in growth control. Nature *273*, 345-349.

104) Follain, G., Osmani, N., Azevedo, A. S., Allio, G., Mercier, L., Karreman, M. A., Solecki, G., Garcia Leon, M. J., Lefebvre, O., Fekonja, N., *et al.* (2018). Hemodynamic Forces Tune the Arrest, Adhesion, and Extravasation of Circulating Tumor Cells. Dev Cell *45*, 33-52 e12.

105) Fong, H., Hohenstein, K. A., and Donovan, P. J. (2008). Regulation of self-renewal and pluripotency by Sox2 in human embryonic stem cells. Stem Cells *26*, 1931-1938.

106) Fouad, Y. A., and Aanei, C. (2017). Revisiting the hallmarks of cancer. Am J Cancer Res *7*, 1016-1036.

107) Fraga, M. F., Herranz, M., Espada, J., Ballestar, E., Paz, M. F., Ropero, S., Erkek, E., Bozdogan, O., Peinado, H., Niveleau, A., *et al.* (2004). A mouse skin multistage carcinogenesis model reflects the aberrant DNA methylation patterns of human tumors. Cancer Res *64*, 5527-5534.

108) Franken, N. A., Rodermond, H. M., Stap, J., Haveman, J., and van Bree, C. (2006). Clonogenic assay of cells in vitro. Nat Protoc *1*, 2315-2319.

109) Friedl, P., and Alexander, S. (2011). Cancer invasion and the microenvironment: plasticity and reciprocity. Cell *147*, 992-1009.

110) Frisch, S. M., and Francis, H. (1994). Disruption of epithelial cell-matrix interactions induces apoptosis. J Cell Biol *124*, 619-626.

111) Frisch, S. M., Schaller, M., and Cieply, B. (2013). Mechanisms that link the oncogenic epithelial-mesenchymal transition to suppression of anoikis. J Cell Sci *126*, 21-29.

112) Fukushige, S., and Horii, A. (2013). DNA methylation in cancer: a gene silencing mechanism and the clinical potential of its biomarkers. Tohoku J Exp Med *229*, 173-185.

113) Gade, P., and Kalvakolanu, D. V. (2011). Chromatin immunoprecipitation assay as a tool for analyzing transcription factor activity. Methods Mol Biol *809*, 85-104.

114) Garcia-Gomez, R., Bustelo, X. R., and Crespo, P. (2018). Protein-Protein Interactions: Emerging Oncotargets in the RAS-ERK Pathway. Trends Cancer *4*, 616-633.

115) Gaspar-Maia, A., Alajem, A., Meshorer, E., and Ramalho-Santos, M. (2010). Open chromatin in pluripotency and reprogramming. Nat Rev Mol Cell Biol *12*, 36-47.

116) Gay, L. J., and Felding-Habermann, B. (2011). Contribution of platelets to tumour metastasis. Nat Rev Cancer *11*, 123-134.

117) Gialeli, C., Theocharis, A. D., and Karamanos, N. K. (2010). Roles of matrix metalloproteinases in cancer progression and their pharmacological targeting. FEBS J *278*, 16-27.

118) Gilbert, B., and Alves, L. F. (2003). Synergy in plant medicines. Curr Med Chem *10*, 13-20.

119) Giridharan, S., and Srinivasan, M. (2018). Mechanisms of NF-kappaB p65 and strategies for therapeutic manipulation. J Inflamm Res *11*, 407-419.

120) Giudice, F. S., Pinto, D. S., Jr., Nor, J. E., Squarize, C. H., and Castilho, R. M. (2013). Inhibition of histone deacetylase impacts cancer stem cells and induces epithelial-mesenchyme transition of head and neck cancer. PLoS One *8*, e58672.

121) Gonzalez-Gonzalez, L., and Alonso, J. (2018). Periostin: A Matricellular Protein With Multiple Functions in Cancer Development and Progression. Front Oncol *8*, 225.

122) Goodell, M. A., Brose, K., Paradis, G., Conner, A. S., and Mulligan, R. C. (1996). Isolation and functional properties of murine hematopoietic stem cells that are replicating in vivo. J Exp Med *183*, 1797-1806.

123) Goodell, M. A., Rosenzweig, M., Kim, H., Marks, D. F., DeMaria, M., Paradis, G., Grupp, S. A., Sieff, C. A., Mulligan, R. C., and Johnson, R. P. (1997). Dye efflux studies suggest that hematopoietic stem cells expressing low or undetectable levels of CD34 antigen exist in multiple species. Nat Med *3*, 1337-1345.

124) Gou, W. F., Zhao, Y., Lu, H., Yang, X. F., Xiu, Y. L., Zhao, S., Liu, J. M., Zhu, Z. T., Sun, H. Z., Liu, Y. P., *et al.* (2014). The role of RhoC in epithelial-to-mesenchymal transition of ovarian carcinoma cells. BMC Cancer *14*, 477.

125) Goyal, R., Reinhardt, R., and Jeltsch, A. (2006). Accuracy of DNA methylation pattern preservation by the Dnmt1 methyltransferase. Nucleic Acids Res *34*, 1182-1188.

126) Greaves, M., and Maley, C. C. (2012). Clonal evolution in cancer. Nature *481*, 306-313.

127) Greenberg, M. V. C., and Bourc'his, D. (2019). The diverse roles of DNA methylation in mammalian development and disease. Nat Rev Mol Cell Biol *20*, 590-607.

128) Grosso, S., Doyen, J., Parks, S.K., Bertero, T., Paye, A., Cardinaud, B., Gounon, P., Lacas-Gervais, S., Noël, A., Pouysségur, J., Barbry, P., Mazure, N.M., Mari, B. (2013). MiR-210 promotes a hypoxic phenotype and increases radioresistance in human lung cancer cell lines. Cell Death Dis. *4(3)*, 14.

129) Grundmann, E. (1985). [The concept of Julius Cohnheim on tumor formation and metastasis from the viewpoint of new research results]. Zentralbl Allg Pathol *130*, 323-331.

130) Gu, G., Yuan, J., Wills, M., and Kasper, S. (2007). Prostate cancer cells with stem cell characteristics reconstitute the original human tumor in vivo. Cancer Res *67*, 4807-4815.

131) Guan, X. (2015). Cancer metastases: challenges and opportunities. Acta Pharm Sin B *5*, 402-418.

132) Guo, H., Hu, B., Yan, L., Yong, J., Wu, Y., Gao, Y., Guo, F., Hou, Y., Fan, X., Dong, J., *et al.* (2016). DNA methylation and chromatin accessibility profiling of mouse and human fetal germ cells. Cell Res *27*, 165-183.

133) Guo, Y. J., Pan, W. W., Liu, S. B., Shen, Z. F., Xu, Y., and Hu, L. L. (2020). ERK/MAPK signalling pathway and tumorigenesis. Exp Ther Med *19*, 1997-2007.

134) Gyorffy, B., Bottai, G., Fleischer, T., Munkacsy, G., Budczies, J., Paladini, L., Borresen-Dale, A. L., Kristensen, V. N., and Santarpia, L. (2015). Aberrant DNA methylation impacts gene expression and prognosis in breast cancer subtypes. Int J Cancer *138*, 87-97.

135) Hall, A. (1992). Ras-related GTPases and the cytoskeleton. Mol Biol Cell *3*, 475-479.

136) Hall, A. (1998). Rho GTPases and the actin cytoskeleton. Science *279*, 509-514.

137) Hall, A. (2005). Rho GTPases and the control of cell behaviour. Biochem Soc Trans *33*, 891-895.

138) Hall, A., Paterson, H. F., Adamson, P., and Ridley, A. J. (1993). Cellular responses regulated by rho-related small GTP-binding proteins. Philos Trans R Soc Lond B Biol Sci *340*, 267-271.

139) Hamilton, W. B., and Brickman, J. M. (2014). Erk signaling suppresses embryonic stem cell self-renewal to specify endoderm. Cell Rep *9*, 2056-2070.

140) Harini, L., Srivastava, S., Gnanakumar, G. P., Karthikeyan, B., Ross, C., Krishnakumar, V., Kannan, V. R., Sundar, K., and Kathiresan, T. (2019). An ingenious non-spherical mesoporous silica nanoparticle cargo with curcumin induces mitochondria-mediated apoptosis in breast cancer (MCF-7) cells. Oncotarget *10*, 1193-1208.

141) Hashimoto, K., Kokubun, S., Itoi, E., and Roach, H. I. (2007). Improved quantification of DNA methylation using methylation-sensitive restriction enzymes and real-time PCR. Epigenetics *2*, 86-91.

142) Hayden, M. S., and Ghosh, S. (2008). Shared principles in NF-kappaB signaling. Cell *132*, 344-362.

143) He, X., Qian, Y., Cai, H., Yang, S., Cai, J., and Wang, Z. (2015). RhoC is essential in TGF-beta1 induced epithelial-mesenchymal transition in cervical cancer cells. Oncol Lett *10*, 985-989.

144) Heberle, E., and Bardet, A. F. (2019). Sensitivity of transcription factors to DNA methylation. Essays Biochem *63*, 727-741.

145) Hemmings, B. A., and Restuccia, D. F. (2012). PI3K-PKB/Akt pathway. Cold Spring Harb Perspect Biol *4*, a011189.

146) Herrmann, C., Avgousti, D. C., and Weitzman, M. D. (2017). Differential Salt Fractionation of Nuclei to Analyze Chromatin-associated Proteins from Cultured Mammalian Cells. Bio Protoc *7*.

147) Hirschmann-Jax, C., Foster, A. E., Wulf, G. G., Nuchtern, J. G., Jax, T. W., Gobel, U., Goodell, M. A., and Brenner, M. K. (2004). A distinct "side

population" of cells with high drug efflux capacity in human tumor cells. Proc Natl Acad Sci U S A *101*, 14228-14233.

148) Hjelmeland, A. B., and Rich, J. N. (2011). Molecular targeting of neural cancer stem cells: TTAGGG, you're it! Clin Cancer Res *17*, 3-5.

149) Hoeppner, L. H., Sinha, S., Wang, Y., Bhattacharya, R., Dutta, S., Gong, X., Bedell, V. M., Suresh, S., Chun, C., Ramchandran, R., *et al.* (2015). RhoC maintains vascular homeostasis by regulating VEGF-induced signaling in endothelial cells. J Cell Sci *128*, 3556-3568.

150) Hoffmann, M. J., and Schulz, W. A. (2005). Causes and consequences of DNA hypomethylation in human cancer. Biochem Cell Biol *83*, 296-321.

151) Holland, J. D., Klaus, A., Garratt, A. N., and Birchmeier, W. (2013). Wnt signaling in stem and cancer stem cells. Curr Opin Cell Biol *25*, 254-264.

152) Hollern, D. P., Swiatnicki, M. R., Rennhack, J. P., Misek, S. A., Matson, B. C., McAuliff, A., Gallo, K. A., Caron, K. M., and Andrechek, E. R. (2019). E2F1 Drives Breast Cancer Metastasis by Regulating the Target Gene FGF13 and Altering Cell Migration. Sci Rep *9*, 10718.

153) Howe, F. S., Fischl, H., Murray, S. C., and Mellor, J. (2016). Is H3K4me3 instructive for transcription activation? Bioessays *39*, 1-12.

154) Hu, C., Li, H., Li, J., Zhu, Z., Yin, S., Hao, X., Yao, M., Zheng, S., and Gu, J. (2008). Analysis of ABCG2 expression and side population identifies intrinsic drug efflux in the HCC cell line MHCC-97L and its modulation by Akt signaling. Carcinogenesis *29*, 2289-2297.

155) Hu, S. (2017). Co-targeting cancer stem-like cells and bulk cancer cells with a bispecific antibody. Mol Cell Oncol *4*, e1308851.

156) Hussain, A., Sharma, C., Khan, S., Shah, K., and Haque, S. (2015). Aloe vera inhibits proliferation of human breast and cervical cancer cells and acts synergistically with cisplatin. Asian Pac J Cancer Prev *16*, 2939-2946.

157) Iiizumi, M., Bandyopadhyay, S., Pai, S. K., Watabe, M., Hirota, S., Hosobe, S., Tsukada, T., Miura, K., Saito, K., Furuta, E., *et al.* (2008). RhoC promotes metastasis via activation of the Pyk2 pathway in prostate cancer. Cancer Res *68*, 7613-7620.

158) Ikoma, T., Takahashi, T., Nagano, S., Li, Y. M., Ohno, Y., Ando, K., Fujiwara, T., Fujiwara, H., and Kosai, K. (2004). A definitive role of RhoC

in metastasis of orthotopic lung cancer in mice. Clin Cancer Res *10*, 1192-1200.

159) Iliakis, G. (2009). Backup pathways of NHEJ in cells of higher eukaryotes: cell cycle dependence. Radiother Oncol *92*, 310-315.

160) Imamura, A., Kajiya, H., Fujisaki, S., Maeshiba, M., Yanagi, T., Kojima, H., and Ohno, J. (2020). Three-dimensional spheroids of mesenchymal stem/stromal cells promote osteogenesis by activating stemness and Wnt/beta-catenin. Biochem Biophys Res Commun *523*, 458-464.

161) Islam, M., Sharma, S., Kumar, B., and Teknos, T. N. (2013). Atorvastatin inhibits RhoC function and limits head and neck cancer metastasis. Oral Oncol *49*, 778-786.

162) Islam, M., Sharma, S., and Teknos, T. N. (2014). RhoC regulates cancer stem cells in head and neck squamous cell carcinoma by overexpressing IL-6 and phosphorylation of STAT3. PLoS One *9*, e88527.

163) Issa, J. P. (2000). The epigenetics of colorectal cancer. Ann N Y Acad Sci *910*, 140-153; discussion 153-145.

164) Ivashkevich, A., Redon, C. E., Nakamura, A. J., Martin, R. F., and Martin, O. A. (2012). Use of the gamma-H2AX assay to monitor DNA damage and repair in translational cancer research. Cancer Lett *327*, 123-133.

165) Iyoda, T., and Fukai, F. (2011). Modulation of Tumor Cell Survival, Proliferation, and Differentiation by the Peptide Derived from Tenascin-C: Implication of beta1-Integrin Activation. Int J Cell Biol *2012*, 647594.

166) Jacob, M. C., Favre, M., and Bensa, J. C. (1991). Membrane cell permeabilization with saponin and multiparametric analysis by flow cytometry. Cytometry *12*, 550-558.

167) Jang, G. B., Kim, J. Y., Cho, S. D., Park, K. S., Jung, J. Y., Lee, H. Y., Hong, I. S., and Nam, J. S. (2015). Blockade of Wnt/beta-catenin signaling suppresses breast cancer metastasis by inhibiting CSC-like phenotype. Sci Rep *5*, 12465.

168) Jayant, K., Sankaranarayanan, R., Thorat, R. V., Muwonge, R., Hingmire, S. J., Panse, N. S., Shastri, S. S., Malvi, S. G., and Nene, B. (2016). Improved Survival of Cervical Cancer Patients in a Screened Population in Rural India. Asian Pac J Cancer Prev *17*, 4837-4844.

169) Jeggo, P. A., Geuting, V., and Lobrich, M. (2011). The role of homologous recombination in radiation-induced double-strand break repair. Radiother Oncol *101*, 7-12.

170) Jin, B., Li, Y., and Robertson, K. D. (2011). DNA methylation: superior or subordinate in the epigenetic hierarchy? Genes Cancer *2*, 607-617.

171) Jolly, M. K., Jia, D., Boareto, M., Mani, S. A., Pienta, K. J., Ben-Jacob, E., and Levine, H. (2015). Coupling the modules of EMT and stemness: A tunable 'stemness window' model. Oncotarget *6*, 25161-25174.

172) Jolly, M. K., Mani, S. A., and Levine, H. (2018). Hybrid epithelial/mesenchymal phenotype(s): The 'fittest' for metastasis? Biochim Biophys Acta Rev Cancer *1870*, 151-157.

173) Jones, P. L., and Wolffe, A. P. (1999). Relationships between chromatin organization and DNA methylation in determining gene expression. Semin Cancer Biol *9*, 339-347.

174) Josefson, D. (1999). Adding chemotherapy improves survival in cervical cancer. BMJ *318*, 623.

175) Kaboord, B., and Perr, M. (2008). Isolation of proteins and protein complexes by immunoprecipitation. Methods Mol Biol *424*, 349-364.

176) Kahn, M. (2014). Can we safely target the WNT pathway? Nat Rev Drug Discov *13*, 513-532.

177) Kamai, T., Tsujii, T., Arai, K., Takagi, K., Asami, H., Ito, Y., and Oshima, H. (2003). Significant association of Rho/ROCK pathway with invasion and metastasis of bladder cancer. Clin Cancer Res *9*, 2632-2641.

178) Kamdar, S., Isserlin, R., Van der Kwast, T., Zlotta, A. R., Bader, G. D., Fleshner, N. E., and Bapat, B. (2019). Exploring targets of TET2-mediated methylation reprogramming as potential discriminators of prostate cancer progression. Clin Epigenetics *11*, 54.

179) Karamboulas, C., and Ailles, L. (2013). Developmental signaling pathways in cancer stem cells of solid tumors. Biochim Biophys Acta *1830*, 2481-2495.

180) Karin, M. (2009). NF-kappaB as a critical link between inflammation and cancer. Cold Spring Harb Perspect Biol *1*, a000141.

181) Karlic, R., Chung, H. R., Lasserre, J., Vlahovicek, K., and Vingron, M. (2010). Histone modification levels are predictive for gene expression. Proc Natl Acad Sci U S A *107*, 2926-2931.

182) Kass, S. U., Pruss, D., and Wolffe, A. P. (1997). How does DNA methylation repress transcription? Trends Genet *13*, 444-449.

183) Kelly, P. N., Dakic, A., Adams, J. M., Nutt, S. L., and Strasser, A. (2007). Tumor growth need not be driven by rare cancer stem cells. Science *317*, 337.

184) Kim, H. S., Kacew, S., and Lee, B. M. (1999). In vitro chemopreventive effects of plant polysaccharides (Aloe barbadensis miller, Lentinus edodes, Ganoderma lucidum and Coriolus versicolor). Carcinogenesis *20*, 1637-1640.

185) Kim, J. H., Xu, C., Keum, Y. S., Reddy, B., Conney, A., and Kong, A. N. (2006). Inhibition of EGFR signaling in human prostate cancer PC-3 cells by combination treatment with beta-phenylethyl isothiocyanate and curcumin. Carcinogenesis *27*, 475-482.

186) Kim, J. Y., Banerjee, T., Vinckevicius, A., Luo, Q., Parker, J. B., Baker, M. R., Radhakrishnan, I., Wei, J. J., Barish, G. D., and Chakravarti, D. (2014). A role for WDR5 in integrating threonine 11 phosphorylation to lysine 4 methylation on histone H3 during androgen signaling and in prostate cancer. Mol Cell *54*, 613-625.

187) Kim, J. Y., Nelson, A. L., Algon, S. A., Graves, O., Sturla, L. M., Goumnerova, L. C., Rowitch, D. H., Segal, R. A., and Pomeroy, S. L. (2003). Medulloblastoma tumorigenesis diverges from cerebellar granule cell differentiation in patched heterozygous mice. Dev Biol *263*, 50-66.

188) Kimura, K., Ito, M., Amano, M., Chihara, K., Fukata, Y., Nakafuku, M., Yamamori, B., Feng, J., Nakano, T., Okawa, K., *et al.* (1996). Regulation of myosin phosphatase by Rho and Rho-associated kinase (Rho-kinase). Science *273*, 245-248.

189) Kocik, J., Balan, B. J., Zdanowski, R., Jung, L., Skopinska-Rozewska, E., and Skopinski, P. (2014). Feeding mice with Aloe vera gel diminishes L-1 sarcoma-induced early neovascular response and tumor growth. Cent Eur J Immunol *39*, 14-18.

190) Kohno, M., and Pouyssegur, J. (2006). Targeting the ERK signaling pathway in cancer therapy. Ann Med *38*, 200-211.

191) Korotayev, K., Chaussepied, M., and Ginsberg, D. (2008). ERK activation is regulated by E2F1 and is essential for E2F1-induced S phase entry. Cell Signal *20*, 1221-1226.

192) Kyutoku, M., Taniyama, Y., Katsuragi, N., Shimizu, H., Kunugiza, Y., Iekushi, K., Koibuchi, N., Sanada, F., Oshita, Y., and Morishita, R. (2011). Role of periostin in cancer progression and metastasis: inhibition of breast cancer progression and metastasis by anti-periostin antibody in a murine model. Int J Mol Med *28*, 181-186.

193) Lagana, A., Dorn, J. F., De Rop, V., Ladouceur, A. M., Maddox, A. S., and Maddox, P. S. (2010). A small GTPase molecular switch regulates epigenetic centromere maintenance by stabilizing newly incorporated CENP-A. Nat Cell Biol *12*, 1186-1193.

194) Lahtz, C., and Pfeifer, G. P. (2011). Epigenetic changes of DNA repair genes in cancer. J Mol Cell Biol *3*, 51-58.

195) Lamarche, B. J., Orazio, N. I., and Weitzman, M. D. (2010). The MRN complex in double-strand break repair and telomere maintenance. FEBS Lett *584*, 3682-3695.

196) Lamarche, N., and Hall, A. (1994). GAPs for rho-related GTPases. Trends Genet *10*, 436-440.

197) Lambert, A. W., Wong, C. K., Ozturk, S., Papageorgis, P., Raghunathan, R., Alekseyev, Y., Gower, A. C., Reinhard, B. M., Abdolmaleky, H. M., and Thiagalingam, S. (2015). Tumor Cell-Derived Periostin Regulates Cytokines That Maintain Breast Cancer Stem Cells. Mol Cancer Res *14*, 103-113.

198) Lamson, D. W., and Brignall, M. S. (2000). Antioxidants and cancer, part 3: quercetin. Altern Med Rev *5*, 196-208.

199) Lang, S., Busch, H., Boerries, M., Brummer, T., Timme, S., Lassmann, S., Aktories, K., and Schmidt, G. (2017). Specific role of RhoC in tumor invasion and metastasis. Oncotarget *8*, 87364-87378.

200) Langley, R. R., and Fidler, I. J. (2011). The seed and soil hypothesis revisited--the role of tumor-stroma interactions in metastasis to different organs. Int J Cancer *128*, 2527-2535.

201) Lapidot, T., Sirard, C., Vormoor, J., Murdoch, B., Hoang, T., Caceres-Cortes, J., Minden, M., Paterson, B., Caligiuri, M. A., and Dick, J. E. (1994). A cell initiating human acute myeloid leukaemia after transplantation into SCID mice. Nature *367*, 645-648.

202) Lechman, E. R., Gentner, B., Ng, S. W. K., Schoof, E. M., van Galen, P., Kennedy, J. A., Nucera, S., Ciceri, F., Kaufmann, K. B., Takayama, N., *et al.*

(2016). miR-126 Regulates Distinct Self-Renewal Outcomes in Normal and Malignant Hematopoietic Stem Cells. Cancer Cell *29*, 602-606.

203) Lee, S. H., Do, S. I., Lee, H. J., Kang, H. J., Koo, B. S., and Lim, Y. C. (2016). Notch1 signaling contributes to stemness in head and neck squamous cell carcinoma. Lab Invest *96*, 508-516.

204) Leontovich, A. A., Jalalirad, M., Salisbury, J. L., Mills, L., Haddox, C., Schroeder, M., Tuma, A., Guicciardi, M. E., Zammataro, L., Gambino, M. W., *et al.* (2018). NOTCH3 expression is linked to breast cancer seeding and distant metastasis. Breast Cancer Res *20*, 105.

205) Lequeux, A., Noman, M. Z., Xiao, M., Sauvage, D., Van Moer, K., Viry, E., Bocci, I., Hasmim, M., Bosseler, M., Berchem, G., and Janji, B. (2019). Impact of hypoxic tumor microenvironment and tumor cell plasticity on the expression of immune checkpoints. Cancer Lett *458*, 13-20.

206) Li, B., Carey, M., and Workman, J. L. (2007). The role of chromatin during transcription. Cell *128*, 707-719.

207) Li, C. L., Yang, D., Cao, X., Wang, F., Hong, D. Y., Wang, J., Shen, X. C., and Chen, Y. (2017). Fibronectin induces epithelial-mesenchymal transition in human breast cancer MCF-7 cells via activation of calpain. Oncol Lett *13*, 3889-3895.

208) Li, Q., Wen, J., Yu, K., Shu, Y., He, W., Chu, H., Zhang, B., and Ge, C. (2018). Aloe-emodin induces apoptosis in human oral squamous cell carcinoma SCC15 cells. BMC Complement Altern Med *18*, 296.

209) Liang, Y. X., Lu, J. M., Mo, R. J., He, H. C., Xie, J., Jiang, F. N., Lin, Z. Y., Chen, Y. R., Wu, Y. D., Luo, H. W., *et al.* (2016). E2F1 promotes tumor cell invasion and migration through regulating CD147 in prostate cancer. Int J Oncol *48*, 1650-1658.

210) Liao, J., Qian, F., Tchabo, N., Mhawech-Fauceglia, P., Beck, A., Qian, Z., Wang, X., Huss, W. J., Lele, S. B., Morrison, C. D., and Odunsi, K. (2014). Ovarian cancer spheroid cells with stem cell-like properties contribute to tumor generation, metastasis and chemotherapy resistance through hypoxia-resistant metabolism. PLoS One *9*, e84941.

211) Linder, D., and Gartler, S. M. (1965). Glucose-6-phosphate dehydrogenase mosaicism: utilization as a cell marker in the study of leiomyomas. Science *150*, 67-69.

212) Lister, R., Pelizzola, M., Dowen, R. H., Hawkins, R. D., Hon, G., Tonti-Filippini, J., Nery, J. R., Lee, L., Ye, Z., Ngo, Q. M., *et al.* (2009). Human DNA methylomes at base resolution show widespread epigenomic differences. Nature *462*, 315-322.

213) Liu, M., Sakamaki, T., Casimiro, M. C., Willmarth, N. E., Quong, A. A., Ju, X., Ojeifo, J., Jiao, X., Yeow, W. S., Katiyar, S., *et al.* (2010). The canonical NF-kappaB pathway governs mammary tumorigenesis in transgenic mice and tumor stem cell expansion. Cancer Res *70*, 10464-10473.

214) Liu, N., Zhang, G., Bi, F., Pan, Y., Xue, Y., Shi, Y., Yao, L., Zhao, L., Zheng, Y., and Fan, D. (2007). RhoC is essential for the metastasis of gastric cancer. J Mol Med (Berl) *85*, 1149-1156.

215) Liu, S., Cheng, K., Zhang, H., Kong, R., Wang, S., and Mao, C. (2020). Methylation Status of the Nanog Promoter Determines the Switch between Cancer Cells and Cancer Stem Cells. Adv Sci (Weinh) *7*, 1903035.

216) Locke, W. J., Guanzon, D., Ma, C., Liew, Y. J., Duesing, K. R., Fung, K. Y. C., and Ross, J. P. (2019). DNA Methylation Cancer Biomarkers: Translation to the Clinic. Front Genet *10*, 1150.

217) Lopez, J., Poitevin, A., Mendoza-Martinez, V., Perez-Plasencia, C., and Garcia-Carranca, A. (2012). Cancer-initiating cells derived from established cervical cell lines exhibit stem-cell markers and increased radioresistance. BMC Cancer *12*, 48.

218) Lowndes, N. F., and Toh, G. W. (2005). DNA repair: the importance of phosphorylating histone H2AX. Curr Biol *15*, R99-R102.

219) Lowy, D. R., and Schiller, J. T. (2006). Prophylactic human papillomavirus vaccines. J Clin Invest *116*, 1167-1173.

220) Lu, X., Guo, H., Chen, X., Xiao, J., Zou, Y., Wang, W., and Chen, Q. (2016). Effect of RhoC on the epithelial-mesenchymal transition process induced by TGF-beta1 in lung adenocarcinoma cells. Oncol Rep *36*, 3105-3112.

221) Ma, X., Gao, Y., Fan, Y., Ni, D., Zhang, Y., Chen, W., Zhang, P., Song, E., Huang, Q., Ai, Q., *et al.* (2013). Overexpression of E2F1 promotes tumor malignancy and correlates with TNM stages in clear cell renal cell carcinoma. PLoS One *8*, e73436.

222) Maddala, R., Deng, P. F., Costello, J. M., Wawrousek, E. F., Zigler, J. S., and Rao, V. P. (2004). Impaired cytoskeletal organization and membrane

integrity in lens fibers of a Rho GTPase functional knockout transgenic mouse. Lab Invest *84*, 679-692.

223) Maehle, A. H. (2011). Ambiguous cells: the emergence of the stem cell concept in the nineteenth and twentieth centuries. Notes Rec R Soc Lond *65*, 359-378.

224) Mah, L. J., El-Osta, A., and Karagiannis, T. C. (2010). gammaH2AX: a sensitive molecular marker of DNA damage and repair. Leukemia *24*, 679-686.

225) Mahaffy, R. E., and Pollard, T. D. (2008). Influence of phalloidin on the formation of actin filament branches by Arp2/3 complex. Biochemistry *47*, 6460-6467.

226) Malanchi, I., Peinado, H., Kassen, D., Hussenet, T., Metzger, D., Chambon, P., Huber, M., Hohl, D., Cano, A., Birchmeier, W., and Huelsken, J. (2008). Cutaneous cancer stem cell maintenance is dependent on beta-catenin signalling. Nature *452*, 650-653.

227) Mamun, M. A., Mannoor, K., Cao, J., Qadri, F., and Song, X. (2018). SOX2 in cancer stemness: tumor malignancy and therapeutic potentials. J Mol Cell Biol *12*, 85-98.

228) Mani, S. A., Guo, W., Liao, M. J., Eaton, E. N., Ayyanan, A., Zhou, A. Y., Brooks, M., Reinhard, F., Zhang, C. C., Shipitsin, M., *et al.* (2008). The epithelial-mesenchymal transition generates cells with properties of stem cells. Cell *133*, 704-715.

229) Martello, G., Bertone, P., and Smith, A. (2013). Identification of the missing pluripotency mediator downstream of leukaemia inhibitory factor. EMBO J *32*, 2561-2574.

230) Mascetti, G., Carrara, S., and Vergani, L. (2001). Relationship between chromatin compactness and dye uptake for in situ chromatin stained with DAPI. Cytometry *44*, 113-119.

231) Matsui, W. H. (2016). Cancer stem cell signaling pathways. Medicine (Baltimore) *95*, S8-S19.

232) Mauch, P., Constine, L., Greenberger, J., Knospe, W., Sullivan, J., Liesveld, J. L., and Deeg, H. J. (1995). Hematopoietic stem cell compartment: acute and late effects of radiation therapy and chemotherapy. Int J Radiat Oncol Biol Phys *31*, 1319-1339.

233) McCubrey, J. A., Steelman, L. S., Chappell, W. H., Abrams, S. L., Wong, E. W., Chang, F., Lehmann, B., Terrian, D. M., Milella, M., Tafuri, A., *et al.* (2007). Roles of the Raf/MEK/ERK pathway in cell growth, malignant transformation and drug resistance. Biochim Biophys Acta *1773*, 1263-1284.

234) McKinnon, K. M. (2018). Flow Cytometry: An Overview. Curr Protoc Immunol *120*, 5 1 1-5 1 11.

235) Meng, P., and Ghosh, R. (2014). Transcription addiction: can we garner the Yin and Yang functions of E2F1 for cancer therapy? Cell Death Dis *5*, e1360.

236) Metsalu, T., and Vilo, J. (2015). ClustVis: a web tool for visualizing clustering of multivariate data using Principal Component Analysis and heatmap. Nucleic Acids Res *43*, W566-570.

237) Miller, S. A., Dykes, D. D., and Polesky, H. F. (1988). A simple salting out procedure for extracting DNA from human nucleated cells. Nucleic Acids Res *16*, 1215.

238) Moon, S. Y., and Zheng, Y. (2003). Rho GTPase-activating proteins in cell regulation. Trends Cell Biol *13*, 13-22.

239) Moran-Crusio, K., Reavie, L., Shih, A., Abdel-Wahab, O., Ndiaye-Lobry, D., Lobry, C., Figueroa, M. E., Vasanthakumar, A., Patel, J., Zhao, X., *et al.* (2011). Tet2 loss leads to increased hematopoietic stem cell self-renewal and myeloid transformation. Cancer Cell *20*, 11-24.

240) Morris, M., Eifel, P. J., Lu, J., Grigsby, P. W., Levenback, C., Stevens, R. E., Rotman, M., Gershenson, D. M., and Mutch, D. G. (1999). Pelvic radiation with concurrent chemotherapy compared with pelvic and para-aortic radiation for high-risk cervical cancer. N Engl J Med *340*, 1137-1143.

241) Mullis, K., Faloona, F., Scharf, S., Saiki, R., Horn, G., and Erlich, H. (1986). Specific enzymatic amplification of DNA in vitro: the polymerase chain reaction. Cold Spring Harb Symp Quant Biol *51 Pt 1*, 263-273.

242) Munoz, P., Iliou, M. S., and Esteller, M. (2012). Epigenetic alterations involved in cancer stem cell reprogramming. Mol Oncol *6*, 620-636.

243) Muraoka, M., Konishi, M., Kikuchi-Yanoshita, R., Tanaka, K., Shitara, N., Chong, J. M., Iwama, T., and Miyaki, M. (1996). p300 gene alterations in colorectal and gastric carcinomas. Oncogene *12*, 1565-1569.

244) Nakazawa, Y., Taniyama, Y., Sanada, F., Morishita, R., Nakamori, S., Morimoto, K., Yeung, K. T., and Yang, J. (2018). Periostin blockade

overcomes chemoresistance via restricting the expansion of mesenchymal tumor subpopulations in breast cancer. Sci Rep *8*, 4013.

245) Neilsen, B. K., Chakraborty, B., McCall, J. L., Frodyma, D. E., Sleightholm, R. L., Fisher, K. W., and Lewis, R. E. (2018). WDR5 supports colon cancer cells by promoting methylation of H3K4 and suppressing DNA damage. BMC Cancer *18*, 673.

246) Nelson, M., Raschke, E., and McClelland, M. (1993). Effect of site-specific methylation on restriction endonucleases and DNA modification methyltransferases. Nucleic Acids Res *21*, 3139-3154.

247) Nes, W. D. (2011). Biosynthesis of cholesterol and other sterols. Chem Rev *111*, 6423-6451.

248) Newell-Price, J., Clark, A. J., and King, P. (2000). DNA methylation and silencing of gene expression. Trends Endocrinol Metab *11*, 142-148.

249) Nieto, M. A., Huang, R. Y., Jackson, R. A., and Thiery, J. P. (2016). Emt: 2016. Cell *166*, 21-45.

250) Nobili, S., Lippi, D., Witort, E., Donnini, M., Bausi, L., Mini, E., and Capaccioli, S. (2009). Natural compounds for cancer treatment and prevention. Pharmacol Res *59*, 365-378.

251) Nout, R. A., Putter, H., Jurgenliemk-Schulz, I. M., Jobsen, J. J., Lutgens, L. C., van der Steen-Banasik, E. M., Mens, J. W., Slot, A., Stenfert Kroese, M. C., Nijman, H. W., *et al.* (2011). Five-year quality of life of endometrial cancer patients treated in the randomised Post Operative Radiation Therapy in Endometrial Cancer (PORTEC-2) trial and comparison with norm data. Eur J Cancer *48*, 1638-1648.

252) Nowell, P. C. (1976). The clonal evolution of tumor cell populations. Science *194*, 23-28.

253) O'Brien, C. A., Kreso, A., and Jamieson, C. H. (2010). Cancer stem cells and self-renewal. Clin Cancer Res *16*, 3113-3120.

254) O'Farrell, P. H. (1975). High resolution two-dimensional electrophoresis of proteins. J Biol Chem *250*, 4007-4021.

255) Odho, Z., Southall, S. M., and Wilson, J. R. (2010). Characterization of a novel WDR5-binding site that recruits RbBP5 through a conserved motif to enhance methylation of histone H3 lysine 4 by mixed lineage leukemia protein-1. J Biol Chem *285*, 32967-32976.

256) Ogawa, K., Yoshioka, Y., Isohashi, F., Seo, Y., Yoshida, K., and Yamazaki, H. (2013). Radiotherapy targeting cancer stem cells: current views and future perspectives. Anticancer Res *33*, 747-754.

257) Okano, M., Bell, D. W., Haber, D. A., and Li, E. (1999). DNA methyltransferases Dnmt3a and Dnmt3b are essential for de novo methylation and mammalian development. Cell *99*, 247-257.

258) Olofsson, B. (1999). Rho guanine dissociation inhibitors: pivotal molecules in cellular signalling. Cell Signal *11*, 545-554.

259) Organista-Nava, J., Gomez-Gomez, Y., Ocadiz-Delgado, R., Garcia-Villa, E., Bonilla-Delgado, J., Lagunas-Martinez, A., Tapia, J. S., Lambert, P. F., Garcia-Carranca, A., and Gariglio, P. (2016). The HPV16 E7 oncoprotein increases the expression of Oct3/4 and stemness-related genes and augments cell self-renewal. Virology *499*, 230-242.

260) Ouwens, D. M., de Ruiter, N. D., van der Zon, G. C., Carter, A. P., Schouten, J., van der Burgt, C., Kooistra, K., Bos, J. L., Maassen, J. A., and van Dam, H. (2002). Growth factors can activate ATF2 via a two-step mechanism: phosphorylation of Thr71 through the Ras-MEK-ERK pathway and of Thr69 through RalGDS-Src-p38. EMBO J *21*, 3782-3793.

261) Paget, S. (1889). The distribution of secondary growths in cancer of the breast. 1889. Cancer Metastasis Rev *8*, 98-101.

262) Pal, A., and Kundu, R. (2020). Human Papillomavirus E6 and E7: The Cervical Cancer Hallmarks and Targets for Therapy. Front Microbiol *10*, 3116.

263) Pastushenko, I., and Blanpain, C. (2019). EMT Transition States during Tumor Progression and Metastasis. Trends Cell Biol *29*, 212-226.

264) Pastushenko, I., Brisebarre, A., Sifrim, A., Fioramonti, M., Revenco, T., Boumahdi, S., Van Keymeulen, A., Brown, D., Moers, V., Lemaire, S., *et al.* (2018). Identification of the tumour transition states occurring during EMT. Nature *556*, 463-468.

265) Pattabiraman, D. R., and Weinberg, R. A. (2014). Tackling the cancer stem cells - what challenges do they pose? Nat Rev Drug Discov *13*, 497-512.

266) Peacock, C. D., Wang, Q., Gesell, G. S., Corcoran-Schwartz, I. M., Jones, E., Kim, J., Devereux, W. L., Rhodes, J. T., Huff, C. A., Beachy, P. A., *et al.*

(2007). Hedgehog signaling maintains a tumor stem cell compartment in multiple myeloma. Proc Natl Acad Sci U S A *104*, 4048-4053.

267) Pearson, G. W. (2019). Control of Invasion by Epithelial-to-Mesenchymal Transition Programs during Metastasis. J Clin Med *8*.

268) Pecere, T., Gazzola, M. V., Mucignat, C., Parolin, C., Vecchia, F. D., Cavaggioni, A., Basso, G., Diaspro, A., Salvato, B., Carli, M., and Palu, G. (2000). Aloe-emodin is a new type of anticancer agent with selective activity against neuroectodermal tumors. Cancer Res *60*, 2800-2804.

269) Peinado, H., Lavotshkin, S., and Lyden, D. (2011). The secreted factors responsible for pre-metastatic niche formation: old sayings and new thoughts. Semin Cancer Biol *21*, 139-146.

270) Peinado, H., Zhang, H., Matei, I. R., Costa-Silva, B., Hoshino, A., Rodrigues, G., Psaila, B., Kaplan, R. N., Bromberg, J. F., Kang, Y., *et al.* (2017). Pre-metastatic niches: organ-specific homes for metastases. Nat Rev Cancer *17*, 302-317.

271) Pellegrini, P., Cordero, A., Gallego, M. I., Dougall, W. C., Munoz, P., Pujana, M. A., and Gonzalez-Suarez, E. (2013). Constitutive activation of RANK disrupts mammary cell fate leading to tumorigenesis. Stem Cells *31*, 1954-1965.

272) Peng, C., Zhang, W., Dai, C., Li, W., Shen, X., Yuan, Y., Yan, L., and Yao, M. (2019). Study of the aqueous extract of Aloe vera and its two active components on the Wnt/beta-catenin and Notch signaling pathways in colorectal cancer cells. J Ethnopharmacol *243*, 112092.

273) Penuelas, S., Anido, J., Prieto-Sanchez, R. M., Folch, G., Barba, I., Cuartas, I., Garcia-Dorado, D., Poca, M. A., Sahuquillo, J., Baselga, J., and Seoane, J. (2009). TGF-beta increases glioma-initiating cell self-renewal through the induction of LIF in human glioblastoma. Cancer Cell *15*, 315-327.

274) Peterson, S. C., Eberl, M., Vagnozzi, A. N., Belkadi, A., Veniaminova, N. A., Verhaegen, M. E., Bichakjian, C. K., Ward, N. L., Dlugosz, A. A., and Wong, S. Y. (2015). Basal cell carcinoma preferentially arises from stem cells within hair follicle and mechanosensory niches. Cell Stem Cell *16*, 400-412.

275) Petrova, R., and Joyner, A. L. (2014). Roles for Hedgehog signaling in adult organ homeostasis and repair. Development *141*, 3445-3457.

276) Phi, L. T. H., Sari, I. N., Yang, Y. G., Lee, S. H., Jun, N., Kim, K. S., Lee, Y. K., and Kwon, H. Y. (2018). Cancer Stem Cells (CSCs) in Drug Resistance and their Therapeutic Implications in Cancer Treatment. Stem Cells Int *2018*, 5416923.

277) Podhorecka, M., Skladanowski, A., and Bozko, P. (2010). H2AX Phosphorylation: Its Role in DNA Damage Response and Cancer Therapy. J Nucleic Acids *2010*.

278) Poli, V., Fagnocchi, L., Fasciani, A., Cherubini, A., Mazzoleni, S., Ferrillo, S., Miluzio, A., Gaudioso, G., Vaira, V., Turdo, A., *et al.* (2018). MYC-driven epigenetic reprogramming favors the onset of tumorigenesis by inducing a stem cell-like state. Nat Commun *9*, 1024.

279) Ponti, D., Costa, A., Zaffaroni, N., Pratesi, G., Petrangolini, G., Coradini, D., Pilotti, S., Pierotti, M. A., and Daidone, M. G. (2005). Isolation and in vitro propagation of tumorigenic breast cancer cells with stem/progenitor cell properties. Cancer Res *65*, 5506-5511.

280) Pranatharthi, A., Thomas, P., Udayashankar, A. H., Bhavani, C., Suresh, S. B., Krishna, S., Thatte, J., Srikantia, N., Ross, C. R., and Srivastava, S. (2019). RhoC regulates radioresistance via crosstalk of ROCK2 with the DNA repair machinery in cervical cancer. J Exp Clin Cancer Res *38*, 392.

281) Prasad, S., Ravindran, J., and Aggarwal, B. B. (2010). NF-kappaB and cancer: how intimate is this relationship. Mol Cell Biochem *336*, 25-37.

282) Puck, T. T., and Marcus, P. I. (1956). Action of x-rays on mammalian cells. J Exp Med *103*, 653-666.

283) Puig, I., Tenbaum, S. P., Chicote, I., Arques, O., Martinez-Quintanilla, J., Cuesta-Borras, E., Ramirez, L., Gonzalo, P., Soto, A., Aguilar, S., *et al.* (2018). TET2 controls chemoresistant slow-cycling cancer cell survival and tumor recurrence. J Clin Invest *128*, 3887-3905.

284) Pulvirenti, T., Van Der Heijden, M., Droms, L. A., Huse, J. T., Tabar, V., and Hall, A. (2011). Dishevelled 2 signaling promotes self-renewal and tumorigenicity in human gliomas. Cancer Res *71*, 7280-7290.

285) Punzi, S., Balestrieri, C., D'Alesio, C., Bossi, D., Dellino, G. I., Gatti, E., Pruneri, G., Criscitiello, C., Lovati, G., Meliksetyan, M., *et al.* (2019). WDR5 inhibition halts metastasis dissemination by repressing the mesenchymal phenotype of breast cancer cells. Breast Cancer Res *21*, 123.

286) Qin, C., Huang, R. Y., and Wang, Z. X. (2015). Potential role of miR-100 in cancer diagnosis, prognosis, and therapy. Tumour Biol. *36(3)*, 1403-9.

287) Qin, J., Wen, B., Liang, Y., Yu, W., and Li, H. (2020). Histone Modifications and their Role in Colorectal Cancer (Review). Pathol Oncol Res *26*, 2023-2033.

288) Quintana, E., Shackleton, M., Foster, H. R., Fullen, D. R., Sabel, M. S., Johnson, T. M., and Morrison, S. J. (2010). Phenotypic heterogeneity among tumorigenic melanoma cells from patients that is reversible and not hierarchically organized. Cancer Cell *18*, 510-523.

289) Quintana, E., Shackleton, M., Sabel, M. S., Fullen, D. R., Johnson, T. M., and Morrison, S. J. (2008). Efficient tumour formation by single human melanoma cells. Nature *456*, 593-598.

290) Radford, I. R. (1985). The level of induced DNA double-strand breakage correlates with cell killing after X-irradiation. Int J Radiat Biol Relat Stud Phys Chem Med *48*, 45-54.

291) Rafehi, H., Orlowski, C., Georgiadis, G. T., Ververis, K., El-Osta, A., and Karagiannis, T. C. (2011). Clonogenic assay: adherent cells. J Vis Exp.

292) Ramsahoye, B. H., Biniszkiewicz, D., Lyko, F., Clark, V., Bird, A. P., and Jaenisch, R. (2000). Non-CpG methylation is prevalent in embryonic stem cells and may be mediated by DNA methyltransferase 3a. Proc Natl Acad Sci U S A *97*, 5237-5242.

293) Rasmussen, K. D., and Helin, K. (2016). Role of TET enzymes in DNA methylation, development, and cancer. Genes Dev *30*, 733-750.

294) Rasoanaivo, P., Wright, C. W., Willcox, M. L., and Gilbert, B. (2011). Whole plant extracts versus single compounds for the treatment of malaria: synergy and positive interactions. Malar J *10 Suppl 1*, S4.

295) Razin, A., and Cedar, H. (1991). DNA methylation and gene expression. Microbiol Rev *55*, 451-458.

296) Reya, T., Morrison, S. J., Clarke, M. F., and Weissman, I. L. (2001). Stem cells, cancer, and cancer stem cells. Nature *414*, 105-111.

297) Reymond, N., d'Agua, B. B., and Ridley, A. J. (2013). Crossing the endothelial barrier during metastasis. Nat Rev Cancer *13*, 858-870.

298) Reymond, N., Im, J. H., Garg, R., Cox, S., Soyer, M., Riou, P., Colomba, A., Muschel, R. J., and Ridley, A. J. (2015). RhoC and ROCKs regulate cancer cell interactions with endothelial cells. Mol Oncol *9*, 1043-1055.

299) Ricci-Vitiani, L., Lombardi, D. G., Pilozzi, E., Biffoni, M., Todaro, M., Peschle, C., and De Maria, R. (2007). Identification and expansion of human colon-cancer-initiating cells. Nature *445*, 111-115.

300) Ridley, A. J. (1997). The GTP-binding protein Rho. Int J Biochem Cell Biol *29*, 1225-1229.

301) Ridley, A. J. (2006). Rho GTPases and actin dynamics in membrane protrusions and vesicle trafficking. Trends Cell Biol *16*, 522-529.

302) Ridley, A. J. (2013). RhoA, RhoB and RhoC have different roles in cancer cell migration. J Microsc *251*, 242-249.

303) Riverso, M., Montagnani, V., and Stecca, B. (2017). KLF4 is regulated by RAS/RAF/MEK/ERK signaling through E2F1 and promotes melanoma cell growth. Oncogene *36*, 3322-3333.

304) Roberts, P. J., Mitin, N., Keller, P. J., Chenette, E. J., Madigan, J. P., Currin, R. O., Cox, A. D., Wilson, O., Kirschmeier, P., and Der, C. J. (2008). Rho Family GTPase modification and dependence on CAAX motif-signaled posttranslational modification. J Biol Chem *283*, 25150-25163.

305) Robertson, K. D. (2002). DNA methylation and chromatin - unraveling the tangled web. Oncogene *21*, 5361-5379.

306) Robertson, K. D. (2005). DNA methylation and human disease. Nat Rev Genet *6*, 597-610.

307) Rodrigues, C., Pattabiraman, C., Vijaykumar, A., Arora, R., Narayana, S. M., Kumar, R. V., Notani, D., Varga-Weisz, P., and Krishna, S. (2019). A SUV39H1-low chromatin state characterises and promotes migratory properties of cervical cancer cells. Exp Cell Res *378*, 206-216.

308) Rogakou, E. P., Boon, C., Redon, C., and Bonner, W. M. (1999). Megabase chromatin domains involved in DNA double-strand breaks in vivo. J Cell Biol *146*, 905-916.

309) Rojowska, A., Lammens, K., Seifert, F. U., Direnberger, C., Feldmann, H., and Hopfner, K. P. (2014). Structure of the Rad50 DNA double-strand break repair protein in complex with DNA. EMBO J *33*, 2847-2859.

310) Rose, P. G., Bundy, B. N., Watkins, E. B., Thigpen, J. T., Deppe, G., Maiman, M. A., Clarke-Pearson, D. L., and Insalaco, S. (1999). Concurrent cisplatin-based radiotherapy and chemotherapy for locally advanced cervical cancer. N Engl J Med *340*, 1144-1153.

311) Rosenthal, D. T., Zhang, J., Bao, L., Zhu, L., Wu, Z., Toy, K., Kleer, C. G., and Merajver, S. D. (2012). RhoC impacts the metastatic potential and abundance of breast cancer stem cells. PLoS One *7*, e40979.

312) Ross, S. E., Radomska, H. S., Wu, B., Zhang, P., Winnay, J. N., Bajnok, L., Wright, W. S., Schaufele, F., Tenen, D. G., and MacDougald, O. A. (2004). Phosphorylation of C/EBPalpha inhibits granulopoiesis. Mol Cell Biol *24*, 675-686.

313) Ruth, M. C., Xu, Y., Maxwell, I. H., Ahn, N. G., Norris, D. A., and Shellman, Y. G. (2006). RhoC promotes human melanoma invasion in a PI3K/Akt-dependent pathway. J Invest Dermatol *126*, 862-868.

314) Ruthenburg, A. J., Wang, W., Graybosch, D. M., Li, H., Allis, C. D., Patel, D. J., and Verdine, G. L. (2006). Histone H3 recognition and presentation by the WDR5 module of the MLL1 complex. Nat Struct Mol Biol *13*, 704-712.

315) Saibishkumar, E. P., Patel, F. D., and Sharma, S. C. (2006). Evaluation of late toxicities of patients with carcinoma of the cervix treated with radical radiotherapy: an audit from India. Clin Oncol (R Coll Radiol) *18*, 30-37.

316) Sandberg, A. A., and Hossfeld, D. K. (1970). Chromosomal abnormalities in human neoplasia. Annu Rev Med *21*, 379-408.

317) Sanders, B., Ray, A. M., Goldberg, S., Clark, T., McDaniel, H. R., Atlas, S. E., Farooqi, A., Konefal, J., Lages, L. C., Lopez, J., *et al.* (2017). Anti-cancer effects of aloe-emodin: a systematic review. J Clin Transl Res *3*, 283-296.

318) Sang, X. B., Sun, K. X., Wang, L. L., Chen, S., Wu, D. D., Zong, Z. H., and Zhao, Y. (2016). Effects and mechanism of RhoC downregulation in suppressing ovarian cancer stem cell proliferation, drug resistance, invasion and metastasis. Oncol Rep *36*, 3267-3274.

319) Santos-Rosa, H., Schneider, R., Bannister, A. J., Sherriff, J., Bernstein, B. E., Emre, N. C., Schreiber, S. L., Mellor, J., and Kouzarides, T. (2002). Active genes are tri-methylated at K4 of histone H3. Nature *419*, 407-411.

320) Sasaki, N., Ishiwata, T., Hasegawa, F., Michishita, M., Kawai, H., Matsuda, Y., Arai, T., Ishikawa, N., Aida, J., Takubo, K., and Toyoda, M. (2018).

Stemness and anti-cancer drug resistance in ATP-binding cassette subfamily G member 2 highly expressed pancreatic cancer is induced in 3D culture conditions. Cancer Sci *109*, 1135-1146.

321) Schackert, G., and Fidler, I. J. (1988). Site-specific metastasis of mouse melanomas and a fibrosarcoma in the brain or meninges of syngeneic animals. Cancer Res *48*, 3478-3484.

322) Schmeler, K. M., Jhingran, A., Iyer, R. B., Sun, C. C., Eifel, P. J., Soliman, P. T., Ramirez, P. T., Frumovitz, M., Bodurka, D. C., and Sood, A. K. (2010). Pelvic fractures after radiotherapy for cervical cancer: implications for survivors. Cancer *116*, 625-630.

323) Schubeler, D. (2015). Function and information content of DNA methylation. Nature *517*, 321-326.

324) Schuhmacher, J., Heidu, S., Balchen, T., Richardson, J. R., Schmeltz, C., Sonne, J., Schweiker, J., Rammensee, H. G., Thor Straten, P., Roder, M. A., *et al.* (2020). Vaccination against RhoC induces long-lasting immune responses in patients with prostate cancer: results from a phase I/II clinical trial. J Immunother Cancer *8*.

325) Schulz, A., Meyer, F., Dubrovska, A., and Borgmann, K. (2019). Cancer Stem Cells and Radioresistance: DNA Repair and Beyond. Cancers (Basel) *11*.

326) Segawa, K., and Nagata, S. (2015). An Apoptotic 'Eat Me' Signal: Phosphatidylserine Exposure. Trends Cell Biol *25*, 639-650.

327) Seyfried, T. N., and Huysentruyt, L. C. (2013). On the origin of cancer metastasis. Crit Rev Oncog *18*, 43-73.

328) Shackleton, M., Quintana, E., Fearon, E. R., and Morrison, S. J. (2009). Heterogeneity in cancer: cancer stem cells versus clonal evolution. Cell *138*, 822-829.

329) Shackleton, M., Vaillant, F., Simpson, K. J., Stingl, J., Smyth, G. K., Asselin-Labat, M. L., Wu, L., Lindeman, G. J., and Visvader, J. E. (2006). Generation of a functional mammary gland from a single stem cell. Nature *439*, 84-88.

330) Sharma, S., Kelly, T. K., and Jones, P. A. (2010). Epigenetics in cancer. Carcinogenesis *31*, 27-36.

331) Sheaffer, K. L., Elliott, E. N., and Kaestner, K. H. (2016). DNA Hypomethylation Contributes to Genomic Instability and Intestinal Cancer Initiation. Cancer Prev Res (Phila) *9*, 534-546.

332) Shepherd, J., Cobbe, S. M., Ford, I., Isles, C. G., Lorimer, A. R., MacFarlane, P. W., McKillop, J. H., and Packard, C. J. (1995). Prevention of coronary heart disease with pravastatin in men with hypercholesterolemia. West of Scotland Coronary Prevention Study Group. N Engl J Med *333*, 1301-1307.

333) Sherry, M. M., Reeves, A., Wu, J. K., and Cochran, B. H. (2009). STAT3 is required for proliferation and maintenance of multipotency in glioblastoma stem cells. Stem Cells *27*, 2383-2392.

334) Shibue, T., and Weinberg, R. A. (2017). EMT, CSCs, and drug resistance: the mechanistic link and clinical implications. Nat Rev Clin Oncol *14*, 611-629.

335) Shikada, Y., Yoshino, I., Okamoto, T., Fukuyama, S., Kameyama, T., and Maehara, Y. (2003). Higher expression of RhoC is related to invasiveness in non-small cell lung carcinoma. Clin Cancer Res *9*, 5282-5286.

336) Shinto, E., Tsuda, H., Matsubara, O., and Mochizuki, H. (2003). [Significance of RhoC expression in terms of invasion and metastasis of colorectal cancer]. Nihon Rinsho *61 Suppl 7*, 215-219.

337) Shiozawa, Y., Nie, B., Pienta, K. J., Morgan, T. M., and Taichman, R. S. (2013). Cancer stem cells and their role in metastasis. Pharmacol Ther *138*, 285-293.

338) Shope, R. E., and Hurst, E. W. (1933). Infectious Papillomatosis of Rabbits : With a Note on the Histopathology. J Exp Med *58*, 607-624.

339) Siebert, H. C., Lu, S. Y., Frank, M., Kramer, J., Wechselberger, R., Joosten, J., Andre, S., Rittenhouse-Olson, K., Roy, R., von der Lieth, C. W., *et al.* (2002). Analysis of protein-carbohydrate interaction at the lower size limit of the protein part (15-mer peptide) by NMR spectroscopy, electrospray ionization mass spectrometry, and molecular modeling. Biochemistry *41*, 9707-9717.

340) Simbulan-Rosenthal, C. M., Rosenthal, D. S., Boulares, A. H., Hickey, R. J., Malkas, L. H., Coll, J. M., and Smulson, M. E. (1998). Regulation of the expression or recruitment of components of the DNA synthesome by poly(ADP-ribose) polymerase. Biochemistry *37*, 9363-9370.

341) Singh, S. K., Hawkins, C., Clarke, I. D., Squire, J. A., Bayani, J., Hide, T., Henkelman, R. M., Cusimano, M. D., and Dirks, P. B. (2004). Identification of human brain tumour initiating cells. Nature *432*, 396-401.

342) Smejkal, G. B. (2004). The Coomassie chronicles: past, present and future perspectives in polyacrylamide gel staining. Expert Rev Proteomics *1*, 381-387.

343) Smith, P. K., Krohn, R. I., Hermanson, G. T., Mallia, A. K., Gartner, F. H., Provenzano, M. D., Fujimoto, E. K., Goeke, N. M., Olson, B. J., and Klenk, D. C. (1985). Measurement of protein using bicinchoninic acid. Anal Biochem *150*, 76-85.

344) Smith, Z. D., and Meissner, A. (2013). DNA methylation: roles in mammalian development. Nat Rev Genet *14*, 204-220.

345) Son, H., and Moon, A. (2010). Epithelial-mesenchymal Transition and Cell Invasion. Toxicol Res *26*, 245-252.

346) Song, B., Kim, D. K., Shin, J., Bae, S. H., Kim, H. Y., Won, B., Kim, J. K., Youn, H. D., Kim, S. T., Kang, S. W., and Jang, H. (2018). OCT4 directly regulates stemness and extracellular matrix-related genes in human germ cell tumours. Biochem Biophys Res Commun *503*, 1980-1986.

347) Song, W. S., Yang, Y. P., Huang, C. S., Lu, K. H., Liu, W. H., Wu, W. W., Lee, Y. Y., Lo, W. L., Lee, S. D., Chen, Y. W., *et al.* (2016). Sox2, a stemness gene, regulates tumor-initiating and drug-resistant properties in CD133-positive glioblastoma stem cells. J Chin Med Assoc *79*, 538-545.

348) Srivastava, S., and Krishna, S. (2009). Cancer stem cells: an approach to identify newer therapeutic targets. J Stem Cells *4*, 123-131.

349) Srivastava, S., Ramdass, B., Nagarajan, S., Rehman, M., Mukherjee, G., and Krishna, S. (2009). Notch1 regulates the functional contribution of RhoC to cervical carcinoma progression. Br J Cancer *102*, 196-205.

350) Stine, R. R., and Matunis, E. L. (2013). JAK-STAT signaling in stem cells. Adv Exp Med Biol *786*, 247-267.

351) Stockert, J. C., Horobin, R. W., Colombo, L. L., and Blazquez-Castro, A. (2018). Tetrazolium salts and formazan products in Cell Biology: Viability assessment, fluorescence imaging, and labeling perspectives. Acta Histochem *120*, 159-167.

352) Storms, R. W., Goodell, M. A., Fisher, A., Mulligan, R. C., and Smith, C. (2000). Hoechst dye efflux reveals a novel CD7(+)CD34(-) lymphoid progenitor in human umbilical cord blood. Blood *96*, 2125-2133.

353) Sugimura, T. (2002). [The principles of cancer treatment--changes in chemotherapy]. Gan To Kagaku Ryoho *29*, 1263-1278.

354) Surjushe, A., Vasani, R., and Saple, D. G. (2008). Aloe vera: a short review. Indian J Dermatol *53*, 163-166.

355) Suwa, H., Ohshio, G., Imamura, T., Watanabe, G., Arii, S., Imamura, M., Narumiya, S., Hiai, H., and Fukumoto, M. (1998). Overexpression of the rhoC gene correlates with progression of ductal adenocarcinoma of the pancreas. Br J Cancer *77*, 147-152.

356) Suzuki, M., Suzuki, T., Matsuura, M., Iwasaki, M., Tanaka, R., Ito, E., Fujii, M., and Saito, T. (2010). Prediction of histologic type and lymph node metastasis for advanced ovarian cancer on uterine cervical and endometrial cytology. Acta Cytol *54*, 575-581.

357) Szklarczyk, D., Gable, A. L., Lyon, D., Junge, A., Wyder, S., Huerta-Cepas, J., Simonovic, M., Doncheva, N. T., Morris, J. H., Bork, P., *et al.* (2018). STRING v11: protein-protein association networks with increased coverage, supporting functional discovery in genome-wide experimental datasets. Nucleic Acids Res *47*, D607-D613.

358) Tahiliani, M., Koh, K. P., Shen, Y., Pastor, W. A., Bandukwala, H., Brudno, Y., Agarwal, S., Iyer, L. M., Liu, D. R., Aravind, L., and Rao, A. (2009). Conversion of 5-methylcytosine to 5-hydroxymethylcytosine in mammalian DNA by MLL partner TET1. Science *324*, 930-935.

359) Tanabe, S., Quader, S., Cabral, H., and Ono, R. (2020). Interplay of EMT and CSC in Cancer and the Potential Therapeutic Strategies. Front Pharmacol *11*, 904.

360) Thankamony, A. P., Saxena, K., Murali, R., Jolly, M. K., and Nair, R. (2020). Cancer Stem Cell Plasticity - A Deadly Deal. Front Mol Biosci *7*, 79.

361) Thomas, P., Pranatharthi, A., Ross, C., and Srivastava, S. (2019). RhoC: a fascinating journey from a cytoskeletal organizer to a Cancer stem cell therapeutic target. J Exp Clin Cancer Res *38*, 328.

362) Thomson, S. P., and Meyskens, F. L., Jr. (1982). Method for measurement of self-renewal capacity of clonogenic cells from biopsies of metastatic human malignant melanoma. Cancer Res *42*, 4606-4613.

363) Thouri, A., Chahdoura, H., El Arem, A., Omri Hichri, A., Ben Hassin, R., and Achour, L. (2017). Effect of solvents extraction on phytochemical components and biological activities of Tunisian date seeds (var. Korkobbi and Arechti). BMC Complement Altern Med *17*, 248.

364) Toh, T. B., Lim, J. J., and Chow, E. K. (2017). Epigenetics in cancer stem cells. Mol Cancer *16*, 29.

365) Toledo-Guzman, M. E., Hernandez, M. I., Gomez-Gallegos, A. A., and Ortiz-Sanchez, E. (2018). ALDH as a Stem Cell Marker in Solid Tumors. Curr Stem Cell Res Ther *14*, 375-388.

366) Towbin, H., Staehelin, T., and Gordon, J. (1979). Electrophoretic transfer of proteins from polyacrylamide gels to nitrocellulose sheets: procedure and some applications. Proc Natl Acad Sci U S A *76*, 4350-4354.

367) Tsuruo, T., Iida, H., Tsukagoshi, S., and Sakurai, Y. (1981). Overcoming of vincristine resistance in P388 leukemia in vivo and in vitro through enhanced cytotoxicity of vincristine and vinblastine by verapamil. Cancer Res *41*, 1967-1972.

368) Ulasov, I. V., Mijanovic, O., Savchuk, S., Gonzalez-Buendia, E., Sonabend, A., Xiao, T., Timashev, P., and Lesniak, M. S. (2019). TMZ regulates GBM stemness via MMP14-DLL4-Notch3 pathway. Int J Cancer *146*, 2218-2228.

369) Valastyan, S., and Weinberg, R. A. (2011). Tumor metastasis: molecular insights and evolving paradigms. Cell *147*, 275-292.

370) Valencia-Gonzalez, H. A., Ruiz, G., Ortiz-Sanchez, E., and Garcia-Carranca, A. (2019). Cancer Stem Cells from Tumor Cell Lines Activate the DNA Damage Response Pathway after Ionizing Radiation More Efficiently Than Noncancer Stem Cells. Stem Cells Int *2019*, 7038953.

371) van Golen, K. L., Bao, L. W., Pan, Q., Miller, F. R., Wu, Z. F., and Merajver, S. D. (2002). Mitogen activated protein kinase pathway is involved in RhoC GTPase induced motility, invasion and angiogenesis in inflammatory breast cancer. Clin Exp Metastasis *19*, 301-311.

372) van Golen, K. L., Wu, Z. F., Qiao, X. T., Bao, L., and Merajver, S. D. (2000a). RhoC GTPase overexpression modulates induction of angiogenic factors in breast cells. Neoplasia *2*, 418-425.

373) van Golen, K. L., Wu, Z. F., Qiao, X. T., Bao, L. W., and Merajver, S. D. (2000b). RhoC GTPase, a novel transforming oncogene for human mammary epithelial cells that partially recapitulates the inflammatory breast cancer phenotype. Cancer Res *60*, 5832-5838.

374) van Zijl, F., Krupitza, G., and Mikulits, W. (2011). Initial steps of metastasis: cell invasion and endothelial transmigration. Mutat Res *728*, 23-34.

375) Varnat, F., Duquet, A., Malerba, M., Zbinden, M., Mas, C., Gervaz, P., and Ruiz i Altaba, A. (2009). Human colon cancer epithelial cells harbour active HEDGEHOG-GLI signalling that is essential for tumour growth, recurrence, metastasis and stem cell survival and expansion. EMBO Mol Med *1*, 338-351.

376) Vermes, I., Haanen, C., and Reutelingsperger, C. (2000). Flow cytometry of apoptotic cell death. J Immunol Methods *243*, 167-190.

377) Vermes, I., Haanen, C., Steffens-Nakken, H., and Reutelingsperger, C. (1995). A novel assay for apoptosis. Flow cytometric detection of phosphatidylserine expression on early apoptotic cells using fluorescein labelled Annexin V. J Immunol Methods *184*, 39-51.

378) Viswanathan, A. N., Lee, L. J., Eswara, J. R., Horowitz, N. S., Konstantinopoulos, P. A., Mirabeau-Beale, K. L., Rose, B. S., von Keudell, A. G., and Wo, J. Y. (2014). Complications of pelvic radiation in patients treated for gynecologic malignancies. Cancer *120*, 3870-3883.

379) Volkel, P., and Angrand, P. O. (2007). The control of histone lysine methylation in epigenetic regulation. Biochimie *89*, 1-20.

380) Waalwijk, C., and Flavell, R. A. (1978). MspI, an isoschizomer of hpaII which cleaves both unmethylated and methylated hpaII sites. Nucleic Acids Res *5*, 3231-3236.

381) Waddington, C. H. (2012). The epigenotype. 1942. Int J Epidemiol *41*, 10-13.

382) Wade, P. A. (2001). Methyl CpG-binding proteins and transcriptional repression. Bioessays *23*, 1131-1137.

383) Wainwright, E. N., and Scaffidi, P. (2017). Epigenetics and Cancer Stem Cells: Unleashing, Hijacking, and Restricting Cellular Plasticity. Trends Cancer *3*, 372-386.

384) Wang, J., Sakariassen, P. O., Tsinkalovsky, O., Immervoll, H., Boe, S. O., Svendsen, A., Prestegarden, L., Rosland, G., Thorsen, F., Stuhr, L., *et al.* (2008a). CD133 negative glioma cells form tumors in nude rats and give rise to CD133 positive cells. Int J Cancer *122*, 761-768.

385) Wang, S. S., Jiang, J., Liang, X. H., and Tang, Y. L. (2015). Links between cancer stem cells and epithelial-mesenchymal transition. Onco Targets Ther *8*, 2973-2980.

386) Wang, W., Wu, F., Fang, F., Tao, Y., and Yang, L. (2008b). RhoC is essential for angiogenesis induced by hepatocellular carcinoma cells via regulation of endothelial cell organization. Cancer Sci *99*, 2012-2018.

387) Wang, W., Yang, L. Y., Yang, Z. L., Huang, G. W., and Lu, W. Q. (2003). Expression and significance of RhoC gene in hepatocellular carcinoma. World J Gastroenterol *9*, 1950-1953.

388) Wang, X., Liu, J., Wang, Z., Huang, Y., Liu, W., Zhu, X., Cai, Y., Fang, X., Lin, S., Yuan, L., and Ouyang, G. (2013). Periostin contributes to the acquisition of multipotent stem cell-like properties in human mammary epithelial cells and breast cancer cells. PLoS One *8*, e72962.

389) Wang, Z., Da Silva, T. G., Jin, K., Han, X., Ranganathan, P., Zhu, X., Sanchez-Mejias, A., Bai, F., Li, B., Fei, D. L., *et al.* (2014). Notch signaling drives stemness and tumorigenicity of esophageal adenocarcinoma. Cancer Res *74*, 6364-6374.

390) Wang, Z., and Ouyang, G. (2012). Periostin: a bridge between cancer stem cells and their metastatic niche. Cell Stem Cell *10*, 111-112.

391) Washburn, M. P., Wolters, D., and Yates, J. R., 3rd (2001). Large-scale analysis of the yeast proteome by multidimensional protein identification technology. Nat Biotechnol *19*, 242-247.

392) Wee, B., Pietras, A., Ozawa, T., Bazzoli, E., Podlaha, O., Antczak, C., Westermark, B., Nelander, S., Uhrbom, L., Forsberg-Nilsson, K., *et al.* (2016). ABCG2 regulates self-renewal and stem cell marker expression but not tumorigenicity or radiation resistance of glioma cells. Sci Rep *6*, 25956.

393) Wennerberg, K., and Der, C. J. (2004). Rho-family GTPases: it's not only Rac and Rho (and I like it). J Cell Sci *117*, 1301-1312.

394) Whitney, C. W., Sause, W., Bundy, B. N., Malfetano, J. H., Hannigan, E. V., Fowler, W. C., Jr., Clarke-Pearson, D. L., and Liao, S. Y. (1999). Randomized comparison of fluorouracil plus cisplatin versus hydroxyurea as an adjunct to radiation therapy in stage IIB-IVA carcinoma of the cervix with negative para-aortic lymph nodes: a Gynecologic Oncology Group and Southwest Oncology Group study. J Clin Oncol *17*, 1339-1348.

395) Winkler, C., Denker, K., Wortelkamp, S., and Sickmann, A. (2007). Silver- and Coomassie-staining protocols: detection limits and compatibility with ESI MS. Electrophoresis *28*, 2095-2099.

396) Witt, A. E., Lee, C. W., Lee, T. I., Azzam, D. J., Wang, B., Caslini, C., Petrocca, F., Grosso, J., Jones, M., Cohick, E. B., *et al.* (2017). Identification of a cancer stem cell-specific function for the histone deacetylases, HDAC1 and HDAC7, in breast and ovarian cancer. Oncogene *36*, 1707-1720.

397) Wong, A. D., and Searson, P. C. (2017). Mitosis-Mediated Intravasation in a Tissue-Engineered Tumor-Microvessel Platform. Cancer Res *77*, 6453-6461.

398) Wortzel, I., and Seger, R. (2011). The ERK Cascade: Distinct Functions within Various Subcellular Organelles. Genes Cancer *2*, 195-209.

399) Wu, X., and Zhang, Y. (2017). TET-mediated active DNA demethylation: mechanism, function and beyond. Nat Rev Genet *18*, 517-534.

400) Wu, Y., Tao, Y., Chen, Y., and Xu, W. (2012). RhoC regulates the proliferation of gastric cancer cells through interaction with IQGAP1. PLoS One *7*, e48917.

401) Xiao, X., Li, B. X., Mitton, B., Ikeda, A., and Sakamoto, K. M. (2010). Targeting CREB for cancer therapy: friend or foe. Curr Cancer Drug Targets *10*, 384-391.

402) Xie, S., Zhu, M., Lv, G., Geng, Y., Chen, G., Ma, J., and Wang, G. (2013). Overexpression of Ras homologous C (RhoC) induces malignant transformation of hepatocytes in vitro and in nude mouse xenografts. PLoS One *8*, e54493.

403) Xu, X. D., Shen, H. B., Zhu, L., Lu, J. Q., Zhang, L., Luo, Z. Y., and Wu, Y. Q. (2017). Anti-RhoC siRNAs inhibit the proliferation and invasiveness of

breast cancer cells via modulating the KAI1, MMP9, and CXCR4 expression. Onco Targets Ther *10*, 1827-1834.

404) Yamaguchi, H., and Condeelis, J. (2007). Regulation of the actin cytoskeleton in cancer cell migration and invasion. Biochim Biophys Acta *1773*, 642-652.

405) Yamazaki, D., Kurisu, S., and Takenawa, T. (2005). Regulation of cancer cell motility through actin reorganization. Cancer Sci *96*, 379-386.

406) Yan, L. H., Wei, W. Y., Cao, W. L., Zhang, X. S., Xie, Y. B., and Xiao, Q. (2014). Overexpression of E2F1 in human gastric carcinoma is involved in anti-cancer drug resistance. BMC Cancer *14*, 904.

407) Yang, Z., Li, C., Fan, Z., Liu, H., Zhang, X., Cai, Z., Xu, L., Luo, J., Huang, Y., He, L., *et al.* (2017). Single-cell Sequencing Reveals Variants in ARID1A, GPRC5A and MLL2 Driving Self-renewal of Human Bladder Cancer Stem Cells. Eur Urol *71*, 8-12.

408) Yang, Z. J., and Wechsler-Reya, R. J. (2007). Hit 'em where they live: targeting the cancer stem cell niche. Cancer Cell *11*, 3-5.

409) Yoshida, K., and Miki, Y. (2004). Role of BRCA1 and BRCA2 as regulators of DNA repair, transcription, and cell cycle in response to DNA damage. Cancer Sci *95*, 866-871.

410) Yu, B., Wu, K., Wang, X., Zhang, J., Wang, L., Jiang, Y., Zhu, X., Chen, W., and Yan, M. (2018). Periostin secreted by cancer-associated fibroblasts promotes cancer stemness in head and neck cancer by activating protein tyrosine kinase 7. Cell Death Dis *9*, 1082.

411) Yu, K. R., Yang, S. R., Jung, J. W., Kim, H., Ko, K., Han, D. W., Park, S. B., Choi, S. W., Kang, S. K., Scholer, H., and Kang, K. S. (2012). CD49f enhances multipotency and maintains stemness through the direct regulation of OCT4 and SOX2. Stem Cells *30*, 876-887.

412) Yun, C., and DasGupta, R. (2014). Luciferase reporter assay in Drosophila and mammalian tissue culture cells. Curr Protoc Chem Biol *6*, 7-23.

413) Zeineddine, D., Hammoud, A. A., Mortada, M., and Boeuf, H. (2014). The Oct4 protein: more than a magic stemness marker. Am J Stem Cells *3*, 74-82.

414) Zeisberg, M., and Neilson, E. G. (2009). Biomarkers for epithelial-mesenchymal transitions. J Clin Invest *119*, 1429-1437.

415) Zeng, J., Liu, Z., Sun, S., Xie, J., Cao, L., Lv, P., Nie, S., Zhang, B., Xie, B., Peng, S., and Jiang, B. (2018a). Tumor-associated macrophages recruited by periostin in intrahepatic cholangiocarcinoma stem cells. Oncol Lett *15*, 8681-8686.

416) Zeng, Y. F., Xiao, Y. S., Liu, Y., Luo, X. J., Wen, L. D., Liu, Q., and Chen, M. (2018b). Formin-like 3 regulates RhoC/FAK pathway and actin assembly to promote cell invasion in colorectal carcinoma. World J Gastroenterol *24*, 3884-3897.

417) Zhang, L., Rayner, S., Katoku-Kikyo, N., Romanova, L., and Kikyo, N. (2007). Successful co-immunoprecipitation of Oct4 and Nanog using cross-linking. Biochem Biophys Res Commun *361*, 611-614.

418) Zhang, P., Lee, H., Brunzelle, J. S., and Couture, J. F. (2012). The plasticity of WDR5 peptide-binding cleft enables the binding of the SET1 family of histone methyltransferases. Nucleic Acids Res *40*, 4237-4246.

419) Zhang, W., Sui, Y., Ni, J., and Yang, T. (2016). Insights into the Nanog gene: A propeller for stemness in primitive stem cells. Int J Biol Sci *12*, 1372-1381.

420) Zhao, L., Zhao, Y., Schwarz, B., Mysliwietz, J., Hartig, R., Camaj, P., Bao, Q., Jauch, K. W., Guba, M., Ellwart, J. W., *et al.* (2016). Verapamil inhibits tumor progression of chemotherapy-resistant pancreatic cancer side population cells. Int J Oncol *49*, 99-110.

421) Zhao, M., Mishra, L., and Deng, C. X. (2018). The role of TGF-beta/SMAD4 signaling in cancer. Int J Biol Sci *14*, 111-123.

422) Zhao, W., Li, Y., and Zhang, X. (2017). Stemness-Related Markers in Cancer. Cancer Transl Med *3*, 87-95.

423) Zhao, Z., and Shilatifard, A. (2019). Epigenetic modifications of histones in cancer. Genome Biol *20*, 245.

424) Zheng, Y. (2001). Dbl family guanine nucleotide exchange factors. Trends Biochem Sci *26*, 724-732.

425) Zhong, H., Li, X., Zhang, J., and Wu, X. (2019). Overexpression of periostin is positively associated with gastric cancer metastasis through promoting tumor metastasis and invasion. J Cell Biochem *120*, 9927-9935.

426) Zhou, H. M., Zhang, J. G., Zhang, X., and Li, Q. (2021). Targeting cancer stem cells for reversing therapy resistance: mechanism, signaling, and prospective agents. Signal Transduct Target Ther *6*, 62.

427) Zhou, J., Wulfkuhle, J., Zhang, H., Gu, P., Yang, Y., Deng, J., Margolick, J. B., Liotta, L. A., Petricoin, E., 3rd, and Zhang, Y. (2007). Activation of the PTEN/mTOR/STAT3 pathway in breast cancer stem-like cells is required for viability and maintenance. Proc Natl Acad Sci U S A *104*, 16158-16163.

428) Zhou, K., Guo, H., Zhang, J., Zhao, D., Zhou, Y., Zheng, Z., Xu, Y., Li, Y., and Wang, D. (2019). Potential role of TET2 in gastric cancer cisplatin resistance. Pathol Res Pract *215*, 152637.

429) Zhou, S., Schuetz, J. D., Bunting, K. D., Colapietro, A. M., Sampath, J., Morris, J. J., Lagutina, I., Grosveld, G. C., Osawa, M., Nakauchi, H., and Sorrentino, B. P. (2001). The ABC transporter Bcrp1/ABCG2 is expressed in a wide variety of stem cells and is a molecular determinant of the side-population phenotype. Nat Med *7*, 1028-1034.

430) Zhou, W., Ke, S. Q., Huang, Z., Flavahan, W., Fang, X., Paul, J., Wu, L., Sloan, A. E., McLendon, R. E., Li, X., *et al.* (2015). Periostin secreted by glioblastoma stem cells recruits M2 tumour-associated macrophages and promotes malignant growth. Nat Cell Biol *17*, 170-182.

431) Zhu. L., Wang. A., Gao. M., Duan. X., Li. Z. (2020). LncRNA MIR4435-2HG triggers ovarian cancer progression by regulating miR-128-3p/CKD14 axis. Cancer Cell Int. *20*, 145.

432) Zhuang, J., Huo, Q., Yang, F., and Xie, N. (2020). Perspectives on the Role of Histone Modification in Breast Cancer Progression and the Advanced Technological Tools to Study Epigenetic Determinants of Metastasis. Front Genet *11*, 603552.